Drug and device testing in a preclinical model sensitive to cardiac arrhythmias

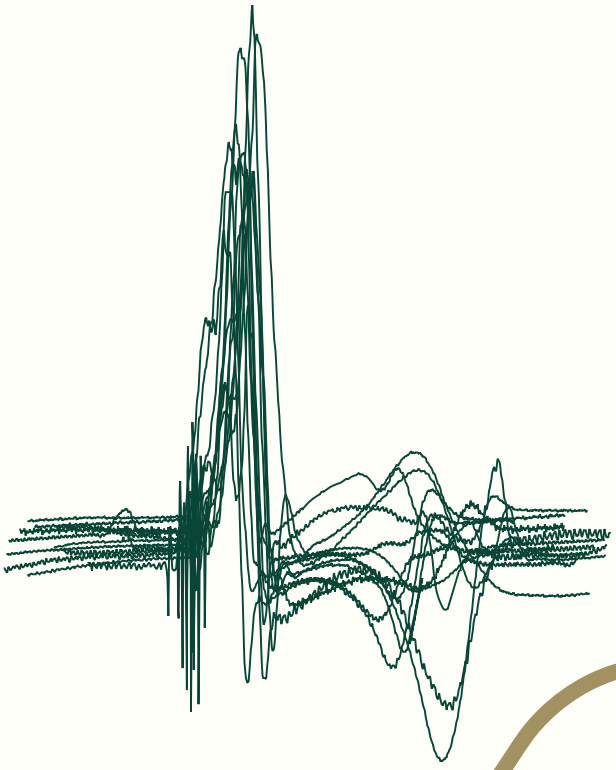

Joanne J.A. van Bavel

Drug and device testing in a preclinical model sensitive to cardiac arrhythmias

Joanne J.A. van Bavel

ISBN: 978-94-6419-880-5
Cover design: Joanne van Bavel
Lay-out: Joanne van Bavel
Printing: Gildeprint B.V. | www.gildeprint.nl

Drug and device testing in a preclinical model sensitive to cardiac arrhythmias

Medicijn en hartapparaat testen in een preklinisch model gevoelig voor hartritmestoornissen

(met een samenvatting in het Nederlands)

Proefschrift

ter verkrijging van de graad van doctor aan de
Universiteit Utrecht
op gezag van de
rector magnificus, prof.dr. H.R.B.M. Kummeling,
ingevolge het besluit van het college voor promoties
in het openbaar te verdedigen op

donderdag 28 september 2023 des middags te 12.15 uur

door

Joanne Johanne Arianne van Bavel

geboren op 18 september 1993
te Angerlo

Promotor:
Prof. dr. M.A. Vos

Copromotor:
Dr. M.A.G. van der Heyden

Beoordelingscommissie:
Prof. dr. ir. J.P.W.M. Bakkers
Dr. M. Pešl
Prof. dr. H.V.M. van Rijen (voorzitter)
Prof. dr. D. Salvatori
Prof. dr. D. Thijssen

The research described in this thesis was performed at the Department of Medical Physiology from the Division Heart & Lungs of the University Medical Center Utrecht, within the PhD programme of Cardiovascular Research from the Graduate School of Life Sciences, Utrecht University.

The research described in this thesis was partly funded by the European Union's Horizon 2020 research and innovation programme under grant number 732170 as part of the CResPace consortium.

Financial support by the Dutch Heart Foundation for the publication of this thesis is gratefully acknowledged.

‘t Komt wel goed.

Contents

1

General introduction

Joanne J.A. van Bavel

Introduction

Alterations in the electrical activity of heart cells (cardiomyocytes) forming an action potential is the fundamental mechanism of generating a heart rhythm. A cardiac action potential wave starts its journey in the natural pacemaker of the heart: the sinoatrial node located in the right atrium. Next, it propagates through the atrial cells until it reaches the atrioventricular (AV) node, where it is shortly delayed allowing the atria to contract. Then, it follows a fast path through the bundle of His and the bundle branches to the apex of the heart. From there, an action potential wave through the Purkinje fibers induces depolarization of cardiomyocytes with biventricular contraction as result. The action potential is formed by the properties of ion channels localized over the cell membranes and differs between the compartments of the conduction system. The ventricular action potential consists of different phases including 0) depolarization (rapid influx of Na^+ ions by opening of the voltage-gated Na^+ channels), 1) early repolarization (slight drop in potential due to closure of the voltage-gated Na^+ channels and activation of the transient outward K^+ current), 2) plateau (influx of Ca^{2+} by opening of voltage-gated L-type Ca^{2+} channels balances the K^+ efflux by opening of the slow delayed rectifier K^+ channels), 3) repolarization (efflux of K^+ by the slow and rapid delayed rectifier K^+ channels), and 4) resting (diastole). Under physiological circumstances, the electrical conduction system with a proper rhythm and succeeding contraction can comply with the body's demands in terms of blood flow and gas exchange.

Under pathological conditions, disturbances in the electrical conduction system can lead to various rhythm disorders, called arrhythmias, of which ventricular fibrillation is the most severe. When sustained, this type of arrhythmia causes prolonged loss of cardiac output and subsequently death. Importantly, sudden cardiac death is still the leading cause of mortality worldwide and in 50-70% of the cases related to ventricular tachyarrhythmia.[1,2] The process of initiation and perpetuation of ventricular arrhythmias is complex and coincides with (a combination of) diverse substrates, triggers, and underlying electrophysiological mechanisms. Adaptation (remodeling) of the heart in a pathological situation involves alterations on a structural, functional, electrophysiological, and neurohormonal level which form an arrhythmic substrate.[3] With age, family history, lifestyle habits (e.g., diet, smoking, alcohol consumption, physical inactivity), medications, and comorbidities such as coronary artery disease, chronic kidney disease, lung disease, and sleep apnea, the risk for arrhythmia

occurrence increases.[4-7] Under these proarrhythmic conditions, any disturbances in the electrical conduction system can initiate arrhythmic events. Automatic activity of ventricular cardiomyocytes (abnormal automaticity), and early and delayed afterdepolarizations occurring during or after the repolarization phase (triggered activity) give rise to premature ventricular contractions (PVCs) which can perpetuate into ventricular tachyarrhythmias.[8] An anatomical or functional block in the electrical conduction wave propagating around the ventricles can cause a closed loop forming the reentry mechanism for arrhythmia occurrence.[9]

Ventricular arrhythmia therapy

Electrocardiographic monitoring, exercise testing, imaging, and genetic testing act as diagnostic tools for arrhythmias with a sporadic behavior or as symptom of an underlying disease.[10] When life threatening, management of ventricular arrhythmias includes acute correction of reversible causes, and/or interventional therapy, pharmacotherapy, and device therapy for long-term treatment.[10] Most antiarrhythmic drugs are classified and further split into subgroups based on their effect on the cardiac electrical system: Na^+ channel blockade, beta-adrenergic blockade, K^+ channel blockade, and Ca^{2+} channel blockade.[11] Antiarrhythmic drug therapy should contemplate with the hemodynamic and rhythmic status of a patient, especially due to the negative inotropic effect many of these drugs can have. Moreover, pharmacological treatment of patients with a high risk for ventricular arrhythmias and comorbidities affecting cardiac function also cover inhibition of the renin-angiotensin system and SGLT2, and activation of the aldosterone receptor.[12] In terms of cardiac devices, therapy has been strongly improved since the development of an external pace system in 1951.[13] Currently, the most common therapy includes implantation of an implantable cardioverter defibrillator (ICD) device in patients surviving a cardiac arrest (secondary prevention) or at high risk for undergoing one (primary prevention).[10] Here, drug therapy combined with ICD therapy reduces the risk for recurrent ventricular arrhythmia.[14] Other device therapies are biventricular pacing by cardiac resynchronization therapy (CRT) in heart failure patients and permanent pacing in case of e.g., bradyarrhythmia.[15]

Ventricular arrhythmia research

In the research field of cardiac electrophysiology, arrhythmia management is still improving and focusses on evaluating proarrhythmic responses of new developed compounds, the discovery of new pharmacological targets, and improvement of antiarrhythmic strategies. Experimental approaches make use of *in silico* and *in vitro* systems, small and large preclinical animal models, and healthy and diseased human participants. Guidelines by the Food and Drug Administration (FDA) and European Medicines Agency (EMA) describe proarrhythmic risk assessment by performance of *in vitro* I_{Kr} assays and *in vivo* QT assays to evaluate potential drug-induced QT prolongation before entering further progress to clinical trials.[16] Next, a clinical evaluation of QT/QTc interval prolongation and proarrhythmic potential is performed in safety studies in patients.[17] In addition, the comprehensive *in vitro* proarrhythmia assay (CiPA) initiative covers multi-ion channel targeting besides solely I_{Kr}.[18]

The focus on alternatives for animal use in science is expanding tremendously, though it faces challenges in approaching the physiological state of a living organism and thereby being of translational significance. For example, induced-pluripotent stem cell derived cardiomyocytes (iPSC-CMs) show an immature phenotype and beat spontaneously,[19] and in general single cells lack organ-dependent factors and cell-cell interactions. Moreover, even small animal models, such as zebrafish with two heart chambers and the commonly used rat and mice models with aberrant ion channel levels compared to human display their drawbacks. Currently, a complete removal of animal testing in biomedical science seems unrealistic. It is therefore of utmost importance that every experimental approach consists of thorough evaluation on what model approximates an optimal translational value. A preclinical model standardized for electrophysiological research, best resembling human electrophysiology, hemodynamics, pharmacodynamics etc., is of crucial value in examining pro- and antiarrhythmic drug and device responses. The canine heart shares a moderate resemblance in cardiac electrophysiology with that of the human, and is recommended as appropriate research model in electrophysiology studies as incorporated in the ICH S7B guidelines.[16]

The AV block dog: a preclinical model sensitive to cardiac arrhythmias

The dog with complete AV block[20] induced by radiofrequency ablation of the His bundle[21] has been standardized over the last three decades with a strong focus on pro- and antiarrhythmic

properties in pharmacological research.[22,23] Immediately after AV block, the dissociation in electrical conduction between the atria and the ventricles exchanges sinus rhythm (SR) for an escape rhythm from the ventricles, the idioventricular rhythm (IVR). The ventricular rate decreases from 100 bpm at SR to 50 bpm at IVR (**Figure 1A, red line**) which induces volume overload. This is accompanied by a sudden drop in cardiac output (**Figure 1A, black line**) and demands compensation by cardiac remodeling[24] in order to maintain a proper blood flow to the demanding tissues. Remodeling occurs at different levels, starting with an increase in contractility (LV dP/dt_{max}) (**Figure 1A, green line**)[25] partly due to enhanced neurohormonal levels.[26] On a structural level, the growth of single cardiomyocytes – hypertrophy – takes over on a much slower pace (**Figure 1A, yellow line**)[27] and the contractility declines. Lastly, a downregulation of the slow and rapid delayed rectifier outward potassium currents (I_{Ks} and I_{Kr})[28] prolongs the action potential duration and thereby the QT interval on the ECG (**Figure 1A, blue line**). This reduces the repolarization reserve; a safety net which normally includes the compensation of one channel when the other is affected.[29]

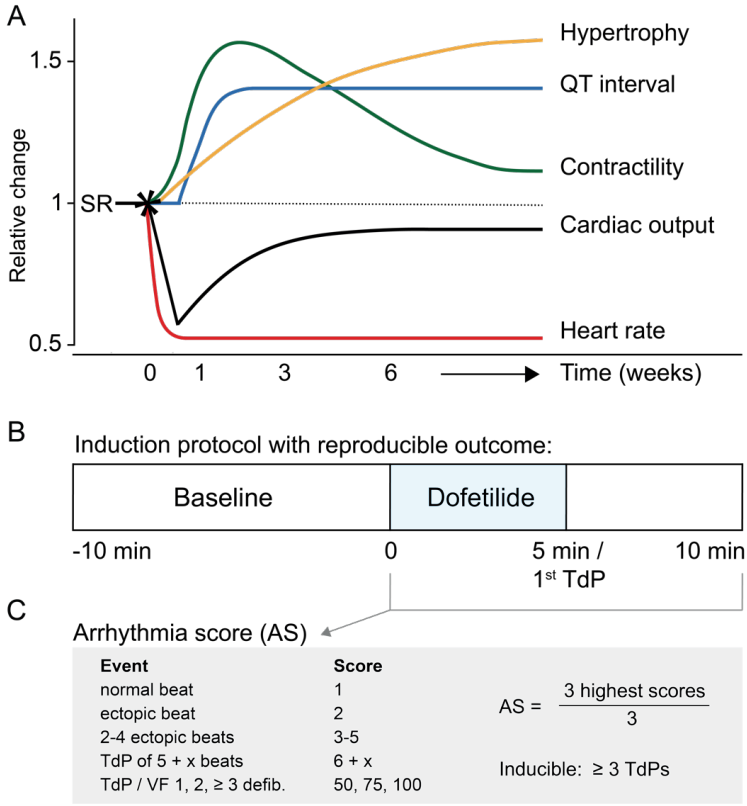

Figure 1. A) Overview of the different remodeling stages after atrioventricular (AV) block induction over time. The star symbol refers to AV block induction at timepoint zero. **B**) Flowchart of the standardized protocol of Torsade de Pointes (TdP) arrhythmia induction using the I_{Kr} blocker dofetilide for 5 minutes or until the occurrence of the first TdP arrhythmia. **C**) The arrhythmia score (AS) is based on the three highest scored arrhythmic events during the 10-minute time window after the onset of dofetilide. A TdP and ventricular fibrillation (VF) demanding 1, 2, ≥3 defibrillations (defib.) receive a score of 50, 75, 100, respectively. Dogs are considered inducible when showing three or more TdP arrhythmias in the 10-minute time window. Panel A was adapted from Bourgonje et al.[24]

Under anesthesia, a combination of the preceding components of bradycardia-induced remodeling makes the AV block heart susceptible for Torsade de Pointes (TdP) arrhythmias. This type of ventricular tachycardia is depicted as voltage signals turning around the isoelectric line on the ECG and is considered as model of triggered activity in its origin and reentry-based for longer lasting episodes (>14 beats).[30] From two weeks after AV block, infusion of dofetilide as additional hit induces TdP arrhythmias in approximately 75% of the animals and this number is highly reproducible and stable over time.[20]

The protocol of testing TdP sensitivity includes a 10-minute baseline recording of electrophysiological signals followed by dofetilide infusion for 5 minutes or until the first TdP arrhythmia occurs (**Figure 1B**). TdP sensitivity is quantified by the arrhythmia score (AS)[31] and determined in the 10 minutes after the onset of dofetilide infusion (**Figure 1C**). Each arrhythmic event contains a specific score of which the sum of the three highest scores, within the 10-minute time window, divided by three forms the AS. A dog is considered inducible for TdP arrhythmias when showing three or more TdP episodes in the 10-minute time window. In general, the continuously recorded signals include surface ECG, monophasic action potentials (MAP) from the left ventricular apex and/or the right ventricular mid-free wall, and occasionally left ventricular pressure signals for further analysis. Extraction of the beat-to-beat variability of repolarization of the MAP signals is quantified by short term variability (STV) of repolarization and characterizes the temporal dispersion of repolarization. Enhanced STV is associated with induction of TdP arrhythmias.[32]

Thesis outline

Testing of the proarrhythmic risk or antiarrhythmic properties of drugs and devices occurs in an induction or prevention strategy in the AV block dog model. In terms of compounds, affecting cardiac repolarization and thereby evaluating proarrhythmic risk can be indirectly via cellular processes or via direct channel modulation. The degradation of cellular material called autophagy is a crucial process in cellular physiology and therefore a valuable target in anticancer treatment. Compounds targeting one of its main pathways (PI3K) are described to affect ion channels in cardiac repolarization and concerns have raised within the field of cardiac safety testing. Furthermore, cardiac safety studies mainly focus on targeting I_{Kr}, yet the most common type of long QT syndrome is caused by mutations in the *KCNQ1* gene encoding for the channel conducting I_{Ks}.[33] We explored the effect of pharmacologically targeting cardiac repolarization indirectly via a PI3K inhibitor and directly via I_{Ks} inhibition and activation in the AV block dog model.

Automated recording of STV and thereby monitoring arrhythmia prediction[34] and evaluation of high septal pacing[35] are examples of previously tested device properties in the AV block dog model. Device optimization currently focusses on miniaturization, leadless devices, and chemo-sensor development. Incorporation of multiple physiological variables in a pacing

algorithm is the basis of the CResPace consortium. It aims to restore respiratory sinus arrhythmia, the fluctuation in heart rate upon each respiratory cycle, and adapting the pacing rate to varying oxygen levels and blood pressure to improve cardiac function.

The studies incorporated in this thesis concentrate on two parts for targeting ventricular arrhythmias. 1) Drug testing: with a focus on targeting the second main repolarizing current I_{Ks} and the establishment of underlying proarrhythmic triggers for ventricular arrhythmias, and 2) Device testing: by preparing the AV block dog model in terms of exercise and respiratory behavior for testing a new pacing strategy.

In **chapter 2** we describe the role of antiarrhythmic drugs at the level of cellular autophagy, followed by **chapter 3** which presents the proarrhythmic effects of the PI3K inhibitor omipalisib that targets crucial cellular processes such as survival and autophagy. In **chapter 4** we determined the proarrhythmic effects of I_{Ks} inhibitor JNJ303 with enhanced inotropy as additional trigger. In **chapter 5** we discuss the potential antiarrhythmic effects of activating I_{Ks} by the compound ML277. **Chapter 6** includes a critical analysis on the cardiac responses of the AV block dog to elaborate on why one dog is more sensitive to arrhythmias than the other.

In **chapter 7** we present the exercising AV block dog model and examine the exercise tolerance at different stages of cardiac remodeling. In **chapter 8** we established the variability in heart rate after AV block to explore the value of the AV block model in restoring respiratory sinus arrhythmia. **Chapter 9** gives an overview of the role of the AV block dog model in the CResPace consortium which aims to develop a pacing device that adapts to physiological parameters. A general discussion of all previous chapters is provided in **Chapter 10**.

References

1. Wong CX, Brown A, Lau DH, et al. Epidemiology of sudden cardiac death: global and regional perspectives. *Heart Lung Circ.* 2019;28(1):6-14.
2. Goldberger JJ, Buxton AE, Cain M, et al. Risk stratification for arrhythmic sudden cardiac death: identifying the roadblocks. *Circulation.* 2011;123(21):2423-2430.
3. Zhang D, Tu H, Wadman MC, Li YL. Substrates and potential therapeutics of ventricular arrhythmias in heart failure. *Eur J Pharmacol.* 2018;833:349-356.
4. Hayashi M, Shimizu W, Albert CM. The spectrum of epidemiology underlying sudden cardiac death. *Circ Res.* 2015;116(12):1887-1906.
5. Tisdale JE, Chung MK, Campbell KB, et al. Drug-induced arrhythmias: a scientific statement from the american Heart Association. *Circulation.* 2020;142(15):e214-e233.
6. Kendir C, Van den Akker M, Vos R, Metsemakers J. Cardiovascular disease patients have increased risk for comorbidity: A cross-sectional study in the Netherlands. *Eur J Gen Pract.* 2018;24(1):45-50.
7. May AM, Van Wagoner DR, Mehra R. OSA and cardiac arrhythmogenesis: Mechanistic Insights. *Chest.* 2017;151(1):225-241.
8. Binah O, Rosen MR. Mechanisms of ventricular arrhythmias. *Circulation.* 1992;85(1 Suppl):I25-31.
9. Antzelevitch C. Basic mechanisms of reentrant arrhythmias. *Curr Opin Cardiol.* 2001;16(1):1-7.
10. Zeppenfeld K, Tfelt-Hansen J, de Riva M, et al. 2022 ESC Guidelines for the management of patients with ventricular arrhythmias and the prevention of sudden cardiac death. *Eur Heart J.* 2022;43(40):3997-4126.
11. Larson J, Rich L, Deshmukh A, Judge EC, Liang JJ. Pharmacologic management for ventricular arrhythmias: overview of anti-arrhythmic drugs. *J Clin Med.* 2022;11(11):3233.
12. Heidenreich PA, Bozkurt B, Aguilar D, et al. 2022 AHA/ACC/HFSA Guideline for the management of heart failure: executive summary: a report of the American College of Cardiology/American Heart Association Joint Committee on clinical practice guidelines. *Circulation.* 2022;145(18):e876-e894.
13. Haydock P, Camm AJ. History and evolution of pacing and devices. *Heart.* 2022;108(10):794-799.
14. Santangeli P, Muser D, Maeda S, et al. Comparative effectiveness of antiarrhythmic drugs and catheter ablation for the prevention of recurrent ventricular tachycardia in patients with implantable cardioverter-defibrillators: A systematic review and meta-analysis of randomized controlled trials. *Heart Rhythm.* 2016;13(7):1552-1559.
15. Epstein AE, Dimarco JP, Ellenbogen KA, et al. ACC/AHA/HRS 2008 guidelines for device-based therapy of cardiac rhythm abnormalities: executive summary. *Heart Rhythm.* 2008;5(6):934-955.
16. ICH S7B guidance, The nonclinical evaluation of the potential for delayed ventricular repolarization (QT interval prolongation) by Human Pharmaceuticals. 2005; https://www.ema.europa.eu/en/documents/scientific-guideline/ich-s-7-b-nonclinical-evaluation-potential-delayed-ventricular-repolarization-qt-interval_en.pdf.
17. ICH E14 guidance, The clinical evaluation of QT/QTc interval prolongation and proarrhythmic potential for non-antiarrhythmic drugs. 2005; https://www.ema.europa.eu/en/documents/scientific-guideline/ich-e-14-clinical-evaluation-qt/qts-interval-prolongation-proarrhythmic-potential-non-antiarrhythmic-drugs-step-5_en.pdf.
18. Fermini B, Hancox JC, Abi-Gerges N, et al. A new perspective in the field of cardiac safety testing through the comprehensive in vitro proarrhythmia assay paradigm. *J Biomol Screen.* 2016;21(1):1-11.
19. Wallis R, Benson C, Darpo B, et al. CiPA challenges and opportunities from a non-clinical, clinical and regulatory perspectives. An overview of the safety pharmacology scientific discussion. *J Pharmacol Toxicol Methods.* 2018;93:15-25.
20. Oros A, Beekman JD, Vos MA. The canine model with chronic, complete atrio-ventricular block. *Pharmacol Ther.* 2008;119(2):168-178.
21. Timmermans C, Rodriguez LM, Van Suylen RJ, et al. Catheter-based cryoablation produces permanent bidirectional cavotricuspid isthmus conduction block in dogs. *J Interv Card Electrophysiol.*

2002;7(2):149-155.

22. Verduyn SC, Van Opstal JM, Leunissen JD, Vos MA. Assessment of the pro-arrhythmic potential of anti-arrhythmic drugs: an experimental approach. *J Cardiovasc Pharmacol Ther.* 2001;6(1):89-97.
23. Loen V, Vos MA, Van der Heyden MAG. The canine chronic atrioventricular block model in cardiovascular preclinical drug research. *Br J Pharmacol.* 2022;179(5):859-881.
24. Bourgonje VJA, Van Veen TAB, Vos MA. Ventricular electrical remodeling in compensated cardiac hypertrophy. In: Gussak I, Antzelevitch C, eds. *Electrical Diseases of the Heart*. London: Springer-Verlag; 2013:387-398.
25. De Groot SH, Schoenmakers M, Molenschot MM, Leunissen JD, Wellens HJ, Vos MA. Contractile adaptations preserving cardiac output predispose the hypertrophied canine heart to delayed afterdepolarization-dependent ventricular arrhythmias. *Circulation.* 2000;102(17):2145-2151.
26. Vos MA, de Groot SH, Verduyn SC, et al. Enhanced susceptibility for acquired torsade de pointes arrhythmias in the dog with chronic, complete AV block is related to cardiac hypertrophy and electrical remodeling. *Circulation.* 1998;98(11):1125-1135.
27. Verduyn SC, Ramakers C, Snoep G, Leunissen JD, Wellens HJ, Vos MA. Time course of structural adaptations in chronic AV block dogs: evidence for differential ventricular remodeling. *Am J Physiol Heart Circ Physiol.* 2001;280(6):H2882-2890.
28. Volders PG, Sipido KR, Vos MA, et al. Downregulation of delayed rectifier K(+) currents in dogs with chronic complete atrioventricular block and acquired torsades de pointes. *Circulation.* 1999;100(24):2455-2461.
29. Biliczki P, Virag L, Iost N, Papp JG, Varró A. Interaction of different potassium channels in cardiac repolarization in dog ventricular preparations: role of repolarization reserve. *Br J Pharmacol.* 2002;137(3):361-368.
30. Vandersickel N, Bossu A, De Neve J, et al. Short-lasting episodes of torsade de pointes in the chronic atrioventricular block dog model have a focal mechanism, while longer-lasting episodes are maintained by re-entry. *JACC Clin Electrophysiol.* 2017;3(13):1565-1576.
31. Stams TRG, Winckels SKG, Oros A, et al. Novel parameters to improve quantification of repolarization reserve and arrhythmogenesis using a dofetilide challenge. *Heart Rhythm.* 2013;10(11):1745-1746.
32. Thomsen MB, Volders PG, Beekman JD, Matz J, Vos MA. Beat-to-Beat variability of repolarization determines proarrhythmic outcome in dogs susceptible to drug-induced torsades de pointes. *J Am Coll Cardiol.* 2006;48(6):1268-1276.
33. Krahn AD, Laksman Z, Sy RW, et al. Congenital long QT syndrome. *JACC Clin Electrophysiol.* 2022;8(5):687-706.
34. Smoczyńska A, Loen V, Aranda A, Beekman HDM, Meine M, Vos MA. High-rate pacing guided by short-term variability of repolarization prevents imminent ventricular arrhythmias automatically by an implantable cardioverter-defibrillator in the chronic atrioventricular block dog model. *Heart Rhythm.* 2020;17(12):2078-2085.
35. Winckels SK, Thomsen MB, Oosterhoff P, et al. High-septal pacing reduces ventricular electrical remodeling and proarrhythmia in chronic atrioventricular block dogs. *J Am Coll Cardiol.* 2007;50(9):906-913.

Part I

Drug testing

2

Cardiac arrhythmias and antiarrhythmic drugs: an autophagic perspective

Joanne J.A. van Bavel[1], Marc A. Vos[1], Marcel A.G. van der Heyden[1]

[1] Department of Medical Physiology, Division of Heart and Lungs, University Medical Center Utrecht, Utrecht, the Netherlands

***Frontiers in Physiology*, 2018, 9:127**

Abstract

Degradation of cellular material by lysosomes is known as autophagy, and its main function is to maintain cellular homeostasis for growth, proliferation, and survival of the cell. In recent years, research has focused on the characterization of autophagy pathways. Targeting of autophagy mediators has been described predominantly in cancer treatment, but also in neurological and cardiovascular diseases. Although the number of studies is still limited, there are indications that activity of autophagy pathways increases under arrhythmic conditions. Moreover, an increasing number of antiarrhythmic and non-cardiac drugs are found to affect autophagy pathways. We, therefore, suggest that future work should recognize the largely unaddressed effects of antiarrhythmic agents and other classes of drugs on autophagy pathway activation and inhibition.

Keywords

Autophagy, AMPK, antiarrhythmic drugs, arrhythmias, mTOR, heart

Introduction

Degradation of cellular material occurs mainly via two pathways: the ubiquitin-proteasome system (UPS) and the autophagy-lysosome pathway. The UPS targets mainly short-lived or misfolded proteins, whereas autophagy includes the degradation, digestion, and recycling of autophagy substrates, by lysosomes.[1] In healthy conditions, autophagy acts principally as a protective and control mechanism by maintaining cellular growth, proliferation, survival, and clearance of dying cells.[2] Over the last decade, an increasing amount of research has focused on autophagy and attention has been paid to the association between autophagy and cardiac diseases, including ischemia and hypertrophy. Thus far, a potential link between arrhythmic conditions and changes in autophagy activity has gained little attention, although the evidence for such interaction currently expands. There remains a need for increased research focus on the association between pro- and antiarrhythmic drugs and autophagy pathways in the heart. We review the link between cardiac autophagy and arrhythmic conditions, and the limitations regarding the effect of antiarrhythmic drugs on autophagy. Only a few years from now we can determine whether the current niche of arrhythmias and autophagy research will emerge in a mature field of investigation.

Autophagy types and targets

Autophagy substrates (referred to as cellular material) include proteins, proteasomes, lysosomes, endoplasmic reticulum (ER), mitochondria, lipid droplets, polyribosomes, peroxisomes, bacteria, viruses, and ruptured phagosomes. These substrates are targeted for degradation as long as they are freely accessible in the cytosol.[3] Three types of autophagic targeting are recognized (**Figure 1A**). Microautophagy is the least studied type of autophagy, which involves the direct uptake of soluble cellular substrates from the cytoplasm by invaginations in lysosomal membranes.[1] Macroautophagy, the best characterized variant of autophagy, is used synonymous with the term autophagy. It refers to both selective and non-selective capture of cellular components in double-membraned vesicles in the cytosol, and subsequent transport of the content to lysosomes.[4] Chaperone-mediated autophagy (CMA) is a selective autophagic mechanism, which is mediated by the recognition of a peptide sequence in substrate proteins by chaperones e.g., hsc70.[5] The substrate binds to lysosome-associated membrane protein 2A (LAMP-2A) and translocates into the lysosome for degradation. The main and most important function of the strictly organized process of

autophagy is to maintain cellular homeostasis.[6] Autophagy can act selectively, which includes the degradation of specific cargo selected by receptor proteins, and non-selectively by maintenance of intracellular nutrient supply with starvation as its main trigger.[7] Besides small cellular components, selective autophagy can target specific cell components e.g., mitochondria (mitophagy), ER (reticulophagy), ribosomes (ribophagy), lipids (lipophagy), and ion channels (channelophagy).[8,9] Autophagic processes are either continuously active (constitutive) or triggered (inducible). The primary stimulus of autophagy in yeast is nutrient withdrawal, whereas in mammals several stimuli can trigger autophagy, of which the most important are nutritional changes (e.g., starvation), organelle damage, hormonal regulation, infectious agents, hypoxia (such as in cardiac ischemia), and intracellular accumulation of toxic products (e.g., some antiarrhythmic drugs).[6,10,11] The first reports on autophagic processes appeared in 1955. Christian de Duve coined the term "autophagy" in 1963, which was based on the discovery of self-eating lysosomes in rat hepatic cells.[12] The following decades, research focused on studying molecular autophagy mechanisms in yeast, which differ from autophagy processes in mammals.[10,13] Furthermore, genetic screens revealed the existence of AuTophaGy-related (ATG) genes, of which the role in autophagy is associated to various processes in health and disease.[4,14] Recently, the field of autophagy was honored by a Nobel Prize awarded to Yoshinori Ohsumi in 2016.[15]

Autophagy-related proteins and their use as therapeutical targets

ATG proteins are mainly described in macroautophagy because of its best-known machinery and are illustrated in **Figure 1B**. Two important regulators of autophagy initiation are AMP-activated protein kinase (AMPK) and mechanistic target of rapamycin complex 1 (mTORC1). Active AMPK stimulates autophagy initiation, whereas mTORC1 inhibits autophagy.[16] In autophagy stimulation, the ULK1/2-Atg13-FIP200 complex becomes active, ATG proteins are recruited and a phagophore is formed.[17] The class III phosphatidylinositol 3-kinase (PI3KCIII) complex (beclin-1, VPS34, VPS15, and Atg14L) mediates nucleation of the phagophore.[18] Different ubiquitin-like conjugation systems (Atg12-Atg5 and Atg8/LC3) are central in the next autophagic step; elongation of the phagophore, and proteins and lipids involved in autophagosome formation and maturation are recruited by the PI3KCIII complex.[4,17] Beclin-1 is part of the PI3KCIII complex and plays a key role in autophagosome formation and maturation.[17] Mature autophagosomes move along microtubules and fuse with lysosomes in

a process that involves gamma-aminobutyric acid receptor-associated proteins (GABARAP) and soluble NSF attachment protein receptor (SNARE) family proteins.[19,20] Autophagy's final step is degradation of the autophagolysosome cargo by different types of proteases.[21] Detailed overviews of the macroautophagy machinery are given by Feng et al. and Xie et al.[4,17]

Inability to maintain cellular homeostasis due to defective autophagy associates with a variety of systemic diseases, such as cancer, neurodegeneration, liver disease and (cardio-) myopathies.[14] Distinct ATG proteins are considered as interesting targets for autophagy modulation (**Figure 1B, Table 1**), in which the field of cancer therapy progressed furthest.[22] Rapamycin and its analogs (rapalogs) inhibit mTORC1 resulting in autophagy activation and are used in certain cancer treatments.[23] Other recognized mTORC1 inhibitors are perhexiline (antianginal agent), niclosamide (used in treating worm infections), and rottlerin (natural product, known to open potassium channels).[24] Activation of autophagy can also result from AMPK activators, such as commonly used antidiabetic agents metformin and phenformin, and AMP analog 5-aminoimidazole-4-carboxamide-1-β-D-ribofuranoside (AICAR).[25-27] Common inhibitors of AMPK include adenine 9-beta-D-arabinofuranoside (Ara-A, or vidarabine) and compound C.[25,28] Antitumor drug wogonin can affect the next step in the autophagy pathway (phagophore nucleation) by targeting the beclin-1/PI3K complex, and thereby inducing autophagy in human pancreatic cancer cells.[29] The antimalarial and anti-inflammatory agent chloroquine targets the last step in the autophagy pathway by inhibiting fusion of autophagosomes and lysosomes.[30] Although certain compounds seem to target autophagy pathways effectively, former mentioned compounds can act directly with a positive effect (e.g., tumor regression), as well as indirectly causing side effects.

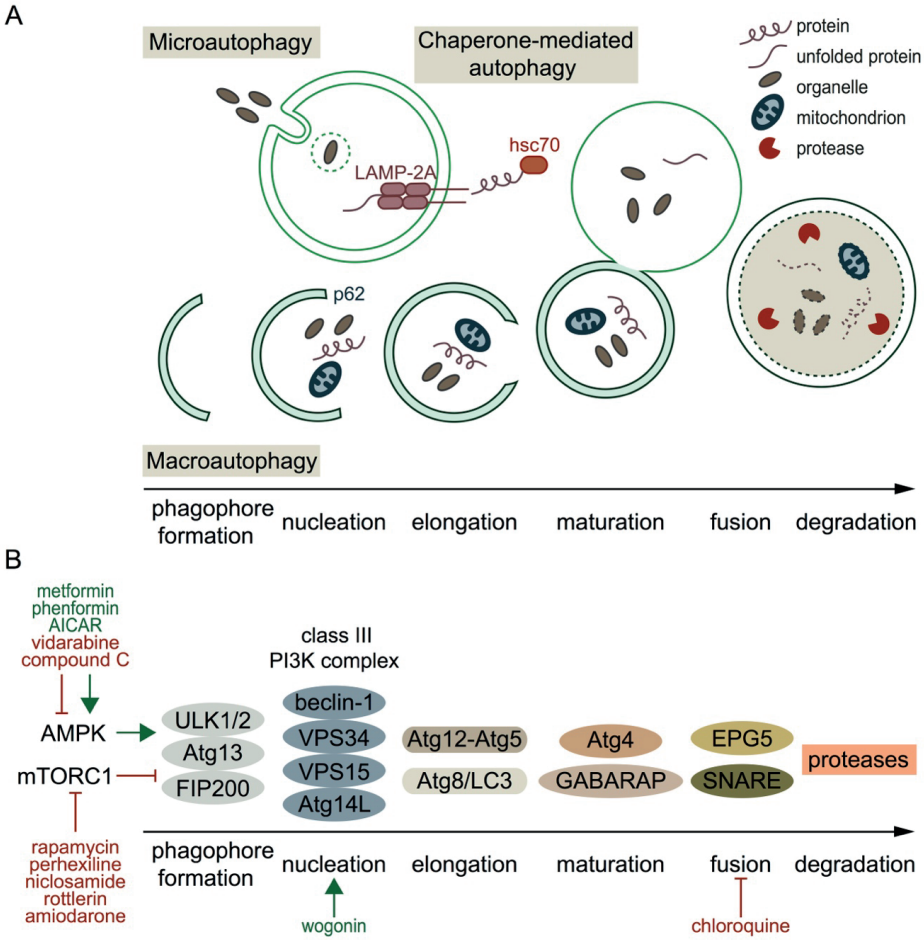

Figure 1. Autophagy types, processes, molecular players, and pharmacological regulators. **A**) Schematic presentation of the three autophagy types. Microautophagy refers to the direct uptake of soluble cellular substrates from the cytoplasm by invaginations in lysosomal membranes. Chaperone-mediated autophagy includes targeting of a specific motif in a substrate protein, translocation of the substrate to the lysosome by heat shock-cognate protein of 70 kDa (hsc70), and translocation into the lysosome by lysosome-associated membrane protein 2A (LAMP-2A) on the lysosomal membrane. Macroautophagy starts with formation of a double-membraned phagophore, at which proteins and lipids are recruited by, among others, p62 (nucleation). Then, the phagophore elongates, matures, and the autophagosome fuses with a lysosome. **B**) Overview of the mediators involved in macroautophagy and some of their stimulators/inhibitors (green and red respectively). Autophagy initiation occurs by activated AMPK, which phosphorylates the ULK1/2-Atg13-FIP200 complex. mTORC1 inhibits this complex. Once the autophagy pathway is activated, a phagophore is formed and the class III PI3K complex is responsible for nucleation. Two different conjugation systems are important for elongation of the phagophore (Atg12-Atg5 and Atg8/LC3). GABARAP and Atg4 are involved in autophagosome maturation, and fusion of the autophagosome with a lysosome is mediated by EPG5 and SNARE proteins. Finally, the cargo is degraded by proteases.

Autophagy in the heart: some lessons from gene defects

Autophagy is important for maintenance of the highly organized cardiac structure, function, and homeostasis. Nutrient insufficient conditions lead to the inactivation of mTORC1: rapamycin interacts with and inhibits mTORC1 activating unc-51-like kinase 1 and 2 (ULK1 and ULK2), leading to autophagy induction.[31] Activation of sensitive nutrient sensor AMPK occurs when ATP/AMP levels decrease due to exercise, ischemia, or lack of glucose, resulting in autophagy initiation.[32] Other important autophagy mediators in the cardiovascular system include inositol 1,4,5-triphosphate (IP_3), transcription factor 53 (TP53), cyclic AMP-dependent protein kinase A (PKA), histone acetyltransferases (HATs) and histone deacetylases (HDACs), glycogen synthase kinase 3β (GSK3β), nicotinamide adenine dinucleotide (NAD^+), and microRNAs, which can initiate and inhibit autophagy, as reviewed by Lavandero et al.[31] Impaired autophagy pathway signaling, due to ATG protein deficiency, may cause cardiac pathologies. Mice with Atg5 and Atg7 deficiency, ATG proteins involved in phagophore elongation, displayed dilated cardiomyopathy and contractile dysfunction, and accumulation of defective proteins and organelles, respectively.[33,34] Ectopic P-granules autophagy protein 5 (EPG5), important in translocation of autophagosomes to lysosomes, deficient individuals suffer from the Vici syndrome; a multisystem disorder with autophagy malfunction.[35] Cardiac symptoms, predominantly hypertrophy and left ventricular dilatation, are present in 90% of the Vici syndrome patients.[36] Deficiency of LAMP-2, required for the fusion of autophagosomes with endosomes and lysosomes,[37] leads to Danon disease causing intellectual disability, skeletal myopathy and severe cardiomyopathy.[38] LAMP-2 deficient mice have a high mortality rate, show autophagosome accumulation in the pancreas, liver, kidney, skeletal muscle and heart, and possess cardiomyocytes filled with large vacuoles. The latter might be the cause of a reduced heart muscle contractility observed in these mice.[39] Apart from the reductive, but instructive, ATG deficient models, most studies however focus on ischemia/reperfusion (I/R) and hypertrophy models to examine the role of cardiac autophagy.[31]

Autophagy in cardiac ischemia/reperfusion and hypertrophy models

Both protective (clearance and removal of misfolded proteins and roles in energy homeostasis) and detrimental (massive digestion of cellular components and cross-talk to other forms of cell death) functions of autophagy have been presented in ischemic and

hypertrophy models.[40] In the ischemic heart, upregulation of autophagy associates with a reduction in infarct size and apoptosis, and vice versa, suggested to work cardioprotective by maintaining energy levels.[41] In this situation, the drop in ATP levels during ischemia activates AMPK leading to an upregulation of autophagy activation.[42] In mice hearts however that underwent I/R, when oxygen and nutrient supply is impaired and subsequently restored, AMPK is inactivated, mTOR is upregulated, and beclin-1 is highly upregulated, suggesting an inhibition of autophagy.[43] Remarkably, these mice showed an increase in autophagosome levels and a decrease in apoptosis.

Cardiac hypertrophy is associated with an upregulation of autophagy. Weng et al. presented an increase in autophagic gene (Atg5 and Atg16) expression, and increased beclin-1 and microtubule-associated protein 1A/1B chain 3 phosphatidylethanolamine conjugate (LC3-II) levels in transverse aortic constriction (TAC), to induce pressure overload, operated mice.[44] Furthermore, AMPK induces autophagy in TAC operated hearts by regulating the mTORC1 pathway, leading to inhibition of cardiac hypertrophy and improved cardiac function.[45] Cardiac-specific knockout of mTOR showed an impaired hypertrophic response and enhanced heart failure progression after TAC mediated pressure-overload in mice, suggesting detrimental effects when mTOR is lacking.[46] However, pharmacologic inhibition of mTOR indicates a cardiac protective effect: rapamycin treatment in TAC operated mice showed an inhibitory effect on cardiac hypertrophy development.[47] Moreover, treatment of rapamycin in cardiac transplant recipients resulted in reduced left ventricular mass and improved diastolic function.[48] Altogether, current evidence states that regulation of autophagy levels is crucial in protecting cardiomyocytes under ischemic and hypertrophic conditions.

Increased autophagy activation in arrhythmic conditions

Connexin43 (Cx43) proteins form gap junctions, which are responsible for the propagation of cardiac action potentials between cardiomyocytes. In the recent years, literature has been growing regarding the role of autophagy in degradation of Cx43.[49] A lowered expression of Cx43 was also linked to arrhythmias: among others, Shu et al., 2017 showed a lowered Cx43 protein expression in a canine model with atrial fibrillation (AF) induced by rapid atrial pacing (RAP).[50] It remains to be identified if a lowered Cx43 expression in arrhythmic conditions was mediated by autophagic degradation. As an indication of autophagy activation, levels of

autophagy mediators have been examined in several arrhythmic conditions. A RAP canine model, vulnerable to AF, showed an increase in LC3B-II (LC3 family member) and phosphorylated AMPK (p-AMPK) protein levels.[51] Moreover, in the same study, it was presented that these autophagy mediators were increased in human patients suffering from AF. Furthermore, beclin-1 and LC3B-II expression levels were increased in I/R-injured fibrillated mouse hearts.[52] The increased levels of these autophagy mediators suggest increased autophagy activation in response to arrhythmias. Although the number of autophagic vacuoles was elevated in patients who underwent coronary artery bypass grafting with postoperative atrial fibrillation, decreased levels of LC3B-II levels were found in these patients.[53] A decrease in vesicle degradation and an impaired autophagic flow can clarify the elevated vesicle levels and the decreased LC3B-II levels, respectively.[53] These exciting findings, albeit just a few, appear to outpoint that autophagy pathways are becoming activated in arrhythmic conditions, and are therefore of interest as potential therapeutic targets. Nonetheless, the exact mechanistic relationship between autophagy and cardiac arrhythmias clearly remains to be elucidated.

Antiarrhythmic drugs affect autophagy pathways

Along with limited research into autophagy occurrence and regulation in arrhythmic conditions, only a few studies have thus far focused on the effect of antiarrhythmic drugs on autophagy activation and the results are interesting. **Table 1** demonstrates the effect on autophagic regulation, the effective concentrations affecting autophagy, the clinical effective concentrations, and a possible association with arrhythmias of the compounds discussed in this perspective. The effective concentrations of the compounds on autophagy regulation, although tested *in vitro* with limited concentration ranges, can be compared to drug plasma levels in patients. Overlapping concentrations indicate that a number of clinically used compounds are likely to influence autophagy regulation. Antiarrhythmic drugs are classified by the effect on the targets whose actions form the cardiac action potential. Class I drugs block Na^+ channels, class II drugs are adrenergic receptor antagonists, class III drugs are K^+ channel blockers, and the AV-node conduction is slowed down by class IV drugs usually by blockage of L-type calcium channels (LTCCs). The antiarrhythmic effects of Na^+ channel blocker ranolazine, initially developed as antianginal agent, are convincing.[54] Huang et al. (2010) showed induced autophagy activation after ranolazine treatment in HL-1 cells and

isolated rat cardiomyocytes.[55] Commonly used beta-blocker propranolol is reported as autophagy inhibitor: increased LC3-II levels, autophagosome formation, and p62 (which degrades during autophagy stimulation) levels were measured in HepG2 cells, suggesting an inhibition of hepatic autophagy by propranolol at a later stage due to reduced degradation.[56] Class III antiarrhythmic drug amiodarone inhibits mTORC1 leading to stimulation of the autophagy pathway, which was explored *in vitro.*[24] In another *in vitro* study, we indicated lysosomal impairment by amiodarone and its synthetic analogue dronedarone, which resulted in increased inward rectifier potassium channel $K_{ir}2.1$ expression and intracellular accumulation.[57] The well-known drawback of amiodarone is its high incidence of side effects, including thyroid toxicity, pulmonary toxicity, hepatic toxicity, neurological toxicity, which seem to be related to the lifetime cumulative dose of the drug.[58] However, pharmacological activation of autophagy by amiodarone has been shown to improve liver regeneration after partial hepatectomy in mice.[59] LTCC blocker nifedipine, used as arterial vasodilator, increases autophagic flow, as shown by increased presence of autophagosomes and LC3-II levels, and lower p62 levels in isolated rat cardiomyocytes.[60] LTCC blocker verapamil, used in treating angina and arrhythmias, increases autophagic flux, which was shown by elevated LC3-II levels in PC12 cells and in a series of human cell lines, in which the latter also included increased development of autophagic vacuoles.[61,62] These studies, although limited in number, clearly represent the existing link between antiarrhythmic drugs and autophagy, and the direct outcomes can be both activation and inhibition of autophagy.

Non-cardiac drugs can act proarrhythmic and affect autophagy

As well as antiarrhythmic compounds, non-cardiac drugs can have the tendency to act proarrhythmic e.g., by prolonging the QT interval with an increased risk for Torsade de Pointes (TdP) arrhythmias,[63] and they can affect the autophagic pathway. Many compounds with increased proarrhythmic risk are clinically used, or only reached phase I of clinical trials, to treat various disease areas. The former discussed drug chloroquine, which increases the lysosomal pH and thereby prevents the degradation of certain autophagy substrates, is reported as proarrhythmic. Accumulated levels of $K_{ir}2.1$ were found intracellularly and I_{K1} densities increased due to chloroquine treatment.[64] From an autophagic perspective these results can be linked to the chloroquine-induced QT prolongation, conduction disturbances and cardiomyopathy at high doses, as reviewed by White.[65] The proarrhythmic effect of

antiprotozoal drug pentamidine has been firstly reported in 1987 by the description of two case reports with occurrence of TdP arrhythmias after administration of pentamidine, which results have been confirmed later on.[66,67] We suggested a link between pentamidine and autophagy, in which pentamidine may induce lysosomal degradation of potassium channel $K_{ir}2.1$.[68] Pentamidine analogues have been, and still are, tested to finally develop efficient and specific $K_{ir}2.x$ ion-channel-carried inward rectifier current (I_{K1}) inhibitors for treating atrial fibrillation and short QT syndrome type 3.[69,70] Antipsychotic drug paliperidone, which inhibits human ether-a-go-go-related gene (hERG) K^+ channel, has also been characterized to increase the QT interval and increase the risk for TdP arrhythmia.[71,72] It may be assumed that it also affects autophagy, since mTOR was identified as a downstream effector of paliperidone-induced extrapyramidal symptoms (side effect of antipsychotics), as observed in a network analysis of gene expression.[73] The role of autophagy in cancer has been characterized as paradoxical because of its pro-survival and pro-death outcomes.[74] A frequently altered pathway in cancer includes PI3K and its inhibitors seem to treat solid tumors and hematologic malignancies.[75] Nilotinib, dasatinib, and sunitinib are examples of PI3K inhibitors, which are approved by the FDA to treat certain cancer types and are shown to induce autophagy pathways in cancer cell models.[76-78] However, a recent study by Cohen et al., presented a prolongation of the action potential by former named PI3K inhibitors, and thereby clearly suggests that drug safety testing should be improved.[79] The compounds discussed in this paragraph, either approved by the FDA or currently in clinical trials, seem to affect the autophagy pathway and cardiac action potential, while their original purpose is not to affect those. Causality, however, needs to be demonstrated.

Table 1. The effect of the discussed compounds on autophagy activation, their effective concentration on autophagy regulation, their therapeutic plasma concentrations, and their potential link to arrhythmic conditions.

Compound	Autophagic activation	Concentrations		Associated with arrhythmias[a]	References
AICAR	↑	AMPK activation Plasma levels	500 μM not reported	+ hERG inhibition	25,80
Amiodarone	↑	mTORC1 inhibition Plasma levels	>10 μM 0.8-3.9 μM	+ QT prolongation	24,81,82
Chloroquine	↓	Autolysosome fusion ↓ Mean peak plasma level	120 μM 0.4 μM	+ at high dose	30,65,83
Compound C	↓	AMPK inhibition Plasma levels	20 μM not reported	↓ (potentially) by hERG activation	25,80
Dronedarone	↑	Autophagy activation Steady-state plasma levels	2 μM 0.15-0.3 μM	+ QT prolongation	84-86
Metformin	↑	AMPK activation Steady-state plasma levels	>2 μM 10-40 μM	↓ AF in DM patients	25,87
Niclosamide	↑	mTORC1 inhibition Serum concentration range	1 μM 0.76-18.32 μM	not reported	24,88
Nifedipine	↑	Autophagy activation Mean peak plasma level	10 μM 0.35 μM	↓ LTCC blocker	60,89,90
Paliperidone	↑	Downstream effector mTOR Mean plasma level	not reported 84.4 nM	+ hERG inhibition	71,73,91
Pentamidine	↑	$K_{ir}2.1$ degradation Plasma levels	5-10 μM 0.5-2.4 μM	+ risk for TdP	67,68,92
Perhexiline	↑	mTORC1 inhibition Serum concentration range	1-10 μM 0.8-3.8 μM	+ hERG inhibition	24,93,94
Phenformin	↑	AMPK activation Plasma level	>0.3 mM 0.27 μM	+ hERG inhibition	80,95,96
PI3K inhibitors[b]	↑	AMPK activation[c] Mean peak plasma level[c]	5 μM 3.6 μM	+ APD prolongation	76,79,97
Propranolol	↓	Late block in autophagy Plasma levels	10 μM 20-428 μM	↓ shorter QT in LQT1	56,98,99
Ranolazine	↑	Autophagy activation Mean steady-state level	1 μM 6 μM	↓ AF episodes	55,100,101
Rapamycin	↑	mTORC1 inhibition Target concentration range	0.5-100 nM 4-22 nM	+ >28 nM	102-104
Rottlerin	↑	mTORC1 inhibition Plasma levels	1-3 μM not reported	+ APD shortening	24,105
Verapamil	↑	Autophagy activation Mean peak plasma level	1 μM 0.8 μM	+ LTCC and hERG inhibition	61,90,106
Vidarabine	↓	AMPK inhibition Mean peak plasma level	>0.5 mM 3.7 μM	-	28,107,108
Wogonin	↑	Beclin-1/PI3K activation Plasma levels	40 μM not reported	↓ in ischemic model	29,109

Abbreviations: AF, atrial fibrillation; APD, action potential duration; DM, diabetes mellitus; LQT1, long QT syndrome 1; LTCC, L-type calcium channel; TdP, Torsade de Pointes.

Compound association with arrhythmias (+), no association (-), preventive effect (↓) or 'not reported'.

[a] Arrhythmic associations tested in human, animal, or *in vitro* models.

[b] PI3K inhibitor examples are, as mentioned in the text, nilotinib, dasatinib and sunitinib.

[c] Nilotinib concentration.

Conclusion and future perspectives

Autophagy regulation is crucial in basal and diseased conditions, and has been shown to act both protective and detrimental in cardiac disease models. Up to now, evidence has brought forward that autophagy activation changes in arrhythmic conditions of the heart. In addition, some antiarrhythmic drugs have been shown to affect autophagy pathways and this may associate with adverse effects. The direct effects and deciphering of the complex underlying

mechanisms of antiarrhythmic drugs on autophagy mediation in the heart remain to be determined. Ion channels are crucial in maintaining a regular cardiac rhythm and some are also involved in autophagy regulation, as reviewed by Kondratskyi et al. (2017),[9] indicating a possible direction of future research. Another research aim should be to understand the dependent role of remodeling on autophagy in cardiac arrhythmic conditions. Gene defect models and arrhythmia-induced models are promising in understanding the mechanistic relationship between autophagy and arrhythmias. We also suggest that future work should include the examination of autophagy effects in exploring the effectiveness of antiarrhythmic drugs. This may improve drug development to provide safer antiarrhythmic drugs by removal of autophagy pathway disturbances. Antiarrhythmic drugs may then not further worsen autophagy dysregulation in arrhythmic conditions. Beyond doubt, from an autophagic perspective; focus should increase on its regulation under arrhythmic conditions, and on the effects of its unknown targeting by antiarrhythmic compounds and other drugs.

References

1. Li WW, Li J, Bao JK. Microautophagy: lesser-known self-eating. *Cell Mol Life Sci.* 2012;69(7):1125-1136.
2. Filippi-Chiela EC, Viegas MS, Thome MP, Buffon A, Wink MR, Lenz G. Modulation of Autophagy by Calcium Signalosome in Human Disease. *Mol Pharmacol.* 2016;90(3):371-384.
3. Galluzzi L, Baehrecke EH, Ballabio A, et al. Molecular definitions of autophagy and related processes. *EMBO J.* 2017;36(13):1811-1836.
4. Feng Y, He D, Yao Z, Klionsky DJ. The machinery of macroautophagy. *Cell Res.* 2014;24(1):24-41.
5. Cuervo AM, Wong E. Chaperone-mediated autophagy: roles in disease and aging. *Cell Res.* 2014;24(1):92-104.
6. Singh R, Cuervo AM. Autophagy in the cellular energetic balance. *Cell Metab.* 2011;13(5):495-504.
7. Svenning S, Johansen T. Selective autophagy. *Essays Biochem.* 2013;55:79-92.
8. Klionsky DJ, Cuervo AM, Dunn WA, Jr., Levine B, Van der Klei I, Seglen PO. How shall I eat thee? *Autophagy.* 2007;3(5):413-416.
9. Kondratskyi A, Kondratska K, Skryma R, Klionsky DJ, Prevarskaya N. Ion channels in the regulation of autophagy. *Autophagy.* 2018;14(1):3-21.
10. Reggiori F, Klionsky DJ. Autophagic processes in yeast: mechanism, machinery and regulation. *Genetics.* 2013;194(2):341-361.
11. Kudenchuk PJ, Pierson DJ, Greene HL, Graham EL, Sears GK, Trobaugh GB. Prospective evaluation of amiodarone pulmonary toxicity. *Chest.* 1984;86(4):541-548.
12. De Duve C, Pressman BC, Gianetto R, Wattiaux R, Appelmans F. Tissue fractionation studies. 6. Intracellular distribution patterns of enzymes in rat-liver tissue. *Biochem J.* 1955;60(4):604-617.
13. Matsuura A, Tsukada M, Wada Y, Ohsumi Y. Apg1p, a novel protein kinase required for the autophagic process in Saccharomyces cerevisiae. *Gene.* 1997;192(2):245-250.
14. Schneider JL, Cuervo AM. Autophagy and human disease: emerging themes. *Curr Opin Genet Dev.* 2014;26:16-23.
15. Levine B, Klionsky DJ. Autophagy wins the 2016 Nobel Prize in Physiology or Medicine: Breakthroughs in baker's yeast fuel advances in biomedical research. *Proc Natl Acad Sci U S A.* 2017;114(2):201-205.

16. Kim J, Kundu M, Viollet B, Guan KL. AMPK and mTOR regulate autophagy through direct phosphorylation of Ulk1. *Nat Cell Biol.* 2011;13(2):132-141.
17. Xie Y, Kang R, Sun X, et al. Posttranslational modification of autophagy-related proteins in macroautophagy. *Autophagy.* 2015;11(1):28-45.
18. Baskaran S, Carlson LA, Stjepanovic G, et al. Architecture and dynamics of the autophagic phosphatidylinositol 3-kinase complex. *Elife.* 2014;3:e05115.
19. Itakura E, Kishi-Itakura C, Mizushima N. The hairpin-type tail-anchored SNARE syntaxin 17 targets to autophagosomes for fusion with endosomes/lysosomes. *Cell.* 2012;151(6):1256-1269.
20. Nair U, Jotwani A, Geng J, et al. SNARE proteins are required for macroautophagy. *Cell.* 2011;146(2):290-302.
21. Kaminskyy V, Zhivotovsky B. Proteases in autophagy. *Biochim Biophys Acta.* 2012;1824(1):44-50.
22. Levy JMM, Towers CG, Thorburn A. Targeting autophagy in cancer. *Nat Rev Cancer.* 2017;17(9):528-542.
23. Li J, Kim SG, Blenis J. Rapamycin: one drug, many effects. *Cell Metab.* 2014;19(3):373-379.
24. Balgi AD, Fonseca BD, Donohue E, et al. Screen for chemical modulators of autophagy reveals novel therapeutic inhibitors of mTORC1 signaling. *PLoS One.* 2009;4(9):e7124.
25. Zhou G, Myers R, Li Y, et al. Role of AMP-activated protein kinase in mechanism of metformin action. *J Clin Invest.* 2001;108(8):1167-1174.
26. Yang L, Sha H, Davisson RL, Qi L. Phenformin activates the unfolded protein response in an AMP-activated protein kinase (AMPK)-dependent manner. *J Biol Chem.* 2013;288(19):13631-13638.
27. Ducommun S, Ford RJ, Bultot L, et al. Enhanced activation of cellular AMPK by dual-small molecule treatment: AICAR and A769662. *Am J Physiol Endocrinol Metab.* 2014;306(6):E688-696.
28. Pelletier A, Joly E, Prentki M, Coderre L. Adenosine 5'-monophosphate-activated protein kinase and p38 mitogen-activated protein kinase participate in the stimulation of glucose uptake by dinitrophenol in adult cardiomyocytes. *Endocrinology.* 2005;146(5):2285-2294.
29. Li SJ, Sun SJ, Gao J, Sun FB. Wogonin induces Beclin-1/PI3K and reactive oxygen species-mediated autophagy in human pancreatic cancer cells. *Oncol Lett.* 2016;12(6):5059-5067.
30. Yoon YH, Cho KS, Hwang JJ, Lee SJ, Choi JA, Koh JY. Induction of lysosomal dilatation, arrested autophagy, and cell death by chloroquine in cultured ARPE-19 cells. *Invest Ophthalmol Vis Sci.* 2010;51(11):6030-6037.
31. Lavandero S, Troncoso R, Rothermel BA, Martinet W, Sadoshima J, Hill JA. Cardiovascular autophagy: concepts, controversies, and perspectives. *Autophagy.* 2013;9(10):1455-1466.
32. Hardie DG, Ross FA, Hawley SA. AMPK: a nutrient and energy sensor that maintains energy homeostasis. *Nat Rev Mol Cell Biol.* 2012;13(4):251-262.
33. Nakai A, Yamaguchi O, Takeda T, et al. The role of autophagy in cardiomyocytes in the basal state and in response to hemodynamic stress. *Nat Med.* 2007;13(5):619-624.
34. Komatsu M, Waguri S, Ueno T, et al. Impairment of starvation-induced and constitutive autophagy in Atg7-deficient mice. *J Cell Biol.* 2005;169(3):425-434.
35. Cullup T, Kho AL, Dionisi-Vici C, et al. Recessive mutations in EPG5 cause Vici syndrome, a multisystem disorder with defective autophagy. *Nat Genet.* 2013;45(1):83-87.
36. Byrne S, Dionisi-Vici C, Smith L, Gautel M, Jungbluth H. Vici syndrome: a review. *Orphanet J Rare Dis.* 2016;11:21.
37. Endo Y, Furuta A, Nishino I. Danon disease: a phenotypic expression of LAMP-2 deficiency. *Acta Neuropathol.* 2015;129(3):391-398.
38. D'Souza R S, Levandowski C, Slavov D, et al. Danon disease: clinical features, evaluation, and management. *Circ Heart Fail.* 2014;7(5):843-849.
39. Tanaka Y, Guhde G, Suter A, et al. Accumulation of autophagic vacuoles and cardiomyopathy in LAMP-2-deficient mice. *Nature.* 2000;406(6798):902-906.
40. Sciarretta S, Hariharan N, Monden Y, Zablocki D, Sadoshima J. Is autophagy in response to ischemia and

reperfusion protective or detrimental for the heart? *Pediatr Cardiol.* 2011;32(3):275-281.
41. Sciarretta S, Yee D, Shenoy V, Nagarajan N, Sadoshima J. The importance of autophagy in cardioprotection. *High Blood Press Cardiovasc Prev.* 2014;21(1):21-28.
42. Takagi H, Matsui Y, Hirotani S, Sakoda H, Asano T, Sadoshima J. AMPK mediates autophagy during myocardial ischemia in vivo. *Autophagy.* 2007;3(4):405-407.
43. Matsui Y, Takagi H, Qu X, et al. Distinct roles of autophagy in the heart during ischemia and reperfusion: roles of AMP-activated protein kinase and Beclin 1 in mediating autophagy. *Circ Res.* 2007;100(6):914-922.
44. Weng LQ, Zhang WB, Ye Y, et al. Aliskiren ameliorates pressure overload-induced heart hypertrophy and fibrosis in mice. *Acta Pharmacol Sin.* 2014;35(8):1005-1014.
45. Li Y, Chen C, Yao F, et al. AMPK inhibits cardiac hypertrophy by promoting autophagy via mTORC1. *Arch Biochem Biophys.* 2014;558:79-86.
46. Zhang D, Contu R, Latronico MV, et al. MTORC1 regulates cardiac function and myocyte survival through 4E-BP1 inhibition in mice. *J Clin Invest.* 2010;120(8):2805-2816.
47. McMullen JR, Sherwood MC, Tarnavski O, et al. Inhibition of mTOR signaling with rapamycin regresses established cardiac hypertrophy induced by pressure overload. *Circulation.* 2004;109(24):3050-3055.
48. Raichlin E, Chandrasekaran K, Kremers WK, et al. Sirolimus as primary immunosuppressant reduces left ventricular mass and improves diastolic function of the cardiac allograft. *Transplantation.* 2008;86(10):1395-1400.
49. Falk MM, Kells RM, Berthoud VM. Degradation of connexins and gap junctions. *FEBS Lett.* 2014;588(8):1221-1229.
50. Shu C, Huang W, Zeng Z, et al. Connexin 43 is involved in the sympathetic atrial fibrillation in canine and canine atrial myocytes. *Anatol J Cardiol.* 2017;18(1):3-9.
51. Yuan Y, Zhao J, Yan S, et al. Autophagy: a potential novel mechanistic contributor to atrial fibrillation. *Int J Cardiol.* 2014;172(2):492-494.
52. Meyer G, Czompa A, Reboul C, et al. The cellular autophagy markers Beclin-1 and LC3B-II are increased during reperfusion in fibrillated mouse hearts. *Curr Pharm Des.* 2013;19(39):6912-6918.
53. Garcia L, Verdejo HE, Kuzmicic J, et al. Impaired cardiac autophagy in patients developing postoperative atrial fibrillation. *J Thorac Cardiovasc Surg.* 2012;143(2):451-459.
54. Gupta T, Khera S, Kolte D, Aronow WS, Iwai S. Antiarrhythmic properties of ranolazine: A review of the current evidence. *Int J Cardiol.* 2015;187:66-74.
55. Huang C, Yitzhaki S, Perry CN, et al. Autophagy induced by ischemic preconditioning is essential for cardioprotection. *J Cardiovasc Transl Res.* 2010;3(4):365-373.
56. Farah BL, Sinha RA, Wu Y, et al. Beta-adrenergic agonist and antagonist regulation of autophagy in HepG2 cells, primary mouse hepatocytes, and mouse liver. *PLoS One.* 2014;9(6):e98155.
57. Ji Y, Takanari H, Qile M, et al. Class III antiarrhythmic drugs amiodarone and dronedarone impair K(IR) 2.1 backward trafficking. *J Cell Mol Med.* 2017;21(10):2514-2523.
58. Santangeli P, Di Biase L, Burkhardt JD, et al. Examining the safety of amiodarone. *Expert Opin Drug Saf.* 2012;11(2):191-214.
59. Lin CW, Chen YS, Lin CC, et al. Amiodarone as an autophagy promoter reduces liver injury and enhances liver regeneration and survival in mice after partial hepatectomy. *Sci Rep.* 2015;5:15807.
60. Pushparaj C, Das A, Purroy R, et al. Voltage-gated calcium channel blockers deregulate macroautophagy in cardiomyocytes. *Int J Biochem Cell Biol.* 2015;68:166-175.
61. Williams A, Sarkar S, Cuddon P, et al. Novel targets for Huntington's disease in an mTOR-independent autophagy pathway. *Nat Chem Biol.* 2008;4(5):295-305.
62. Kania E, Pajak B, O'Prey J, et al. Verapamil treatment induces cytoprotective autophagy by modulating cellular metabolism. *FEBS J.* 2017;284(9):1370-1387.
63. Bossu A, Van der Heyden MA, de Boer TP, Vos MA. A 2015 focus on preventing drug-induced arrhythmias. *Expert Rev Cardiovasc Ther.* 2016;14(2):245-253.

64. Jansen JA, de Boer TP, Wolswinkel R, et al. Lysosome mediated Kir2.1 breakdown directly influences inward rectifier current density. *Biochem Biophys Res Commun.* 2008;367(3):687-692.
65. White NJ. Cardiotoxicity of antimalarial drugs. *Lancet Infect Dis.* 2007;7(8):549-558.
66. Wharton JM, Demopulos PA, Goldschlager N. Torsade de pointes during administration of pentamidine isethionate. *Am J Med.* 1987;83(3):571-576.
67. Antoniou T, Gough KA. Early-onset pentamidine-associated second-degree heart block and sinus bradycardia: case report and review of the literature. *Pharmacotherapy.* 2005;25(6):899-903.
68. Nalos L, de Boer TP, Houtman MJ, Rook MB, Vos MA, Van der Heyden MA. Inhibition of lysosomal degradation rescues pentamidine-mediated decreases of K(IR)2.1 ion channel expression but not that of K(v)11.1. *Eur J Pharmacol.* 2011;652(1-3):96-103.
69. Takanari H, Nalos L, Stary-Weinzinger A, et al. Efficient and specific cardiac IK(1) inhibition by a new pentamidine analogue. *Cardiovasc Res.* 2013;99(1):203-214.
70. Ji Y, Veldhuis MG, Zandvoort J, et al. PA-6 inhibits inward rectifier currents carried by V93I and D172N gain-of-function K(IR)2.1 channels, but increases channel protein expression. *J Biomed Sci.* 2017;24(1):44.
71. Vigneault P, Kaddar N, Bourgault S, et al. Prolongation of cardiac ventricular repolarization under paliperidone: how and how much? *J Cardiovasc Pharmacol.* 2011;57(6):690-695.
72. Hagiwara M, Kambayashi R, Aimoto M, Nagasawa Y, Takahara A. In vivo analysis of torsadogenic potential of an antipsychotic drug paliperidone using the acute atrioventricular block rabbit as a proarrhythmia model. *J Pharmacol Sci.* 2016;132(1):48-54.
73. Mas S, Gasso P, Parellada E, Bernardo M, Lafuente A. Network analysis of gene expression in peripheral blood identifies mTOR and NF-kappaB pathways involved in antipsychotic-induced extrapyramidal symptoms. *Pharmacogenomics J.* 2015;15(5):452-460.
74. Helgason GV, Holyoake TL, Ryan KM. Role of autophagy in cancer prevention, development and therapy. *Essays Biochem.* 2013;55:133-151.
75. Mayer IA, Arteaga CL. The PI3K/AKT pathway as a target for cancer treatment. *Annu Rev Med.* 2016;67:11-28.
76. Yu HC, Lin CS, Tai WT, Liu CY, Shiau CW, Chen KF. Nilotinib induces autophagy in hepatocellular carcinoma through AMPK activation. *J Biol Chem.* 2013;288(25):18249-18259.
77. Le XF, Mao W, Lu Z, Carter BZ, Bast RC, Jr. Dasatinib induces autophagic cell death in human ovarian cancer. *Cancer.* 2010;116(21):4980-4990.
78. Wang B, Lu D, Xuan M, Hu W. Antitumor effect of sunitinib in human prostate cancer cells functions via autophagy. *Exp Ther Med.* 2017;13(4):1285-1294.
79. Cohen IS, Lin RZ, Ballou LM. Acquired long QT syndrome and phosphoinositide 3-kinase. *Trends Cardiovasc Med.* 2017;27(7):451-459.
80. Almilaji A, Munoz C, Elvira B, et al. AMP-activated protein kinase regulates hERG potassium channel. *Pflugers Arch.* 2013;465(11):1573-1582.
81. Hrudikova Vyskocilova E, Grundmann M, Duricova J, Kacirova I. Therapeutic monitoring of amiodarone: pharmacokinetics and evaluation of the relationship between effect and dose/concentration. *Biomed Pap Med Fac Univ Palacky Olomouc Czech Repub.* 2017;161(2):134-143.
82. Tarapues M, Cereza G, Arellano AL, Montane E, Figueras A. Serious QT interval prolongation with ranolazine and amiodarone. *Int J Cardiol.* 2014;172(1):e60-61.
83. Walker O, Dawodu AH, Adeyokunnu AA, Salako LA, Alvan G. Plasma chloroquine and desethylchloroquine concentrations in children during and after chloroquine treatment for malaria. *Br J Clin Pharmacol.* 1983;16(6):701-705.
84. Piccoli E, Nadai M, Caretta CM, et al. Amiodarone impairs trafficking through late endosomes inducing a Niemann-Pick C-like phenotype. *Biochem Pharmacol.* 2011;82(9):1234-1249.
85. Patel C, Yan GX, Kowey PR. Dronedarone. *Circulation.* 2009;120(7):636-644.
86. Wadhani N, Sarma JS, Singh BN, Radzik D, Gaud C. Dose-dependent effects of oral dronedarone on the

circadian variation of RR and QT intervals in healthy subjects: implications for antiarrhythmic actions. *J Cardiovasc Pharmacol Ther.* 2006;11(3):184-190.

87. Chang SH, Wu LS, Chiou MJ, et al. Association of metformin with lower atrial fibrillation risk among patients with type 2 diabetes mellitus: a population-based dynamic cohort and in vitro studies. *Cardiovasc Diabetol.* 2014;13:123.
88. Andrews P, Thyssen J, Lorke D. The biology and toxicology of molluscicides, Bayluscide. *Pharmacol Ther.* 1982;19(2):245-295.
89. Van Bortel L, Bohm R, Mooij J, Schiffers P, Rahn KH. Total and free steady-state plasma levels and pharmacokinetics of nifedipine in patients with terminal renal failure. *Eur J Clin Pharmacol.* 1989;37(2):185-189.
90. Redfern WS, Carlsson L, Davis AS, et al. Relationships between preclinical cardiac electrophysiology, clinical QT interval prolongation and torsade de pointes for a broad range of drugs: evidence for a provisional safety margin in drug development. *Cardiovasc Res.* 2003;58(1):32-45.
91. Nazirizadeh Y, Vogel F, Bader W, et al. Serum concentrations of paliperidone versus risperidone and clinical effects. *Eur J Clin Pharmacol.* 2010;66(8):797-803.
92. Waalkes TP, Denham C, DeVita VT. Pentamidine: clinical pharmacologic correlations in man and mice. *Clin Pharmacol Ther.* 1970;11(4):505-512.
93. Pilcher J, Cooper JD, Turnell DC, Matenga J, Paul R, Lockhart JD. Investigations of long-term treatment with perhexiline maleate using therapeutic monitoring and electromyography. *Ther Drug Monit.* 1985;7(1):54-60.
94. Walker BD, Valenzuela SM, Singleton CB, et al. Inhibition of HERG channels stably expressed in a mammalian cell line by the antianginal agent perhexiline maleate. *Br J Pharmacol.* 1999;127(1):243-251.
95. Vincent EE, Coelho PP, Blagih J, Griss T, Viollet B, Jones RG. Differential effects of AMPK agonists on cell growth and metabolism. *Oncogene.* 2015;34(28):3627-3639.
96. Marchetti P, Benzi L, Cecchetti P, et al. Plasma biguanide levels are correlated with metabolic effects in diabetic patients. *Clin Pharmacol Ther.* 1987;41(4):450-454.
97. Fava C, Kantarjian H, Cortes J, Jabbour E. Development and targeted use of nilotinib in chronic myeloid leukemia. *Drug Des Devel Ther.* 2009;2:233-243.
98. Castleden CM, Kaye CM, Parsons RL. The effect of age on plasma levels of propranolol and practolol in man. *Br J Clin Pharmacol.* 1975;2(4):303-306.
99. Ahn J, Kim HJ, Choi JI, et al. Effectiveness of beta-blockers depending on the genotype of congenital long-QT syndrome: A meta-analysis. *PLoS One.* 2017;12(10):e0185680.
100. Inc. CT. Data from: Ranexa (Ranolazine) Tablet, Film Coated, Extended Release. 2017. https://dailymed.nlm.nih.gov/dailymed/archives/fdaDrugInfo.cfm?archiveid=5376.
101. Guerra F, Romandini A, Barbarossa A, Belardinelli L, Capucci A. Ranolazine for rhythm control in atrial fibrillation: A systematic review and meta-analysis. *Int J Cardiol.* 2017;227:284-291.
102. Foster DA, Toschi A. Targeting mTOR with rapamycin: one dose does not fit all. *Cell Cycle.* 2009;8(7):1026-1029.
103. Stenton SB, Partovi N, Ensom MH. Sirolimus: the evidence for clinical pharmacokinetic monitoring. *Clin Pharmacokinet.* 2005;44(8):769-786.
104. Karakas NM, Erdogan I, Ozdemir B, Sezgin A. Pain syndrome and ventricular arrhythmia induced by sirolimus and resolved by dosage adjustment in a child after heart transplant: a case report. *Exp Clin Transplant.* 2016. 1(1).
105. Lu HR, Vlaminckx E, Hermans AN, et al. Predicting drug-induced changes in QT interval and arrhythmias: QT-shortening drugs point to gaps in the ICHS7B Guidelines. *Br J Pharmacol.* 2008;154(7):1427-1438.
106. Frishman W, Kirsten E, Klein M, et al. Clinical relevance of verapamil plasma levels in stable angina pectoris. *Am J Cardiol.* 1982;50(5):1180-1184.
107. Whitley RJ, Tucker BC, Kinkel AW, et al. Pharmacology, tolerance, and antiviral activity of vidarabine

monophosphate in humans. *Antimicrob Agents Chemother.* 1980;18(5):709-715.

108. Wada T, Nakamura Y, Cao X, et al. Antiviral drug vidarabine possessing cardiac type 5 adenylyl cyclase inhibitory property did not affect cardiohemodynamic or electrophysiological variables in the halothane-anesthetized dogs. *J Toxicol Sci.* 2016;41(1):115-122.

109. Lee YM, Cheng PY, Chen SY, Chung MT, Sheu JR. Wogonin suppresses arrhythmias, inflammatory responses, and apoptosis induced by myocardial ischemia/reperfusion in rats. *J Cardiovasc Pharmacol.* 2011;58(2):133-42

3

PI3K/mTOR inhibitor omipalisib prolongs cardiac repolarization along with a mild proarrhythmic outcome in the AV block dog model

Joanne J.A. van Bavel[1], Caroline Pham[1], Henriëtte D.M. Beekman[1], Marien J.C. Houtman[1], Alexandre Bossu[1], Rolf W. Sparidans[2], Marcel A.G. van der Heyden[1], Marc A. Vos[1]

[1] Department of Medical Physiology, Division of Heart and Lungs, University Medical Center Utrecht, Utrecht, the Netherlands
[2] Division Pharmacology, Department of Pharmaceutical Sciences, Faculty of Science, Utrecht University, Utrecht, the Netherlands

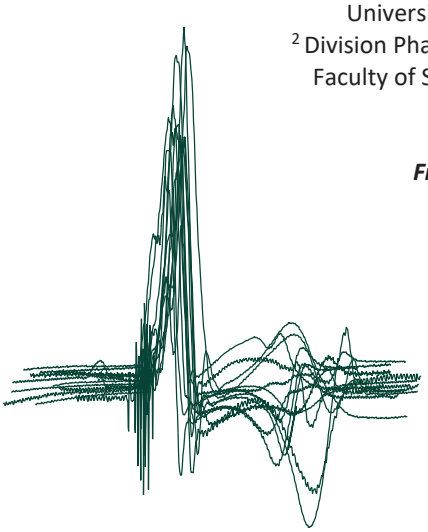

***Frontiers in Cardiovascular Medicine*, 2022, 9:956538**

Abstract

The phosphoinositide 3-kinase (PI3K) signaling pathway is an interesting target in cancer treatment. The awareness of the proarrhythmic risk of PI3K inhibitors was raised because PI3K is also involved in regulating signaling towards cardiac ion channels. Canine cardiomyocytes treated with PI3K inhibitors show an increased action potential duration and reduced cardiac repolarizing currents. Now, the potential proarrhythmic effect of chronic treatment of PI3K/mTOR inhibitor GSK2126458 (omipalisib) was investigated in the atrioventricular (AV) block dog model.

Purpose-bred Mongrel dogs received complete AV block by ablation of the bundle of His and their hearts were paced in the right ventricular apex at VDD-mode (RVA-VDD). In this way, sinus rhythm was maintained for 15 ± 1 days and thereby bradycardia-induced cardiac remodeling was prevented. Dogs received 1 mg/kg omipalisib once (n=3) or twice (n=10) a day via oral administration for 7 days. Under standardized conditions (anesthesia, bradycardia at 60 beats/minute, and a dofetilide challenge), potential proarrhythmic effects of omipalisib were investigated.

Twice-daily dosing of omipalisib increased accumulative plasma levels compared to once-daily dosing accompanied with adverse events. Omipalisib prolonged the QT interval at baseline and more strongly after the dofetilide challenge (490 ± 37 to 607 ± 48 ms). The arrhythmic outcome after omipalisib resulted in single ectopic beats in 30% of dogs perpetuating in multiple ectopic beats and TdP arrhythmia in 20% of dogs. Isolated ventricular cardiomyocytes from omipalisib-treated dogs showed a diminished I_{Ks} current density.

Chronic treatment of PI3K/mTOR inhibitor omipalisib prolonged the QT interval in a preclinical model under standardized proarrhythmic conditions. Furthermore, this study showed that electrical remodeling induced by omipalisib had a mild proarrhythmic outcome.

Keywords

PI3K inhibition, omipalisib, QT prolongation, ventricular arrhythmias, AV block dog model

Introduction

The PI3K signaling pathway is involved in a wide range of cellular processes important for cell growth, cell proliferation, cell survival and autophagy.[1] Enhanced activity of the PI3K signaling pathway is a hallmark of a broad spectrum of human cancers, associated with increased angiogenesis and cell survival. Mutations in genes of members of the PI3K pathway, such as *PIK3CA* (p110α), *AKT*, and *PTEN* have been found in various cancer types.[2,3] Aside from cancer, PI3K signaling is involved in triggering other human diseases, such as tuberous sclerosis and psoriasis.[4-6] Certainly, targeting PI3K pathway elements is of interest in the development of therapeutic interventions.[7] Chemotherapeutic agents that target or interfere with PI3K signaling include pan-PI3K inhibitors (targeting p110 isoforms), isoform-specific PI3K inhibitors, and dual PI3K/mTOR inhibitors, which are tested in clinical trials alone or in combined conditions.[8] Though, the significant role of the complex PI3K signaling pathway in functioning of the cell is accompanied with challenges in the development of therapeutic interventions that aim to target the pathway. Combination therapies are shown to be more effective than monotherapy but bring complexity issues and adverse effects, such as drug-related toxicity and compensatory signaling, resulting in resistance causing failure of the drug in clinical trials.[9]

Cardiovascular toxicity is a side effect of anti-cancer treatment that emerged the cardio-oncology discipline.[10] Regulation of the PI3K signaling pathway in the cardiovascular research field concerns crucial cellular processes such as survival and autophagy.[11,12] Adverse cardiac effects accompanied with PI3K inhibition include a reduction in adaptive responses (e.g., hypertrophy and angiogenesis) to pathologic stressors, and a higher risk for cardiovascular disease in diabetic patients due to reduced glucose oxidation.[13] In terms of cardiac electrophysiology, the PI3K pathway is involved in regulating signaling towards cardiac ion channels.[14] Transgenic mice with cardiac-specific constitutively active PI3Kα showed upregulated mRNA levels of ion channels responsible for the slow delayed rectifier current (I_{Ks}), sodium current (I_{Na}) and calcium current ($I_{Ca,L}$).[15] Suppression of PI3K signaling in isolated dog cardiomyocytes for two hours prolonged the action potential duration (APD), reduced rapid delayed rectifier current (I_{Kr}), I_{Ks}, $I_{Ca,L}$ and $I_{Na\text{-}peak}$ densities, and enhanced $I_{Na\text{-}late}$ density.[16] Furthermore, the decreased PI3K signaling caused prolongation of the QT interval recorded from isolated hearts of PI3Kα$^{-/-}$ mice and isolated hearts of wildtype mice perfused with

tyrosine kinase inhibitor nilotinib.[16] We aimed to investigate the potential proarrhythmic effect of chronic inhibition of the PI3K pathway in a preclinical animal model.

GSK2126458 (omipalisib) was presented in 2010 as dual PI3K/mTOR inhibitor.[17] It is highly active against all PI3K isoforms and both mTOR complexes and it is more potent than BEZ235 and GDC-0941.[17] Its promising role as potential therapeutic agent is shown in *in vitro* studies reflecting a variety of cancer types and idiopathic pulmonary fibrosis.[18-21] Chronic treatment of $Tsc2^{+/-}$ mice, a model of tuberous sclerosis, with omipalisib reduced the number and size of solid renal tumors.[22] The compound is currently tested in phase I clinical trials, and to date, three publications have documented drug tolerance, dosing safety, clinical outcome, and drug combination effectivity in human patients.[23-25] ECG parameters were addressed in one article, and besides a clinically insignificant reduced heart rate, no cardiac abnormalities were reported as adverse events after omipalisib treatment.[25]

The sensitive atrioventricular (AV) block dog model has been used for the last three decades to test potential pro- and antiarrhythmic effects of pharmacological compounds.[26] A combination of AV block-induced cardiac remodeling, anesthesia, bradycardia, and infusion of I_{Kr} blocker dofetilide as the final hit, predisposes the heart to Torsade de Pointes (TdP) ventricular arrhythmias.[27] The electrical component of cardiac remodeling includes a reduced repolarization reserve, which is caused by a downregulation of I_{Kr} and I_{Ks} and results in QT prolongation.[28,29] It is yet unclear whether diminished ion current densities induced by chronic PI3K inhibition result in proarrhythmic conditions. Therefore, we investigated the proarrhythmic risk of PI3K/mTOR inhibitor omipalisib by replacing AV block-induced electrical remodeling by chronic omipalisib treatment.

Materials and Methods

Animals

Animal handling and care were in accordance with the Directive 2010/63/EU of the European Parliament and of the Council of 22 September 2010 on the protection of animals used for scientific purposes and the Dutch law on animal experimentation. Experiments were approved by the Central Authority for Scientific Procedures on Animals. Dogs were housed in pairs in kennels containing wooden bedding material, had ad libitum access to drinking water

and received food pellets twice a day. The animals were allowed to play outside once a day and their welfare was checked daily.

Animal preparation

Adult purpose-bred mongrel dogs (n=13, Marshall, New York, USA) were included in the experimental protocol. The dogs were fasted overnight and received premedication (0.02 mg/kg atropine, 0.5 mg/kg methadone, and 0.5 mg/kg acepromazine i.m.) 30 minutes prior to the surgical procedure. General anesthesia was induced by sodium pentobarbital (Nembutal, 25 mg/kg i.v.) and maintained by 1.5% isoflurane in O_2 and N_2O (1:2 ratio) via mechanical ventilation at twelve breaths/minute. To minimize pain and the risk of inflammation, dogs received analgesics (0.1 mg/kg Metacam s.c. before surgery and 0.3 mg Temgesic i.m. after surgery) and antibiotics (1000 mg ampicillin i.v. before and i.m. after surgery).

Control experiment

Two serial experiments were performed under general anesthesia with each dog serving as its own control (**Figure 1**). The first experiment under general anesthesia included implantation of a pacemaker device (Medtronic, Maastricht, The Netherlands) with a right atrial lead sensing native atrial activity and a screw-in lead for stimulation of the right ventricular (RV) apex. A transmural needle biopsy was obtained from the left ventricular (LV) apex and immediately frozen using liquid nitrogen for later protein analysis. Radiofrequency ablation of the His bundle induced complete and irreversible AV block to induce bradycardia. The arrhythmic status of the heart at this control time point was tested according to our standardized protocol: under anesthesia, at bradycardia (continuous RV pacing at 60 bpm, VVI 60), and infusion of I_{Kr} blocker dofetilide (Biorbyt, dissolved in 100 μl 0.1 M HCl and diluted in saline, 25 μg/kg i.v.) for 5 minutes or until the first TdP arrhythmia occurred.

Pacing at VDD mode

After the control experiment, AV block-induced cardiac remodeling on a structural, electrical, and contractile level was prevented by continuous pacing at VDD mode (electrical conduction sensed in the atria was perpetuated via pacing in the RV apex). In this way, sinus rhythm was resembled and maintained until the induction experiment.

Chronic treatment with omipalisib

Eight days after the control experiment, dogs received 1 mg/kg omipalisib daily for seven days (**Figure 1**). First, three dogs (all females, bodyweight: 21 ± 2 kg, age: 12 ± 0 months at control experiment) received omipalisib once a day at 8:00 AM, based on results from a human clinical trial.[23] For optimization of target inhibition across a 24-hour interval and omipalisib concentration in plasma >30 ng/ml,[17,23,25] dosing frequency was increased to twice a day for the next group. Ten dogs (three females and seven males, bodyweight: 25 ± 3 kg, age: 14 ± 2 months at control experiment) received omipalisib at 8:00 AM and 5:00 PM. The compound was administered orally via powder-filled capsules (size 0). One dog received no omipalisib capsule on day 7 due to severe adverse events. Venous blood samples were taken via the cephalic vein on day 1 and day 7 (one hour after administration) for once-daily dosing, and on day 1 (one, four, eight, and 24 hours after administration) and day 7 (one hour after administration) for twice-daily dosing. The welfare and body weight (BW) of the animals were checked daily.

Induction experiment

The second experiment under general anesthesia included testing of the arrhythmic status of the heart after omipalisib treatment (**Figure 1**). The procedure was performed on day 7 of omipalisib treatment, corresponding to 15 ± 1 days after the control experiment. Similar to the control experiment, the arrhythmic status of the heart was tested under anesthesia, bradycardia (the pacing rate at VVD mode was reduced to VVI 60), and a dofetilide challenge. At the end of the procedure, heparin (10.000 IU, i.v.) was infused and hearts were excised (of dogs dosed twice/day) by right-sided thoracotomy, weighed, and used for single cell isolation.

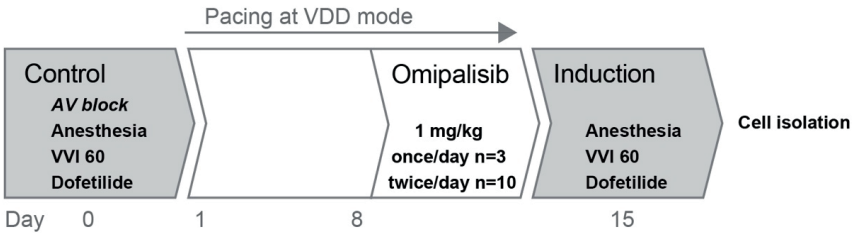

Figure 1. Overview of the experimental protocol. Two experiments were performed in series: control and induction, before and after omipalisib treatment to examine the potential proarrhythmic effect of omipalisib in the AV block dog model.

Data acquisition

Experiments included a continuous recording of the surface electrocardiogram (ECG) and endocardial LV and RV monophasic action potential (LV and RV MAP) signals (catheter from Hugo Sachs Elektronik, Germany). LV pressure (LV-P) signals were acquired for three dogs with a 7F pressure catheter (CD Leycom Inc., Zoetermeer, The Netherlands). All signals were acquired at a sampling rate of 1 kHz using EP-Tracer software (Cardiotek, Maastricht, The Netherlands).

Analysis of electrophysiological and pressure signals

ECG parameters were measured from five consecutive complexes on lead II of the surface ECG. The RR, PP, QRS, and QT intervals were determined via offline analysis by manually setting the markers in EP-Tracer. Ten consecutive complexes were included for RR and PP interval analysis from awake dogs. The JT interval was obtained by subtracting the QRS interval from the QT interval, and the QT corrected for heart rate (QTc) was calculated using the Van de Water formula.[30] The LV MAP and RV MAP duration (LV MAPD, RV MAPD) at 80% of repolarization of five consecutive action potentials were measured semi-automatically using custom-made software (AutoMAPD, MATLAB, Mathworks, Natick, MA, USA). Temporal dispersion or beat-to-beat variation of repolarization was quantified as short-term variability (STV) of repolarization and was calculated from 31 consecutive beats using the formula:

$$\mathrm{STV} = \sum |\mathrm{D_{n+1}} - \mathrm{D_n}| / \left[30 * \sqrt{2}\right]$$

with D referring to LV MAPD and RV MAPD.[31] Ectopic beats and complexes with a P-wave in the T-wave end were excluded.

The maximum of the derivative of the LV pressure signal, referring to the point where the slope of the pressure rise is the steepest ($LVdP/dt_{max}$), was manually measured offline using AutoMAPD. The mean $LVdP/dt_{max}$ was based on five consecutive pressure cycles. The duration of five consecutive LV-P cycles was manually measured in EP tracer by selecting the start of the QRS on the surface ECG and the end of the pressure cycle ($QLVP_{end}$). Calculation of the electromechanical window (EMW) was performed by subtraction of the QT interval from the $QLVP_{end}$.[32] The maximum and minimum of the derivative of the LV-P signal, referring to the point where the slope of the pressure rise and fall is the steepest ($LVdP/dt_{max}$ and $LVdP/dt_{min}$,

respectively), were manually measured offline using AutoMAPD (MATLAB, Mathworks, Natick, MA, USA). The mean LVdP/dt was based on five consecutive LV-P cycles. Time point baseline corresponds to the complexes before the onset of dofetilide infusion. Time point dofetilide corresponds to 5 minutes after the onset of infusion, or the occurrence of an ectopic beat within these 5 minutes (for ECG parameters: n=1, and for MAPD and STV parameters: n=6). Signals that were invalid for reliable analysis were excluded.

Quantification of arrhythmic outcome

The arrhythmia score (AS) is a quantification of the severity of the arrhythmic outcome,[33,34] and is the average of the three highest scored arrhythmic events that occurred in 10 minutes after the onset of dofetilide infusion. A regular beat is scored with 1 point, single ectopic beats (sEB) are scored with 2 points, multiple ectopic beats (mEB) are scored with 3-5 points, and TdP arrhythmias from 6 complexes or more are scored with 6-49 points. TdP arrhythmias lasting longer than 10 seconds were defibrillated and scored with 50, 75, and 100 points depending on the number of shocks that were required.

Quantification of omipalisib in blood plasma

Blood samples were centrifuged at 4696 g for 5 minutes at 4°C and plasma was stored at -80°C until further analysis. Omipalisib concentration in plasma was determined using protein precipitation and liquid chromatography-tandem mass spectrometry (LC-MS/MS) as previously described.[35]

Cellular electrophysiology

Hearts from omipalisib-treated dogs (n=7, dosed twice-daily, three females and four males, bodyweight: 21 ± 2 kg, age: 15 ± 3 months at day of heart isolation) and healthy surplus beagle dogs (n=6, three females and three males, bodyweight: 10 ± 2 kg, age: 1-3 years, Charles River Laboratories, 's-Hertogenbosch, The Netherlands) were excised and put on a Langendorff system via ligation of the left circumflex coronary artery and right coronary artery. A transmural biopsy of the LV apex was obtained from the omipalisib-treated dogs and immediately frozen using liquid nitrogen for protein analysis. LV and RV cardiomyocytes were enzymatically isolated and stored as previously described.[36] Cells were stored at room temperature (RT) in 0.2 mM Ca^{2+} standard buffer solution (in mM: 130 NaCl, 5.4 KCl, 1.2

KH_2PO_4, 1.2 $MgSO_4$, 6 HEPES and 20 glucose, pH 7.2 corrected with NaOH) until used for whole-cell patch clamp experiments at the same day. Action potentials and potassium currents were recorded using Clampex 10 software (Molecular Devices, Sunnyvale, CA, USA). Action potentials were analyzed using Peaks, a custom Matlab script, which is freely available through the Open Science Framework (https://osf.io/86ufe/). Potassium currents were analyzed using Clampfit 10 software (Molecular Devices, Sunnyvale, CA, USA).

For action potential recordings, cells from SR (n=3) and omipalisib-treated dogs (n=3) were stimulated with 2 ms current injections at 0.5 Hz in a temperature-controlled chamber perfused with (in mM) 137 NaCl, 5.4 KCl, 0.5 $MgCl_2$, 1.8 $CaCl_2$, 11.8 HEPES and 10 glucose (pH 7.4) at 37°C. Patch pipettes with a 1.5-2.5 MΩ resistance were filled with (in mM) 10 NaCl, 130 KCl, 0.5 $MgCl_2$, 5 MgATP and 10 HEPES (pH 7.2). Action potentials after 10 minutes of stable recording were used to obtain action potential duration (APD) at 90% of repolarization and STV.

For potassium current measurements, cells from SR (n=3) and omipalisib-treated dogs (n=4) were perfused with bath solution containing (in mM) 145 NaCl, 4 KCl, 1 $MgCl_2$, 1.8 $CaCl_2$, 10 HEPES, 11 glucose and 0.005 nifedipine (pH 7.4) at 37°C. Pipette solution consisted of (in mM) 20 KCl, 1 $MgCl_2$, 5 MgATP, 5 HEPES, 125 K-aspartate and 10 EGTA (pH 7.2). Cells were kept at a holding potential of -80 mV and a voltage protocol was applied that consisted of the following steps: -80 mV for 100 ms, -40 mV for 500 ms, -20 to +60 mV with 10 mV increments for 2000 ms, -50 mV for 1000 ms, -80 mV for 150 ms, -100 mV for 200 ms and -80 mV for 100 ms. After recording the total current (I_K), the I_{Ks}-sensitive current was determined by adding 500 nM HMR 1556 followed by the addition of 1 μM dofetilide to obtain the I_{Kr}-sensitive current. The interval between the addition of the two inhibitors was ±3 minutes. Current levels were determined as peak tail-current at -50 mV (after the 60 mV step pulse) and corrected for the cell capacitance to obtain current densities.

Immunoblotting

Frozen cardiac biopsies were pulverized using a liquid nitrogen-cooled mortar and lysates were made using RIPA buffer: (in mM) 20 Tris, 150 NaCl, 10 $Na_2HPO_4.2H_2O$, 1% Triton X-100, 1% Na-deoxycholate, 0.1% SDS, 1 Na_2EDTA, 50 NaF (pH 7.4) supplemented with 1 mM

phenylmethylsulfonyl fluoride (PMSF) and 10 μg/ml aprotinin. Protein lysates prepared in Laemmli sample buffer were incubated for 5 minutes at 37°C and 30 μg was separated by 10% SDS-PAGE and blotted on a nitrocellulose membrane. Equal protein loading was revealed by ponceau S staining. Membranes were blocked with 5% BSA in Tris-buffered saline/ Tween 20 (20 mM Tris-HCl pH 8.0, 150 mM NaCl, 0.05% Tween-20) for 1.5 hour at RT. Phospho-Akt protein was detected by incubation with polyclonal anti-pAkt primary antibody (1:1000, Cell Signaling Technology, Danvers, Massachusetts, USA) overnight and HRP-conjugated anti-rabbit secondary antibody (1:7000, Bio-Rad Laboratories, Hercules, USA) for 2 hours at RT. Final detection was performed by a standard chemiluminescence procedure (Cytiva, Amersham, United Kingdom) with ChemiDocXRS system (Bio-Rad Laboratories, Veenendaal, The Netherlands). Signal analysis was performed using Image Lab software (version 6.1, Bio-Rad Laboratories, Veenendaal, The Netherlands).

Statistical analysis

Data are presented as mean ± standard deviation (SD). Data were analyzed using a paired Student's *t*-test, (repeated measures) one-way analysis of variance (ANOVA) with Tukey's multiple comparisons test, or a repeated measures two-way ANOVA with Tukey's or Bonferroni's multiple comparisons test. Statistical analyses were performed with GraphPad Prism (version 9.3.1, GraphPad Software, San Diego, USA). A value of $p<0.05$ was considered statistically significant.

Results

ECG parameters and dose testing after once-daily omipalisib

Omipalisib was administered once a day to three dogs for seven days to determine plasma levels and its effect on electrophysiological parameters and arrhythmic outcome. The ECG parameters under anesthesia during baseline and after dofetilide, before (control) and after omipalisib treatment are presented in **Table 1**. Though not significant, dofetilide prolonged the QT and JT interval during the control experiment (**Table 1, Figure 2A**). These repolarization intervals were significantly prolonged by dofetilide after chronic omipalisib treatment. During the control experiment, solely ectopic beats occurred in all animals during the dofetilide challenge, whereas ectopic beats perpetuated in multiple ectopic beats and TdP arrhythmia in one animal after omipalisib treatment (**Figure 2C**). The AS increased from 1 to 18.7 for this

dog (**Figure 2D**) due to the sudden-onset TdP arrhythmia demanding defibrillation (**Figure 2E**), while the AS was unaltered for the other two animals (**Figures 2D**). Accumulative omipalisib levels in plasma on day seven of treatment increased to 15.9 – 34.5 ng/ml and were below the target concentration of 30 ng/ml for two out of three dogs (**Figure 2B**).

Table 1. Electrophysiological parameters of anesthetized dogs (n=3) before treatment (control) and after 1 mg/kg omipalisib treatment for once a day.

	Control		**Omipalisib**	
Parameter	**Baseline**	**Dofetilide**	**Baseline**	**Dofetilide**
RR	1000 ± 0	1000 ± 0	1000 ± 0	1000 ± 0
PP	574 ± 46	700 ± 46	416 ± 67	535 ± 67
QRS	113 ± 3	114 ± 2	112 ± 4	114 ± 5
QT	379 ± 30	489 ± 79	361 ± 30	535 ± 82 *#
JT	266 ± 31	375 ± 77	248 ± 29	423 ± 80 *#

Parameters in ms. Data as mean ± SD. Repeated measures two-way ANOVA with Tukey's multiple comparisons test. *p<0.05 compared to control baseline and #p<0.05 compared to omipalisib baseline.

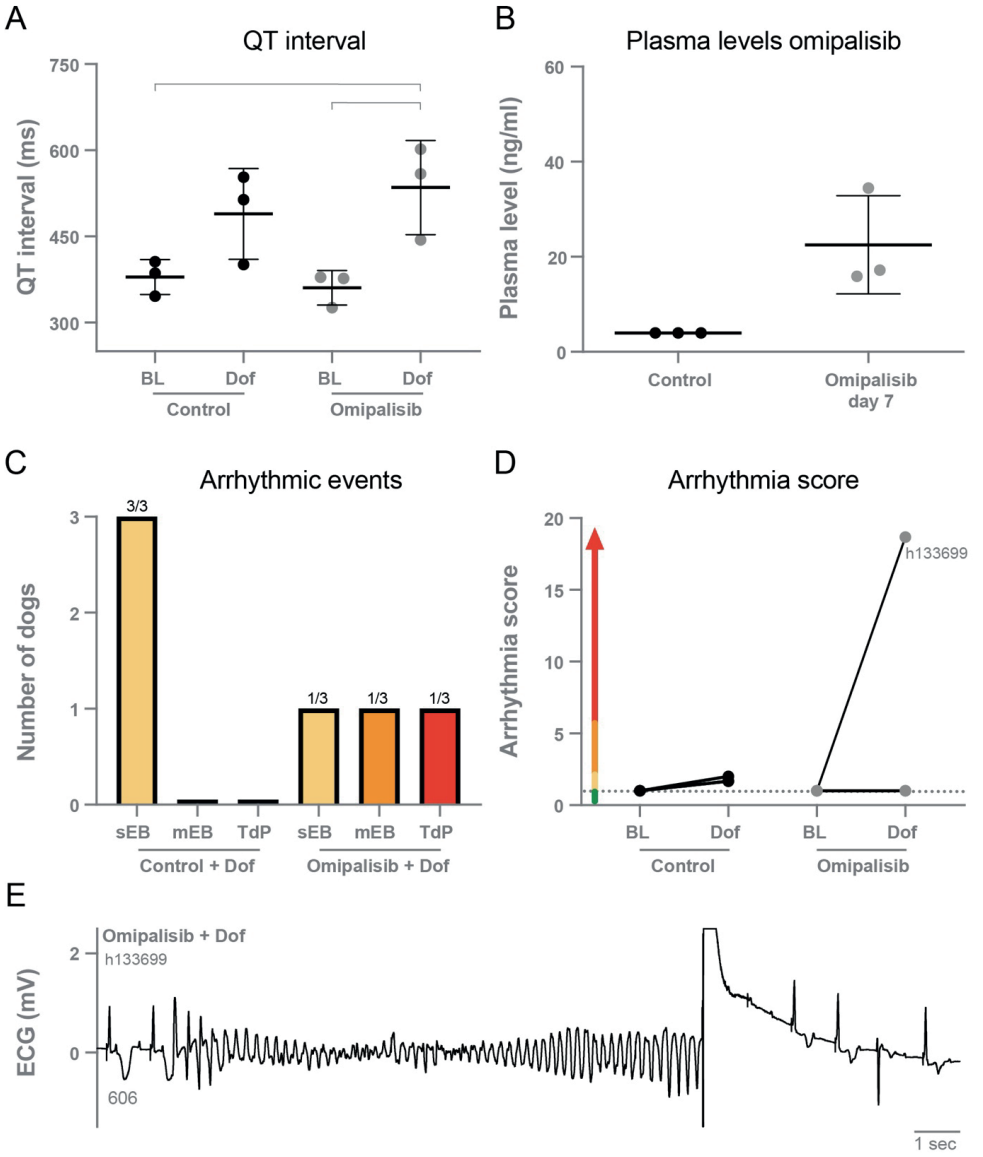

Figure 2. A) QT interval during baseline and dofetilide before treatment (control) and after omipalisib treatment (1 mg/kg once a day). Repeated measures two-way ANOVA with Tukey's multiple comparisons, bars refer to $p<0.05$. **B**) Plasma levels of omipalisib before (values <4 ng/ml) and after 7 days of omipalisib treatment. Data are presented as mean ± SD. **C**) Incidence of arrhythmic events. **D**) Arrhythmia score of dogs before (control) and after 1 mg/kg omipalisib once a day. Single ectopic beats (sEB, scored with 2 points), multiple ectopic beats (mEB, scored with 3-5 points), and Torsade de Pointes (TdP) arrhythmia (scored with 6-49 points). TdP arrhythmia demanding defibrillation was scored with 50, 75 or 100 points depending on the number of shocks. **E**) ECG lead II showing a defibrillated TdP arrhythmia after omipalisib treatment and dofetilide infusion in dog h133699. The QT interval (ms) of the complex before the TdP is stated below the T wave.

Adverse events and increased plasma levels after twice-daily omipalisib

Omipalisib was administered twice a day to ten dogs to examine if this higher dose would increase plasma levels to its target levels and the risk for proarrhythmic conditions. Drug-related adverse events were determined, with infected stitches, fever and weight loss as the most common reactions (**Figure 3A**). Inhibition of the PI3K/mTOR pathway by omipalisib was confirmed by reduced pAkt protein levels in isolated ventricular biopsies (**Figure 3B**). The weight of the isolated hearts (HW) of omipalisib treated dogs was 238 ± 32 g and the HW/BW corrected for omipalisib-induced weight loss (by taking the BW before treatment) was 9.6 ± 1.3 g/kg. Indeed, on day one at four hours after administration of omipalisib, the accumulative omipalisib levels in plasma were >30 ng/ml in all dogs and maintained above this target concentration at eight hours after the first capsule in 80% of the dogs (**Figure 3C**). Accumulative omipalisib levels at the last day of treatment were 164 ± 229 ng/ml, with levels above the target concentration in 80% of the dogs (**Figure 3C**).

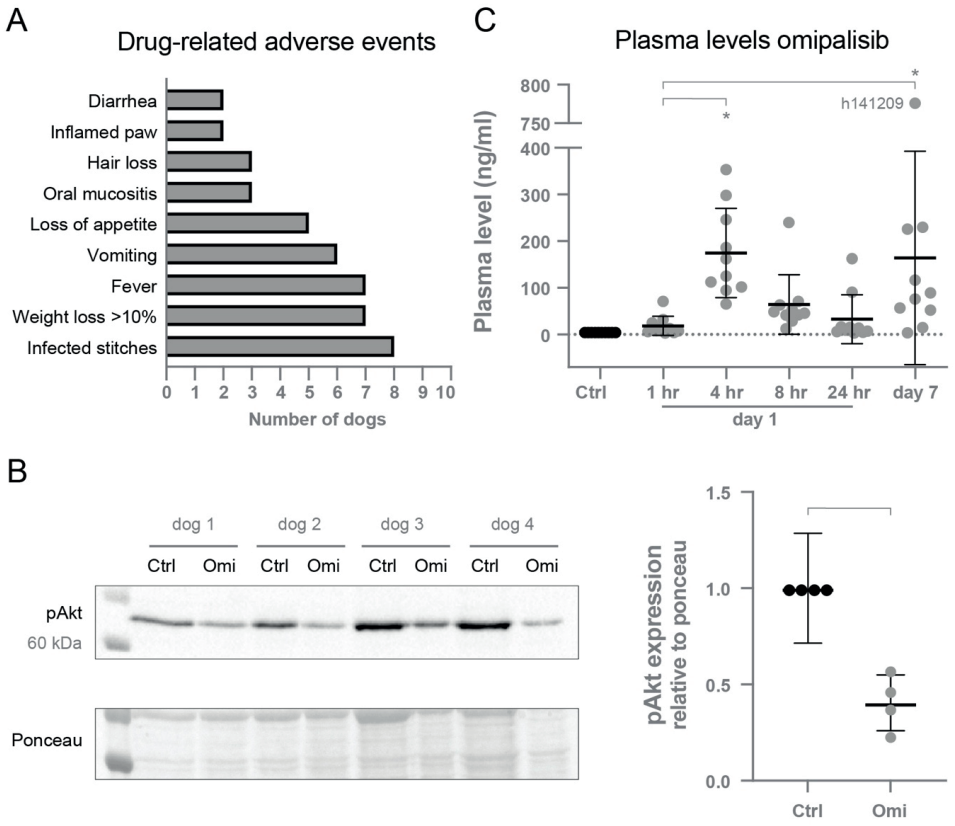

Figure 3. A) Drug-related adverse events induced by omipalisib. **B**) Reduced pAkt protein expression relative to ponceau after omipalisib treatment (Omi) compared to control (Ctrl) measured in cardiac biopsies. Paired t-test, bar refers to p<0.05. **C**) Levels of omipalisib in blood plasma from dogs (n=10) treated with 1 mg/kg omipalisib twice a day. Repeated measures one-way ANOVA with Tukey's multiple comparisons test, *p<0.05 compared to Ctrl and for bars. Data are presented as mean ± SD.

Repolarization duration is not affected by VDD pacing and omipalisib treatment in awake dogs

Alternative to the physiological path of ventricular conduction through the septum in SR, pacing at VDD mode (to maintain ventricular rate at SR) initiated ventricular conduction from the right ventricular apex. Accordingly, the possible effect of RVA-VDD pacing and omipalisib treatment was examined by analyzing ECG parameters of awake dogs through the experimental protocol (**Table 2**). Both interventions did not affect the RR interval but prolonged the QRS, QT, and QTc intervals compared to SR. The JTc interval, reflecting the repolarization duration by exclusion of the QRS duration from the QTc interval, was not affected by pacing and omipalisib treatment.

Table 2. Effect of RVA-VDD pacing and omipalisib treatment on electrophysiological parameters in awake dogs (n=9).

	No treatment			**Omipalisib**
	Sinus rhythm	**RVA-VDD pacing**		
Parameter	**day -2**	**day 1**	**day 8**	**day 14**
RR	604 ± 94	653 ± 102	535 ± 94	582 ± 138
QRS	77 ± 3	124 ± 9 *	116 ± 8 *^	121 ± 9 *
QT	212 ± 8	277 ± 10 *	248 ± 13 *^	267 ± 9 *$^{\#}$
QTc	247 ± 5	308 ± 13 *	290 ± 6 *^	302 ± 12 *
JTc	170 ± 4	184 ± 16	174 ± 7	181 ± 15

Parameters in ms. Data as mean ± SD. Repeated measures one-way ANOVA with Tukey's multiple comparisons test, *p<0.05 compared to sinus rhythm at day -2, ^p<0.05 compared to RVA-VDD pacing day 1, and $^{\#}$p<0.05 compared to RVA-VDD pacing day 8. Parameters of one dog were excluded because of pacing defects at day 14.

Twice-daily omipalisib prolongs repolarization duration

In the control experiment, dofetilide prolonged the PP interval and all (intra)cardiac repolarization parameters (QT, JT, LV MAPD, and RV MAPD, **Table 3**). Interestingly, chronic omipalisib treatment prolonged repolarization parameters QT, JT, and RV MAPD during baseline and more strongly during dofetilide for all repolarization parameters (**Table 3, Figure 4A**). Furthermore, the temporal dispersion of repolarization – quantified by the STV – was

increased after omipalisib treatment combined with dofetilide (**Table 3, Figure 4B**). A measure of spatial dispersion of repolarization, quantified by the △MAPD, remained unaltered upon dofetilide infusion or omipalisib treatment (**Table 3**).

Table 3. Electrophysiological parameters of anesthetized dogs (n=10) before treatment (control) and after 1 mg/kg omipalisib treatment twice a day.

	Control		Omipalisib	
Parameter	Baseline	Dofetilide	Baseline	Dofetilide
RR	1000 ± 0	1000 ± 0	1000 ± 0	1000 ± 0
PP	471 ± 54	615 ± 60 *	506 ± 64	661 ± 118 *#
QRS	123 ± 7	125 ± 7	134 ± 9 *	134 ± 8 *^
QT	364 ± 17	490 ± 37 *	432 ± 36 *	607 ± 48 *^#
JT	241 ± 15	365 ± 39 *	298 ± 29 *	473 ± 48 *^#
LV MAPD	248 ± 21	352 ± 52 *	282 ± 18	459 ± 54 *^#
RV MAPD	222 ± 25	274 ± 29 *	271 ± 13 *	408 ± 35 *^#
△MAPD	25 ± 15	75 ± 49	17 ± 12	41 ± 25
STV LV MAPD	0.70 ± 0.42	1.83 ± 0.84	0.94 ± 0.84	3.54 ± 2.84 *
STV RV MAPD	0.62 ± 0.24	1.13 ± 0.64	0.83 ± 0.49	5.26 ± 4.42 *^#

Parameters in ms. Data as mean ± SD. PP interval: n=9. Monophasic action potential duration from the left ventricle (LV MAPD, n=9) and right ventricle (RV MAPD, n=8) at 80% of repolarization. △MAPD = LV MAPD – RV MAPD. STV = short term variability. Repeated measures two-way ANOVA with Tukey's multiple comparisons test, *p<0.05 compared to control baseline, ^p<0.05 compared to control dofetilide, and #p<0.05 compared to omipalisib baseline.

Omipalisib has a mild proarrhythmic outcome in the AV block dog model

After omipalisib treatment and the dofetilide challenge, 30% of the dogs showed sEB which perpetuated in mEB and TdP in 20% of the dogs (**Figure 4C**). The TdP arrhythmias that occurred in the ten-minute time window after the onset of dofetilide included 15 self-terminating TdP arrhythmias scored with 6-9 points for one dog and a self-terminating TdP scored with 17 points for the other dog (h141209) (**Figure 4E**). Their arrhythmia score increased from 1 to 7.7 and 1 to 8.3 (**Figure 4D**) and both dogs showed the highest omipalisib plasma levels in plasma on day 7. The proarrhythmic effect of an additional trigger in the form of enhanced contractility was examined supplementary to omipalisib treatment. Contractility was enhanced by Na^+/K^+-ATPase pump inhibitor ouabain in three dogs from the twice-daily omipalisib-treated group (**Suppl. table 1 and Suppl. figure 1B**). However, the ouabain challenge did not increase the proarrhythmic outcome (**Suppl. figure 1C and D**).

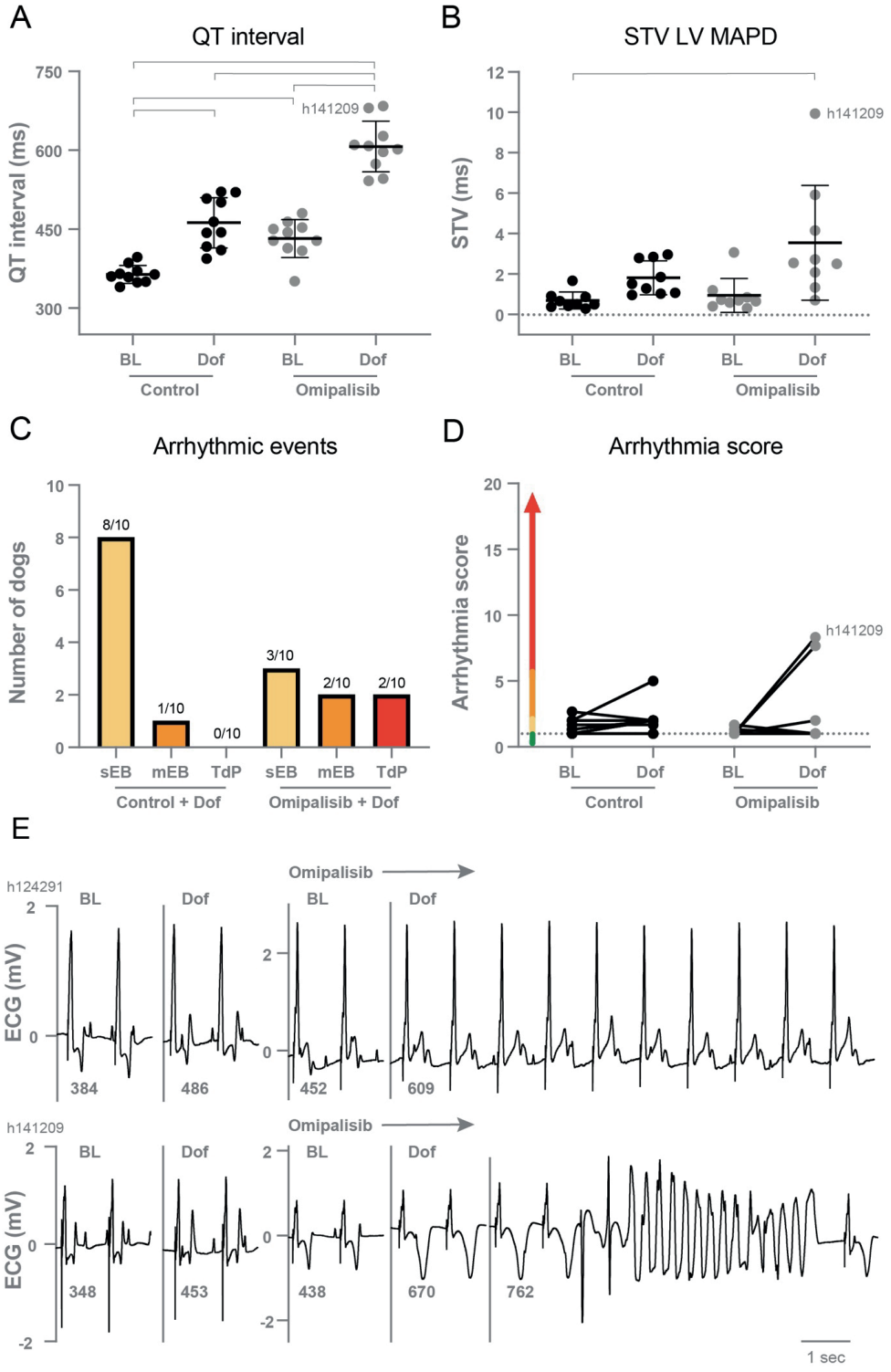
A
QT interval
QT interval (ms)
750
600
450
300
h141209
BL
Dof
BL
Dof
Control
Omipalisib
B
STV LV MAPD
STV (ms)
12
10
8
6
4
2
0
h141209
BL
Dof
BL
Dof
Control
Omipalisib
C
Arrhythmic events
Number of dogs
10
8
6
4
2
0
8/10
1/10
0/10
3/10
2/10
2/10
sEB
mEB
TdP
sEB
mEB
TdP
Control + Dof
Omipalisib + Dof
D
Arrhythmia score
Arrhythmia score
20
15
10
5
0
h141209
BL
Dof
BL
Dof
Control
Omipalisib
E
h124291
Omipalisib
BL
Dof
BL
Dof
ECG (mV)
2
0
384
486
452
609
h141209
Omipalisib
BL
Dof
BL
Dof
ECG (mV)
2
0
-2
348
453
438
670
762
1 sec

Figure 4. A) QT interval (n=10) and **B**) short term variability of repolarization (STV LV MAPD, n=9) in dogs before (Control) and after 1 mg/kg omipalisib twice a day during baseline (BL) and dofetilide (Dof). Data are presented as mean ± SD. Repeated measures two-way ANOVA with Tukey's multiple comparisons test, bars refer to $p<0.05$. **C**) Incidence of arrhythmic events and **D**) arrhythmia score during 10 min after start of Dof before and after omipalisib treatment. Single ectopic beats (sEB, score: 2 points), multiple ectopic beats (mEB, scored with 3-5 points), and Torsade de Pointes (TdP) arrhythmia (scored with 6-49 points). TdP arrhythmia demanding defibrillation were scored with 50, 75 or 100 points depending on the number of shocks. **E**) ECG lead II of the two dogs: h124291 with arrhythmia score of 1, and h141209 with a self-terminating TdP arrhythmia and arrhythmia score of 8.3.

Diminished I_{Ks} density in isolated cardiomyocytes from omipalisib-treated dogs

To determine the effect of chronic omipalisib treatment on the different potassium currents, electrophysiological measurements were performed on isolated cardiomyocytes from the LV and RV. Representative potassium current tracings from cells of healthy and omipalisib-treated dogs are presented in **Figure 5A**. Relative to the total I_K, cells from omipalisib-treated dogs showed a reduced I_{Ks} (**Figure 5B**). Representative APD tracings are depicted in **Figure 5C**, and APD at 90% of repolarization of cells from omipalisib-treated dogs (291 ± 61 ms) was marginally shorter compared to SR cells (353 ± 65 ms, $p<0.05$) (**Figure 5D**). The APD at 50% of repolarization was 253 ± 58 ms in cells from omipalisib-treated dogs and 317 ± 61 ms in SR cells ($p<0.05$). The STV of the isolated single cells was not altered after omipalisib (**Figure 5E**).

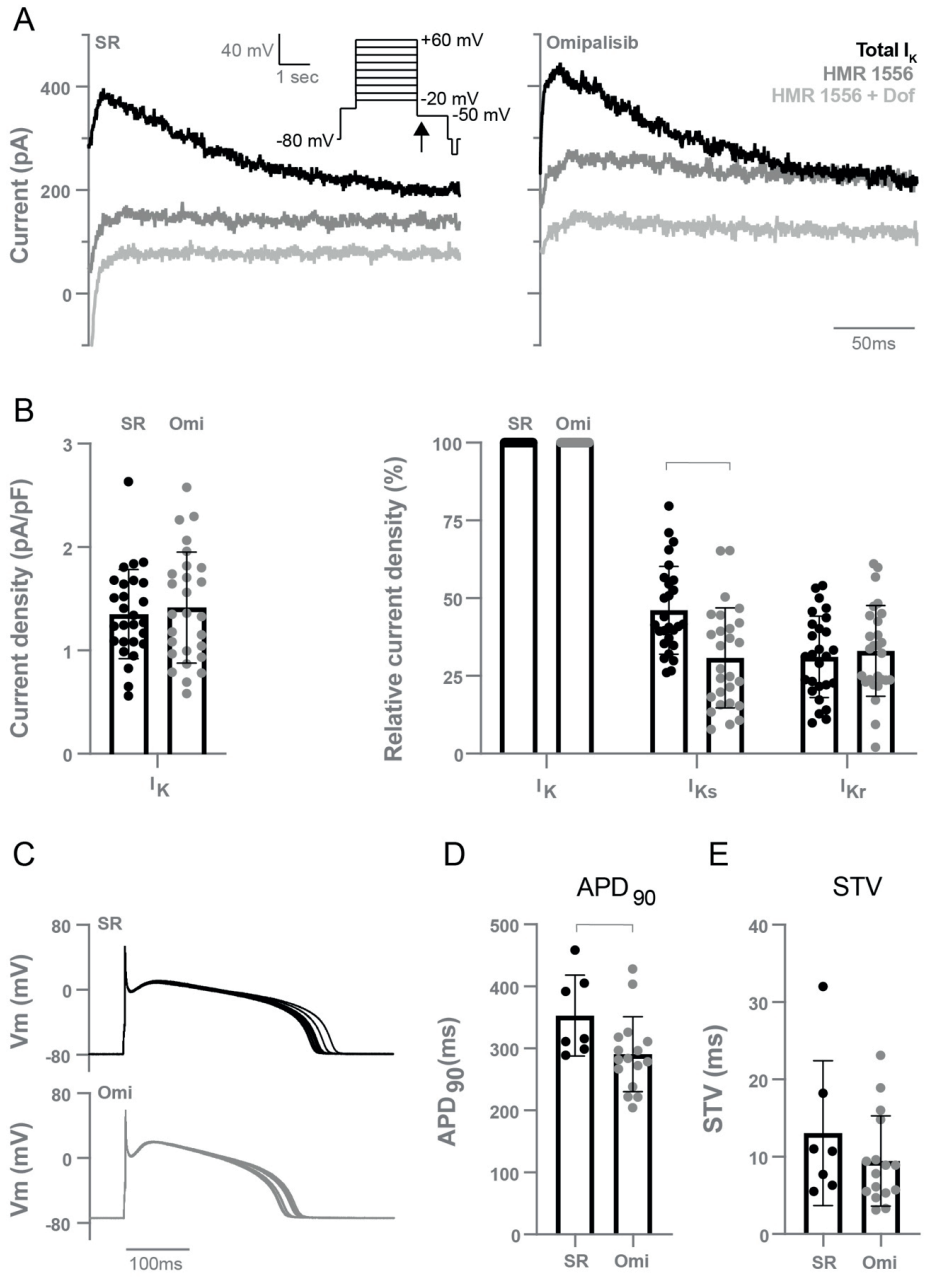

Figure 5. Electrophysiological measurements of isolated cardiomyocytes from the left and right ventricle of dogs in sinus rhythm (SR) and after 1 mg/kg omipalisib twice a day (Omi). **A**) Representative peak tail current tracings at -50 mV (arrow). **B**) Current density of total I_K (left graph, n=27, unpaired t-test, not significant) and relative current density of I_{Ks} and I_{Kr} to total I_K (right graph, n=27, repeated measures two-way ANOVA with Bonferroni's multiple comparisons test SR vs Omi, bar refers to $p<0.05$). I_{Ks} refers to the current blocked by 500 nM HMR 1556 and I_{Kr} refers to the current blocked by 1 μM dofetilide (Dof). **C**) Representative action potential tracings.

Membrane potential (Vm). **D**) Action potential duration at 90% of repolarization (APD_{90}) and **E**) short term variability (STV) of repolarization at SR (n=7) and Omi (n=16). Unpaired t-test, bar refers to $p<0.05$. Data are presented as mean ± SD.

Discussion

This study presents the electrophysiological effects of chronic treatment with the PI3K/mTOR inhibitor omipalisib in a preclinical model. Twice-daily dosing was required to reach the omipalisib target concentration. Right ventricular pacing at SR rate and omipalisib did not affect repolarization duration in an awake situation. Yet, omipalisib induced repolarization prolongation under standardized conditions in baseline which further increased after a dofetilide challenge. Furthermore, cardiomyocytes isolated from omipalisib-treated dogs showed a diminished I_{Ks} density. Electrical remodeling induced by omipalisib triggered the occurrence of ectopic beats in 30% of dogs which perpetuated in multiple ectopic beats and TdP arrhythmias in 20% of dogs, resulting in a mild proarrhythmic outcome.

Role of cardiac remodeling in this study

Cardiac remodeling of the chronic AVB dog model is characterized by bradycardia-induced adaptation on a structural, electrical, and contractile level.[37] In the current study design, we prevented these elements of remodeling from occurring by pacing the RV apex at VDD mode to maintain SR rate. A limitation of this pacing protocol is a change in the physiological ventricular conduction pathway causing asynchronous contraction of the ventricles. This can result in LV systolic dysfunction and an increased risk for heart failure.[38] Continuation of SR conduction following AV block by so-called His bundle pacing is preferred but coincides with implantation difficulties.[39] In the current study, pacing the RV apex at VDD mode and eliminating its effects on repolarization duration by ECG analysis served as the optimal approach towards the maintenance of ventricular rate at SR in the AV block dog model. When focusing on the individual remodeling components, omipalisib did not induce structural remodeling in the form of hypertrophy as the HW and HW/BW were lower compared to previously reported results from chronic AVB dogs, and were similar to SR dogs.[40,41] In addition, the contractile parameter $LVdP/dt_{max}$ was unaltered after omipalisib treatment compared to the control timepoint including values lower than those of previously reported results of chronic AV block remodeled hearts.[42] At initiation of this study, it was hypothesized that PI3K/mTOR inhibition by chronic omipalisib treatment could replace AV block-induced

electrical remodeling (QT prolongation due to diminished I_{Ks} and I_{Kr}) by omipalisib. Indeed, omipalisib induced prolongation of the QT and JT intervals at baseline and more strongly after dofetilide under proarrhythmic conditions. Furthermore, cardiomyocytes isolated from hearts of omipalisib-treated dogs showed a diminished I_{Ks} current. These results demonstrate that chronic PI3K/mTOR inhibition indeed induces proarrhythmic cardiac electrical remodeling to an extent that, at least partially, reflects chronic AV block induced remodeling.

PI3K inhibition and cardiac electrophysiology

Examination of the role of PI3K inhibition on cardiac electrophysiology is currently predominantly addressed in *in vitro* studies. Isolated cardiomyocytes from healthy dogs incubated by PI3K inhibitors for two hours showed a prolonged APD_{90} and diminished densities of the two main repolarizing currents (I_{Ks} and I_{Kr}).[16] Despite the diminished I_{Ks} found in the current study, we could not confirm APD_{90} lengthening in isolated cells from hearts after chronic treatment of PI3K inhibitor omipalisib. The diminished $I_{Ca,L}$ density in dog cells incubated with PI3K inhibitor nilotinib[16] and in cells isolated from p110α deficient mice[43] could serve as an explanation for the shorter APD of isolated cells from omipalisib-treated dogs. Furthermore, APD_{50} shortening with similar absolute levels as APD_{90} shortening supports this view on a role of decreased $I_{Ca,L}$ densities. Clearly, absence of measuring $I_{Ca,L}$ densities in the isolated myocytes must be regarded as a limitation of the current study. Nevertheless, as is known, 1) the gap between single-cell measurements lacking environmental influences and *in vivo* proarrhythmic conditions (anesthesia and bradycardia), and 2) incubation duration differences between our and previous studies may add to the contrasting outcome of this and earlier studies on APD_{90} in isolated cells.

PI3K signaling is also involved in glucose regulation and inhibition of the pathway is linked to development of hyperglycemia.[44] A study in mongrel dogs with diabetes showed prolongation of the QT interval and a diminished I_{Ks} density, which could be prevented by insulin.[45] Despite the similar findings on I_{Ks} density and hyperglycemia as common side effect of PI3K inhibition, the lack of assessment of glucose markers in the current study cannot reveal a link between omipalisib-induced effects on glucose metabolism and repolarization prolongation.

In clinical trials, detailed insight into electrophysiological effects of omipalisib is lacking while examination of cardiac toxicity is a standard item of investigation in drug testing. ECG parameters were addressed in one article and, besides a clinically insignificant reduced heart rate, no abnormalities were reported as adverse events.[25] Omipalisib was combined with the RAS/RAF/MEK pathway inhibitor trametinib in a phase Ib trial and showed poor tolerability due to overlapping adverse events.[24] ECG and echocardiogram were included in the study design, but unfortunately no outcome was reported.

Mild proarrhythmic outcome: safe or warning?

Under standardized proarrhythmic conditions – including anesthesia, bradycardia, and a dofetilide challenge – chronic omipalisib treatment induces prolongation of the QT interval of >100 ms and increases STV. Current guidelines in evaluating drug safety focus on I_{Kr} block and QT prolongation, while compounds can affect multiple ion channels as is shown for omipalisib. STV was suggested as a parameter superior to QT interval prolongation in evaluating the proarrhythmic risk of compounds as established in the AV block dog model.[46,47] Furthermore, 20% of the dogs showed arrhythmic events in the form of ectopic beats perpetuating in self-terminating TdP arrhythmias after omipalisib treatment. Intervening with defibrillation was not required in the animals treated with omipalisib for twice a day, though the initiation of such ventricular arrhythmias can be fatal when sustained. Both dogs with TdP arrhythmias showed the highest omipalisib plasma levels at the induction experiment (day 7), and plasma levels were highly diverse between animals. It should be acknowledged that the accuracy of pharmacokinetics suffers from interindividual[48] and interspecies variability.[49] Omipalisib plasma concentrations were compared to target concentrations found in clinical trials, in which plasma level variability and similar adverse events were determined.[23] Obviously, the effectiveness of anti-cancer treatment should be weighed against the accompanied cardiotoxic effects. This, with a special focus on cardioprotection in patients susceptible to the development of cardiac disease based on additional risk factors, comorbidity, and genetic profile.[10] Integration of knowledge in the cardiology and oncology field is crucial here.

Study limitations

As a first approach, three dogs received omipalisib once a day to determine its effect on electrophysiological parameters and if target levels were reached. The small sample size may have affected the reliability of the described findings. Furthermore, inhibition of the PI3K pathway affects many more cellular processes than solely cardiac electrical remodeling. Underlying mechanisms resulting from drug-induced adverse effects and potential omipalisib metabolites may have interfered in the study. In addition, the effect of the drug-drug interaction between omipalisib and dofetilide cannot be excluded.

Acknowledgments

We thank Dr. T.P. de Boer (Department of Medical Physiology, UMC Utrecht) for supporting the cellular electrophysiology experiments.

References

1. Yu JS, Cui W. Proliferation, survival and metabolism: the role of PI3K/AKT/mTOR signalling in pluripotency and cell fate determination. *Development.* 2016;143(17):3050-3060.
2. Samuels Y, Waldman T. Oncogenic mutations of PIK3CA in human cancers. *Curr Top Microbiol Immunol.* 2010;347:21-41.
3. Kandoth C, McLellan MD, Vandin F, et al. Mutational landscape and significance across 12 major cancer types. *Nature.* 2013;502(7471):333-339.
4. Varshney P, Saini N. PI3K/AKT/mTOR activation and autophagy inhibition plays a key role in increased cholesterol during IL-17A mediated inflammatory response in psoriasis. *Biochim Biophys Acta Mol Basis Dis.* 2018;1864(5 Pt A):1795-1803.
5. Zucco AJ, Pozzo VD, Afinogenova A, Hart RP, Devinsky O, D'Arcangelo G. Neural progenitors derived from tuberous sclerosis complex patients exhibit attenuated PI3K/AKT signaling and delayed neuronal differentiation. *Mol Cell Neurosci.* 2018;92:149-163.
6. Fruman DA, Chiu H, Hopkins BD, Bagrodia S, Cantley LC, Abraham RT. The PI3K pathway in human disease. *Cell.* 2017;170(4):605-635.
7. Vanhaesebroeck B, Perry MWD, Brown JR, Andre F, Okkenhaug K. PI3K inhibitors are finally coming of age. *Nat Rev Drug Discov.* 2021;20(10):741-769.
8. Mayer IA, Arteaga CL. The PI3K/AKT pathway as a target for cancer treatment. *Annu Rev Med.* 2016;67:11-28.
9. Mishra R, Patel H, Alanazi S, Kilroy MK, Garrett JT. PI3K inhibitors in cancer: clinical implications and adverse effects. *Int J Mol Sci.* 2021;22(7):3464.
10. Teske AJ, Linschoten M, Kamphuis JAM, et al. Cardio-oncology: an overview on outpatient management and future developments. *Neth Heart J.* 2018;26(11):521-532.
11. Durrant TN, Hers I. PI3K inhibitors in thrombosis and cardiovascular disease. *Clin Transl Med.* 2020;9(1):8.
12. Van Bavel JJA, Vos MA, Van der Heyden MAG. Cardiac arrhythmias and antiarrhythmic drugs: an autophagic perspective. *Front Physiol.* 2018;9:127.
13. McLean BA, Zhabyeyev P, Pituskin E, Paterson I, Haykowsky MJ, Oudit GY. PI3K inhibitors as novel cancer therapies: implications for cardiovascular medicine. *J Card Fail.* 2013;19(4):268-282.

14. Ballou LM, Lin RZ, Cohen IS. Control of cardiac repolarization by phosphoinositide 3-kinase signaling to ion channels. *Circ Res.* 2015;116(1):127-137.
15. Yang KC, Tseng YT, Nerbonne JM. Exercise training and PI3Kalpha-induced electrical remodeling is independent of cellular hypertrophy and Akt signaling. *J Mol Cell Cardiol.* 2012;53(4):532-541.
16. Lu Z, Wu CY, Jiang YP, et al. Suppression of phosphoinositide 3-kinase signaling and alteration of multiple ion currents in drug-induced long QT syndrome. *Sci Transl Med.* 2012;4(131):131ra150.
17. Knight SD, Adams ND, Burgess JL, et al. Discovery of GSK2126458, a highly potent inhibitor of PI3K and the mammalian target of rapamycin. *ACS Med Chem Lett.* 2010;1(1):39-43.
18. Leung E, Kim JE, Rewcastle GW, Finlay GJ, Baguley BC. Comparison of the effects of the PI3K/mTOR inhibitors NVP-BEZ235 and GSK2126458 on tamoxifen-resistant breast cancer cells. *Cancer Biol Ther.* 2011;11(11):938-946.
19. Feng Y, Jiang Y, Hao F. GSK2126458 has the potential to inhibit the proliferation of pancreatic cancer uncovered by bioinformatics analysis and pharmacological experiments. *J Transl Med.* 2021;19(1):373.
20. Zhu DS, Dong JY, Xu YY, Zhang XT, Fu SB, Liu W. Omipalisib inhibits esophageal squamous cell carcinoma growth through inactivation of phosphoinositide 3-kinase (PI3K)/AKT/Mammalian target of rapamycin (mTOR) and ERK signaling. *Med Sci Monit.* 2020;26:e927106.
21. Mercer PF, Woodcock HV, Eley JD, et al. Exploration of a potent PI3 kinase/mTOR inhibitor as a novel anti-fibrotic agent in IPF. *Thorax.* 2016;71(8):701-711.
22. Narov K, Yang J, Samsel P, Jones A, Sampson JR, Shen MH. The dual PI3K/mTOR inhibitor GSK2126458 is effective for treating solid renal tumours in Tsc2(+/-) mice through suppression of cell proliferation and induction of apoptosis. *Oncotarget.* 2017;8(35):58504-58512.
23. Munster P, Aggarwal R, Hong D, et al. First-in-human phase I study of GSK2126458, an oral pan-class I phosphatidylinositol-3-kinase inhibitor, in patients with advanced solid tumor malignancies. *Clin Cancer Res.* 2016;22(8):1932-1939.
24. Grilley-Olson JE, Bedard PL, Fasolo A, et al. A phase Ib dose-escalation study of the MEK inhibitor trametinib in combination with the PI3K/mTOR inhibitor GSK2126458 in patients with advanced solid tumors. *Invest New Drugs.* 2016;34(6):740-749.
25. Lukey PT, Harrison SA, Yang S, et al. A randomised, placebo-controlled study of omipalisib (PI3K/mTOR) in idiopathic pulmonary fibrosis. *Eur Respir J.* 2019;53(3):1801992.
26. Loen V, Vos MA, Van der Heyden MAG. The canine chronic atrioventricular block model in cardiovascular preclinical drug research. *Br J Pharmacol.* 2022;179(5):859-881.
27. Oros A, Beekman JD, Vos MA. The canine model with chronic, complete atrio-ventricular block. *Pharmacol Ther.* 2008;119(2):168-178.
28. Volders PG, Sipido KR, Vos MA, et al. Downregulation of delayed rectifier K(+) currents in dogs with chronic complete atrioventricular block and acquired torsades de pointes. *Circulation.* 1999;100(24):2455-2461.
29. Ramakers C, Vos MA, Doevendans PA, et al. Coordinated down-regulation of KCNQ1 and KCNE1 expression contributes to reduction of I(Ks) in canine hypertrophied hearts. *Cardiovasc Res.* 2003;57(2):486-496.
30. Van de Water A, Verheyen J, Xhonneux R, Reneman RS. An improved method to correct the QT interval of the electrocardiogram for changes in heart rate. *J Pharmacol Methods.* 1989;22(3):207-217.
31. Thomsen MB, Verduyn SC, Stengl M, et al. Increased short-term variability of repolarization predicts d-sotalol-induced torsades de pointes in dogs. *Circulation.* 2004;110(16):2453-2459.
32. Van der Linde HJ, Van Deuren B, Somers Y, Loenders B, Towart R, Gallacher DJ. The electro-mechanical window: a risk marker for torsade de pointes in a canine model of drug induced arrhythmias. *Br J Pharmacol.* 2010;161(7):1444-1454.
33. Stams TRG, Winckels SKG, Oros A, et al. Novel parameters to improve quantification of repolarization reserve and arrhythmogenesis using a dofetilide challenge. *Heart Rhythm.* 2013;10(11):1745-1746.
34. Smoczyńska A, Beekman HD, Vos MA. The increment of short-term variability of repolarisation

determines the severity of the imminent arrhythmic outcome. *Arrhythm Electrophysiol Rev.* 2019;8(3):166-172.

35. Dolman ME, Westerhout EM, Hamdi M, Schellens JH, Beijnen JH, Sparidans RW. Liquid chromatography-tandem mass spectrometric assay for the PI3K/mTOR inhibitor GSK2126458 in mouse plasma and tumor homogenate. *J Pharm Biomed Anal.* 2015;107:403-408.
36. Bossu A, Houtman MJC, Meijborg VMF, et al. Selective late sodium current inhibitor GS-458967 suppresses torsades de pointes by mostly affecting perpetuation but not initiation of the arrhythmia. *Br J Pharmacol.* 2018;175(12):2470-2482.
37. Bourgonje VJA, Van Veen TAB, Vos MA. Ventricular electrical remodeling in compensated cardiac hypertrophy. In: Gussak I, Antzelevitch C, eds. *Electrical Diseases of the Heart*. London: Springer-Verlag; 2013:387-398.
38. Gould J, Sieniewicz B, Porter B, Sidhu B, Rinaldi CA. Chronic right ventricular pacing in the heart failure population. *Curr Heart Fail Rep.* 2018;15(2):61-69.
39. Lewis AJM, Foley P, Whinnett Z, Keene D, Chandrasekaran B. His bundle pacing: a new strategy for physiological ventricular activation. *J Am Heart Assoc.* 2019;8(6):e010972.
40. Vos MA, de Groot SH, Verduyn SC, et al. Enhanced susceptibility for acquired torsade de pointes arrhythmias in the dog with chronic, complete AV block is related to cardiac hypertrophy and electrical remodeling. *Circulation.* 1998;98(11):1125-1135.
41. Antoons G, Volders PG, Stankovicova T, et al. Window Ca2+ current and its modulation by Ca2+ release in hypertrophied cardiac myocytes from dogs with chronic atrioventricular block. *J Physiol.* 2007;579(Pt 1):147-160.
42. De Groot SH, Schoenmakers M, Molenschot MM, Leunissen JD, Wellens HJ, Vos MA. Contractile adaptations preserving cardiac output predispose the hypertrophied canine heart to delayed afterdepolarization-dependent ventricular arrhythmias. *Circulation.* 2000;102(17):2145-2151.
43. Lu Z, Jiang YP, Wang W, et al. Loss of cardiac phosphoinositide 3-kinase p110 alpha results in contractile dysfunction. *Circulation.* 2009;120(4):318-325.
44. Khan KH, Wong M, Rihawi K, et al. Hyperglycemia and phosphatidylinositol 3-kinase/protein kinase B/mammalian target of rapamycin (PI3K/AKT/mTOR) inhibitors in phase I trials: incidence, predictive factors, and management. *Oncologist.* 2016;21(7):855-860.
45. Lengyel C, Virag L, Biro T, et al. Diabetes mellitus attenuates the repolarization reserve in mammalian heart. *Cardiovasc Res.* 2007;73(3):512-520.
46. Varkevisser R, Wijers SC, Van der Heyden MA, Beekman JD, Meine M, Vos MA. Beat-to-beat variability of repolarization as a new biomarker for proarrhythmia in vivo. *Heart Rhythm.* 2012;9(10):1718-1726.
47. Bossu A, Varkevisser R, Beekman HDM, Houtman MJC, Van der Heyden MAG, Vos MA. Short-term variability of repolarization is superior to other repolarization parameters in the evaluation of diverse antiarrhythmic interventions in the chronic atrioventricular block dog. *J Cardiovasc Pharmacol.* 2017;69(6):398-407.
48. Nicolas JM, Espie P, Molimard M. Gender and interindividual variability in pharmacokinetics. *Drug Metab Rev.* 2009;41(3):408-421.
49. Daublain P, Feng KI, Altman MD, et al. Analyzing the potential root causes of variability of pharmacokinetics in preclinical species. *Mol Pharm.* 2017;14(5):1634-1645.

Supplementary material

Suppl. table 1. Electrophysiological and contractile parameters of dogs (n=3) before and after 1 mg/kg omipalisib twice a day during baseline followed by dofetilide and ouabain.

	Control			Omipalisib		
Parameter	**Baseline**	**Dofetilide**	**Ouabain**	**Baseline**	**Dofetilide**	**Ouabain**
RR	1000 ± 0	1000 ± 0	1000 ± 0	1000 ± 0	1000 ± 0	1000 ± 0
PP	496 ± 56	617 ± 89	681 ± 85 *	530 ± 101	613 ± 173	651 ± 170 *
QRS	128 ± 9	128 ± 9	130 ± 11	139 ± 9 *	136 ± 7	136 ± 9
QT	375 ± 19	500 ± 49 *	534 ± 36 *	451 ± 27 *	636 ± 44 *^#	582 ± 10 *#&
JT	248 ± 20	372 ± 55 *	404 ± 46 *	312 ± 19 *	500 ± 49 *^#	446 ± 13 *#
$QLVP_{end}$	470 ± 41	478 ± 48	467 ± 20	424 ± 60	422 ± 51	404 ± 38
EMW	94 ± 52	-22 ± 96 *	-67 ± 54 *^	-27 ± 59 *	-214 ± 16 *^#	-177 ± 31 *$#&
$LVdP/dt_{max}$	1185 ± 500	1443 ± 474	2424 ± 667 *^	1058 ± 145	1489 ± 227 #	2290 ± 244 *#&
$LVdP/dt_{min}$	-1211 ± 430	-1363 ± 282	-1955 ± 422 *	-1028 ± 301	-1391 ± 258	-1939 ± 93 *#

Parameters in ms, except for $LVdP/dt_{max}$ and LVdP/dt in mmHg/s. Data as mean ± SD. Timepoint ouabain: 15 min after onset of infusion. Repeated measures two-way ANOVA with Tukey's multiple comparisons test. *p<0.05 compared to control baseline, ^p<0.05 compared to control dofetilide, $^{\$}$p<0.05 compared to control ouabain, $^{\#}$p<0.05 compared to omipalisib baseline, and $^{\&}$p<0.05 compared to omipalisib dofetilide.

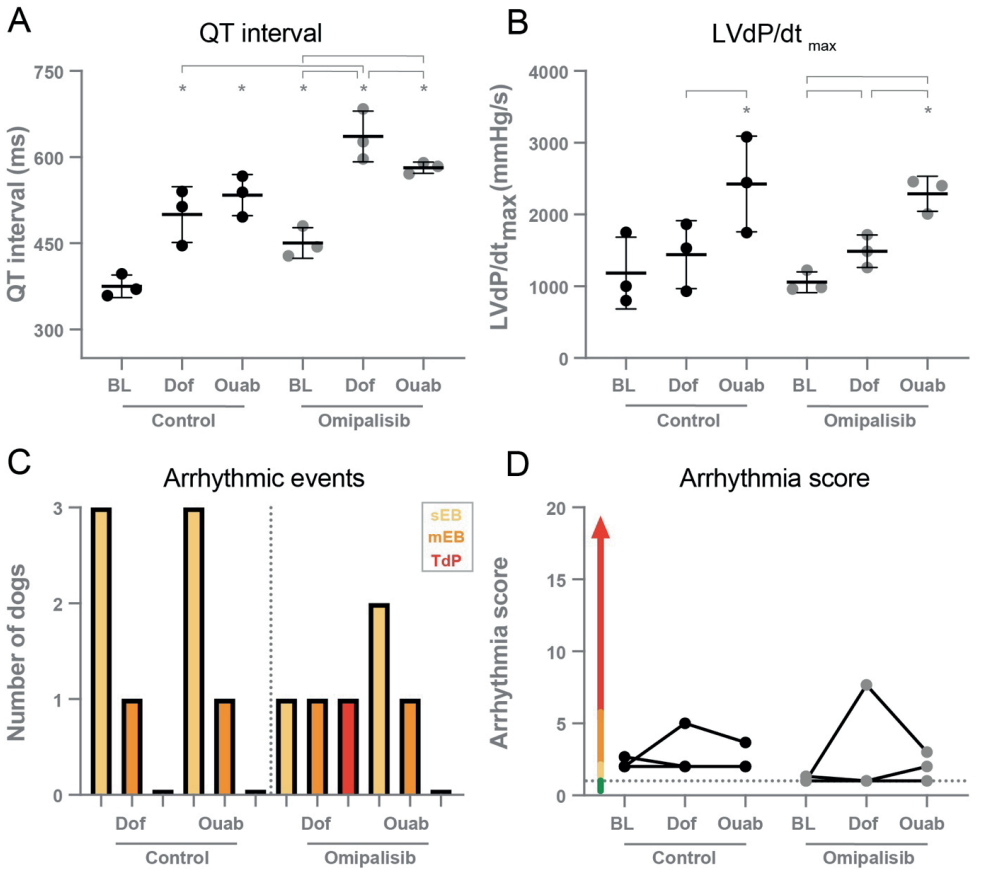

Suppl. figure 1. A) QT interval and **B**) LVdP/dt_{max} of dogs before and after 1mg/kg omipalisib twice a day at baseline (BL), dofetilide (Dof), and 15 min after start ouabain (Ouab). Data are presented as mean ± SD. Repeated measures two-way ANOVA with Tukey's multiple comparisons test. *p<0.05 compared to control BL, and for bars. **C**) Incidence of arrhythmic events and **D**) arrhythmia score before and after omipalisib during 10 min after start Dof and 15 min after start Ouab. Single ectopic beats (sEB, score: 2 points), multiple ectopic beats (mEB, scored with 3-5 points), and Torsade de Pointes (TdP) arrhythmia (scored with 6-49 points). TdP arrhythmia demanding defibrillation were scored with 50, 75, or 100 points depending on the number of shocks.

4

I_{Ks} inhibitor JNJ303 prolong the QT interval and perpetuates arrhythmia when combined with enhanced inotropy in the CAVB dog

Joanne J.A. van Bavel[1], Henriëtte D.M. Beekman[1], Valerie Y.H. van Weperen[1], Henk J. van der Linde[2], Marcel A.G. van der Heyden[1], Marc A. Vos[1]

[1] Department of Medical Physiology, Division of Heart and Lungs, University Medical Center Utrecht, Utrecht, the Netherlands
[2] Janssen Research & Development, Division of Janssen Pharmaceutica NV, Beerse, Belgium

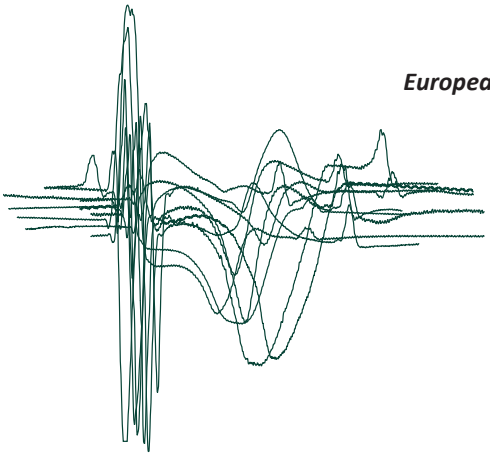

***European Journal of Pharmacology*, 2022, 932:175218**

Abstract

Impaired I_{Ks} induced by drugs or due to a KCNQ1 mutation, diagnosed as long QT syndrome type 1 (LQT1) prolongs the QT interval and predisposes the heart to Torsade de Pointes (TdP) arrhythmias. The anesthetized chronic AV block (CAVB) dog is inducible for TdP after remodeling and I_{Kr} inhibitor dofetilide. We tested the proarrhythmic effect of I_{Ks} inhibition in the CAVB dog, and the proarrhythmic role of increased contractility herein.

Dofetilide-inducible animals were included to test the proarrhythmic effect of 1) I_{Ks} inhibition by JNJ303 (0.63 mg/kg/10min i.v.; n=4), 2) I_{Ks} inhibition combined with enhanced inotropy (ouabain, 0.045 mg/kg/1min i.v.; n=6), and 3) the washout period of the anesthetic regime (n=10).

JNJ303 prolonged the QTc interval (from 477 ± 53 ms to 565 ± 14 ms, P<0.02) resembling standardized dofetilide-induced QTc prolongation. Single ectopic beats (n=4) and ventricular tachycardia (VT) (n=3) were present, increasing the arrhythmia score (AS) from 1.0 ± 0 to 7.1 ± 6.5. JNJ303 combined with ouabain increased contractile parameters ($LVdP/dt_{max}$ from 1725 ± 273 to 4147 ± 611 mmHg/s, P<0.01). Moreover, TdP arrhythmias were induced in 4/6 dogs and AS increased from 1.0 ± 0 to 20.2 ± 19.0 after JNJ303 and ouabain (P<0.05). Finally, TdP arrhythmias were induced in 4/10 dogs during the anesthesia washout period and the AS increased from 1.1 ± 0.3 to 9.2 ± 11.2.

Mimicking LQT1 using I_{Ks} inhibitor JNJ303 prolongs the QTc interval and triggers ectopic beats and non-sustained VT in the CAVB dog. Induction of the more severe arrhythmic events (TdP) demands a combination of I_{Ks} inhibition with enhanced inotropy or ending the anesthetic regime.

Keywords

JNJ303, I_{Ks}, CAVB dog model, ventricular arrhythmia, QT interval, contractility

Introduction

The repolarization phase of the cardiac action potential is a highly regulated process in which various ion channels, pumps, and the autonomic nervous system all play an essential role. In drug development, the mandatory evaluation of repolarization prolongation and proarrhythmic risk is limited to hERG channel (responsible for I_{Kr}, main repolarizing current) assays and non-clinical and clinical QT assays as reflected in the ICH S7B and E14 guidelines. Nevertheless, during the last decade focus of testing has changed towards the inclusion of multiple ion channels as proposed by the CiPA initiative and in enhancing the value of nonclinical assays by linking the ICH S7B and E14 guidelines.[1,2]

In terms of ion currents other than I_{Kr}, the second main potassium current active during the repolarization phase of the cardiac action potential is the slow delayed rectifier potassium current (I_{Ks}). A faster heart rate is associated with increased I_{Ks} as the sympathetic nervous system stimulates I_{Ks} through a signaling pathway involving β-adrenergic receptors, cAMP and protein-kinase A.[3] A loss-of-function mutation in the KCNQ1 gene causes long QT syndrome type 1 (LQT1), which is characterized by a high risk for Torsade de Pointes (TdP) arrhythmias with exercise and emotional stress as predominant triggers.[4,5]

The interest of screening for safety issues caused by I_{Ks} block has increased over the last two decades as more laboratories developed new screening methods for compounds that block I_{Ks}. JNJ38445303 (JNJ303) was synthesized as analogue from a compound with high potency for 11β-hydroxysteroid dehydrogenase type 1 enzyme inhibition as potential anti-obesity/diabetes drug.[6] JNJ303 solely blocking I_{Ks} was suggested as cause of arrhythmic events in beagle dogs since binding profile assays revealed that JNJ303 has little or no effect on other ion channels involved in ventricular repolarization.[6] A disturbed calcium handling was one of the other suggested possible contributors to the proarrhythmic conditions. Intracellular Ca^{2+} overload and spontaneous Ca^{2+} release can cause early and delayed afterdepolarizations especially in situations of repolarization prolongation, resulting in electrical heterogeneity and thereby arrhythmic conditions. The perspective on I_{Ks} block in safety screening reported no further details on QT prolongation and arrhythmia quantification.

We examined if JNJ303 induced repolarization prolongation and proarrhythmic conditions in a translational dog model with proarrhythmic vulnerability. The chronic atrioventricular (AV) block (CAVB) dog is a model of compensated hypertrophy, and remodeling-induced contractile (altered calcium handling) and electrical (diminished I_{Kr} and I_{Ks}) changes. A combination of ventricular remodeling after AV block, a reduced repolarization reserve, bradycardia and anesthesia predispose the heart to TdP arrhythmias, and I_{Kr} blocker dofetilide acts as final hit for TdP induction with high reproducibility.[7,8] This model has been standardized over the last decades and experimental protocols predominantly included I_{Kr} as target for affecting the repolarization reserve.

In this study, we hypothesize that disturbance of the repolarization reserve by inhibition of I_{Ks} with JNJ303 initiates repolarization prolongation in the remodeled CAVB dog. Addition of an enhanced inotropic response – above the AV block-induced alterations in calcium handling – to the prolonged repolarization is a potential trigger of ectopic beats and more severe arrhythmic events. In these conditions, the proarrhythmic outcome was further examined.

Materials and methods

Animals

Animal care and experimentation were approved by the Committee for Experiments on Animals of Utrecht University (application approval number: AVD115002016531) and were in accordance with the Directive 2010/63/EU of the European Parliament and the Dutch law on animal experimentation. Dogs were housed in pairs in kennels with wooden bedding material, had ad libitum access to water and received food pellets twice a day. The animals were allowed to play outside once a day for 2 h with access to playing toys, and their welfare was checked daily.

Anesthetic regime and AV block

Animals were fasted overnight and received premedication (0.02 mg/kg i.m. atropine, 0.5 mg/kg i.m. methadone, 0.5 mg/kg i.m. acepromazine and 0.1 mg/kg s.c. Meloxicam) half an hour prior to the surgical procedure. The anesthetic regime was induced by sodium pentobarbital (Pentobarbital, 25 mg/kg i.v.) and maintained by 1.5% isoflurane in O_2 and N_2O (1:2 ratio) via mechanical ventilation at 12 breaths/min. Ampicillin (1000 mg) was

administered before (i.v.) and after (i.m.) surgery, and Buprenorphine (0.3 mg, i.m.) was provided after surgery.

AV block was induced by radiofrequency ablation of the His bundle.[9] After ventricular remodeling for 3 ± 0.5 weeks, the dogs underwent the inducibility experiment at which I_{Kr} blocker dofetilide (0.025 mg/kg, i.v.) was infused for 5 min or until the first TdP (ventricular arrhythmia >6 complexes) occurred. Dogs were considered inducible when showing three or more TdP arrhythmias within 10 min after the start of dofetilide infusion.

Experimental protocol

Two groups of anesthetized dogs inducible for TdP arrhythmias by dofetilide were included in the subsequent JNJ303 protocol.

First, the effect of I_{Ks} inhibitor JNJ303 on the QT interval and arrhythmic outcome in the CAVB dog was examined (**Figure 1A**). Four inducible purpose-bred mongrel dogs (Marshall, New York, USA, one male and three females, bodyweight: 24 ± 4 kg, age: 16 ± 2 months) at CAVB for 8 ± 3 weeks received JNJ303 (0.63 mg/kg, i.v.) for 10 min. The dose was identical to the lowest dose tested causing TdP in anesthetized healthy beagle dog.[6] Surface ECG, monophasic action potential from the LV and RV (LV MAP and RV MAP respectively, catheters from Hugo Sachs Elektronik, Germany) and LV pressure (LV-P, using a 7F catheter, CD Leycom Inc., Zoetermeer, the Netherlands) signals were recorded with a sampling rate of 1 kHz continuously during the experiment (10 min infusion time and 50 min follow-up time) using EP Tracer (Cardiotek, Maastricht, The Netherlands).

Secondly, the effect of I_{Ks} inhibition combined with enhanced inotropy was examined by infusion of JNJ303 for 10 min followed by infusion of Na^+/K^+-ATP-pump inhibitor ouabain (0.045 mg/kg, i.v.) for 1 min (**Figure 1B**). The dose was based on previous work by our group in which this single dose of ouabain did not induce arrhythmias in the CAVB dog.[10] Six inducible mongrel dogs (two males and four females, bodyweight: 26 ± 1 kg and age: 14 ± 3 months) at CAVB for 10 ± 1 weeks were included. Again, surface ECG, LV MAP, RV MAP and LV-P signals were recorded continuously during the experiment until 1 h after the start of JNJ303.

After 1 h of follow-up time after the start of JNJ303 infusion, catheters were removed, and the anesthetic regime was ended. All ten dogs were followed for 15 min (including continuous ECG recording) during the washout period of the anesthetic regime (**Figure 1**). The mechanical ventilation was switched to spontaneous ventilation ± 5 min after the stop of isoflurane.

Figure 1. Schematic overview of the experimental protocol. **A**) Four inducible chronic AV block (CAVB) dogs received I_{Ks} blocker JNJ303 (0.63mg/kg, i.v.) for 10 min. **B**) Six inducible CAVB dogs received JNJ303 for 10 min followed by Na^+/K^+-ATPase pump inhibitor ouabain (0.045mg/kg, i.v.) for 1 min. Signals in baseline (BL) were recorded for 5 min and follow-up time was until 1 h after the start of JNJ303 infusion. Asterisk refers to finishing of the experimental protocol, after which the anesthetic regime was ended. ECG signals were recorded for 15 min during the washout period.

Compounds

I_{Kr} blocker dofetilide (Biorbyt, Cambridge, United Kingdom) was dissolved in 0.1M HCl and further prepared in 0.9% saline solution. JNJ303 (Janssen, Beerse, Belgium) was dissolved in 20% hydroxypropyl-β-cyclodextrin at a concentration of 1.25 mg/ml, a pH of 3.75 and an osmolality of 312 mOsmol/kg. Ouabain octahydrate (Sigma-Aldrich, Inc., St. Louis, MO, United States) was dissolved in cold water in a concentration of 10 mg/ml.

Data analysis

Five consecutive beats from lead II were measured manually in EP Tracer to obtain the interval duration of ECG parameters RR, PP, QRS, QT and JT. The QT interval was corrected for heart rate (QTc) using the Van de Water formula.[11] The JT was obtained by subtracting the QRS interval from the QT interval. The interval between the J-point and the peak of the T-wave ($JT_{peak}c$),[12] corrected for heart rate) and the interval between the peak of the T-wave and end of the T-wave (T_{peak}-T_{end})[13] were measured reflecting the early repolarization phase and total dispersion of repolarization (SDR), respectively. Ectopic beats and beats with a P-wave in the

T-wave end were excluded. As a measure of temporal dispersion of repolarization, the short-term variability of repolarization of the QT interval (STV QT) and MAP duration (STV LV MAPD and STV RV MAPD) were calculated by the formula: STV-QT= $\sum|D_{n+1}-D_n|/[30 \times \sqrt{2}]$.[14] D corresponds to the QT intervals of 31 consecutive beats manually measured in EP tracer, and MAP durations of 31 consecutive beats measured semi-automatically using AutoMAPD (MATLAB, Mathworks, Natick, MA, USA). The duration of five consecutive LV-P cycles was manually measured in EP Tracer by selecting the start of the QRS on the surface ECG and the end of the pressure cycle ($QLVP_{end}$). Calculation of the electromechanical window (EMW) was by subtraction of the QT interval from the $QLVP_{end}$.[15] The maximum and minimum of the derivative of the LV-P signal, referring to the point where the slope of the pressure rise and fall is the steepest ($LVdP/dt_{max}$ and $LVdP/dt_{min}$, respectively), were manually measured offline using AutoMAPD (MATLAB, Mathworks, Natick, MA, USA). The mean LVdP/dt was based on five consecutive LV-P cycles.

The arrhythmic outcome was quantified by scoring all arrhythmic events and by calculating the arrhythmia score (quantification of the severity of the arrhythmic outcome).[16,17] Regular beats were scored with 1 point, single ectopic beats (sEB) with 2 points, multiple ectopic beats (mEB) with 3-5 points, and monomorphic ventricular tachycardia (VT, defined as periods of ventricular rates >100 bpm yet with proper cardiac output based on blood pressure signal) and self-terminating TdP arrhythmias with 6-49 points. TdP arrhythmias received a score of 50, 75, or 100 when one, two or three (or more) defibrillations were needed to terminate the arrhythmia, respectively. The arrhythmia score is based on the average of the three highest individual scores within a certain time window,[16] which consisted of 10 min after the onset of dofetilide infusion and 1 h after the onset of JNJ303 infusion.

Statistical analysis

Data are presented as mean ± SD. Serial data were analyzed using a (un)paired Student's *t*-test, repeated measures one-way or two-way analysis of variance (ANOVA), with Tukey's test for multiple comparisons. Statistical analyses were performed with GraphPad Prism (version 9.1.0, GraphPad Software, San Diego, USA). A value of $P<0.05$ was considered statistically significant.

Results

I_{Ks} inhibitor JNJ303 prolongs the QT interval in the CAVB dog

In the serial experiments, both JNJ303 and dofetilide significantly prolonged the PP interval, while the RR and QRS intervals were unaffected (**Table 1, Suppl. table 1**). Repolarization parameters were significantly altered by JNJ303, as presented by a prolonged QT, QTc, and JTc interval (**Table 1**). The prolongation of the QT and QTc interval by JNJ303 was similar to dofetilide (**Table 1, Suppl. table 1**). Temporal dispersion of repolarization was enhanced by JNJ303 in the LV, reflected by a significant increase of the STV LV MAPD. Though not significant, a trend towards an increased SDR was shown by prolonged $JT_{peak}c$ and T_{peak}-T_{end} intervals. Furthermore, JNJ303 increased contractility ($LVdP/dt_{max}$) and prolonged the EMW (**Table 1**). The $QLVP_{end}$ and $LVdP/dt_{min}$ were not significantly altered.

I_{Ks} inhibitor JNJ303 initiates ectopic beats and ventricular tachycardia

Within 1 h after start of JNJ303 infusion, sEB were present in all dogs and three showed monomorphic VTs lasting maximal 27 s during the 1-h time window after the start of JNJ303 (**Figures 2A and 2C, Suppl. figure 1**). Despite the evident QTc prolongation, JNJ303 induced no proarrhythmic events with severe consequences, as no mEB or TdP arrhythmias were determined. The ectopic beats and VT resulted in a small rise of the arrhythmia score from 1 in baseline (no events) to 2.0 - 16.7 after JNJ303 (**Figure 2B**). In the same animals, dofetilide induced sEB which perpetuated into mEB and TdP arrhythmias (**Suppl. figure 1**) in all dogs and increased the arrhythmia score to 50.8 ± 10 (**Suppl. table 1**).

Table 1. Electrophysiological and contractile parameters of dogs with chronic AV block (CAVB) after infusion of JNJ303, and after JNJ303 followed by ouabain.

Parameter	Baseline	JNJ303	% Increase	Baseline	JNJ303 + ouabain	% Increase
RR	1425 ± 98	1498 ± 115	5	1419 ± 159	1537 ± 146	8
PP	565 ± 57	620 ± 57 *	10	540 ± 69	632 ± 72 *	17
QRS	90 ± 10	101 ± 18	12	109 ± 14 ^	96 ± 15	-12
QT	514 ± 58	608 ± 22 *	18	493 ± 69	558 ± 36 *^	13
QTc	477 ± 53	565 ± 14 *	19	456 ± 64	511 ± 32 ^	12
JT	424 ± 60	507 ± 33 *	20	383 ± 71	462 ± 31 *	21
JTc	387 ± 55	464 ± 27 *	20	347 ± 66	415 ± 26 *^	20
$JT_{peak}c$	213 ± 23	244 ± 63	15	192 ± 55	222 ± 32 *	16
T_{peak}-T_{end}	174 ± 45	221 ± 41	27	155 ± 28	193 ± 37	24
STV QT	5.9 ± 1.4	5.1 ± 2.0	-14	5.5 ± 1.8	6.0 ± 1.8	10
LV MAPD	334 ± 40	450 ± 47 *	35	ND	ND	
RV MAPD	290 ± 41	368 ± 91	27	ND	ND	
Δ MAPD	32 ± 72	63 ± 123	98	ND	ND	
STV LV MAPD	0.9 ± 0.2	4.6 ± 1.8 *	420	ND	ND	
STV RV MAPD	1.4 ± 0.7	4.5 ± 3.1	215	ND	ND	
$QLVP_{end}$	399 ± 17	396 ± 18	-1	413 ± 23	372 ± 30 *	-10
EMW	-115 ± 44	-211 ± 22 *	84	-75 ± 79	-184 ± 35 *	131
$LVdP/dt_{max}$	1800 ± 399	2339 ± 701 *	30	1725 ± 273	4147 ± 611 *^	140
$LVdP/dt_{min}$	1464 ± 173	1516 ± 154	4	1442 ± 155	2463 ± 582 *^	66
AS	1.0 ± 0	7.1 ± 6.5		1.0 ± 0	20.2 ± 19.0 *	
TdP	0%	0%		0%	66.7%	

Values are presented as mean ± SD. Parameters are at 30 min after the onset of JNJ303 in dogs at chronic atrioventricular block (CAVB) for 8 ± 3 weeks (n=4), and at 30 ± 8 min after the onset of JNJ303 followed by ouabain in dogs at CAVB for 10 ± 3 weeks (n=6). Increase in percentage of the averaged values. Paired *t*-test, *P<0.05 vs. baseline. Comparison JNJ303 + ouabain experiment vs. JNJ303 experiment, unpaired *t*-test: ^P<0.05. Parameters are in ms, except for $LVdP/dt_{max}$ and $LVdP/dt_{min}$ (mmHg/sec), and for AS and TdP incidence. N=3 for RV MAP, Δ MAPD, and STV RV MAPD. N=5 for $QLVP_{end}$, EMW, and $LVdP/dt_{min}$. AS = arrhythmia score; EMW = electromechanical window; $JT_{peak}c$ = J to T peak interval corrected for heart rate; LV = left ventricular; MAPD = monophasic action potential duration (measured at 80% of repolarization); ND = no data available; $QLVP_{end}$ = interval between Q on ECG and end of LV pressure cycle; QTc and JTc = QT and JT corrected for heart rate using the Van de Water formula; RV = right ventricular; STV = short-term variability of repolarization; TdP = Torsade de Pointes; T_{peak}-T_{end} = T-wave peak to T-wave end interval.

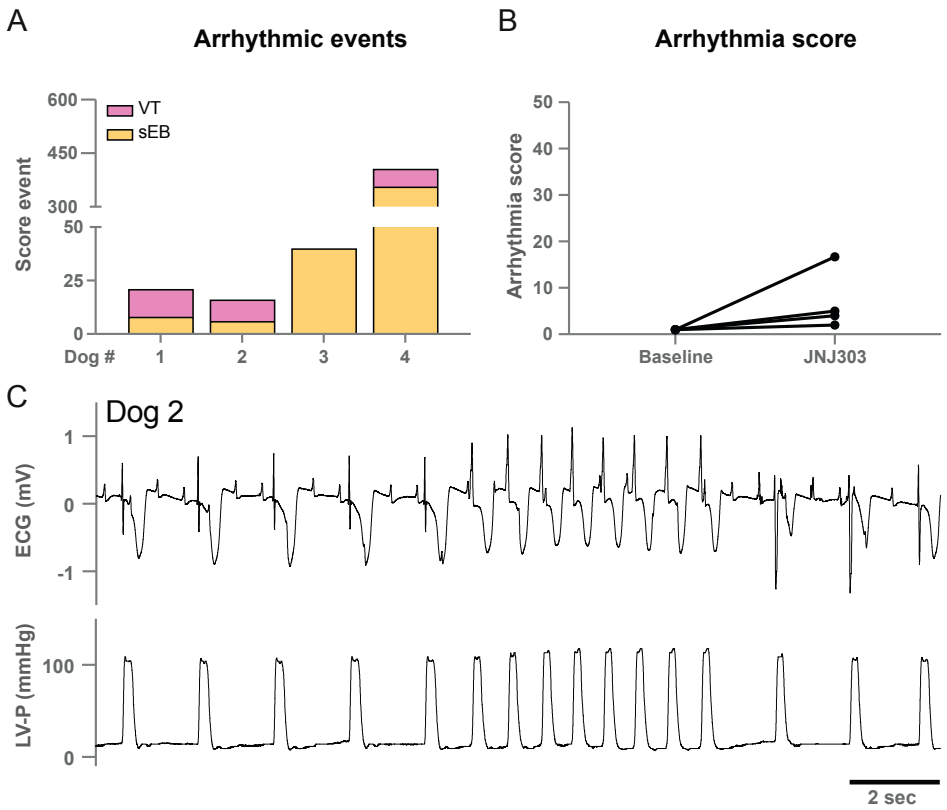

Figure 2. Arrhythmic events after JNJ303. **A**) Score of arrhythmic events and **B**) arrhythmia score per dog during 1 h after the start of JNJ303 infusion. Single ectopic beats (sEB, score: 2 points) and ventricular tachycardia (VT, score: 6-49 points). sEB and VT after JNJ303 infusion increased the arrhythmia score to 2.0 – 16.7. **C**) ECG and left ventricular pressure (LV-P) signals of dog #2 showing a self-terminating VT.

JNJ303 combined with ouabain is highly inotropic

To examine if enhancing contractility could perpetuate sEB, induced by solely JNJ303, into more severe arrhythmic events, ouabain was administered directly after JNJ303 infusion ended. The drug-induced increase in intracellular Ca^{2+}-load by ouabain enhanced inotropy in all six dogs. In **Table 1**, timepoint 'JNJ303 + ouabain' refers to 30 ± 8 min after the start of JNJ303 infusion, which is the average timepoint of the first TdP arrhythmia (dog #5, 6, 8 and 9) and mEB (dog #7) occurrence, and 30 min JNJ303 (dog #10). Similar to infusion of solely JNJ303 or dofetilide, the PP interval was prolonged after JNJ303 + ouabain (**Table 1**). In terms of repolarization, JNJ303 + ouabain prolonged the QT, JT and JTc intervals, though to a smaller extent compared to solely JNJ303 or dofetilide (**Table 1, Suppl. table 1**). Enhanced contractility by ouabain caused intracardiac MAP catheter motion resulting in a loss of stable

recording of the LV- and RVMAP signals, and therefore LV- and RV MAPD and their corresponding STV could not be determined. Similar to JNJ303 and dofetilide, addition of ouabain to JNJ303 did not affect STV QT (**Table 1**). Parameter $JT_{peak}c$ was significantly prolonged after addition of ouabain (from 192 ± 55 to 222 ± 32 ms, P<0.05) and T_{peak}-T_{end} showed a trend towards prolongation (from 155 ± 28 to 193 ± 37 ms, P= 0.08) (**Table 1**). Dofetilide prolonged both parameters (**Suppl. table 1**). In terms of contractility, JNJ303 + ouabain caused a 2.4-fold increase in $LVdP/dt_{max}$ compared to baseline (**Table 1, Figure 3C**). The enhanced inotropic response after ouabain was also acknowledged by the reduced $QLVP_{end}$ and prolonged EMW (**Table 1**). These parameters were also significantly altered by dofetilide. Nonetheless, the $LVdP/dt_{max}$ was certainly more increased after JNJ303 + ouabain compared to dofetilide (**Figure 3C)**.

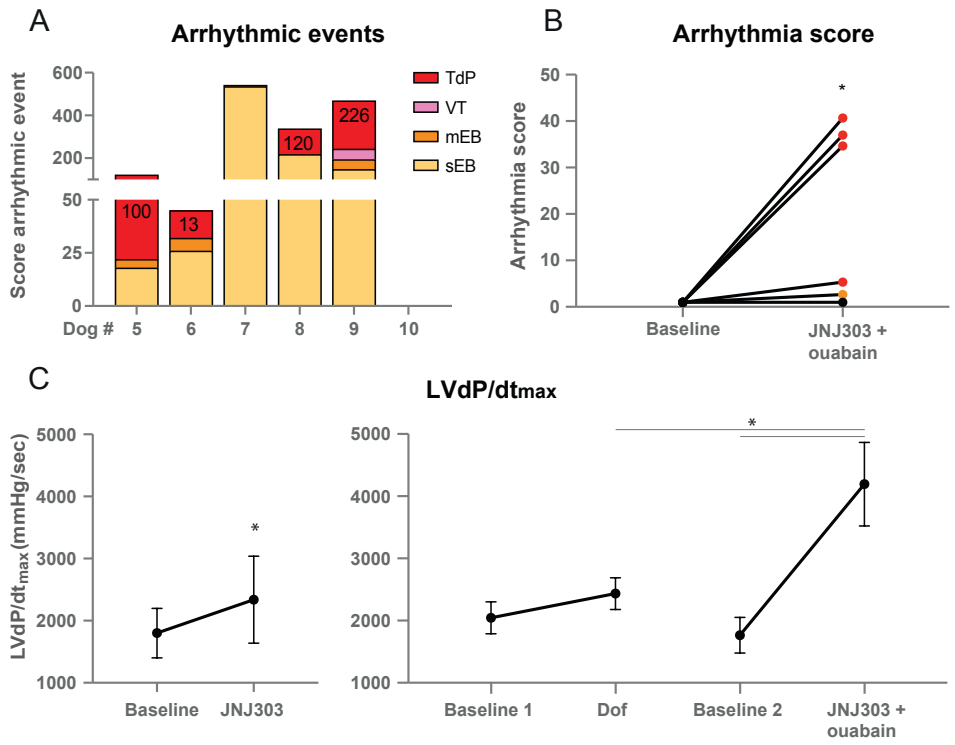

Figure 3. Arrhythmic events and contractility after JNJ303 + ouabain. **A**) Score of arrhythmic events and **B**) arrhythmia score per dog during 1 h after the start of JNJ303 infusion. Single ectopic beats (sEB, score: 2 points), multiple ectopic beats (mEB, score: 3-5 points), ventricular tachycardia (VT) and Torsade de Pointes (TdP) with score: 6-49 points. Score of shocked TdP = 50, 75 or 100 points. The sustained VT for dog #9 (Suppl. figure 2) was scored with 49 points as cardiac output was not affected. Arrhythmia score increased after JNJ303 + ouabain infusion to 1.0 – 40.7. Paired *t*-test, *P<0.05 compared to baseline. **C**) $LVdP/dt_{max}$: left panel; baseline and 30

min after start of JNJ303 (n=4, paired *t*-test, *P<0.05) and right panel; baseline 1 and before the first ectopic beat during dofetilide (Dof), and baseline 2 and 30 ± 8 min after start of JNJ303 (JNJ303 + ouabain, n=5, repeated measures two-way ANOVA, *P<0.05).

JNJ303 combined with ouabain perpetuates ectopic beats into more severe events

JNJ303 + ouabain induced sEB in 5/6 dogs which perpetuated to mEB in 4/6 dogs and TdP arrhythmias in 4/6 dogs (**Figure 3A**). Dog #7 showed solely sEB and mEB, and dog #10 showed no arrhythmic events at all. Dog #9, which exhibited the highest score of TdP also showed a monomorphic VT. The arrhythmic events significantly increased the arrhythmia score ranging from 5.3 to 40.7 for dogs that showed TdP arrhythmias (**Figure 3B**). ECG and LV-P tracings of those dogs are presented in **Figure 4**, including four to five contractions in idioventricular rhythm before the first VT occurred. Dog #5, 8 and 9 showed the typical TdP characterized by a polymorphic VT with the signal twisting around the isoelectric axis initiated by the R on T phenomenon and in the context of QT prolongation. The TdP arrhythmias were terminated by defibrillation in dog #5 and 8, whereas the rate of the consecutive complexes became slower towards the end of the TdP in dog #9 resulting in self-termination of the TdP. The self-terminating TdP of six complexes in dog #6 was accompanied without a complete loss yet reduced LV-P, whereas the LV-P was completely lost during the TdP arrhythmia in the other three dogs (**Figure 4**). In these conditions, no aftercontractions were observed in the LV-P signal before the initiation of the TdP of all dogs. All TdP arrhythmias were preceded by numerous sEB and/or mEB, and this arrhythmic behavior is similar to the events preceding the TdP arrhythmias induced by dofetilide (**Suppl. figure 2**). The number of severe arrhythmic events after JNJ303 and enhanced inotropy was evidently lower compared to dofetilide and followed no specific time course, as dofetilide typically initiates the electrical storm after 2-4 min in inducible dogs (**Suppl. figures 1 and 2**).

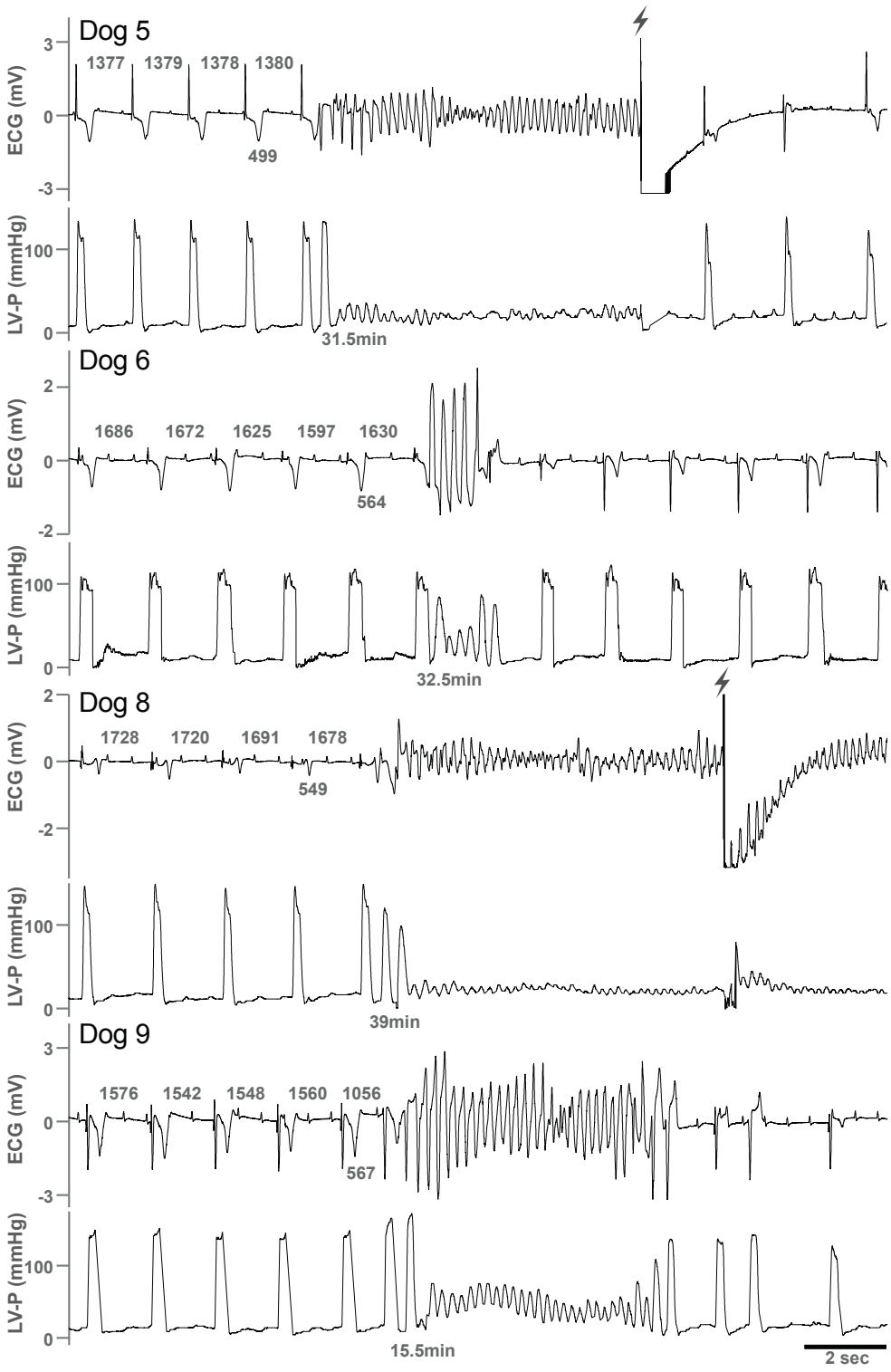
Dog 5
ECG (mV)
3
0
-3
1377
1379
1378
1380
499
LV-P (mmHg)
100
0
31.5min
Dog 6
ECG (mV)
2
0
-2
1686
1672
1625
1597
1630
564
LV-P (mmHg)
100
0
32.5min
Dog 8
ECG (mV)
2
0
-2
1728
1720
1691
1678
549
LV-P (mmHg)
100
0
39min
Dog 9
ECG (mV)
3
0
-3
1576
1542
1548
1560
1056
567
LV-P (mmHg)
100
0
15.5min
2 sec

Figure 4. ECG lead II and LV pressure (LV-P) tracings of dogs after JNJ303 + ouabain infusion. Dogs showed Torsade de Pointes (TdP) arrhythmias of which the first one that occurred is shown. The QT interval (ms) is depicted below the last beat prior to the TdP, and the RR intervals (ms) are depicted above the five beats prior to the TdP. The scale bar indicates 2 s. The shock symbol refers to defibrillation.

Occurrence of arrhythmic events during washout period of anesthetic regime

After the experimental protocol, the surgical procedure was finished, and the anesthetic regime (isoflurane administration) was ended. Moreover, the mechanical ventilation was switched to spontaneous ventilation at 5 min after stop of isoflurane, which corresponds to 110 ± 9 min after the onset of JNJ303 infusion. Interestingly, arrhythmic events occurred after stopping isoflurane. sEB were observed in 7/10 dogs, which perpetuated into TdP arrhythmias in 4/10 dogs (**Figure 5A and 5C**) resulting in an increase of the arrhythmia score from 1.1 ± 0.3 to 9.2 ± 11.2 (**Figure 5B, Table 2**). These results were independent from administration of ouabain after JNJ303, since no difference in arrhythmic outcome was observed between both groups (**Figure 5A, Suppl. figure 3**). Repolarization parameter QTc was significantly prolonged upon the stop of isoflurane or TdP occurrence (**Table 2**). However, correction of the QRS duration showed no effect on the JTc interval, and parameters $JT_{peak}c$, T_{peak}-T_{end}, and STV QT were also not altered. A (more dominant) presence of an adrenergic trigger - activated by the switch to spontaneous ventilation - could not be determined as the RR and PP intervals were not different in the TdP group (red dots) compared to the dogs without TdP (black dots) (**Table 2, Suppl. figure 4**).

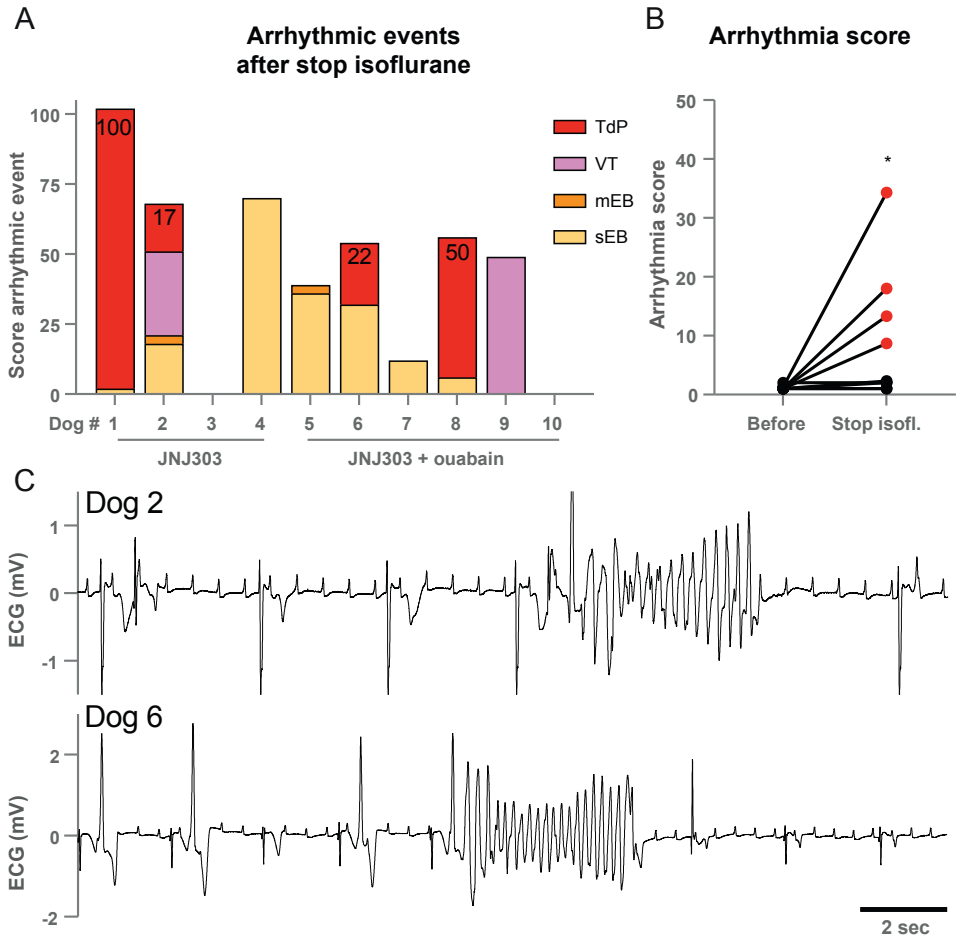

Figure 5. Arrhythmic events after washout of anesthetic regime. **A**) Arrhythmic events during 15 min after stop isoflurane (isofl.) in dogs. 4/10 dogs showed Torsade de Pointes (TdP) arrhythmia (in red, numbers correspond to TdP score). Single ectopic beats (sEB, in yellow, score: 2 points), multiple ectopic beats (mEB, in orange, score: 3-5 points), ventricular tachycardia (VT, in pink), TdP score: 6-49 points and shocked TdP: 50, 75 or 100 points. **B**) Arrhythmia score of dogs (n=9, exclusion of dog 9 with continuous VT). Paired *t*-test, *P<0.05 compared to Before. **C**) ECG lead II tracings of dogs showing self-terminating TdP arrhythmia.

Table 2. Effect of ending anesthetic regime on electrophysiological parameters of dogs with chronic AV block after JNJ303 and JNJ303 combined with ouabain.

Parameter	Before stop isoflurane	TdP / 7min stop isoflurane	% Increase
RR	1703 ± 227	1940 ± 539	14
PP	691 ± 136	683 ± 138	-1
QRS	99 ± 17	109 ± 20	10
QT	559 ± 58	605 ± 104*	8
QTc	498 ± 51	524 ± 72 *	5
JT	460 ± 57	481 ± 71	5
JTc	413 ± 78	415 ± 62	0
$JT_{peak}c$	222 ± 52	241 ± 46	8
T_{peak}-T_{end}	176 ± 31	169 ± 46	-4
STV QT	5.2 ± 0.8	6.7 ± 4.6	28
AS	1.1 ± 0.3	9.2 ± 11.2 *	
TdP	0%	40%	

Values are presented as mean ± SD. Paired *t*-test, *P<0.05 vs. Before stop isoflurane. Timepoint before stop isoflurane was measured after the experimental protocol, and TdP/ 7min stop isoflurane was measured either before the occurrence of a Torsade de Pointes (TdP arrhythmia) or at 7 min after stop of isoflurane. Electrophysiological parameters (in ms, n=9); dog #9 was excluded due to occurrence of ventricular tachycardia. AS and TdP incidence: n=10. AS = arrhythmia score; $JT_{peak}c$ = J to T peak interval corrected for heart rate; QTc and JTc = QT and JT corrected for heart rate using the Van de Water formula; STV = short-term variability of repolarization; TdP = Torsade de Pointes, T_{peak}-T_{end} = T-wave peak to T-wave end interval.

Discussion

This study demonstrates three major conclusions: 1) I_{Ks} blocker JNJ303 induces QT prolongation resembling the QT prolongation induced by I_{Kr} blocker dofetilide in inducible CAVB dogs. 2) JNJ303 evoked sEB and self-terminating VTs which were perpetuated into more severe arrhythmic events including TdP arrhythmias by further challenging the cellular calcium handling using ouabain. 3) Stop of the anesthetic regime induced arrhythmic events after finishing the experimental protocol independent of whether ouabain had been administered.

Arrhythmia initiation with lack of perpetuation by JNJ303

Compared to humans, I_{Ks} in the canine ventricle has a more prominent role in establishing the repolarization reserve,[18] which makes this species favorable in determining cardiac effects of

I_{Ks} inhibiting compounds. The reduced repolarization reserve in the CAVB dog is displayed by the downregulation of I_{Ks} (in both ventricles) and I_{Kr} (in the right ventricle) current densities with 50%.[19] The current study shows that CAVB remodeled hearts exposed to I_{Ks} inhibitor JNJ303 displayed severe prolongation of the QT interval. Interestingly, this is similar to the QT prolongation induced by I_{Kr} blocker dofetilide in serial experiments. While QT prolongation is acknowledged as contributor, STV is recognized as an indicator in evaluating arrhythmogenesis.[16,20] Maintaining a steady repolarization duration is crucial in minimizing temporal dispersion or beat-to-beat variation of repolarization and thereby a depressed STV. I_{Kr} blocker dofetilide increases the STV, and generates an electrical storm of arrhythmic events resulting in more severe arrhythmias.[21,22] The prolongation and temporal dispersion of repolarization are a prerequisite for arrhythmia initiation. Indeed, JNJ303 increased temporal dispersion of repolarization as determined by an increased STV LV MAPD, and evoked EBs and VT. However, in the case of I_{Ks} inhibition by JNJ303, an extra substrate is necessary for the perpetuation of ectopic beats into more severe arrhythmias.

Triggers for induction of severe arrhythmias exceeding I_{Ks} inhibition

Exercise-associated sympathetic activation in a background of impaired I_{Ks} is an important clinical trigger of cardiac arrhythmia.[4] It is therefore not surprising that cardiac sympathetic denervation in patients with LQTS provides antiarrhythmic protection.[23] Modulation of I_{Ks} by beta-adrenergic stimulation is often involved in examining arrhythmias in models mimicking LQT1 syndrome,[24] with a predominant use of isoproterenol positively affecting both inotropy and chronotropy via β1-adrenoreceptor stimulation. Also in isolated dog cardiomyocytes, it has been previously shown that whereas I_{Ks} inhibition has minimal to no effect on APD, beta-adrenergic stimulation enhances the contribution of I_{Ks} to the APD.[25] Moreover, in the study described by Towart et al., beta-adrenergic stimulation after I_{Ks} inhibition evidently enhanced the TdP occurrence.[6] Accumulative administration of JNJ303 at a concentration of 0.63-1.25 mg/kg caused marked QT prolongation and induced spontaneous pause-dependent TdP arrhythmias in 2 out of 4 fentanyl/etomidate-anesthetized beagle (FEAB) dogs tested in sinus rhythm.[6] Addition of isoproterenol after a lower dose of JNJ303 (0.32mg/kg) induced adrenergic-dependent TdP arrhythmias in all 6 tested dogs.[6] Interestingly, they describe their arrhythmic episodes to be either 'adrenergic dependent' or 'pause dependent'. We did not observe such a behavior of arrhythmic episode initiation in dogs exposed to conditions of

increased inotropy and/or ending of the anesthetic regime. The decrease instead of increase in atrial rate – a prolonged PP interval after JNJ303, JNJ303 + ouabain and dofetilide – could be explained by the feedback response to the enhanced inotropy induced by the compounds.

In the CAVB dog, remodeling alters the calcium handling by an increased Ca^{2+} release from the sarcoplasmic reticulum and enhanced Na^{+}/Ca^{2+} exchange.[26] Prior studies by our group have shown that administration of Na^{+}/K^{+}-ATP-pump inhibitor ouabain and the consequential increase in inotropy could induce TdP arrhythmias in a CAVB dog that was previously non-inducible after the standard dofetilide hit.[10] In the current study, targeting the calcium handling by ouabain in the CAVB dog combined with I_{Ks} inhibition induced TdP arrhythmia. Contractility quantified by $LVdP/dt_{max}$ reached levels far above 3000 mmHg/s in those dogs, which could not be reached by hearts infused by solely JNJ303 showing no TdP arrhythmias. The intracellular Ca^{2+} overload and the ability of the structurally remodeled AV block heart to induce such a rise in contractility acted as additional trigger exceeding I_{Ks} inhibition in perpetuation of EBs into TdP arrhythmias. Moreover, the time-window of arrhythmic events and thereby arrhythmia analysis was evidently wider for JNJ303 (1 h) than for the standardized pharmacological hit dofetilide (10 min), though JNJ303 combined with ouabain showed a similar pattern of perpetuating ectopic beats into more severe arrhythmias.

Another documented trigger of TdP arrhythmia is epileptic seizures, induced by autonomic instability in the beagle dog with LQT1 syndrome induced by JNJ303 analogue JNJ282.[27] In our JNJ303 treated CAVB dogs we mimicked a condition of acute autonomic instability by ending the anesthetic regime. Although the adrenergic alteration was not displayed in changes of atrial and ventricular rate, the switch from mechanical to spontaneous breathing after stop of isoflurane induced arrhythmic events. As described earlier, the anesthetic regime is a relevant component for generating TdP vulnerability in the CAVB mongrel dog model.[28] Isoflurane has an inhibiting effect on I_{Ks},[29] though stopping isoflurane after I_{Ks} inhibition by JNJ303 in the CAVB dog contributed to proarrhythmic conditions. Hence, ending I_{Ks} inhibition by isoflurane combined with adrenergic stimulation induced by high CO_2 levels for initiation of spontaneous breathing[30] could result in the proarrhythmic condition after finishing of our experimental protocol.

These findings also illustrate some of the issues the field of cardiac safety pharmacology still faces, and controversies it may raise.[2,31] The QTc prolongation by JNJ303 only is insufficient to induce TdP arrhythmias, and requires an additional hit i.e., ouabain in this study. But more importantly, even in high standardized preclinical models of proarrhythmia, in this case the CAVB dog model,[8] a TdP negative outcome may suddenly transit into an unexpected TdP positive outcome, which here was set off by simply ending anesthesia and finishing mechanical ventilation after completion of the experiment protocol. This was a finding we rarely observed when using dofetilide as pharmacological hit.

A role for spatial dispersion of repolarization after I_{Ks} inhibition

The question now remains if named beta-adrenergic triggers have similar underlying substrates for perpetuation of arrhythmic events. In the CAVB dog, initiation of ectopic beats is suggested to rely on triggered activity with a focal mechanism, where perpetuation of the event is dependent on SDR.[32-34] However, human LV wedges exposed to I_{Ks} inhibition by JNJ303 combined with an adrenergic trigger had no significant impact on transmural dispersion, though I_{Kr} block did increase transmural dispersion of repolarization.[35] In the current study, we again show that I_{Kr} blocker dofetilide prolongs the parameters reflecting early repolarization and global dispersion of repolarization ($JT_{peak}c$ and T_{peak}-T_{end}) in the CAVB dog model. The evolution from the sEB and VT in experiments with only JNJ303 to the presence of mEB and TdP arrhythmias when ouabain was added suggests that more SDR was present in the latter condition. Indeed, parameter T_{peak}-T_{end} reflecting SDR showed a trend towards prolongation after addition of Na^+/K^+-ATPase inhibition by ouabain. Prolongation of early repolarization parameter $JT_{peak}c$ after ouabain reflects the increase in inward currents, e.g. $I_{Ca,L}$ compared to outward currents, e.g. I_{Ks} during this stage of repolarization increasing the risk for the occurrence of early afterdepolarizations and more severe arrhythmic events. Moreover, regional differences of ouabain sensitivity were observed in failing human myocardium,[36] which may further exaggerate existing differences in regional electrical properties upon ouabain application. Electrical mapping using needle electrodes of hearts subjected to the several mentioned beta-adrenergic triggers exceeding I_{Ks} inhibition could establish a more precise role for SDR as underlying mechanism of perpetuation of arrhythmias.

Study limitations

The reliability of the described findings induced by solely JNJ303 might be affected by the small sample size. The diminishing effect of bradycardia and the use of isoflurane in the anesthetic regime on I_{Ks} could be interfering with the effect detection of the drug induced I_{Ks} inhibition. Furthermore, despite a similar arrhythmic sequence induced by JNJ303 and dofetilide, the difference in onset of action could be a cause of multiple factors e.g, differences in drug pharmacokinetic properties, for which insight into the underlying rationale requires additional analysis.

Conclusion

Mimicking LQT1 through reduction of the repolarization reserve using I_{Ks} inhibitor JNJ303 prolongs the QT interval and induces ectopic beats and VT in the CAVB dog. Furthermore, detailed analysis of the arrhythmic outcome shows that perpetuation of the arrhythmic events demands a combination of I_{Ks} inhibition and enhanced inotropy or ending of the anesthetic regime. Finally, it is still required to improve cardiac safety pharmacology in preclinical models to 1) conditions that best mimic human physiology (e.g., changes in autonomic tone, electrolyte status, temperature) and clinical practice (e.g., multiple drug prescription, chronic drug use) and to 2) fine-tune existing and new biomarkers that even better capture electrophysiological phenomena at cellular and tissue level.

References

1. Gintant G, Sager PT, Stockbridge N. Evolution of strategies to improve preclinical cardiac safety testing. *Nat Rev Drug Discov.* 2016;15(7):457-471.
2. Vargas HM, Rolf MG, Wisialowski TA, et al. Time for a fully integrated nonclinical-clinical risk assessment to streamline QT prolongation liability determinations: a pharma industry perspective. *Clin Pharmacol Ther.* 2021;109(2):310-318.
3. Thompson E, Eldstrom J, Westhoff M, McAfee D, Balse E, Fedida D. cAMP-dependent regulation of IKs single-channel kinetics. *J Gen Physiol.* 2017;149(8):781-798.
4. Schwartz PJ, Priori SG, Spazzolini C, et al. Genotype-phenotype correlation in the long-QT syndrome: gene-specific triggers for life-threatening arrhythmias. *Circulation.* 2001;103(1):89-95.
5. Wang Q, Curran ME, Splawski I, et al. Positional cloning of a novel potassium channel gene: KVLQT1 mutations cause cardiac arrhythmias. *Nat Genet.* 1996;12(1):17-23.
6. Towart R, Linders JT, Hermans AN, et al. Blockade of the I(Ks) potassium channel: an overlooked cardiovascular liability in drug safety screening? *J Pharmacol Toxicol Methods.* 2009;60(1):1-10.
7. Bourgonje VJA, Van Veen TAB, Vos MA. Ventricular electrical remodeling in compensated cardiac hypertrophy. In: Gussak I, Antzelevitch C, eds. *Electrical Diseases of the Heart*. London: Springer-Verlag; 2013:387-398.

8. Loen V, Vos MA, Van der Heyden MAG. The canine chronic atrioventricular block model in cardiovascular preclinical drug research. *Br J Pharmacol.* 2022;179(5):859-881.
9. Timmermans C, Rodriguez LM, Van Suylen RJ, et al. Catheter-based cryoablation produces permanent bidirectional cavotricuspid isthmus conduction block in dogs. *J Interv Card Electrophysiol.* 2002;7(2):149-155.
10. Sprenkeler DJ, Bossu A, Beekman JDM, Schoenmakers M, Vos MA. An augmented negative force-frequency relationship and slowed mechanical restitution are associated with increased susceptibility to drug-induced torsade de pointes arrhythmias in the chronic atrioventricular block dog. *Front Physiol.* 2018;9:1086.
11. Van de Water A, Verheyen J, Xhonneux R, Reneman RS. An improved method to correct the QT interval of the electrocardiogram for changes in heart rate. *J Pharmacol Methods.* 1989;22(3):207-217.
12. Johannesen L, Vicente J, Mason JW, et al. Differentiating drug-induced multichannel block on the electrocardiogram: randomized study of dofetilide, quinidine, ranolazine, and verapamil. *Clin Pharmacol Ther.* 2014;96(5):549-558.
13. Opthof T, Coronel R, Wilms-Schopman FJ, et al. Dispersion of repolarization in canine ventricle and the electrocardiographic T wave: Tp-e interval does not reflect transmural dispersion. *Heart Rhythm.* 2007;4(3):341-348.
14. Thomsen MB, Verduyn SC, Stengl M, et al. Increased short-term variability of repolarization predicts d-sotalol-induced torsades de pointes in dogs. *Circulation.* 2004;110(16):2453-2459.
15. Van der Linde HJ, Van Deuren B, Somers Y, Loenders B, Towart R, Gallacher DJ. The electro-mechanical window: a risk marker for torsade de pointes in a canine model of drug induced arrhythmias. *Br J Pharmacol.* 2010;161(7):1444-1454.
16. Smoczyńska A, Beekman HD, Vos MA. The increment of short-term variability of repolarisation determines the severity of the imminent arrhythmic outcome. *Arrhythm Electrophysiol Rev.* 2019;8(3):166-172.
17. Stams TRG, Winckels SKG, Oros A, et al. Novel parameters to improve quantification of repolarization reserve and arrhythmogenesis using a dofetilide challenge. *Heart Rhythm.* 2013;10(11):1745-1746.
18. Jost N, Virag L, Comtois P, et al. Ionic mechanisms limiting cardiac repolarization reserve in humans compared to dogs. *J Physiol.* 2013;591(17):4189-4206.
19. Volders PG, Sipido KR, Vos MA, et al. Downregulation of delayed rectifier K(+) currents in dogs with chronic complete atrioventricular block and acquired torsades de pointes. *Circulation.* 1999;100(24):2455-2461.
20. Bossu A, Varkevisser R, Beekman HDM, Houtman MJC, Van der Heyden MAG, Vos MA. Short-term Variability of Repolarization Is Superior to Other Repolarization Parameters in the Evaluation of Diverse Antiarrhythmic Interventions in the Chronic Atrioventricular Block Dog. *J Cardiovasc Pharmacol.* 2017;69(6):398-407.
21. Oros A, Houtman MJ, Neco P, et al. Robust anti-arrhythmic efficacy of verapamil and flunarizine against dofetilide-induced TdP arrhythmias is based upon a shared and a different mode of action. *Br J Pharmacol.* 2010;161(1):162-175.
22. Van Weperen VYH, Dunnink A, Bossu A, et al. Severe bradycardia increases the incidence and severity of torsade de pointes arrhythmias by augmenting preexistent spatial dispersion of repolarization in the CAVB dog model. *Front Physiol.* 2021;12:642083.
23. Dusi V, Pugliese L, De Ferrari GM, et al. Left cardiac sympathetic denervation for long QT syndrome: 50 years' experience provides guidance for management. *JACC Clin Electrophysiol.* 2022;8(3):281-294.
24. Gallacher DJ, Van de Water A, Van der Linde H, et al. In vivo mechanisms precipitating torsades de pointes in a canine model of drug-induced long-QT1 syndrome. *Cardiovasc Res.* 2007;76(2):247-256.
25. Volders PG, Stengl M, Van Opstal JM, et al. Probing the contribution of IKs to canine ventricular repolarization: key role for beta-adrenergic receptor stimulation. *Circulation.* 2003;107(21):2753-2760.
26. Sipido KR, Volders PG, de Groot SH, et al. Enhanced Ca(2+) release and Na/Ca exchange activity in

hypertrophied canine ventricular myocytes: potential link between contractile adaptation and arrhythmogenesis. *Circulation.* 2000;102(17):2137-2144.

27. Van der Linde H, Kreir M, Teisman A, Gallacher DJ. Seizure-induced torsades de pointes: in a canine drug-induced long-QT1 model. *J Pharmacol Toxicol Methods.* 2021;111:107086.
28. Dunnink A, Sharif S, Oosterhoff P, et al. Anesthesia and arrhythmogenesis in the chronic atrioventricular block dog model. *J Cardiovasc Pharmacol.* 2010;55(6):601-608.
29. Suzuki A, Bosnjak ZJ, Kwok WM. The effects of isoflurane on the cardiac slowly activating delayed-rectifier potassium channel in Guinea pig ventricular myocytes. *Anesth Analg.* 2003;96(5):1308-1315.
30. Bigatello L, Pesenti A. Respiratory physiology for the anesthesiologist. *Anesthesiology.* 2019;130(6):1064-1077.
31. Strauss DG, Wu WW, Li Z, Koerner J, Garnett C. Translational models and tools to reduce clinical trials and improve regulatory decision making for QTc and proarrhythmia risk (ICH E14/S7B Updates). *Clin Pharmacol Ther.* 2021;109(2):319-333.
32. Dunnink A, Stams TRG, Bossu A, et al. Torsade de pointes arrhythmias arise at the site of maximal heterogeneity of repolarization in the chronic complete atrioventricular block dog. *Europace.* 2017;19(5):858-865.
33. Smoczyńska A, Aarnink EW, Dunnink A, et al. Interplay between temporal and spatial dispersion of repolarization in the initiation and perpetuation of torsades de pointes in the chronic atrioventricular block dog. *Am J Physiol Heart Circ Physiol.* 2021;321(3):H569-H576.
34. Vandersickel N, Bossu A, De Neve J, et al. Short-Lasting Episodes of torsade de pointes in the chronic atrioventricular block dog model have a focal mechanism, while longer-lasting episodes are maintained by re-entry. *JACC Clin Electrophysiol.* 2017;3(13):1565-1576.
35. Kang C, Badiceanu A, Brennan JA, et al. beta-adrenergic stimulation augments transmural dispersion of repolarization via modulation of delayed rectifier currents IKs and IKr in the human ventricle. *Sci Rep.* 2017;7(1):15922.
36. Padrini R, Panfili M, Magnolfi G, Piovan D, Casarotto D, Ferrari M. Myocardial region (right or left ventricle) and aetiology of heart failure can influence the inotropic effect of ouabain in failing human myocardium. *Br J Clin Pharmacol.* 1999;48(5):743-749.

Supplementary material

Suppl. table 1. Electrophysiological and contractile parameters of dogs with chronic AV block (CAVB) during baseline and before the first ectopic beat during dofetilide at CAVB for 4 ± 0 weeks (n=4), and during baseline and before the first ectopic beat during dofetilide at CAVB for 3 ± 0 weeks (n=6).

	CAVB (n=4)			CAVB (n=6)		
Parameter	**Baseline**	**Dofetilide**	**% Increase**	**Baseline**	**Dofetilide**	**% Increase**
RR	1524 ± 52	1584 ± 73	4	1298 ± 93	1330 ± 68	2
PP	589 ± 42	657 ± 33 *	12	490 ± 38	538 ± 48 *	10
QRS	97 ± 23	92 ± 21	-5	115 ± 14	116 ± 15	2
QT	501 ± 70	613 ± 74 *	22	489 ± 42	573 ± 38 *	17
QTc	455 ± 67	562 ± 69 *	23	463 ± 46	544 ± 41 *	18
JT	404 ± 64	521 ± 60 *	29	374 ± 39	475 ± 55 *	27
JTc	358 ± 60	470 ± 54 *	31	348 ± 42	428 ± 33 *	23
$JT_{peak}c$	210 ± 19	264 ± 35 *	26	198 ± 48	241 ± 63 *	22
T_{peak}-T_{end}	148 ± 51	207 ± 25 *	39	154 ± 52	207 ± 55 *	35
STV QT	6.2 ± 1.7	5.1 ± 1.0	-17	5.9 ± 1.1	6.7 ± 1.2	14
$QLVP_{end}$	ND	ND		386 ± 27	378 ± 30 *	-2
EMW	ND	ND		-99 ± 27	-216 ± 52 *	119
$LVdP/dt_{max}$	ND	ND		2046 ± 256	2435 ± 255 *	19
$LVdP/dt_{min}$	ND	ND		2348 ± 267	2414 ± 163	3
AS	1.0 ± 0	50.8 ± 10.0 *		1.0 ± 0	60.0 ± 10.0 *	
TdP	0%	100%		0%	100%	

Values are presented as mean ± SD. Increase in percentage of the averaged values. Paired t-test, *P<0.05 vs. baseline. Parameters are in ms, except for $LVdP/dt_{max}$ and $LVdP/dt_{min}$ (mmHg/sec), and for AS and TdP incidence. Baseline and dofetilide at CAVB for 3 ± 0 weeks: n=5 for $QLVP_{end}$, EMW and $LVdP/dt_{max}$, and n=4 for $LVdP/dt_{min}$. AS = arrhythmia score; EMW = electromechanical window; $JT_{peak}c$ = J to T peak interval corrected for heart rate; LV = left ventricular; ND = no data available; $QLVP_{end}$ = interval between Q on ECG and end of LV pressure cycle; QTc and JTc = QT and JT corrected for heart rate using the Van de Water formula; RV = right ventricular; STV = short-term variability of repolarization; TdP = Torsade de Pointes; T_{peak}-T_{end} = T-wave peak to T-wave end interval.

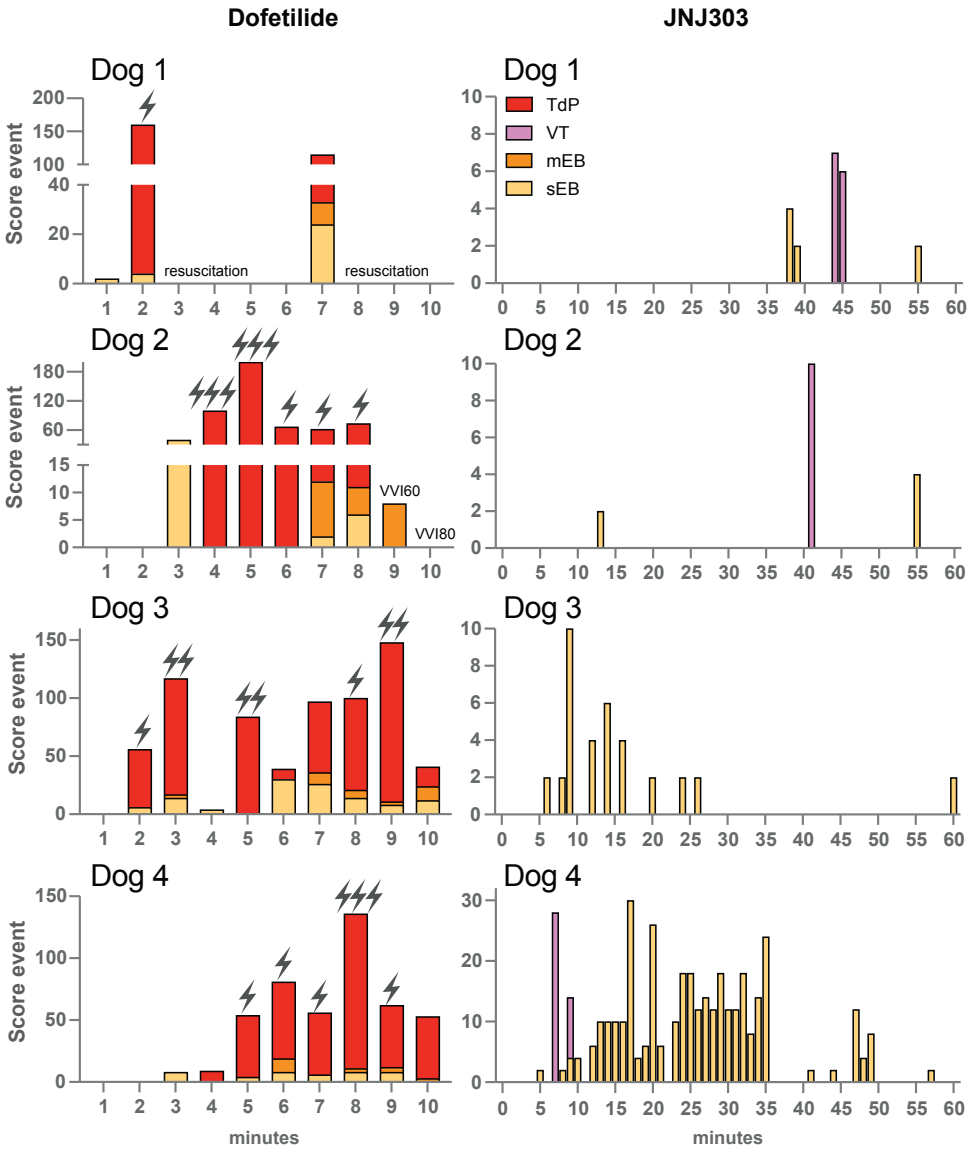

Suppl. figure 1. Score of arrhythmic events of dog #1, 2, 3 and 4 during 10 min after the start of dofetilide infusion (left panel) and during 1 h after the start of JNJ303 infusion (right panel). Single ectopic beats (sEB, score: 2 points), multiple ectopic beats (mEB, score: 3-5 points), ventricular tachycardia (VT) and Torsade de Pointes (TdP) score: 6-49 points and shocked TdP: 50, 75 or 100 points. Dog 2 was paced during dofetilide at 60 bpm (VVI60) at 9 min and VVI80 at 10 min.

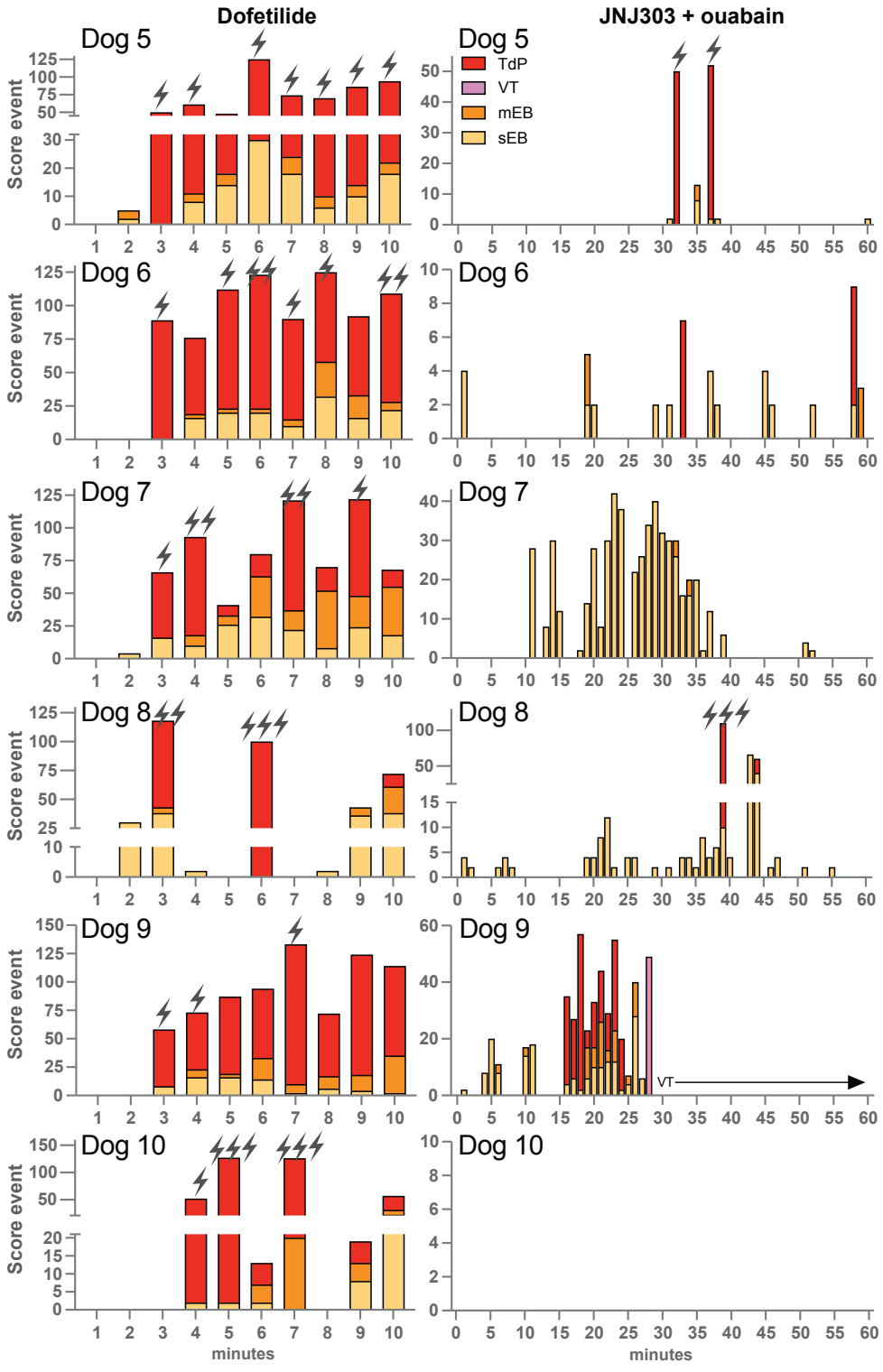
Dofetilide
JNJ303 + ouabain
Dog 5
Dog 6
Dog 7
Dog 8
Dog 9
Dog 10
Score event
TdP
VT
mEB
sEB
VT
minutes
minutes

Suppl. figure 2. Score of arrhythmic events of dog #5, 6, 7, 8, 9 and 10 during 10 min after the start of dofetilide infusion (left panel) and in time window of 1 h after the start of JNJ303 infusion (right panel). Single ectopic beats (sEB, score: 2 points), multiple ectopic beats (mEB, score: 3-5 points), ventricular tachycardia (VT), Torsade de Pointes (TdP) score: 6-49 points and shocked TdP: 50, 75 or 100 points. Shock symbols refer to defibrillated TdP. VT for dog #9 was scored with 49 points.

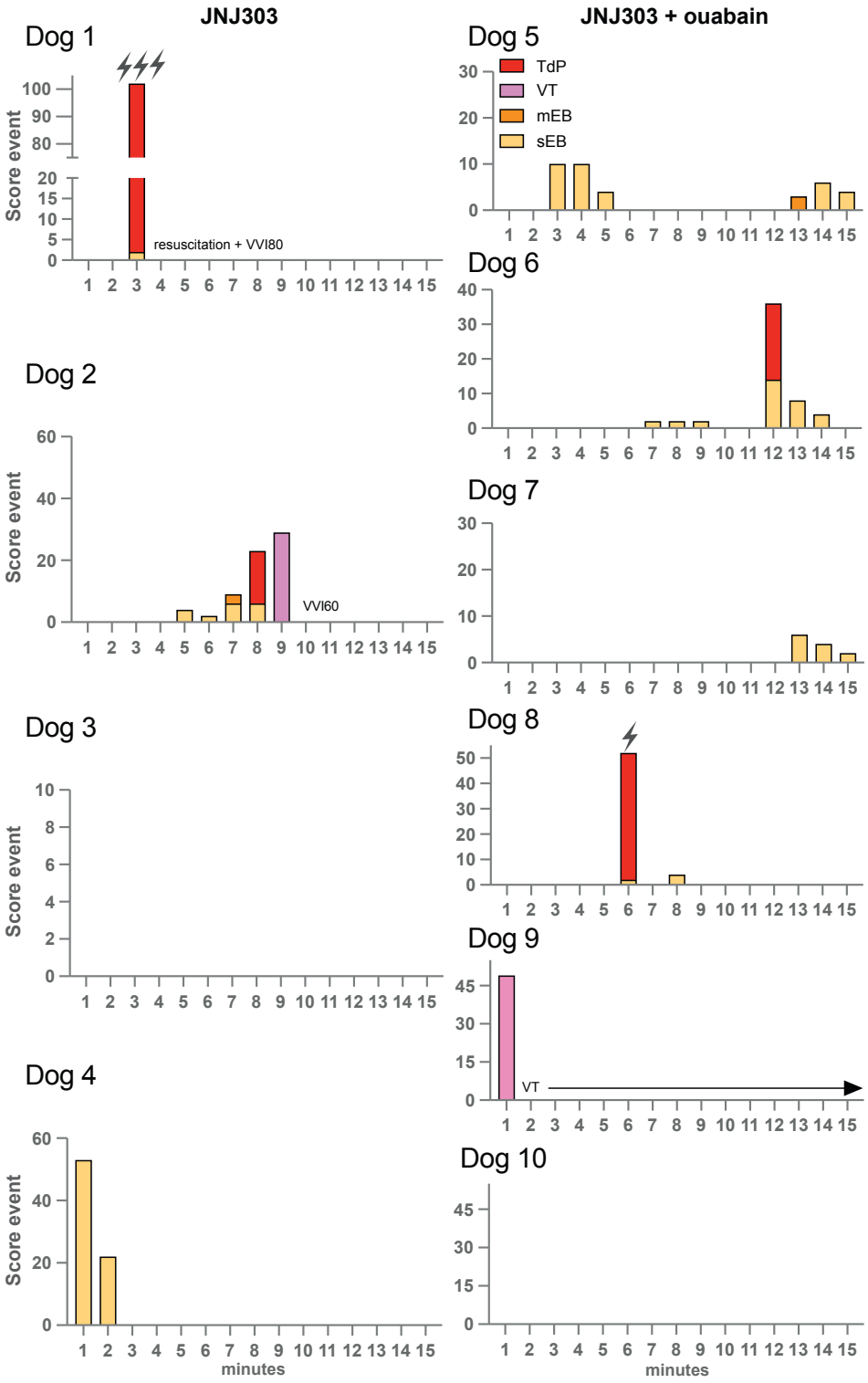
JNJ303
JNJ303 + ouabain
Dog 1
Dog 5
TdP
VT
mEB
sEB
Score event
resuscitation + VVI80
Dog 6
Dog 2
VVI60
Dog 7
Dog 3
Dog 8
Dog 9
VT
Dog 4
Dog 10
minutes
minutes

Suppl. figure 3. Score of arrhythmic events of all dogs during 15 min after the stop of isoflurane. Left panel: #1, 2, 3, and 4 received JNJ303, and right panel: #5, 6, 7, 8, 9 and 10 received JNJ303 + ouabain. Single ectopic beats (sEB, score: 2 points), multiple ectopic beats (mEB, score: 3-5 points), ventricular tachycardia (VT), Torsade de Pointes (TdP) score: 6-49 points and shocked TdP: 50, 75 or 100 points.

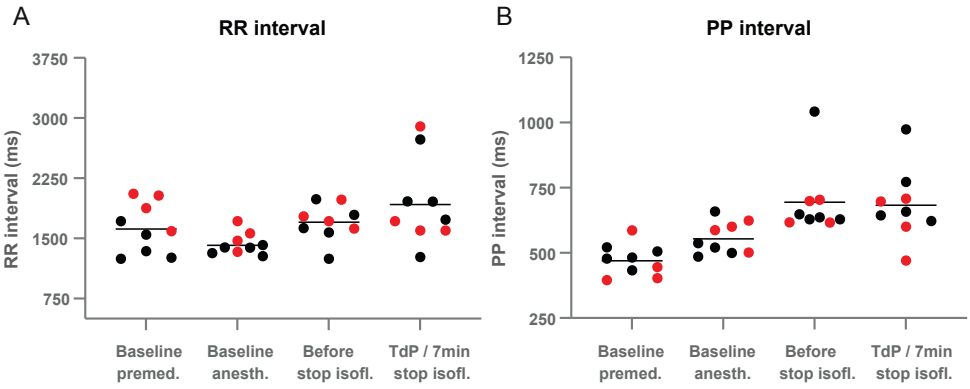

Suppl. figure 4. RR and PP interval of dogs (n=9) during premedication and anesthesia, and before and after stop of isoflurane. Dogs showing TdP arrhythmias after stop isoflurane are depicted in red, with an average time after isoflurane stop of 7 ± 4 min. Dogs showing no TdP arrhythmias after stop isoflurane are depicted in black and parameters were measured at 7 min after stop of isoflurane. Dog #9 with continuous ventricular tachycardia was excluded. The horizontal lines refer to the mean.

5

I_{Ks} activator ML277 mildly affects repolarization and arrhythmic outcome in the CAVB dog model

Joanne J.A. van Bavel[1], Henriëtte D.M. Beekman[1], Agnieszka Smoczyńska[1], Marcel A.G. van der Heyden[1], Marc A. Vos[1]

[1] Department of Medical Physiology, Division of Heart and Lungs, University Medical Center Utrecht, Utrecht, the Netherlands

***Biomedicines*, 2023, 11(4):1147**

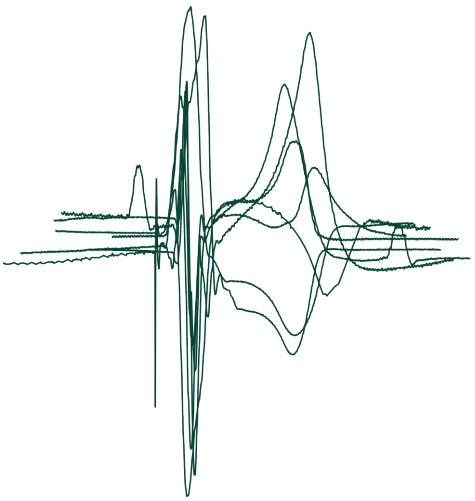

Abstract

Long QT syndrome type 1 with affected I_{Ks} is associated with a high risk for developing Torsade de Pointes (TdP) arrhythmias and eventually sudden cardiac death. Therefore, it is of high interest to explore drugs that target I_{Ks} as antiarrhythmics.

We examined the antiarrhythmic effect of I_{Ks} channel activator ML277 in the chronic atrioventricular block (CAVB) dog model. TdP arrhythmia sensitivity was tested in anesthetized mongrel dogs (n = 7) with CAVB in series: (1) induction experiment at 4 ± 2 weeks CAVB: TdP arrhythmias were induced with our standardized protocol using dofetilide (0.025 mg/kg), and (2) prevention experiment at 10 ± 2 weeks CAVB: the antiarrhythmic effect of ML277 (0.6–1.0 mg/kg) was tested by infusion for 5 min preceding dofetilide.

ML277: (1) temporarily prevented repolarization prolongation induced by dofetilide (QTc: 538 ± 65 ms at induction vs. 393 ± 18 ms at prevention, $p < 0.05$), (2) delayed the occurrence of the first arrhythmic event upon dofetilide (from 129 ± 28 s to 180 ± 51 s, $p < 0.05$), and (3) decreased the arrhythmic outcome with a significant reduction in the number of TdP arrhythmias, TdP score, arrhythmia score and total arrhythmic events (from 669 ± 132 to 401 ± 228, $p < 0.05$).

I_{Ks} channel activation by ML277 temporarily suppressed QT interval prolongation, delayed the occurrence of the first arrhythmic event and reduced the arrhythmic outcome in the CAVB dog model.

Keywords

ML277, AV block dog model, Long QT type 1, ventricular arrhythmia

Introduction

Long QT syndrome (LQTS) can be either congenital or acquired and is characterized by a prolongation of the QT interval on the electrocardiogram (ECG). When inherited, the most common type is caused by a loss-of-function mutation in the *KCNQ1* gene, referred to as LQT type 1 (LQT1), and is found in 40-50% of the LQTS individuals.[1,2] The *KCNQ1* gene encodes the α-subunit of the slow component of the delayed rectifier potassium current (I_{Ks}) and forms a functional channel together with the β-subunit (KCNE1). Specific activation of the channel is present upon enhanced sympathetic stimulation and in maintaining a proper repolarization reserve.[3,4] A loss-of-function mutation in the *KCNQ1* gene results in a reduced I_{Ks} density.[5] The accompanying reduced repolarization reserve predisposes the heart to Torsade de Pointes (TdP) ventricular arrhythmias and possibly sudden cardiac death. Enhanced sympathetic activity, typically by physical exercise or emotional stress, is reported as a trigger.[6]

Insights into regulators of KCNQ1/KCNE1 channels have been reported over the last decades. They range from physiological modulators protein kinase A, phosphatidylinositol 4,5-biphosphate and adenosine triphosphate to pharmacological modulators of which, among others, hexachlorophene, zinc pyrithione, and L-364,373 are presented as I_{Ks} activators.[7-10] The latter are critically discussed regarding their sensitivity of solely KCNQ1 or the KCNQ1/KCNE1 complex and their effect on other (cardiac) ion channels in terms of possible side effects for LQT1 patients.

(R)-N-(4-(4-methoxyphenyl)thiazol-2-yl)-1-tosylpiperidine-2-carboxamide (ML277) was identified as a novel I_{Ks} activator by Mattmann and coworkers in 2012.[11] It is proposed that activation of the I_{Ks} channel is achieved by increasing K^+ conductance and by prolonging the activation and deactivation transitions, and even prevention of channel inactivation, by selectively enhancing the current during the activated open state of the channel.[12-14] Furthermore, ML277 had very modest or no effect on the L-type calcium current (I_{CaL}) and the inward-rectifying current (I_{K1}) shown in guinea pig ventricular cardiomyocytes.[12] Since its identification, a few *in vitro* studies reported on the therapeutic potential of ML277. By acting on KCNQ1 and KCNQ1/KCNE1 complexes, ML277 enhances I_{Ks} density and shortens the action potential duration in canine ventricular cardiomyocytes and human-induced pluripotent stem cell-derived cardiomyocytes (hiPSC-CMs).[12,15] ML277 rescued I_{Ks} dysfunction in hiPSC-CMs

with a patient-specific *KCNQ1* mutation as shown via elevated I_{Ks} density and action potential shortening.[16] Similar results by ML277 were shown in patient-specific hiPSC-CM clusters based on a reduced field potential duration.[17]

To our knowledge, the potential antiarrhythmic efficacy of ML227 *in vivo* has not yet been reported. The chronic atrioventricular (AV) block (CAVB) dog is a model in which TdP arrhythmias can be induced in serial experiments with high reproducibility, and has been widely used to explore pro- and antiarrhythmic drug effects.[18] Ventricular remodeling after AV block in combination with bradycardia and anesthesia predispose the heart to TdP arrhythmias, and the I_{Kr} blocker dofetilide accounts as a final trigger for TdP induction.[19,20] The aim of this study is to examine the potential antiarrhythmic effect of the I_{Ks} activator ML277 in the CAVB dog with a focus on repolarization duration and arrhythmic outcome.

Materials and Methods

Animals

Animal care and experimentation were approved by the Committee for Experiments on Animals of Utrecht University and were in accordance with the Directive 2010/63/EU of the European Parliament and the Dutch law on animal experimentation (application approval number: AVD115002016531, date of approval: 6/8/2016). Dogs were housed in pairs in kennels with wooden bedding material, had ad libitum access to drinking water and received food pellets twice a day. The animals were allowed to play outside once a day with access to playing toys, and their welfare was checked daily.

The experiments were performed with seven purpose-bred mongrel dogs (two females) (Marshall, New York, NY, USA). All dogs had remodeled hearts caused by AV block, which was induced by radiofrequency ablation of the His bundle.[21] The animals had a body weight of 25 ± 3 kg and were 18 ± 2 months old.

Preparation

Animals were fasted overnight and received premedication (0.02 mg/kg i.m. atropine, 0.5 mg/kg i.m. methadone, 0.5 mg/kg i.m. acepromazine and 0.1 mg/kg s.c. meloxicam) half an hour prior to the procedure. General anesthesia was induced by sodium pentobarbital (Nembutal, 25 mg/kg i.v.) and maintained by 1.5% isoflurane in O_2 and N_2O (1:2 ratio) via

mechanical ventilation at 12 breaths/min. Ampicillin (1000 mg) was administered before (i.v.) and after (i.m.) surgery, and buprenorphine (0.3 mg, i.m.) was provided after surgery. A monophasic action potential (MAP) catheter (Hugo Sachs Elektronik, March, Germany) was inserted via the jugular artery to the left ventricular apex. Surface ECG and a MAP signal were recorded continuously during the experiment using EP Tracer (Cardiotek, Maastricht, The Netherlands) with a sampling rate of 1 kHz. Five dogs had an idioventricular rhythm (IVR), whereas two dogs were paced at VVI40-50 due to extreme bradycardia at IVR. The induction and prevention experiments were performed in series.

Compounds

I_{Kr} blocker dofetilide (Biorbyt, Cambridge, United Kingdom, 0.025 mg/kg, i.v.) was dissolved in 0.1M HCl and further prepared in 0.9% saline solution. Infusion time was 5 minutes or until occurrence of the first TdP arrhythmia. I_{Ks} activator ML277 (Bio-Connect B.V., Huissen, The Netherlands, 0.6-1 mg/kg, i.v.) was dissolved in polyethylene glycol 400 (PEG 400) and dimethyl sulfoxide (DMSO) in a 1:1 ratio. The dose was based on absence of electrophysiological and hemodynamic effects upon proof-of-principle cardiac safety experiments in anesthetized sinus rhythm dogs.

Induction experiment

TdP arrhythmias were induced via a standardized protocol. After 10 minutes of baseline (BL) recording, I_{Kr} blocker dofetilide was infused for 5 minutes or until the occurrence of the first TdP (**Figure 1A**). TdP arrhythmias that lasted longer than 10 seconds were terminated via defibrillation. Dogs were considered inducible when they showed at least three TdP arrhythmias (of $\geq$ 5 ectopic beats) within 10 minutes after the start of dofetilide infusion. Seven inducible dogs at 4 ± 2 weeks of CAVB remodeling (CAVB4) were included for the prevention experiment.

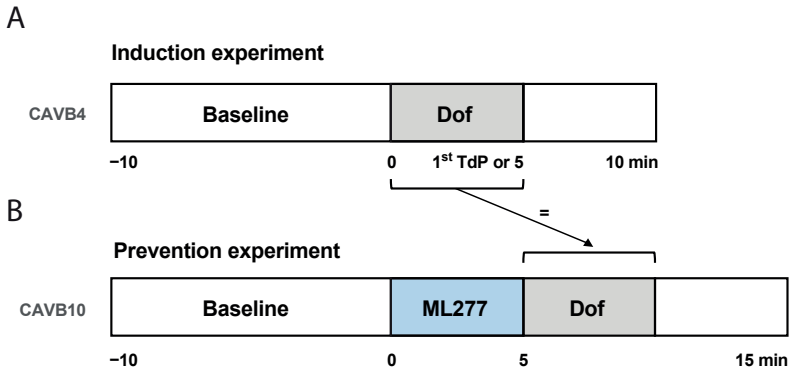

Figure 1. Schematic overview of the experimental setup. Two experiments were performed in series. **A**) Induction experiment at chronic AV block 4 ± 2 weeks (CAVB4): baseline measurement followed by dofetilide (Dof) infusion until first Torsade de Pointes (TdP) arrhythmia or maximum infusion of 5 minutes. **B**) Prevention experiment at CAVB 10 ± 2 weeks (CAVB10): baseline measurement followed by 5 minutes of ML277 and Dof infusion with identical duration as during the induction experiment. Recordings were followed up for 10 minutes after the start of Dof administration.

Prevention experiment

At 10 ± 2 weeks of CAVB remodeling (CAVB10), the antiarrhythmic potential of I_{Ks} activator ML277 was examined in inducible dogs. After 10 minutes of BL recording, ML277 was infused for 5 minutes followed by dofetilide with a similar infusion duration as the induction experiment (**Figure 1B**). Within the same animal, the dofetilide infusion time in the prevention experiment was exactly the same as the dofetilide infusion time during the induction experiment (until the first arrhythmic event or 5 minutes). This timepoint is referred to as dofetilide timepoint 1 (Dof T1).

Data analysis

Five consecutive beats from ECG lead II were measured manually in EP Tracer to obtain the interval duration of ECG parameters RR, PP, QRS, and QT. The QT interval was corrected for heart rate (QTc) using the Van de Water formula.[22] The JTc interval was obtained by subtracting the QRS interval from the QTc interval. The MAP duration of the left ventricle (LV MAPD) at 80% of repolarization was measured semi-automatically using custom-made software (AutoMAPD, MATLAB, MathWorks, Natick, MA, USA). The beat-to-beat variability of repolarization, quantified as short-term variability (STV), was calculated from 31 consecutive beats using the formula: $STV = \sum |D_{n+1} - D_n| / \left(30 * \sqrt{2}\right)$, with D representing the LV MAPD.[23]

Arrhythmic events were scored to quantify the severity of the arrhythmic outcome.[24] Single ectopic beats (sEB) were scored with 2 points, multiple ectopic beats (mEB) were scored with 3-5 points, and self-terminating TdP arrhythmias were scored with 6-49 points. TdP arrhythmias received a score of 50, 75 or 100 points for one, two or three defibrillations, respectively. The arrhythmic outcome was quantified by the relative TdP score (scored TdP arrhythmias relative to the induction experiment), the total number of shocked TdP arrhythmias, and the total score of all arrhythmic events within the 10-minute time window after the start of dofetilide infusion. The arrhythmia score is based on the average of the three highest scored arrhythmic events.[24]

Statistical analysis

Data are presented as mean ± standard deviation (SD). Serial data were analyzed using a paired Student's *t*-test or a one-way analysis of variance (ANOVA) with a Tukey's test to correct for multiple comparisons. All statistical analyses were performed with GraphPad Prism (version 8.3.0, GraphPad Software, San Diego, USA). A value of $p<0.05$ was considered statistically significant.

Results

Temporary suppression of repolarization prolongation

The duration of dofetilide infusion – established during the induction experiment – was identical to the dofetilide duration at the prevention experiment (172 ± 54 seconds, corresponding to 57 ± 18 % of a full dose at 5 minutes), referred to as Dof T1 timepoint. An overview of the delta QTc interval progress upon the induction and prevention experiments is presented in **Figure 2A**. During the induction experiment, dofetilide significantly prolonged the QTc interval. During the prevention experiment, ML277 shortened the QTc interval to some extent in all dogs. Moreover, the QTc interval prolongation during dofetilide was suppressed by the I_{Ks} activator as shown by a shorter QTc interval at Dof T1 (393 ± 18 ms) compared to this timepoint during dofetilide of the induction experiment (538 ± 65 ms, $p<0.05$, **Figure 2A and Table 1**).

Though, this was a temporary effect since dofetilide further prolonged the QTc interval - measured at the timepoint before the actual first arrhythmic event upon dofetilide at the

prevention experiment (479 ± 82 ms, **Figure 2A and Table 1**). Repolarization parameters QT, JTc and LV MAPD showed the same behavior as the QTc interval: prolongation upon dofetilide, trend towards shortening upon ML277, and a delay upon dofetilide following ML277 at Dof T1 (**Table 1**). The progress of the QT interval at the different timepoints is also represented in the ECG lead II tracings of one dog in **Figure 2C**. The RR interval and QRS duration remained stable at all timepoints (**Table 1**). The atrial rate was not affected by ML277, whereas dofetilide showed an increased PP interval compared to baseline in the prevention experiment. The delayed effect by ML277 is also found in the temporal dispersion of repolarization parameter STV: dofetilide duration similarly to the induction experiment (Dof T1) did not increase the STV yet (0.85 ± 0.41, **Table 1**). ML277 infusion alone did not induce any arrhythmic events.

Delay in occurrence of first arrhythmic event

The timepoint at which the first arrhythmic event occurred after the onset of dofetilide infusion is presented in **Figure 2B**. The time-interval at which the first arrhythmic event occurred upon dofetilide following ML277 pretreatment was significantly longer (180 ± 51 seconds) compared to the time at which the first arrhythmic event occurred upon solely dofetilide infusion (129 ± 28 seconds, $p<0.05$).

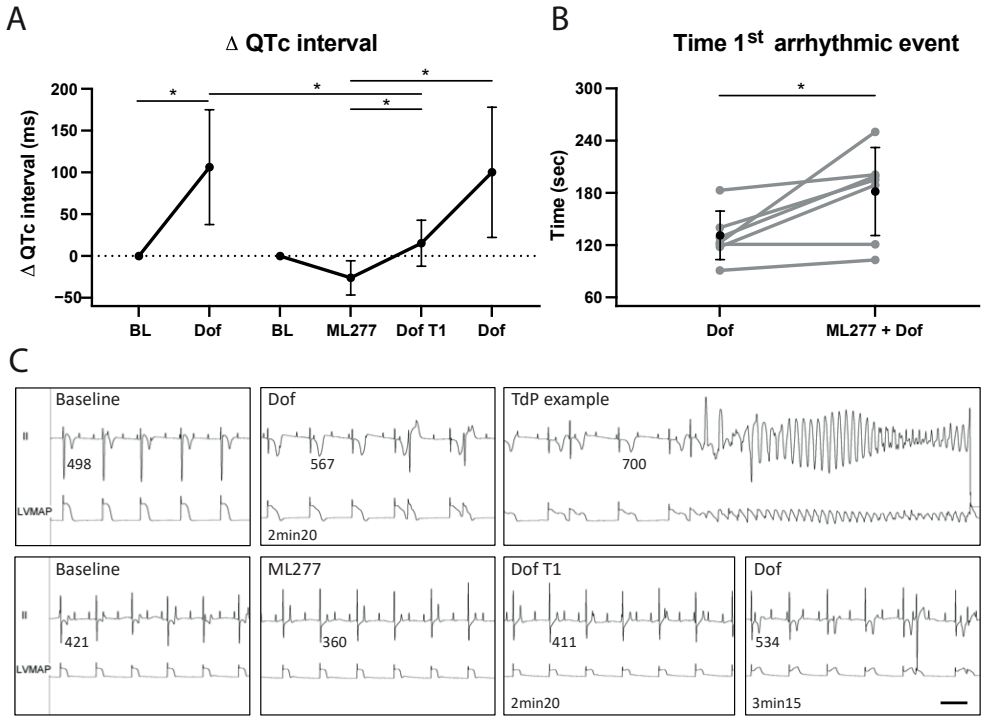

Figure 2. Effect of ML277 in dogs (n=7) with chronic AV block (CAVB). **A**) Progress of the delta QTc interval (in ms) at the induction experiment: chronic AV block (CAVB) 4 weeks at baseline (BL) and before the first arrhythmic event during dofetilide (Dof). The prevention experiment at CAVB10 included timepoints at BL, at 5 minutes of ML277 infusion (ML277), at the same timepoint as the first arrhythmic event during Dof at CAVB4 (Dof T1), and at the actual first arrhythmic event during Dof. Data of individual dogs in grey and mean ± SD in black, repeated measures one-way ANOVA with Tukey's multiple comparisons test, *p<0.05. **B**) Time until the first arrhythmic event occurred during Dof at CAVB4 and during Dof after ML277 at CAVB10. Paired t-test, *P<0.05. **C**) Representative ECG lead II and left ventricular monophasic action potential (LV MAP) tracings (dog #7) with QT intervals (in ms) presented at each measured timepoint and before the shocked Torsade de Pointes (TdP) arrhythmia (example during Dof at CAVB4). The scale bar is 1000 ms.

Table 1. Electrophysiological parameters from seven chronic AV block (CAVB) dogs after dofetilide (Dof), and after ML277 followed by Dof.

	Induction		Prevention			
	BL	**Dof**	**BL**	**ML277**	**Dof T1**	**Dof**
RR	1275 ± 190	1285 ± 180	1322 ± 242	1399 ± 299	1398 ± 301	1432 ± 290
PP	583 ± 113	638 ± 101	577 ± 101	596 ± 114	611 ± 102	672 ± 143*
QRS	104 ± 21	102 ± 27	107 ± 24	107 ± 25	104 ± 27	103 ± 29
QT	456 ± 93	563 ± 70*	406 ± 40	387 ± 36	428 ± 27$^{\#}$	516 ± 77*$^{\&\%}$
QTc	432 ± 84	538 ± 65*	378 ± 26	352 ± 31	393 ± 18$^{\#}$	479 ± 82*$^{\&\%}$
JTc	327 ± 74	436 ± 47*	272 ± 40	245 ± 34	289 ± 19$^{\#}$	376 ± 59*$^{\&\%}$
LV MAPD	308 ± 41	399 ± 77*	278 ± 20	274 ± 26	315 ± 24$^{\#}$	389 ± 53*$^{\&\%}$
STV	1.63 ± 0.50	2.97 ± 0.91	0.78 ± 0.56	0.73 ± 0.33	0.85 ± 0.41	2.31 ± 1.44*$^{\&}$

Parameters in milliseconds, data presented as mean ± SD, at baseline (BL) and before the first arrhythmic event during Dof at the induction experiment at CAVB 4 weeks, and at 5 minutes of ML277 infusion (ML277), at the same timepoint as the first arrhythmic event during Dof at CAVB 4 weeks (Dof T1), and at the actual first arrhythmic event during Dof at the prevention experiment at CAVB 10 weeks. LV MAPD = left ventricular monophasic action potential duration, STV = short term variability of LV MAPD. N=6 for LV MAPD and STV. Repeated measures one-way ANOVA with Tukey's multiple comparisons test. *p<0.05 compared to BL within CAVB group, $^{\#}$p<0.05 compared to Dof CAVB4, $^{\&}$p<0.05 compared to ML277 and $^{\%}$p<0.05 compared to Dof T1.

Mild antiarrhythmic effect: occurrence of TdP arrhythmias

I_{Ks} activation by ML277 not solely delayed the occurrence of the first arrhythmic event: infusion of ML277 before the induction of TdP arrhythmias by dofetilide reduced the relative TdP score in 6 out of 7 dogs by more than 25% (**Figure 3A**). The number of TdP arrhythmias terminated by defibrillation was also significantly lower following ML277 pretreatment (**Figure 3B**). The number of defibrillated vs. self-terminated TdP arrhythmias per dog are presented in **Figure 3C** and show the overall reduction of the arrhythmias after ML277.

The reduced arrhythmic outcome by ML277 is also presented by the significant decrease in arrhythmia score (**Figure 3D**) and total score of arrhythmic events (**Figure 3E**). The 10-minute time window after the onset of dofetilide infusion, in which the arrhythmic events were quantified, was shifted at the prevention experiment to compensate for the delayed occurrence of the first arrhythmic event. A representative overview of the occurrence of arrhythmic events at the prevention and induction experiment is presented in **Figure 3F**. Note the delay of the first arrhythmic event with ML277 (140 seconds at Dof vs. 195 seconds at

ML277 + Dof) and the reduced number of defibrillated TdP arrhythmias with a score equal or higher than 50.

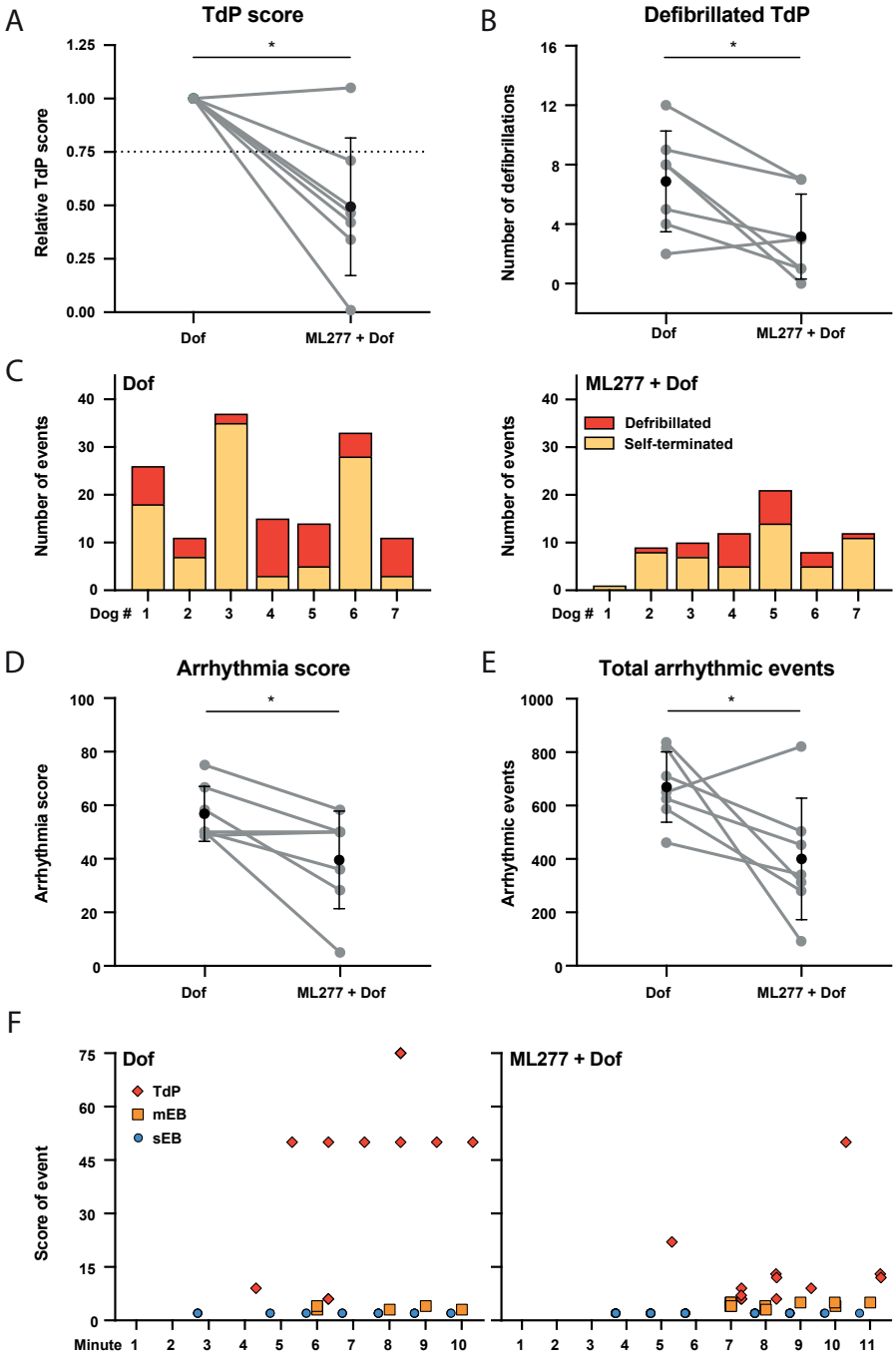

Figure 3. Reduction of Torsade de Pointes (TdP) arrhythmias after ML277. **A**) Relative TdP score and **B**) number of TdP arrhythmias terminated by defibrillation during dofetilide (Dof) infusion and during Dof following ML277. **C**) Overview of defibrillated and self-terminated TdP arrhythmias per dog during Dof and ML277 + Dof. **D**) Arrhythmia score and **E**) total of arrhythmic events during Dof and ML277 + Dof. Data of individual dogs in grey and mean ± SD in black, paired *t*-test with *p<0.05. **F**) Representative overview of arrhythmic events in the 10-minute time window per minute after the start of Dof (left panel) and after Dof following ML277 (right panel). The score of arrhythmic events refers to single ectopic beats (sEB, 2 points), multiple ectopic beats (mEB, 3-5 points), and TdP arrhythmias (TdP, 6-75 points). A TdP terminated with one shock was scored with 50 points, and two defibrillations were scored with 75 points. A delay of 55 seconds of the 10-minute time window is included in the results of ML277 + Dof. Results are from dog #7.

Discussion

In this study, we examined the potential antiarrhythmic effects of I_{Ks} activator ML277 in the CAVB dog model, which allows reproducible inducement of TdP arrhythmias under standardized conditions. ML277 temporarily suppressed dofetilide-induced repolarization prolongation and delayed the occurrence of the first arrhythmic event. Furthermore, the arrhythmic outcome was reduced as quantified by TdP score, number of defibrillated TdP arrhythmias, arrhythmia score, and total score of arrhythmic events.

Targeting I_{Ks} in the CAVB dog model

The I_{Kr} and I_{Ks} are crucial in accomplishing a stable repolarization phase, where I_{Ks} is less dominant compared to I_{Kr}.[25] Furthermore, both currents strongly contribute to a safety mechanism in case of an impaired function of a single potassium channel. The contribution of I_{Ks} to this repolarization reserve is more dominant: I_{Kr} block by dofetilide prolonged the APD by approximately 30%, while around 50% of the prolongation was due to HMR-1556 induced loss of I_{Ks} in dog cardiomyocytes.[25] In the CAVB dog model, the I_{Kr} and I_{Ks} densities are significantly downregulated.[26] This explains the ML277-induced delay in repolarization prolongation upon dofetilide in the CAVB dog, and a lack of ML277-induced QTc modulation in sinus rhythm dogs. I_{Ks} block by JNJ303 prolonged the QT interval in the CAVB model, and in combination with a trigger as enhanced inotropy, ventricular tachycardia and TdP arrhythmias were induced.[27]

In our standardized induction protocol, it is likely that I_{Kr} blocker dofetilide sufficiently prolongs the QT interval in such a way that the remaining I_{Ks} fails to compensate to maintain a proper repolarization reserve on a cellular level. This, in combination with AV block-induced

contractile and structural remodeling of the ventricles, anesthesia, and bradycardia, predisposes the heart to TdP arrhythmias in approximately 75% of the animals.[20] The current study included solely animals inducible for TdP arrhythmias upon dofetilide infusion. ML277 activated the I_{Ks} remaining after AV block-induced downregulation and the inhibiting effect of anesthesia component isoflurane.[28] This is presented by a delay in the occurrence of the first arrhythmic event and a delay in QT interval prolongation. Then, dofetilide challenged the repolarization reserve to such an extent to become reduced and unstable, thereby inducing QT prolongation and arrhythmic events. Here, the prevention approach (ML277 before dofetilide) instead of a suppression experiment (ML277 after dofetilide) allowed the establishment of electrophysiological effects of ML277 itself, and a controlled measurement of electrophysiological parameters such as STV,[29] which would be challenging to obtain upon enhanced arrhythmogenicity when dofetilide was given first. For further investigation, a suppressive approach would be of clinical value in determining a therapeutic effect.

Reproducibility of dofetilide-induced arrhythmias

With I_{Kr} blocker dofetilide as final hit in the standardized protocol of the CAVB dog model, TdP arrhythmia can be reproducibly induced in serial experiments.[30] Here, an average number of 13 TdP arrhythmias occurred in the 10-minute dofetilide time window, of which 20% demanded defibrillation. In the current study, inducible animals highly ranged in number of defibrillations upon dofetilide (2-12). Upon ML277, a significant reduction of the arrhythmic outcome was presented, though the occurrence of TdP arrhythmias – including the severe events demanding defibrillation – could not be suppressed completely. Here, the results of the induction and prevention experiments were compared in order to examine the potential antiarrhythmic outcome of ML277. While the exact reproducibility of the arrhythmic outcome during two serial experiments cannot be excluded, TdP outcome remained relatively stable between serial experiments upon a similar dose of dofetilide.[30]

In terms of cardiac remodeling over time, TdP sensitivity in inducible animals is consistent over the weeks – from CAVB2 weeks on.[20] Moreover, KCNQ1 mRNA and protein levels decreased already at three days, which maintained at least until 30 days after AV block in serial experiments.[31] An essential component for creating vulnerable circumstances for TdP arrhythmias to occur in our CAVB dog model is anesthesia induced by pentobarbital and

maintained by isoflurane. Important to note is that no arrhythmias occur under baseline conditions with this anesthetic regime.[32] On a level of ionic currents, isoflurane has a blocking effect on I_{Ks}.[28] The effect of isoflurane in the current study can be excluded due to serial performance of the induction and prevention experiment under identical conditions.

(Pre)clinical implications

Despite the reduced repolarization prolongation and arrhythmic outcome, the sustained occurrence of TdP arrhythmias after ML277 upon dofetilide infusion fails to consider this I_{Ks} activator as an antiarrhythmic drug in our preclinical model.[33] Yet, this study is the first to determine I_{Ks} activating effects of the compound in an animal model with bradycardia-induced sensitivity to ventricular arrhythmias. Furthermore, it reveals a potential role of I_{Ks} activation in long QT circumstances (temporal antiarrhythmic effect) across the well-determined and more dominant aspect of I_{Kr}.

Study limitations

Despite the extensive electrophysiological evaluation of ML277 in the CAVB dog model, the current data cannot distinguish if dofetilide counteracts with or 'overrules' the ML277-induced electrophysiological effects or if it concerns a potential limited duration of action by ML277. I_{Ks} and action potential recordings are lacking in this study and could have provided further insight into the time and dose dependent behavior of ML277 with a confirming evaluation of the presented *in vivo* electrophysiological effects of ML277. Additional pharmacokinetic analysis is required to elaborate on the peak plasma concentrations and its corresponding time-dependent effect on the presented antiarrhythmic properties.

Conclusions

I_{Ks} activation by ML277 temporarily suppresses dofetilide-induced repolarization prolongation and occurrence of a first arrhythmic event in the CAVB dog model. Whereas the arrhythmic outcome is significantly reduced upon ML277, it fails to completely suppress dofetilide-induced TdP arrhythmias.

References

1. Napolitano C, Priori SG, Schwartz PJ, et al. Genetic testing in the long QT syndrome: development and validation of an efficient approach to genotyping in clinical practice. *JAMA.* 2005;294(23):2975-2980.
2. Kapplinger JD, Tester DJ, Salisbury BA, et al. Spectrum and prevalence of mutations from the first 2,500 consecutive unrelated patients referred for the FAMILION long QT syndrome genetic test. *Heart Rhythm.* 2009;6(9):1297-1303.
3. Banyasz T, Jian Z, Horvath B, Khabbaz S, Izu LT, Chen-Izu Y. Beta-adrenergic stimulation reverses the IKr-IKs dominant pattern during cardiac action potential. *Pflugers Arch.* 2014;466(11):2067-2076.
4. Volders PG, Stengl M, Van Opstal JM, et al. Probing the contribution of IKs to canine ventricular repolarization: key role for beta-adrenergic receptor stimulation. *Circulation.* 2003;107(21):2753-2760.
5. Dvir M, Peretz A, Haitin Y, Attali B. Recent molecular insights from mutated IKs channels in cardiac arrhythmia. *Curr Opin Pharmacol.* 2014;15:74-82.
6. Chen S, Zhang L, Bryant RM, et al. KCNQ1 mutations in patients with a family history of lethal cardiac arrhythmias and sudden death. *Clin Genet.* 2003;63(4):273-282.
7. Zheng Y, Zhu X, Zhou P, et al. Hexachlorophene is a potent KCNQ1/KCNE1 potassium channel activator which rescues LQTs mutants. *PLoS One.* 2012;7(12):e51820.
8. Gao Z, Xiong Q, Sun H, Li M. Desensitization of chemical activation by auxiliary subunits: convergence of molecular determinants critical for augmenting KCNQ1 potassium channels. *J Biol Chem.* 2008;283(33):22649-22658.
9. Nissen JD, Diness JG, Diness TG, Hansen RS, Grunnet M, Jespersen T. Pharmacologically induced long QT type 2 can be rescued by activation of IKs with benzodiazepine R-L3 in isolated guinea pig cardiomyocytes. *J Cardiovasc Pharmacol.* 2009;54(2):169-177.
10. Wu X, Larsson HP. Insights into cardiac IKs (KCNQ1/KCNE1) channels regulation. *Int J Mol Sci.* 2020;21(24):9440.
11. Mattmann ME, Yu H, Lin Z, et al. Identification of (R)-N-(4-(4-methoxyphenyl)thiazol-2-yl)-1-tosylpiperidine-2-carboxamide, ML277, as a novel, potent and selective K(v)7.1 (KCNQ1) potassium channel activator. *Bioorg Med Chem Lett.* 2012;22(18):5936-5941.
12. Xu Y, Wang Y, Zhang M, et al. Probing binding sites and mechanisms of action of an I(Ks) activator by computations and experiments. *Biophys J.* 2015;108(1):62-75.
13. Hou P, Shi J, White KM, Gao Y, Cui J. ML277 specifically enhances the fully activated open state of KCNQ1 by modulating VSD-pore coupling. *Elife.* 2019;8:e48576.
14. Willegems K, Eldstrom J, Kyriakis E, et al. Structural and electrophysiological basis for the modulation of KCNQ1 channel currents by ML277. *Nat Commun.* 2022;13(1):3760.
15. Yu H, Lin Z, Mattmann ME, et al. Dynamic subunit stoichiometry confers a progressive continuum of pharmacological sensitivity by KCNQ potassium channels. *Proc Natl Acad Sci U S A.* 2013;110(21):8732-8737.
16. Ma D, Wei H, Lu J, et al. Characterization of a novel KCNQ1 mutation for type 1 long QT syndrome and assessment of the therapeutic potential of a novel IKs activator using patient-specific induced pluripotent stem cell-derived cardiomyocytes. *Stem Cell Res Ther.* 2015;6:39.
17. Kuusela J, Kim J, Rasanen E, Aalto-Setala K. The effects of pharmacological compounds on beat rate variations in human long QT-syndrome cardiomyocytes. *Stem Cell Rev Rep.* 2016;12(6):698-707.
18. Loen V, Vos MA, Van der Heyden MAG. The canine chronic atrioventricular block model in cardiovascular preclinical drug research. *Br J Pharmacol.* 2022;179(5):859-881.
19. Vos MA, de Groot SH, Verduyn SC, et al. Enhanced susceptibility for acquired torsade de pointes arrhythmias in the dog with chronic, complete AV block is related to cardiac hypertrophy and electrical remodeling. *Circulation.* 1998;98(11):1125-1135.
20. Bourgonje VJA, Van Veen TAB, Vos MA. Ventricular electrical remodeling in compensated cardiac hypertrophy. In: Gussak I, Antzelevitch C, eds. *Electrical Diseases of the Heart*. London: Springer-Verlag; 2013:387-398.

21. Timmermans C, Rodriguez LM, Van Suylen RJ, et al. Catheter-based cryoablation produces permanent bidirectional cavotricuspid isthmus conduction block in dogs. *J Interv Card Electrophysiol.* 2002;7(2):149-155.
22. Van de Water A, Verheyen J, Xhonneux R, Reneman RS. An improved method to correct the QT interval of the electrocardiogram for changes in heart rate. *J Pharmacol Methods.* 1989;22(3):207-217.
23. Thomsen MB, Verduyn SC, Stengl M, et al. Increased short-term variability of repolarization predicts d-sotalol-induced torsades de pointes in dogs. *Circulation.* 2004;110(16):2453-2459.
24. Stams TRG, Winckels SKG, Oros A, et al. Novel parameters to improve quantification of repolarization reserve and arrhythmogenesis using a dofetilide challenge. *Heart Rhythm.* 2013;10(11):1745-1746.
25. Jost N, Virag L, Comtois P, et al. Ionic mechanisms limiting cardiac repolarization reserve in humans compared to dogs. *J Physiol.* 2013;591(17):4189-4206.
26. Volders PG, Sipido KR, Vos MA, et al. Downregulation of delayed rectifier K(+) currents in dogs with chronic complete atrioventricular block and acquired torsades de pointes. *Circulation.* 1999;100(24):2455-2461.
27. Van Bavel JJA, Beekman HDM, Van Weperen VYH, Van der Linde HJ, Van der Heyden MAG, Vos MA. I(Ks) inhibitor JNJ303 prolongs the QT interval and perpetuates arrhythmia when combined with enhanced inotropy in the CAVB dog. *Eur J Pharmacol.* 2022;932:175218.
28. Suzuki A, Bosnjak ZJ, Kwok WM. The effects of isoflurane on the cardiac slowly activating delayed-rectifier potassium channel in Guinea pig ventricular myocytes. *Anesth Analg.* 2003;96(5):1308-1315.
29. Bossu A, Varkevisser R, Beekman HDM, Houtman MJC, Van der Heyden MAG, Vos MA. Short-term variability of repolarization is superior to other repolarization parameters in the evaluation of diverse antiarrhythmic interventions in the chronic atrioventricular block dog. *J Cardiovasc Pharmacol.* 2017;69(6):398-407.
30. Oros A, Beekman JD, Vos MA. The canine model with chronic, complete atrio-ventricular block. *Pharmacol Ther.* 2008;119(2):168-178.
31. Stengl M, Ramakers C, Donker DW, et al. Temporal patterns of electrical remodeling in canine ventricular hypertrophy: focus on IKs downregulation and blunted beta-adrenergic activation. *Cardiovasc Res.* 2006;72(1):90-100.
32. Dunnink A, Sharif S, Oosterhoff P, et al. Anesthesia and arrhythmogenesis in the chronic atrioventricular block dog model. *J Cardiovasc Pharmacol.* 2010;55(6):601-608.
33. Van Weperen VYH, Bossu A, Vos MA. Point of view: electrophysiological endpoints differ when comparing the mode of action of highly successful anti-arrhythmic drugs in the CAVB Dog model with TdP. *J Cardiovasc Pharmacol.* 2019;74(6):499-507.

6

What makes the chronic AV block dog inducible for ventricular arrhythmias?

Joanne J.A. van Bavel[1], Henriëtte D.M. Beekman[1], Marien J.C. Houtman[1], Marc A. Vos[1], Marcel A.G. van der Heyden[1]

[1] Department of Medical Physiology, Division of Heart and Lungs, University Medical Center Utrecht, Utrecht, the Netherlands

A study in progress

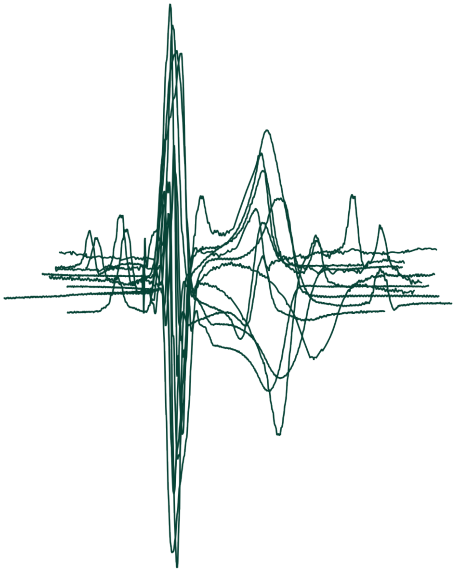

Abstract

The dog with chronic atrioventricular block (CAVB) combines a number of risk factors associated with Torsade de Pointes (TdP) arrhythmias. Nevertheless, approximately 33% of the animals are resistant to dofetilide-induced TdP arrhythmia. Of a group of 78 experimentally identical CAVB dogs, we compared TdP inducible vs. non-inducible animals for a set of basic, and cardiac electrical and mechanical parameters. Body weight, but not sex or age, is associated with TdP inducibility. Of the cardiac parameters, longer ventricular repolarization duration and increased contractility at baseline are associated with dofetilide-induced TdP arrhythmias. Differences in cardiac parameters disappeared upon dofetilide infusion. We discuss that prolonged repolarization and increased contractility may be early indications of calcium mediated early after depolarization that may develop into TdP arrhythmias.

Keywords

AV block dog model, remodeling, torsade de pointes, arrhythmia predisposition

Introduction

The baseline prevalence of cardiac rhythm abnormalities is >2%.[1] Several well-established factors increase the risk for QT prolongation and Torsade de Pointes (TdP) arrhythmias, of which main contributors are female sex, electrolyte imbalance (in particular hypokalemia), age, genetic predisposition, congestive heart failure, and ischemia.[2] Moreover, many widely used medications can induce or exacerbate arrhythmias and much on its underlying mechanism remains unknown.[3] Therefore, an animal model with high and reproducible inducibility rates for ventricular arrhythmias is deemed necessary to test pro- and antiarrhythmic properties of drugs but also new device strategies.

The dog with chronic complete atrioventricular block (CAVB) is already in use for decades as a successful model in cardiac ventricular arrhythmia research.[4] Many pro- and antiarrhythmic drugs and new device properties were evaluated, most often demonstrating congruence with their actions on the heart in humans.[5] The AV block-induced bradycardia causes cardiac adaptation occurring in the weeks succeeding[6] in order to maintain cardiac output as physiologically demanded. Increased neurohormonal levels and calcium handling alterations[7-10] enhance the contractility, which are slowly taken over on a structural level in the form of biventricular hypertrophy[11] without increased fibrosis formation.[7] Moreover, electrical remodeling includes diminished repolarizing I_{Kr} and I_{Ks} densities[12] and is associated with QT prolongation and a reduced repolarization reserve. These outcomes are known proarrhythmic parameters[13] and predispose the animals for drug-induced arrhythmia. Hence, a combination of bradycardia, anesthesia, and infusion of the I_{Kr} blocker dofetilide, leads to TdP arrhythmias in approximately 75% of the animals, which is reproducible when tested again a few weeks later.[4]

Although the high incidence of drug-induced ventricular arrhythmia makes it a useful model, it is still incomprehensible which factors or combination thereof distinguishes “inducible” animals (≥3 TdP arrhythmias in the 10-minute testing period) from “non-inducible” animals (≤2 TdP arrhythmias). Namely, all animals have undergone the same experimental treatments, are of mixed breeds, and even between littermates inducible and non-inducible animals are apparent. In this sense, the model mirrors several human pathological conditions

in which only a proportion of the affected people encounter cardiac arrhythmias, while all have a combination of risk factors.[13]

Most published studies using CAVB dogs present only small experimental groups (4-12 animals),[5] hampering matching presented risk factors to occurrence of cardiac arrhythmia. Moreover, methodology is slightly different between laboratories or change over time, adding to the difficulties in retrospective meta-analysis. Since we have performed many experiments over the last 10 years in CAVB dogs with identical methodology (dog breed and age (1-2 years), generation of AV block, remodeling at idioventricular rhythm (IVR), anesthesia, dofetilide infusion regimen, housing, researcher), we decided to explore our database for currently unpublished general characteristics and cardiac responses of the CAVB dog model in an attempt to answer the question "what makes a CAVB dog inducible?".

Methods

Animals

In this analysis, a total of 78 Marshall Mongrel™ dogs (Marshall, NY, USA) were included that had undergone TdP inducibility testing between the years 2010 and 2020. AV block was induced by radiofrequency ablation of the His-bundle, dogs then underwent remodeling at IVR for >2 weeks, and animals were tested for TdP inducibility with dofetilide (0.025 mg/kg, i.v.) following anesthesia induction with sodium pentobarbital (25 mg/kg i.v.) and maintenance with isoflurane (1.5%). Animal care and experimentation were approved by the Committee for Experiments on Animals of Utrecht University and were in accordance with the Directive 2010//63/EU of the European Parliament and the Dutch law on animal experimentation. Full experimental details including notifications on ARRIVE guidelines can be found in the associated publications.[6,14-20]

Statistics

Data are presented as mean ± SD. Data were analyzed using an unpaired Students *t*-test or a one-way or two-way analysis of variance (ANOVA). Statistical analyses were performed using Graphpad Prism (version 9.3.1, Graphpad Software, San Diego, USA). A value of $p<0.05$ was considered statistically significant.

Results

General characteristics vs. inducibility

With regard to sex, no significant differences were observed in inducibility (62% of the females and 77% of the males were inducible) (**Figure 1A**) and thus the selected group represented the known fraction of inducible animals of approximately 75%. Moreover, no age difference was observed between the two groups (16.9 ± 4.9 vs. 17.4 ± 6.8 months for inducible and non-inducible animals, respectively) (**Figure 1B**). The time of the experiment - in the morning or in the afternoon - had no effect on the inducibility outcome (**Figure 1C**). On a group level, body weight was significantly different between inducible and non-inducible dogs (**Figure 1D**), but in general male dogs were heavier than females (**Figure 1E**). The body weight at heart isolation was lower for non-inducible dogs, though not significant (**Figure 1F**) and the relative heart weight (heart weight *vs*. body weight, *i.e.* an indication of cardiac hypertrophy) was similar between groups (**Figure 1G**). The same holds true for relative lung and liver weight (**Figure 1H, I**) indicating no explicit implications for heart failure. Furthermore, body weight difference between the inducible and non-inducible dogs is rather small, and a substantial overlap between the two groups is apparent. Since all animals were of mixed breed and obtained from the same source (Marshall, NY, USA), no analysis with respect to these factors could be performed. We also do not have complete knowledge on littermates in each group of animals though inclusion of littermates within experimental setups was certainly limited.

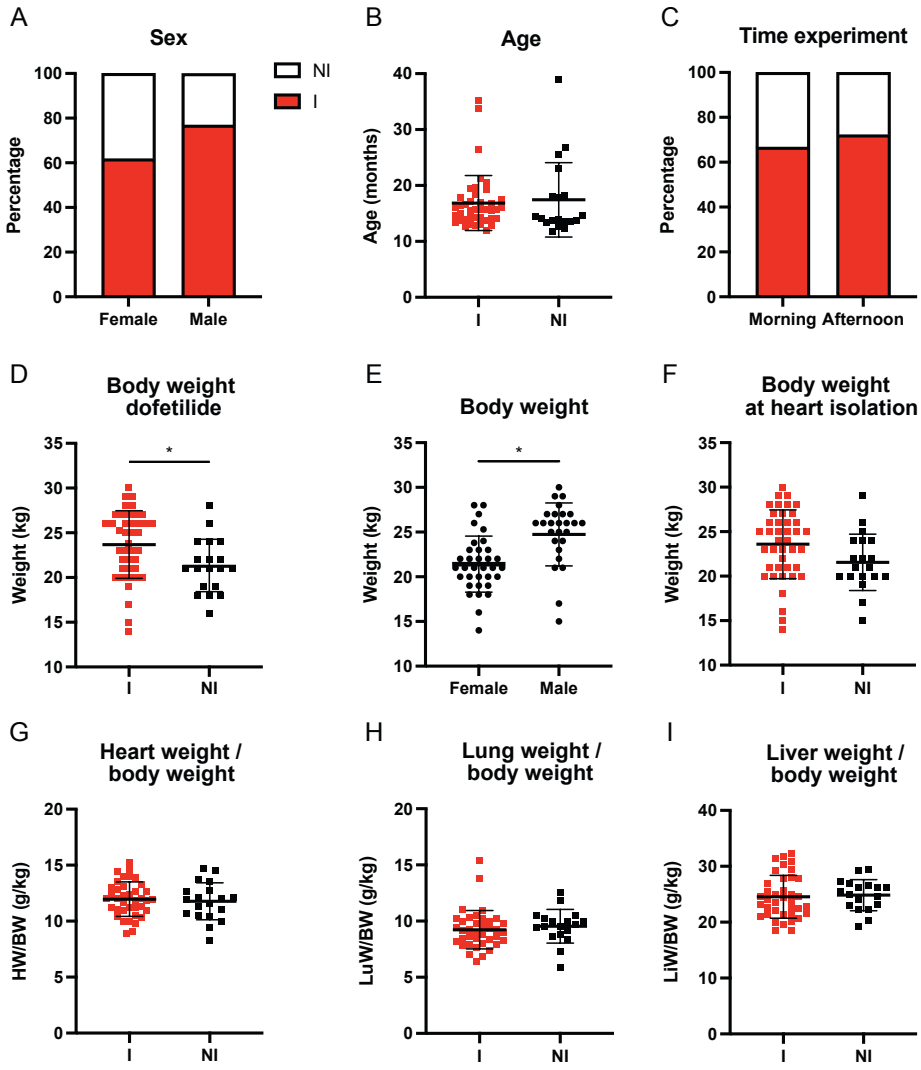

Figure 1. Arrhythmia inducibility per general characteristic of chronic AV block dogs. **A**) Sex (female n=34, male n=27), **B**) age, **C**) time of dofetilide experiment (morning n=43 and afternoon n=18), **D**) body weight during dofetilide experiment, **E**) body weight of female and males, **F**) body weight at heart isolation timepoint, **G**) heart weight/body weight (HW/BW), **H**) lung weight/body weight (LuW/BW), and **I**) liver weight/body weight (LiW/BW) at heart isolation timepoint. I = inducible, and NI = non-inducible. Mean ± SD, two-way ANOVA and unpaired students t-test, * refers to $p<0.05$.

Electrophysiological parameters vs. inducibility

Of all ECG parameters analyzed from remodeled CAVB dogs before dofetilide was added (baseline), only those representing (JT, JTc) or including (QT, QTc) ventricular repolarization intervals are different between inducible and non-inducible animals (**Table 1**). This is, QTc and JTc are approximately 70 ms longer in inducible dogs. Remarkably however, such difference

is not reflected in local MAP duration, either when obtained from the left or right ventricle (LV and RV, respectively). Beat-to-beat variation of repolarization duration quantified by short term variability (STV) in baseline conditions, either from the LV or RV, shows an increased trend in the inducible animals. Dofetilide infusion lengthens repolarization parameters, but more importantly in this respect, eliminates the repolarization differences between inducible and non-inducible CAVB dogs. Similar effects are seen with respect to STV. Only the PP-interval is significantly different between inducible and non-inducible animals, *i.e.* atrial rate is lower in non-inducible animals. In conclusion, a longer repolarization duration at baseline correlates with TdP inducibility, whereas the arrhythmia inducing trigger, dofetilide, eliminates these differences.

Contraction parameters vs. inducibility

In a subset of the dogs, contraction parameters from the LV have been recorded. LV end systolic pressure (ESP) is similar between inducible and non-inducible animals in baseline and dofetilide increases LV ESP in both groups (**Table 1**). No differences can be observed in LV end diastolic pressure (LV EDP), either between inducible *vs*. non-inducible, neither for baseline *vs.* dofetilide. However, the maximal rise in ventricular pressure ($LVdP/dt_{max}$) is higher in inducible animals, and whereas dofetilide increases maximal pressure rise on the one hand, it eliminates differences between inducible *vs.* non-inducible dogs.

Table 1. Electrophysiological and contractile parameters in inducible and non-inducible chronic AV block dogs at baseline and during dofetilide.

	Baseline		**Dofetilide**		
Parameter	**Inducible**	**Non-inducible**	**Inducible**	**Non-inducible**	n (I, NI)
RR	1405 ± 280	1295 ± 157	1550 ± 294*	1510 ± 191*	40, 18
PP	543 ± 74	574 ± 68	635 ± 98*	704 ± 127*^	28, 15
QRS	95 ± 19	91 ± 17	96 ± 21	96 ± 17	39, 18
QT	443 ± 75	364 ± 40^	613 ± 102*	607 ± 69*	40, 18
QTc	407 ± 68	338 ± 34^	565 ± 87*	562 ± 67*	40, 18
JT	347 ± 75	272 ± 36^	520 ± 98*	511 ± 61*	39, 18
JTc	312 ± 68	246 ± 31^	473 ± 83*	467 ± 59*	39, 18
LV MAP	306 ± 50	288 ± 20	479 ± 118*	485 ± 98*	27, 9
RV MAP	260 ± 37	250 ± 29	361 ± 99*	400 ± 78*	23, 10
Δ MAP	41 ± 28	35 ± 28	123 ± 86*	80 ± 72	20, 9
LV STV	1.70 ± 1.24	0.80 ± 0.42	3.57 ± 1.92*	2.54 ± 1.04*	26, 9
RV STV	1.25 ± 0.99	0.76 ± 0.18	2.99 ± 1.70*	3.79 ± 2.41*	15, 7
LVdP/dt$_{max}$	2047 ± 416	1368 ± 205^	2724 ± 520*	2474 ± 554*	10, 5
LV EDP	11 ± 6	8 ± 5	12 ± 5	9 ± 3	13, 4
LV ESP	91 ± 8	85 ± 11	100 ± 7*	102 ± 9*	13, 4

Data presented as mean ± SD. The sample size for inducible (I) and non-inducible (NI) dogs is presented in the last column. Electrophysiological data in ms, LVdP/dt$_{max}$ in mmHg/s, and LV EDP and LV ESP in mmHg. Two-way ANOVA, with Bonferroni's multiple comparisons test. *p<0.05 compared to baseline, and ^p<0.05 compared to inducible dogs.

Arrhythmia indication vs. inducibility

The dominant repolarization prolongation (**Figure 2A**) and the enhanced contractility (**Figure 2B**) of inducible dogs compared to non-inducible dogs at baseline display the indication of the arrhythmic outcome after dofetilide infusion in inducible animals. The clear difference in arrhythmia score reflects the severity of the arrhythmic events in the ten-minute time period after the onset of dofetilide infusion (**Figure 2C**).

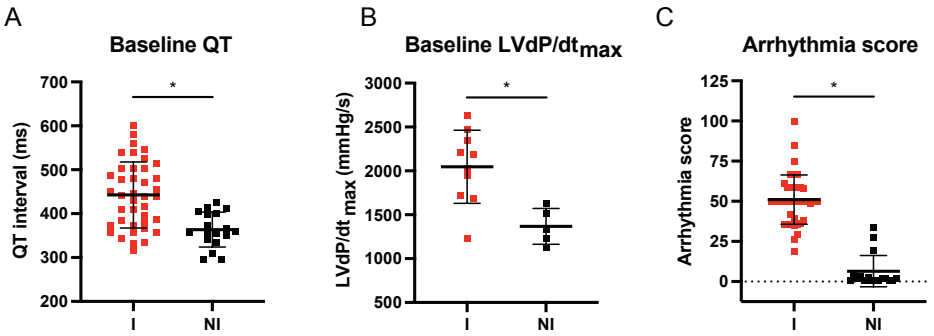

Figure 2. Parameters at baseline indicating arrhythmia outcome. **A**) QT interval and **B**) LVdP/dt_{max} at baseline for inducible (I) and non-inducible (NI) dogs. **C**) Arrhythmia score reflecting the average of the three highest scored arrhythmic events after dofetilide. Mean ± SD, unpaired students t-test, * refers to $p<0.05$.

Cellular data

Ventricular cardiomyocytes from the LV and RV of the CAVB dog have been isolated over the years. Following the final experiment in the experimental protocol, which may differ between the animals (testing of pro- and antiarrhythmic drugs or device interventions), hearts were excised. Cell isolation was performed as described previously.[21] Under baseline patch clamp measuring conditions, there is a strong trend towards a longer action potential duration (APD) in ventricular myocytes isolated from inducible animals than from non-inducible animals (**Figure 3A**). Though, the expected increase in STV of cells from inducible dogs is insignificant (**Figure 3B**). No differences were found when distinguishing cardiomyocytes from the RV and LV (APD90: 439 ± 72 ms (LV) vs. 434 ± 128 ms (RV) for inducible dogs, and 390 ± 63 ms (LV) vs. 381 ± 64 (RV) for non-inducible dogs, STV: 37 ± 20 ms (LV) vs. 49 ± 61 ms (RV) for inducible dogs, and 25 ± 11 ms (LV) vs. 15 ± 6 ms (RV) for non-inducible dogs).

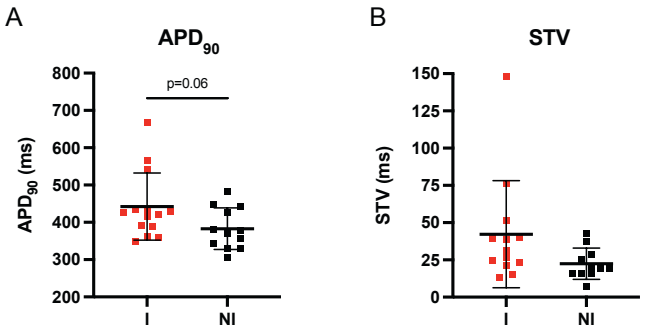

Figure 3. Patch clamp measurements during baseline including **A**) action potential duration at 90% repolarization (APD_{90}) and **B**) short term variability (STV) of the APD_{90} of isolated left and right ventricular cardiomyocytes from inducible (I, n=14 for APD_{90} and n=13 for STV) and non-inducible (NI, n=12 for APD_{90} and n=11 for STV) chronic atrioventricular block dogs. Mean ± SD, unpaired Student's t-test.

Discussion

Sex is not related to TdP inducibility in dogs

A number of studies indicated that in canines QTc duration and other ECG parameters do not differ between males and females,[22] in contrast to humans in which QTc duration is longer in females and sex is considered as a risk factor of TdP (e.g., Drew et al., 2010 and references therein).[13] In clinical practice, dofetilide dose reductions and discontinuations occur more often in women than in men, mainly for reasons of significant QTc prolongation.[23] Importantly, our current analysis indicates that sex is not a risk factor for dofetilide-induced TdP arrhythmias in dogs.

We observed an association between body weight and TdP inducibility in dogs. In our cohort, male dogs were heavier, which may explain the apparent trend of male sex associated increase in higher inducibility. In contrast, we did not observe an association between HW/BW and inducibility. We may consider this as an absence of overt hypertrophy. We have no indications that body fat/muscle distribution changes when animals are heavier, and therefore pharmacokinetics are expected not to be affected by absolute body weight.

Baseline contractility in inducible dogs, a reflection of calcium mediated arrhythmogenesis?

In response to the permanent AV block, cardiac ventricular remodeling occurs in different phases.[4,5] The main mechanism of TdP initiation is through the formation of early after

depolarizations.[24] These result from incorrectly timed cellular calcium increase during the later phases of cardiac repolarization, although the exact mechanisms and players involved have not been resolved completely.[25] Indeed, self-terminating TdPs in the CAVB dog are initiated and maintained by a focal mechanism.[26,27] In strong support of the role of calcium are the findings that calcium antagonists addressing intracellular calcium load (*e.g.* flunarizine, verapamil) are amongst the most effective antiarrhythmics in the CAVB dog model.[6,28-30] As calcium stands at the origin of cardiac contraction, it may indicate that the enhanced contraction parameter in inducible animals at baseline results from excessive remodeling and resulting calcium handling, which may directly link to the underlying mechanism of TdP initiation, and thus arrhythmia risk.

Dofetilide alleviates differences in electrical and contraction parameters between inducible and non-inducible dogs

The cardiac parameters that distinguish inducible from non-inducible dogs at baseline, *i.e.* ECG quantifications of repolarization and LVdP/dt_{max}, increase in both groups of animals in response to dofetilide. However, as the extent of increase is higher in non-inducible animals, these parameters lose their ability to distinguish between both animal groups upon dofetilide infusion. We interpreted this finding as confirmation that prolonged repolarization and increased LVdP/dt_{max} are indicative for proarrhythmic remodeling, but that these are not directly related to triggering TdPs and their maintenance in response to dofetilide.

Over the years, we investigated two different repolarization related parameters and their association with TdP arrhythmias. Firstly, beat-to-beat variability of repolarization, quantified as STV, is a specific type of temporal dispersion of repolarization. It increases upon dofetilide-induced lengthening of repolarization where it can distinguish between inducible and non-inducible animals.[31] Here, **Table 1** indicates that baseline STV values appear to be larger in inducible animals, but did not reach significance. Furthermore, a sudden increase in STV predicts, to a certain extent, a drug (dofetilide, d-sotalol, sertindole) elicited upcoming TdP.[18,31,32] Increased beat-to-beat variability of repolarization likely associates with EAD formation and thus TdP initiation. Though, it should be mentioned that this parameter is sensitive to accurate determination of the end of the MAP signal and therefore demands a proper acquisition and use of cardiac signals. Secondly, spatial dispersion of repolarization

(SDR), that can be measured in diverse orientations in the ventricular free walls e.g., cubic dispersion,[33] quantifies local repolarization heterogeneity. SDR has no predictive value in baseline but can distinguish between inducible and non-inducible animals upon dofetilide infusion.[33] Increased SDR was found to be associated with perpetuation of non-self-terminating TdPs.[34] In a previous study using a smaller group of animals and different anesthesia (halothane *vs.* isoflurane), QTc at baseline was also larger in inducible dogs, and upon dofetilide infusion QTc prolonged in both groups as expected, but QTc remained longer in inducible animals *vs.* non-inducible animals.[31]

Future perspectives

The dog is not useful for investigating sex differences in arrhythmia inducibility. On the other hand, it can be advantageous as sex is not a confounding factor in arrhythmia research using this species. Number of data has to be increased, and we encourage other research teams using the CAVB dogs, albeit with somewhat different methodology, to use their database in similar analyses. More intelligent methods e.g., machine learning based analytics of multiple parameters may be useful to enable prediction of animals at risk for dofetilide-induced TdP.

References

1. Khurshid S, Choi SH, Weng LC, et al. Frequency of cardiac rhythm abnormalities in a half million adults. *Circ Arrhythm Electrophysiol.* 2018;11(7):e006273.
2. Cohagan B, Brandis D. Torsade de Pointes. *StatPearls*. Treasure Island (FL)2023.
3. Tisdale JE, Chung MK, Campbell KB, et al. Drug-induced arrhythmias: a scientific statement from the American Heart Association. *Circulation.* 2020;142(15):e214-e233.
4. Oros A, Beekman JD, Vos MA. The canine model with chronic, complete atrio-ventricular block. *Pharmacol Ther.* 2008;119(2):168-178.
5. Loen V, Vos MA, Van der Heyden MAG. The canine chronic atrioventricular block model in cardiovascular preclinical drug research. *Br J Pharmacol.* 2022;179(5):859-881.
6. Bourgonje VJ, Vos MA, Ozdemir S, et al. Combined Na(+)/Ca(2+) exchanger and L-type calcium channel block as a potential strategy to suppress arrhythmias and maintain ventricular function. *Circ Arrhythm Electrophysiol.* 2013;6(2):371-379.
7. Vos MA, de Groot SH, Verduyn SC, et al. Enhanced susceptibility for acquired torsade de pointes arrhythmias in the dog with chronic, complete AV block is related to cardiac hypertrophy and electrical remodeling. *Circulation.* 1998;98(11):1125-1135.
8. Sipido KR, Volders PG, de Groot SH, et al. Enhanced Ca(2+) release and Na/Ca exchange activity in hypertrophied canine ventricular myocytes: potential link between contractile adaptation and arrhythmogenesis. *Circulation.* 2000;102(17):2137-2144.
9. Antoons G, Volders PG, Stankovicova T, et al. Window Ca2+ current and its modulation by Ca2+ release in hypertrophied cardiac myocytes from dogs with chronic atrioventricular block. *J Physiol.* 2007;579(Pt 1):147-160.
10. Antoons G, Johnson DM, Dries E, et al. Calcium release near L-type calcium channels promotes beat-to-

beat variability in ventricular myocytes from the chronic AV block dog. *J Mol Cell Cardiol.* 2015;89(Pt B):326-334.

11. Volders PG, Sipido KR, Vos MA, Kulcsar A, Verduyn SC, Wellens HJ. Cellular basis of biventricular hypertrophy and arrhythmogenesis in dogs with chronic complete atrioventricular block and acquired torsade de pointes. *Circulation.* 1998;98(11):1136-1147.
12. Volders PG, Sipido KR, Vos MA, et al. Downregulation of delayed rectifier K(+) currents in dogs with chronic complete atrioventricular block and acquired torsades de pointes. *Circulation.* 1999;100(24):2455-2461.
13. Drew BJ, Ackerman MJ, Funk M, et al. Prevention of torsade de pointes in hospital settings: a scientific statement from the American Heart Association and the American College of Cardiology Foundation. *J Am Coll Cardiol.* 2010;55(9):934-947.
14. Bossu A, Houtman MJC, Meijborg VMF, et al. Selective late sodium current inhibitor GS-458967 suppresses Torsades de Pointes by mostly affecting perpetuation but not initiation of the arrhythmia. *Br J Pharmacol.* 2018;175(12):2470-2482.
15. Sprenkeler DJ, Bossu A, Beekman JDM, Schoenmakers M, Vos MA. An augmented negative force-frequency relationship and slowed mechanical restitution are associated with increased susceptibility to drug-induced torsade de pointes arrhythmias in the chronic atrioventricular block dog. *Front Physiol.* 2018;9:1086.
16. Wijers SC, Sprenkeler DJ, Bossu A, et al. Beat-to-beat variations in activation-recovery interval derived from the right ventricular electrogram can monitor arrhythmic risk under anesthetic and awake conditions in the canine chronic atrioventricular block model. *Heart Rhythm.* 2018;15(3):442-448.
17. Smoczyńska A, Loen V, Aranda A, Beekman HDM, Meine M, Vos MA. High-rate pacing guided by short-term variability of repolarization prevents imminent ventricular arrhythmias automatically by an implantable cardioverter-defibrillator in the chronic atrioventricular block dog model. *Heart Rhythm.* 2020;17(12):2078-2085.
18. Smoczyńska A, Sprenkeler DJ, Aranda A, et al. Evaluation of a fully automatic measurement of short-term variability of repolarization on intracardiac electrograms in the chronic atrioventricular block dog. *Front Physiol.* 2020;11:1005.
19. Van Bavel JJA, Beekman HDM, Van Weperen VYH, Van der Linde HJ, Van der Heyden MAG, Vos MA. I(Ks) inhibitor JNJ303 prolongs the QT interval and perpetuates arrhythmia when combined with enhanced inotropy in the CAVB dog. *Eur J Pharmacol.* 2022;932:175218.
20. Van Bavel JJA, Pham C, Beekman HDM, et al. PI3K/mTOR inhibitor omipalisib prolongs cardiac repolarization along with a mild proarrhythmic outcome in the AV block dog model. *Front Cardiovasc Med.* 2022;9:956538.
21. Nalos L, Varkevisser R, Jonsson MK, et al. Comparison of the IKr blockers moxifloxacin, dofetilide and E-4031 in five screening models of pro-arrhythmia reveals lack of specificity of isolated cardiomyocytes. *Br J Pharmacol.* 2012;165(2):467-478.
22. Salama G, Bett GC. Sex differences in the mechanisms underlying long QT syndrome. *Am J Physiol Heart Circ Physiol.* 2014;307(5):H640-648.
23. Pokorney SD, Yen DC, Campbell KB, et al. Dofetilide dose reductions and discontinuations in women compared with men. *Heart Rhythm.* 2018;15(4):478-484.
24. Roden DM. Torsade de pointes. *Clin Cardiol.* 1993;16(9):683-686.
25. Nemec J, Kim JJ, Salama G. The link between abnormal calcium handling and electrical instability in acquired long QT syndrome - Does calcium precipitate arrhythmic storms? *Prog Biophys Mol Biol.* 2016;120(1-3):210-221.
26. Boulaksil M, Jungschleger JG, Antoons G, et al. Drug-induced torsade de pointes arrhythmias in the chronic AV block dog are perpetuated by focal activity. *Circ Arrhythm Electrophysiol.* 2011;4(4):566-576.
27. Vandersickel N, Bossu A, De Neve J, et al. Short-lasting episodes of torsade de pointes in the chronic

atrioventricular block dog model have a focal mechanism, while longer-lasting episodes are maintained by re-entry. *JACC Clin Electrophysiol.* 2017;3(13):1565-1576.

28. Verduyn SC, Vos MA, Gorgels AP, Van der Zande J, Leunissen JD, Wellens HJ. The effect of flunarizine and ryanodine on acquired torsades de pointes arrhythmias in the intact canine heart. *J Cardiovasc Electrophysiol.* 1995;6(3):189-200.
29. Oros A, Houtman MJ, Neco P, et al. Robust anti-arrhythmic efficacy of verapamil and flunarizine against dofetilide-induced TdP arrhythmias is based upon a shared and a different mode of action. *Br J Pharmacol.* 2010;161(1):162-175.
30. Bossu A, Varkevisser R, Beekman HDM, Houtman MJC, Van der Heyden MAG, Vos MA. Short-term variability of repolarization is superior to other repolarization parameters in the evaluation of diverse antiarrhythmic interventions in the chronic atrioventricular block dog. *J Cardiovasc Pharmacol.* 2017;69(6):398-407.
31. Thomsen MB, Oros A, Schoenmakers M, et al. Proarrhythmic electrical remodelling is associated with increased beat-to-beat variability of repolarisation. *Cardiovasc Res.* 2007;73(3):521-530.
32. Thomsen MB, Verduyn SC, Stengl M, et al. Increased short-term variability of repolarization predicts d-sotalol-induced torsades de pointes in dogs. *Circulation.* 2004;110(16):2453-2459.
33. Dunnink A, Stams TRG, Bossu A, et al. Torsade de pointes arrhythmias arise at the site of maximal heterogeneity of repolarization in the chronic complete atrioventricular block dog. *Europace.* 2017;19(5):858-865.
34. Smoczyńska A, Aarnink EW, Dunnink A, et al. Interplay between temporal and spatial dispersion of repolarization in the initiation and perpetuation of torsades de pointes in the chronic atrioventricular block dog. *Am J Physiol Heart Circ Physiol.* 2021;321(3):H569-H576.

Part II

Device testing

7

Remodeling in the AV block dog is essential for tolerating moderate treadmill activity

Joanne J.A. van Bavel[1], Henriëtte D.M. Beekman[1], Arend Schot[2], Philippe C. Wouters[3], Maarten G. van Emst[2], Tim Takken[4], Marcel A.G. van der Heyden[1], Marc A. Vos[1]

[1] Department of Medical Physiology, Division of Heart and Lungs, University Medical Center Utrecht, Utrecht, the Netherlands
[2] Department of Clinical Sciences, Division of Anatomy and Physiology, Faculty of Veterinary Medicine, Utrecht University, the Netherlands
[3] Department of Cardiology, Division of Heart and Lungs, University Medical Center Utrecht, Utrecht, the Netherlands
[4] Child Development and Exercise Center, Wilhelmina Children's Hospital, University Medical Center Utrecht, Utrecht, the Netherlands

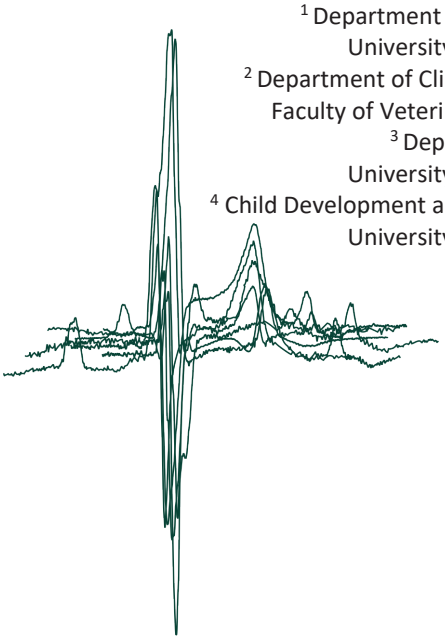

***IJC Heart & Vasculature*, 2023, 44:101169**

Abstract

A preclinical model standardized at different remodeling stages after AV block induction in awake state is suitable for the evaluation of improved cardiac devices. We studied exercise-induced cardiorespiratory parameters at three different timepoints after inducing AV block in dogs.

Mongrel dogs (n=12) were placed on a treadmill with a 10% incline and performed a moderate exercise protocol (10-minute run at 6 km/h). Dogs ran at sinus rhythm (SR), at two days (AVB2d, initiation of remodeling), three weeks (CAVB3) and six weeks (CAVB6, completed remodeling) after AV block.

All dogs completed the exercise protocol at SR, CAVB3 and CAVB6, while 6/12 dogs at AVB2d failed to complete the exercise protocol. The atrial rate was higher at all AV block timepoints (126 ± 20 to 141 ± 19 bpm at rest and 221 ± 10 to 231 ± 13 bpm during exercise) compared to SR (100 ± 29 bpm at rest and 162 ± 28 bpm during exercise, $p<0.05$). Upon exercise, stroke volume increased from 66 ± 15 ml at SR, to 96 ± 21 ml at AVB2d ($p<0.05$), 91 ± 13 ml at CAVB3 ($p<0.05$) and 85 ± 24 ml at CAVB6 but failed to compensate for the AV block-induced bradycardia. Therefore, cardiac output was lower after AV block compared to SR. Exercising dogs at AVB2d showed most arrhythmic events, lowest VO_2, and signs of desaturation and acidification in venous blood.

Dogs with limited remodeling after AV block have a reduced exercise tolerance, which is reflected in changes in cardiorespiratory parameters.

Keywords

Exercise, AV block dog model, remodeling, cardiorespiratory changes, treadmill

Introduction

Management of patients with bradycardia due to atrioventricular block (AV block) includes temporary pacing in the case of reversible causes (e.g., Lyme disease), medical therapy, and chronic therapy in the form of permanent pacing.[1] For young patients with congenital complete AV block (CCAVB), permanent pacing comes with therapeutic dilemmas regarding the decision at what age to implant the pacemaker, what type of pacing (location of pacing leads and mode of pacemaker) gains maximal benefits, and implantation of a device in patients that are asymptomatic.[2] Moreover, chronic pacing will invariably require the replacement of the leads and battery after a certain time period, and long-term side effects such as pacing-induced dyssynchrony resulting in adverse left ventricular remodeling.[2] In the current era of complex digital opportunities, including machine learning, there is high interest in improving cardiovascular device technologies based on physiological input.

Complex device technologies and algorithms developed over the last four decades focus on rate-adaptive pacing based on physiological input, including physical activity,[3] transthoracic impedance,[4] respiration,[5,6] and even a combination of various physiological parameters.[7] However, optimization of sensor sensitivity is challenging, and studies lack significant improvement outcome of the sensors on top of pacing at a fixed rate to treat bradycardia.[8,9] Testing of new developed complex devices and algorithms for treatment of cardiorespiratory diseases by rate-adaptive pacing will benefit from a standardized preclinical model in which evaluation of diverse physiological parameters in conditions of rest and activity are incorporated.

The dog is described as the most predictive species in the cardiac electrophysiological research field.[10] The AV block dog model[11] was standardized over the last four decades as experimental model in pro- and antiarrhythmic drug screening[10] and testing of new device properties.[12] After induction of AV block, the acute bradycardia is accompanied with a decrease in cardiac output and therefore different adaptations are initiated in the subsequent weeks. These are 1) contractile remodeling which includes the enhancement of neurohormonal parameters to increase inotropy upon each cardiac contraction – initiated immediately and maximal after two weeks,[13] 2) electrical remodeling in the form of diminished repolarizing ion currents I_{Kr} and I_{Ks} resulting in prolongation of the action potential

reflected by QT prolongation – completed after two weeks,[14] and 3) structural remodeling referring to the slower process of biventricular hypertrophy which takes over the increase in contractile force – stabilized after four to six weeks.[15] Despite the animal's well-being in daily existence as model of compensated hypertrophy, dogs under anesthesia are sensitive to Torsade de Pointes arrhythmias after a dofetilide-trigger at >2 weeks after AV block.[16] This model allows controlled evaluation of drug safety and device properties in anesthetized and awake conditions at different stages of remodeling.

In view of the necessity of a well characterized preclinical model for evaluating newly developed pacing technology, the aim of this study was to determine exercise tolerance and exercise-induced cardiorespiratory alterations in the moderately exercising AV block dog model without a pacing device at different remodeling stages after induction of AV block using minimally invasive techniques. It was hypothesized that dogs with remodeled hearts as induced by AV block have a better exercise performance than dogs in the first stage(s) of remodeling – with initiated but still limited adaptations – which would provide an optimal time window for future device testing.

Methods

Animals

Animal care and handling were in accordance with the ''Directive 2010/63/EU of the European Parliament and the Council of 22 September 2010 on the protection of animals used for scientific purposes'' and the Dutch law as laid down in the Experiments on Animals Act. Experimental procedures were approved by the Central Authority for Scientific Procedures on Animals. Application approval numbers: AVD115002016531 and AVD11500202114910. Animal studies are reported in compliance with the ARRIVE guidelines.[17] The current study has no implications for replacement, refinement, or reduction.

Twelve purpose-bred mongrel dogs (Marshall, New York, USA) consisting of three females and nine males were included for serial experiments. They had a body weight of 26 ± 2 kg and were 13 ± 1 months old at the time of the first experiment. The animals were housed in pairs in kennels with wooden bedding material, had ad libitum access to water and received food

pellets twice a day. They played outside once a day with access to playing toys, and their welfare was checked daily.

Surgical procedure

Animals were fasted during the night prior to the surgical procedure. Half an hour before the procedure, they received premedication (0.02 mg/kg i.m. atropine, 0.5 mg/kg i.m. methadone, 0.5 mg/kg i.m. acepromazine and 0.1 mg/kg s.c. meloxicam). General anesthesia was induced by sodium pentobarbital (pentobarbital, 25 mg/kg i.v.) and maintained by 1.5% isoflurane in O_2 and N_2O (1:2 ratio) via mechanical ventilation at 12 breaths/minute. Ampicillin (1000 mg) was administered before (i.v.) and after (i.m.) surgery, and buprenorphine (0.3 mg, i.m.) was provided after surgery. During the procedure, AV block was induced by radiofrequency ablation of the bundle of His.[18] A body temperature sensor (IPTT-300, Plexx BV, Elst, The Netherlands) was inserted subcutaneously in the neck of the dog under anesthesia.

Measurements

An overview of the experimental setup to obtain cardiorespiratory parameters is presented in **Figure 1**. Four ECG electrodes were placed in a 10-15 cm distance on the back of the dog: two at both sides at the end of the thoracic spine and two on both sides of the start of the lumbar spine. Six lead ECG tracings were recorded with EP tracer (Cardiotek, Maastricht, The Netherlands) at a sampling frequency of 1,000 Hz. For cardiac impedance measurements with the PhysioFlow® (Manatec Biomedical, Petit Ebersviller, Folschviller, France) two electrodes were placed on the left lateral side of the neck, one at the right 3rd intercostal space on the midclavicular line, one at the left 7th intercostal space on the midclavicular line, and two at the back on the level of the xiphoid process of the sternum. The skin at the location of the electrodes was shaved, gel was added between the skin and the electrodes, and vet wrap was used around the electrodes for proper signal detection. Electrodes and cables were connected to the PhysioFlow® device and body weight, length (from the nose to the base of the tail), and the average of three blood pressure measurements from the tail (PetTrust, BioCare, Taoyuan City, Taiwan) were used for automated signal calibration. The detection of each cardiac cycle and the fiducial points of the Z time derivative signal were checked prior to wireless data acquisition using PhysioFlow® software. Venous blood from the cephalic vein in

the left paw was collected in a heparin flushed syringe (1 ml) and immediately analyzed (GEM Premier 3000, Werfen, Breda, The Netherlands). pH, pCO_2 and pO_2 levels were corrected for body temperature. The treadmill with a custom-build closed chamber of Plexiglass had a continuous flow of 200 l/min and the oxygen uptake (VO_2) and carbon dioxide exhalation (VCO_2) within the chamber were measured via a multi-gas analyzer (Servomex Xentra 4100, Almelo, The Netherlands). The temperature and humidity in the chamber were determined with a thermo hygrometer (Testo 635-1, Testo BV, Almere, The Netherlands) and body temperature was obtained by briefly holding the reader to the sensor in the neck of the dog. Cables and the PhysioFlow® device were surrounded by a vest around the thorax and their position was further secured with masking tape. Except for the minimally invasive collection of venous blood, all techniques were non-invasive.

Experimental protocol

Dogs were familiarized with the treadmill, its environment, and the researchers for six weeks before the first experiment was performed to avoid the effect of stress on the outcome parameters. Signs of acquaintance were determined by the researchers based on the known behavior specific to the individual animal and presence of respiratory sinus arrhythmia on the ECG at resting state. The dogs learned to walk on a leash and to run on the treadmill in step with the belt speed by running short periods of exercise (3-5 minutes, every other day) to avoid intense exercise training. As standard protocol, the dogs were fasted for ±16 hours before the start of each experiment. Surface ECG and PhysioFlow® signals were recorded continuously during the experiment. The temperature, humidity, and VO_2 and VCO_2 levels in the empty chamber were documented after which the dog was placed within the treadmill chamber. At rest, the dogs were in a standing position in the treadmill chamber for 5 minutes, a blood sample and the body temperature were obtained, a VO_2 and VCO_2 steady state was reached, and the chamber temperature and humidity were documented. During moderate exercise, the dogs ran for 10 minutes with a speed of 6 km/h on a 10% inclined treadmill (**Figure 1**). They were positively encouraged to walk by cheering and contact between the researchers and the animal was maintained during the experiment. Blood samples, body temperature, VO_2, VCO_2, and temperature and humidity in the chamber were obtained during exercise. Next, the treadmill was stopped, and the dogs stayed in the treadmill chamber for

5 minutes to recover after which a blood sample, body temperature, VO_2, VCO_2, chamber temperature and humidity were obtained.

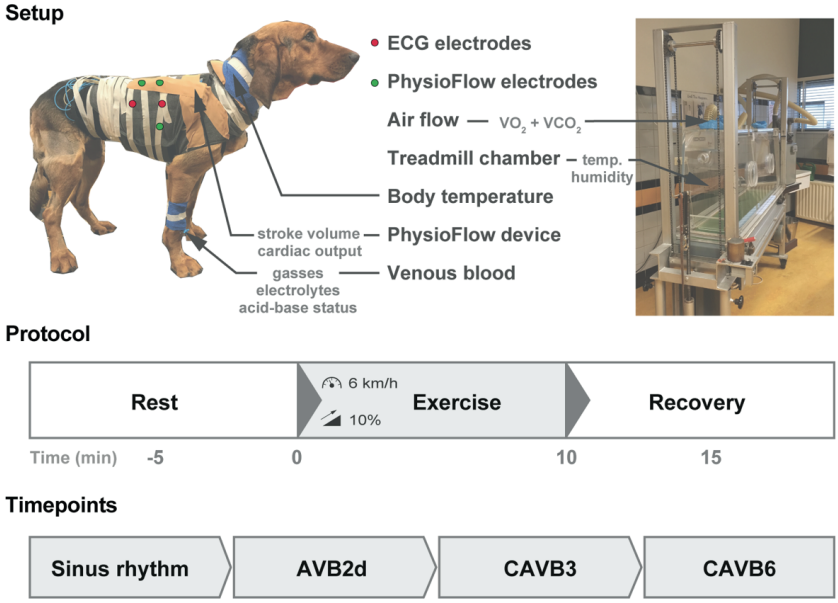

Figure 1. Overview of the experimental design. Setup with overview of techniques and outcome parameters with the dog facing from the right side. Protocol with rest for 5 minutes, exercise for 10 minutes at 6 km/h on a 10% inclined treadmill, and recovery for 5 minutes. Timepoints at which each dog performed the protocol in series: sinus rhythm, and two days (AVB2d), three weeks (CAVB3), and six weeks (CAVB6) after AV block induction.

Experimental timepoints

Animals were not randomized in the present study, and operators were not blinded. Every dog performed the experimental protocol in series at four different timepoints serving as their own controls. These include sinus rhythm (SR), 2 days after AV block (AVB2d, 2.2 ± 0.4 days after induction), three weeks after AV block (CAVB3, 3.0 ± 0 weeks after induction) and six weeks after AV block (CAVB6, 6.2 ± 0.4 weeks after induction) (**Figure 1**). Remodeling is yet limited at AVB2d, whereas the contractile, electrical, and structural compartments of the AV block-induced cardiac adaptation are completed at CAVB6. In between AVB2d and CAVB3, and CAVB3 and CAVB6, the dogs were brought to the treadmill once a week with a run on the treadmill for 3-5 minutes to keep acquainted with the experimental environment.

ECG analysis

Electrophysiological parameters were obtained by manually placing time calipers on lead II of the surface ECG using EP tracer software. Intervals of ten beats were averaged and arrhythmic events were excluded. Parameters covered ventricular rate (from RR interval), atrial rate (from PP interval), QT interval, QTc interval (QT interval corrected for heart rate using the Van de Water formula),[19,20] QRS interval, and JT and JTc interval (QT and QTc corrected for QRS interval, respectively). The occurrence of arrhythmic events in the form of single ectopic beats (sEB) and multiple ectopic beats (mEB), and periods of ventricular tachycardia (VT) were determined during rest (5 minutes), exercise (10 minutes) and recovery (5 minutes).

PhysioFlow® analysis and evaluation

Stroke volume and cardiac output values were obtained from ten cardiac cycles selected from the exported PhysioFlow® files. The number of cycles depended on the signal quality, QRS morphology and heart rate and therefore 1-9 cycles were available for analysis in a few cases. In addition to the reported evaluation of the PhysioFlow® in conscious beagles,[21] the PhysioFlow® was evaluated in mongrel dogs by PV loop recordings, echocardiography, and surface ECG. PV loop tracings were obtained using a 7F pressure catheter in the left ventricle from anesthetized SR dogs laying on the left side (CD Leycom Inc., Hengelo, The Netherlands). Stroke volume was obtained offline from PV loops of 15 selected heart beats via computer software (Conduct NT, CD Leycom). Left ventricular outflow tract (LVOT) and velocity time integral (VTI) from pulsed wave Doppler echocardiograms were used to assess the stroke volume of dogs under anesthesia at SR laying on the left side, and in awake state at SR, AVB2d, and CAVB3 in standing position. Echocardiographic data was analyzed using IntelliSpace Cardiovascular (Philips, Amsterdam, The Netherlands). For data comparison, PhysioFlow® measurements were performed simultaneously with pressure-volume (PV) loop recordings, echocardiography, and surface ECG. Isoprenaline (3 μg/min) was infused at SR and CAVB3 to approach the increase in heart rate and blood pressure during exercise. Under anesthesia, PhysioFlow® electrodes on the back were moved to the xiphoid process of the sternum for proper resting measurements, whereas in awake state they were placed on the back for comparison with measurements during exercise.

Analysis of chamber parameters

VO_2 and VCO_2 in ml/min/kg were calculated based on the flow in the chamber (200 l/min), body weight, and the percentage of O_2 and CO_2 in the empty chamber and with the dog at steady state (at rest, during exercise, and after recovery). The respiratory exchange ratio (RER) is defined as the ratio of the produced carbon dioxide volume and the consumed oxygen volume during respiration and was calculated by dividing VCO_2 by VO_2. The humidity and temperature in the chamber were calculated relative to empty chamber conditions.

Statistical analysis

Data are presented as mean ± standard deviation (SD). Repeated measures two-way analysis of variance (ANOVA) followed by Bonferroni's or Tukey's multiple comparisons test were used to analyze group- and timepoint comparisons of serial data. For comparison of two different groups, the unpaired Student's T test was used. A value of $p<0.05$ was considered statistically significant. All statistical analysis were performed using GraphPad Prism (version 9.3.1, GraphPad Software, San Diego, USA).

Results

AV block dogs with limited remodeling show a lower exercise tolerance

The 10-minute moderate exercise protocol was completed by all dogs at SR, CAVB3, and CAVB6. Although the dogs showed signs of fatigue after the exercise, they were visibly able to complete the exercise without refusing to continue while running. However, after repetitively encouragement to continue the exercise protocol, it had to be ended prematurely for 6/12 dogs at AVB2d (**Figure 2,** red symbols) to avoid a fatal outcome. These animals showed a run duration ranging from 3 minutes and 12 seconds to 8 minutes and 45 seconds (average run duration of n=12, mean ± SD: 8 minutes and 0 seconds ± 2 minutes and 24 seconds). The six dogs that failed the exercise protocol showed more dominant signs of fatigue (panting, head facing forward and stretching the neck for efficient air inhalation, slow response to encouragement, and laying down on the treadmill immediately after stop) compared to SR, CAVB3 and CAVB6. Other reasons of deciding a premature termination of the exercise protocol were a combination of the following: strong refusal to continue (4/6), staggering (5/6), hypoxemia presented by a blue tongue and/or abnormal dark color of the

venous blood sample (6/6), vomiting (1/6), and the occurrence of ventricular tachycardia (2/6).

AV block dogs show increased atrial rate after generated idioventricular rhythm

To avoid missing values from dogs unable to complete the exercise protocol, timepoint exercise refers to 2 minutes of exercise (unless stated otherwise). In SR, exercise increased the atrial and ventricular rate from 100 ± 29 to 162 ± 28 bpm (P<0.05, **Figure 2B, C**). Interestingly, the atrial rate was higher at all AV block timepoints compared to SR in rest and it was further increased upon exercise (P<0.05, **Figure 2B**). The idioventricular rhythm resulting from AV block induction was significantly lower than the ventricular rate at SR in rest; the rate dropped from 100 ± 29 bpm at SR to 47 ± 10 bpm at AVB2d, 45 ± 8 bpm at CAVB3 and 43 ± 7 bpm at CAVB6 (P<0.05, **Figure 2C, Suppl. table 1**). Exercise increased the ventricular rate at SR with more than 60 bpm, whereas after AV block this increase was only ±16 bpm and this was similar at all AV block timepoints. The six dogs that completed the exercise protocol at AVB2d showed a higher ventricular rate upon exercise compared to the six dogs that failed the exercise protocol (P<0.05, **Suppl. figure 1B**). The atrial rate was not different between the completed and failed group. Due to the idioventricular rhythm, the QRS interval was significantly longer at AV block timepoints compared to SR and the interval was not affected by exercise (**Suppl. table 1**). In terms of repolarization, the electrical remodeling induced by AV block is reflected by prolongation of the QT interval corrected for heart rate (QTc) at CAVB3 and CAVB6 (P<0.05, **Suppl. table 1**). Exercise induced shortening of the QT and JT interval at all four tested timepoints. After AV block, this was predominantly heart rate dependent as the QTc and JTc were unaltered upon exercise.

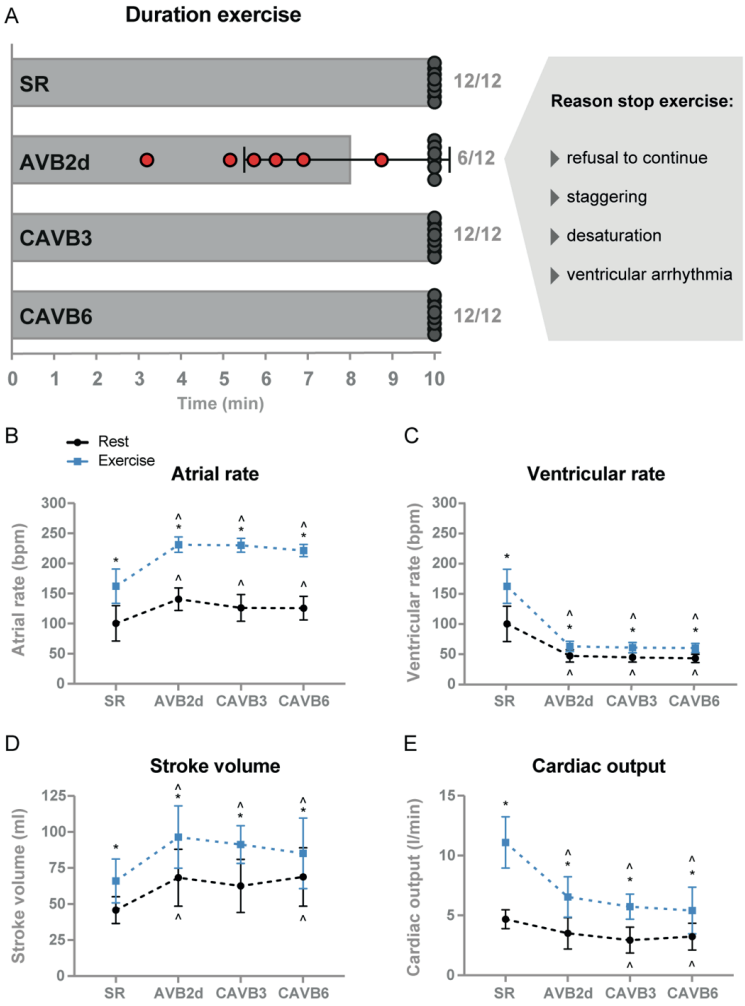

Figure 2. A) Exercise duration per experimental timepoint. Six out of twelve dogs at two days after AV block (AVB2d) failed to complete the 10-minute exercise protocol. Those dogs refused to continue the protocol, were staggering on the treadmill, showed signs of hypoxemia, and ventricular arrhythmias (ectopic beats and ventricular tachycardia) occurred. The protocol was completed by all twelve dogs at sinus rhythm (SR), three weeks (CAVB3), and six weeks (CAVB6) after AV block induction. **B**) Atrial rate, **C**) ventricular rate, **D**) stroke volume, and **E**) cardiac output of dogs (n=12) at rest and during exercise (2 minutes) at SR, AVB2d, CAVB3, and CAVB6. Data are presented as mean ± SD. For CAVB6 exercise: n=11, and for stroke volume and cardiac output at AVB2d: n=10 at rest and n=9 at exercise. Repeated measures two-way ANOVA with Bonferroni's multiple comparisons test for comparing rest vs. exercise and Tukey's multiple comparisons test for comparing SR vs. AV block timepoints. *p<0.05 compared to rest and ^p<0.05 compared to SR.

Exercising dogs are unable to maintain cardiac output after AV block

At rest, stroke volume increased after AV block (P<0.05, **Figure 2D, Suppl. table 1**) and exercise increased stroke volume levels at all measured timepoints. Cardiac output was significantly reduced after AV block remodeling at rest at CAVB3 and CAVB6. Exercise highly increased the cardiac output at SR, though less dominant after AV block (P<0.05, **Figure 2E, Suppl. table 1**). The six dogs that completed the exercise protocol at AVB2d showed a significant higher stroke volume and a trend towards an increased cardiac output upon exercise compared to the six dogs that failed the exercise protocol (P<0.05, P=0.059, **Suppl. figure 1**). A heart weight of 297 ± 33 g and a heart weight/body weight ratio of 11.7 ± 1.0 g/kg were determined after heart isolation at 11 ± 4 weeks of AV block.

The PhysioFlow® technique – used to determine the stroke volume and cardiac output – was evaluated by echocardiography, PV loop measurements and surface ECG, with addition of isoprenaline infusion to simulate a rise in heart rate. This resulted in corresponding heart rate and stroke volume values (**Suppl. figure 2**). The functional adaptation after AV block was confirmed by echocardiography as stroke volume increased after AV block over time (AVB2d and CAVB3).

Proarrhythmia in exercising AV block dogs with limited remodeling

Dogs at SR showed no arrhythmic events during the experimental protocol (**Figure 3A**). Arrhythmic events were mostly present in dogs at AVB2d (**Figure 3B**). Already at rest, four dogs showed EBs and exercise further induced the occurrence of EBs, mEBs and VT. Of the six dogs that failed the exercise protocol at AVB2d, five dogs showed arrhythmic events during exercise. Arrhythmic events were also present at CAVB3 and CAVB6, yet less dominant (**Figure 3C, D**). Moreover, QRS morphology changes - reflecting origin variations of the ventricular pacemaker focus - were predominantly present at AVB2d and the origin was stabilized at CAVB3 and CAVB6 over time. Representative ECG tracings obtained during the experimental protocol illustrate the presence of respiratory sinus arrhythmia in resting dogs at SR, the increase in ventricular rate during exercise, and the specific characteristic of AV block by the absence of a relation between the P waves and the QRS complexes (**Figure 3**). Furthermore, the occurrence of a VT is presented in a dog at AVB2d that stopped the exercise protocol prematurely.

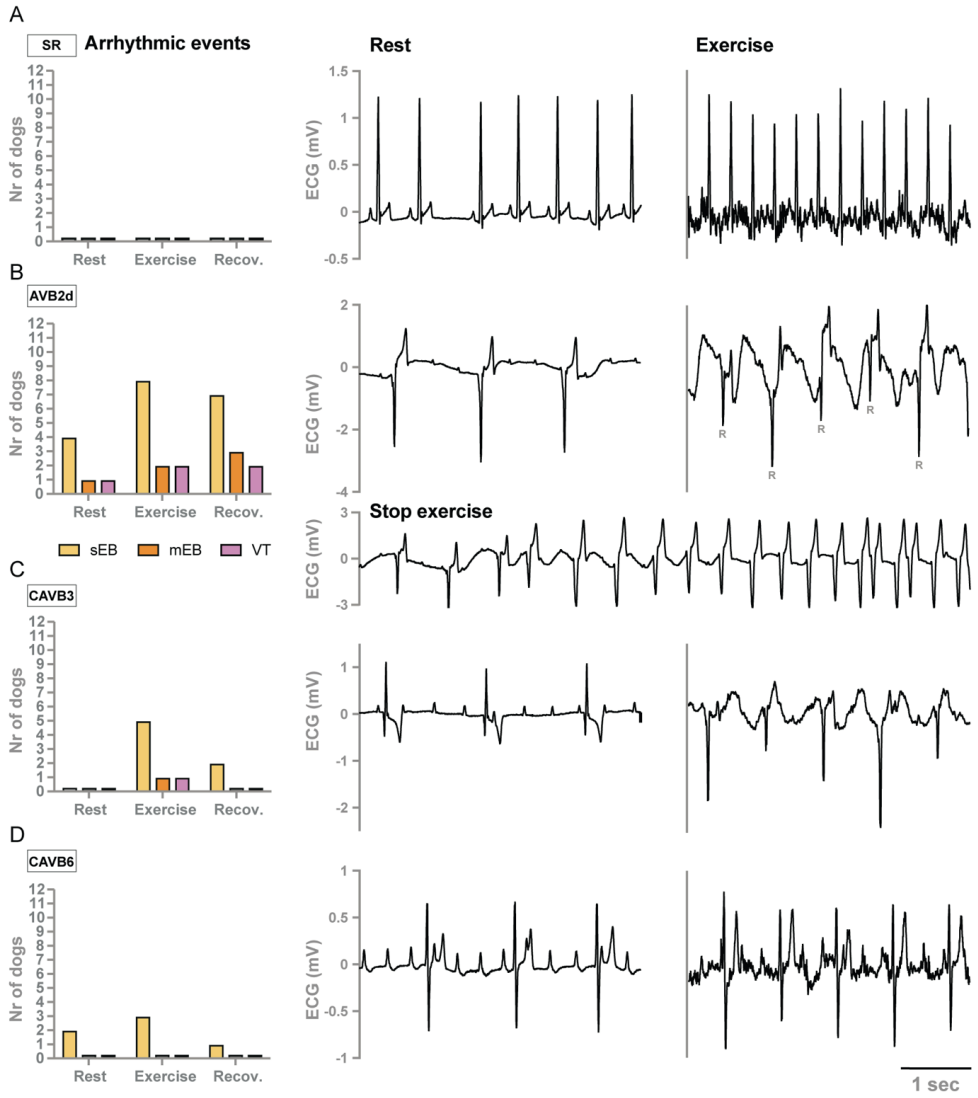

Figure 3. Occurrence of arrhythmic events and representative ECG tracings in dogs (n=12) at **A**) sinus rhythm (SR), **B**) two days after AV block (AVB2d), **C**) three weeks after AV block (CAVB3) and **D**) six weeks after AV block (CAVB6). Arrhythmic events included single ectopic beats (sEB), multiple ectopic beats (mEB) and ventricular tachycardia (VT) observed at rest (5 minutes), during exercise (10 minutes or until premature stop) and recovery period (5 minutes). Representative ECG tracings of dog #168247 at rest and exercise. This dog stopped the exercise protocol prematurely due to VT, hypoxemia, and staggering.

Exercising dogs with limited remodeling have a lower oxygen uptake

At rest, VO_2 and VCO_2 were not different after AV block (**Figure 4A, B**). Exercise increased the VO_2 and VCO_2 significantly in dogs at SR and all AV block timepoints. The VO_2 in dogs at AVB2d

was significantly lower upon exercise compared to SR, CAVB3 and CAVB6 (P<0.05, **Figure 4A**). For VCO_2, values were lower at AVB2d compared to CAVB6 and higher at CAVB6 compared to SR (P<0.05, **Figure 4B**). The RER, a parameter reflecting the fuel selection during exercise based on VCO_2 and VO_2, was not altered after AV block at rest and was increased during exercise at AVB2d and CAVB6 compared to rest (**Figure 4C**). The humidity in the treadmill chamber relative to empty conditions was elevated due to exercise (**Suppl. table 1**), which was more pronounced at CAVB3 and CAVB6 (**Figure 4D**). Exercise increased the temperature in the treadmill chamber at all measured timepoints (P<0.05, **Figure 4E, Suppl. table 1**), and apart from CAVB6 the body temperature was unaffected at rest and exercise (**Figure 4F**).

Hypoxemia and acidification in exercising AV block dogs with limited remodeling

Venous blood was analyzed to determine if the exercise-induced cardiorespiratory changes were reflected in the venous blood parameters. Upon exercise, dogs showed reduced SpO_2 levels at all timepoints and diminished pO_2 levels at SR, AVB2d and CAVB6 (P<0.05, **Figure 4G, H**). Oxygen desaturation was mostly present in exercising dogs at AVB2d, as SpO_2 levels were lowest at that timepoint and significantly different from SR and CAVB3. Moreover, pO_2 levels were significantly lower compared to SR in resting and exercising dogs at AVB2d.

Venous blood from exercising dogs at AVB2d was more acidic as demonstrated by an increase in lactate, and a lower pH and base access (**Figure 4J, K, M**). The latter parameter and HCO_3^- were reduced in exercising dogs at CAVB3 compared to SR (P<0.05, **Figure 4M, L**). Dogs at CAVB6 showed the following alterations in venous blood parameters: exercise reduced SpO_2 and pH, and increased lactate levels compared to SR. However, these values were not different from other AV block timepoints. In terms of electrolytes, sodium levels were significantly higher upon exercise in dogs at AVB2d and CAVB3 (P<0.05, **Figure 4P**). Exercise and AV block did not significantly affect pCO_2, glucose, hematocrit, potassium, and calcium levels (**Figure 4I, N, O, Q, R**).

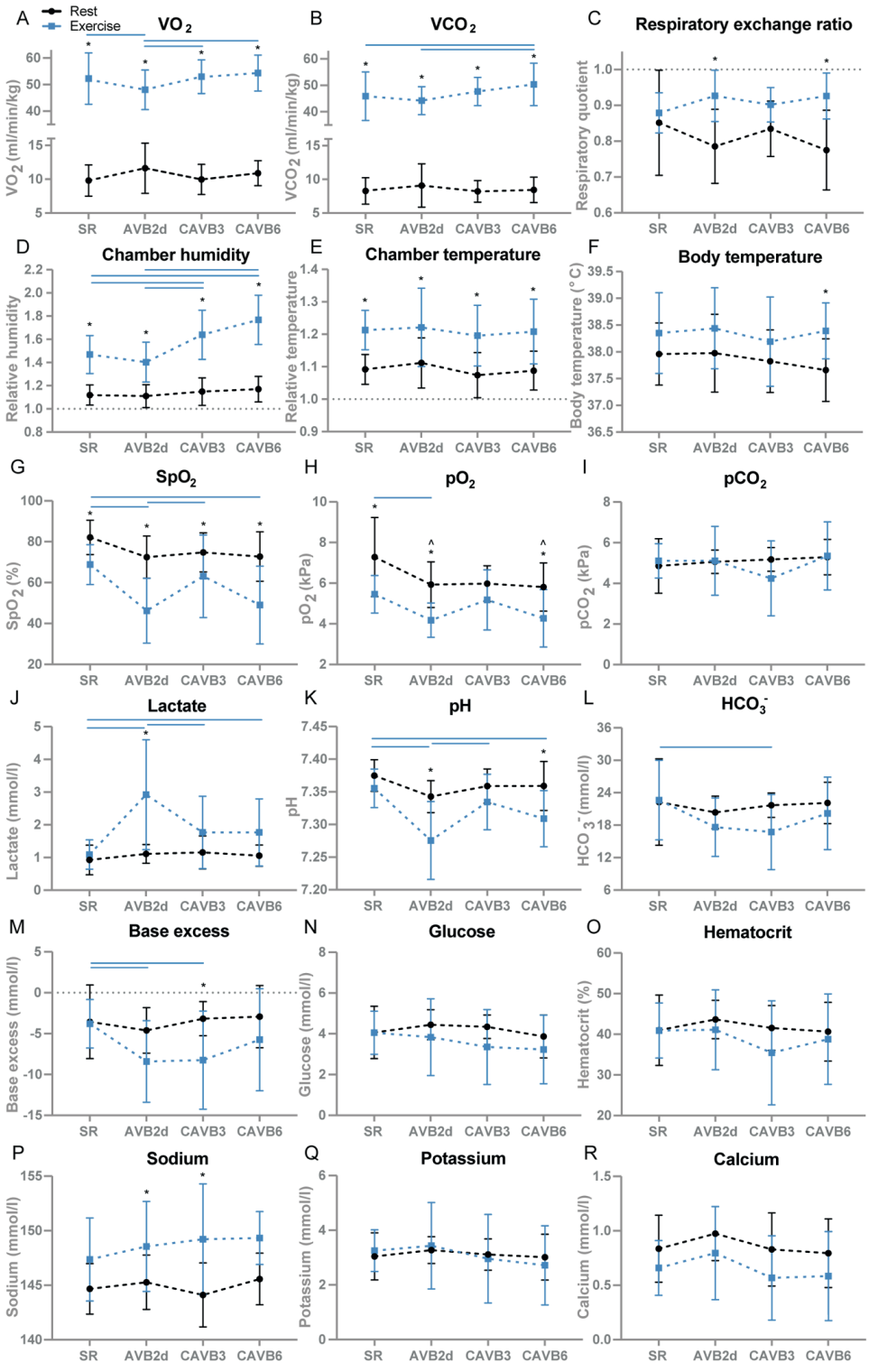
A
Rest
Exercise
VO2
VO2 (ml/min/kg)
B
VCO2
VCO2 (ml/min/kg)
C
Respiratory exchange ratio
Respiratory quotient
D
Chamber humidity
Relative humidity
E
Chamber temperature
Relative temperature
F
Body temperature
Body temperature (°C)
G
SpO2
SpO2 (%)
H
pO2
pO2 (kPa)
I
pCO2
pCO2 (kPa)
J
Lactate
Lactate (mmol/l)
K
pH
pH
L
HCO3-
HCO3- (mmol/l)
M
Base excess
Base excess (mmol/l)
N
Glucose
Glucose (mmol/l)
O
Hematocrit
Hematocrit (%)
P
Sodium
Sodium (mmol/l)
Q
Potassium
Potassium (mmol/l)
R
Calcium
Calcium (mmol/l)
SR
AVB2d
CAVB3
CAVB6

Figure 4. A) Oxygen uptake (VO_2), **B**) carbon dioxide exhalation (VCO_2), **C**) respiratory exchange ratio, **D**) chamber humidity, **E**) chamber temperature and **F**) body temperature of dogs (n=12) at rest and during exercise (10 minutes or steady state when the exercise protocol was stopped prematurely) at sinus rhythm (SR), and two days (AVB2d), three weeks (CAVB3) and six weeks (CAVB6) after AV block induction. Chamber humidity and temperature are relative to empty chamber conditions. Data are presented as mean ± SD, with n=10-12. Repeated measures two-way ANOVA with Bonferroni's multiple comparisons test for comparing rest vs exercise and Tukey's multiple comparisons test for comparing SR vs. AV block timepoints. *p<0.05 compared to rest and blue bars refer to p<0.05 in exercise group. **G-R**) Venous blood parameters of dogs at rest and exercise (2 minutes) at SR, AVB2d, CAVB3, and CAVB6 after AV block induction. Data are presented as mean ± SD. For rest: SR n=12, AVB2d n=11, CAVB3 n=9 and CAVB6 n=7-11. For exercise: SR n=11, AVB2d n=9, CAVB3 n=9 and CAVB6 n=6-10. Repeated measures two-way ANOVA with Bonferroni's multiple comparisons test for comparing rest vs. exercise and Tukey's multiple comparisons test for comparing SR vs. AV block timepoints. *p<0.05 compared to rest/exercise, ^p<0.05 compared to SR and blue bars refer to p<0.05 in exercise group.

Discussion

The exercising AV block dog model

The most frequently used exercise protocol in the clinic is the Bruce treadmill test which includes gradual changes in speed and a slope increase of 22% to assess aerobic exercise capacity.[22] For diseased children, these maximal treadmill protocols at a high incline can be too demanding and therefore individualized protocols were examined.[23] To avoid early loss of our included animals due to a too demanding exercise protocol after the atrioventricular intervention, a constant workload treadmill protocol for 10 minutes at a 10% incline was used in the current study. The protocol was considered moderate as the heart rate of dogs at SR increased to ±55% of the reported maximal heart rate upon exercise.[24,25]

Chronic complete heart block in dogs by a direct incision of the His bundle was first developed as a model of experimental heart failure confirmed by e.g. low exercise tolerance on a treadmill.[26] Later, treadmill experiments in dogs with AV block focused on improvement of cardiac output by pacing[27] and hormone responses to local wall stress.[28] The time course after AV block varied from one week to several months without detailed evaluation of AV block-induced cardiac adaptations, which would highly affect outcome. In the current study, the evaluated timepoints after AV block at AVB2d, CAVB3 and CAVB6 reflect the different remodeling stages that evolve after AV block induction. These include limited remodeling at the early stage, stable contractile and electrical remodeling after two weeks, and stable structural remodeling after four to six weeks.[11] With minimal to non-invasive techniques, we determined cardiorespiratory changes upon exercise at the different remodeling stages.

Exercise induced significant increases in atrial and ventricular rate, stroke volume, cardiac output, VO_2, VCO_2, chamber humidity and temperature, and significant decreases in venous SpO_2 and pO_2 levels. Evaluation of cardiac output includes predominantly invasive methods, though the non-invasive PhysioFlow® system based on cardiac impedance was previously evaluated in conscious beagle dogs.[21] Here, evaluation of the system in anesthetized and awake mongrel dogs, including simulation of increases in heart rate by infusion of isoprenaline, resulted in reliable measures of heart rate and stroke volume when evaluated by ECG, echocardiography, and PV loop analyses. The Physioflow® is considered as a reliable and non-invasive technique to measure cardiac output in awake mongrel dogs.

AV block-induced remodeling and exercise tolerance

Shortening of the PP interval directly after AV block was already reported before[29] and is explained by the enhanced adrenergic activity in order to compensate for the bradycardia-induced drop in cardiac output.[13] This response was further augmented upon exercise (atrial rate >230 bpm) while the ventricular rate only increased to 66 bpm. Unpaced children with AV block are able to increase their ventricular rate upon maximal exercise to 117 ± 48 bpm.[30] The difference in exercise protocol – being moderate in our study – likely explains the lower increase in ventricular rate in our study. The increase in cardiac output during exercise is mainly dependent on the increase in heart rate and partly on the increase in stroke volume.[31] Indeed, the dogs that completed the exercise protocol at AVB2d had a higher ventricular rate. Moreover, their stroke volume was higher than those that failed the exercise protocol, all resulting in a higher cardiac output upon exercise. These results were also found in children with AV block, as the unpaced children showed similar VO_{2peak} levels as paced children.[30] It was suggested that only the 'best' patients stay unpaced. Furthermore, it was implied that children with AV block generate more energy from anaerobic sources during exercise as compensatory mechanism since the peak workload was similar to healthy peers.[30] For the dogs at AVB2d, this can be confirmed by the venous blood parameters showing signs of acidification by a buildup of lactate and the corresponding reduction in venous pH, and hypoxemia by the reduced venous SpO_2 and pO_2. Certainly, these conditions have resulted in premature termination of the exercise protocol as was decided when the dogs at AVB2d were staggering, showed a desaturated tongue and convincingly refused to continue the exercise. Another reason of premature termination was the occurrence of ventricular tachycardia.

Indeed, in addition to the known changes in origin of ventricular pacemaker focus, the dogs at AVB2d showed more arrhythmic events upon exercise. The hypoxic conditions at this timepoint could have contributed to myocardial ischemia resulting in abnormal automaticity and the thereby induced arrhythmic events.[32]

Despite the high dependence of cardiac output on heart rate, stroke volume must increase to a certain level to compensate for the severe bradycardia after AV block in order to maintain cardiac output levels similar to SR. Previous studies showed that AV block dogs with chronic remodeling under anesthetized conditions increased their cardiac output almost to SR conditions due to enhanced inotropic parameters.[15,33] In the current study, cardiac hypertrophy induced by AV block was confirmed as the heart weight and heart weight/body weight values coincide with previously reported results.[13] We also found that the cardiac output was lowest at CAVB3 and CAVB6 at rest in awake conditions, and during exercise it was lower than SR at all AV block timepoints, while all dogs at CAVB3 and CAVB6 completed the exercise protocol. An explanation could be that, in contrast to AVB2d, dogs at CAVB3 and CAVB6 showed a similar steady state VO_2 as at SR. Besides the cardiac remodeling and increased neurohormonal parameters after AV block, a role for remodeling of other organs/tissues important for exercise is implied here. In the AV block dog, chronic remodeling may also include optimization of respiratory ventilation, blood flow regulation, and O_2 extraction in the active muscle which all affect the VO_2.[34]

The exercising AV block dog model: a translational perspective

Software with self-adapting computational neurons based on feedback of various physiological parameters, such as blood pressure, SpO_2, and respiration can be the basis of new cardiac rhythm management.[7] The use of a biofeedback device in cardiac pacing on the respiratory cycle resulted in an improved cardiac output in sheep with heart failure.[35] We suggest that the induction of cardiorespiratory changes upon exercise in the preclinical exercising AV block dog model can be used to test and optimize new device therapies. Improvement of cardiac function and thereby exercise tolerance due to new cardiac device properties can be determined at AVB2d, when the animal's exercise tolerance is most vulnerable.

Study limitations

The lower detection limit of heart rate by the PhysioFlow® was 40 bpm for calibration at resting state resulting in the exclusion of two measurements. The best parameter to describe exercise capacity is VO_{2peak}, though, this study does not include invasive measures of arterial blood and therefore the arteriovenous oxygen difference as part of the VO_{2peak} (according to the Fick equation) could not be determined. The individual remodeling stages over time were not confirmed in the animals included in this study. Moreover, the heterogeneity in activity behavior between animals can represent the variation of human activity in daily life, however, the exact effect of the daily activity in the stables on the experimental outcome cannot be excluded.

Conclusion

In the present study, it was observed that dogs with limited remodeling after AV block at AVB2d have a lower exercise tolerance than dogs with remodeling at three and six weeks after AV block induction. Moreover, the bradycardia-induced adaptations at all AV block timepoints are an increased atrial rate and stroke volume, though these electrical and functional adjustments fail to completely maintain the cardiac output levels as seen at regular sinus rate. The results further demonstrate that exercising dogs at AVB2d show more arrhythmic events, a lower VO_2, and signs of hypoxemia and acidification.

Acknowledgement

The authors thank Dr. Joris Robben for provision of the PetTrust. This study, as part of the CResPace project, has received funding from the European Union's Horizon 2020 research and innovation programme under grant number 732170.

References

1. Kusumoto FM, Schoenfeld MH, Barrett C, et al. 2018 ACC/AHA/HRS Guideline on the evaluation and management of patients with bradycardia and cardiac conduction delay: A report of the American College of Cardiology/American Heart Association Task Force on clinical practice guidelines and the Heart Rhythm Society. *Circulation.* 2019;140(8):e382-e482.
2. Dolara A, Favilli S. Controversies in the therapy of isolated congenital complete heart block. *J Cardiovasc Med (Hagerstown).* 2010;11(6):426-430.
3. Dell'Orto S, Valli P, Greco EM. Sensors for rate responsive pacing. *Indian Pacing Electrophysiol J.* 2004;4(3):137-145.
4. Kay GN, Bubien RS, Epstein AE, Plumb VJ. Rate-modulated cardiac pacing based on transthoracic

impedance measurements of minute ventilation: correlation with exercise gas exchange. *J Am Coll Cardiol.* 1989;14(5):1283-1289.

5. Krause R, Van Bavel JJA, Wu C, Vos MA, Nogaret A, Indiveri G. Robust neuromorphic coupled oscillators for adaptive pacemakers. *Sci Rep.* 2021;11(1):18073.
6. Rossi P, Plicchi G, Canducci G, Rognoni G, Aina F. Respiration as a reliable physiological sensor for controlling cardiac pacing rate. *Br Heart J.* 1984;51(1):7-14.
7. Nogaret A, O'Callaghan EL, Lataro RM, et al. Silicon central pattern generators for cardiac diseases. *J Physiol.* 2015;593(4):763-774.
8. Kaszala K, Ellenbogen KA. Device sensing: sensors and algorithms for pacemakers and implantable cardioverter defibrillators. *Circulation.* 2010;122(13):1328-1340.
9. Clark HI, Pearson MJ, Smart NA. Rate adaptive pacing in people with chronic heart failure increases peak heart rate but not peak exercise capacity: a systematic review. *Heart Fail Rev.* 2022.
10. Loen V, Vos MA, Van der Heyden MAG. The canine chronic atrioventricular block model in cardiovascular preclinical drug research. *Br J Pharmacol.* 2022;179(5):859-881.
11. Oros A, Beekman JD, Vos MA. The canine model with chronic, complete atrio-ventricular block. *Pharmacol Ther.* 2008;119(2):168-178.
12. Smoczyńska A, Loen V, Aranda A, Beekman HDM, Meine M, Vos MA. High-rate pacing guided by short-term variability of repolarization prevents imminent ventricular arrhythmias automatically by an implantable cardioverter-defibrillator in the chronic atrioventricular block dog model. *Heart Rhythm.* 2020;17(12):2078-2085.
13. Vos MA, de Groot SH, Verduyn SC, et al. Enhanced susceptibility for acquired torsade de pointes arrhythmias in the dog with chronic, complete AV block is related to cardiac hypertrophy and electrical remodeling. *Circulation.* 1998;98(11):1125-1135.
14. Volders PG, Sipido KR, Vos MA, et al. Downregulation of delayed rectifier K(+) currents in dogs with chronic complete atrioventricular block and acquired torsades de pointes. *Circulation.* 1999;100(24):2455-2461.
15. Verduyn SC, Ramakers C, Snoep G, Leunissen JD, Wellens HJ, Vos MA. Time course of structural adaptations in chronic AV block dogs: evidence for differential ventricular remodeling. *Am J Physiol Heart Circ Physiol.* 2001;280(6):H2882-2890.
16. Dunnink A, Van Opstal JM, Oosterhoff P, et al. Ventricular remodelling is a prerequisite for the induction of dofetilide-induced torsade de pointes arrhythmias in the anaesthetized, complete atrio-ventricular-block dog. *Europace.* 2012;14(3):431-436.
17. Percie du Sert N, Ahluwalia A, Alam S, et al. Reporting animal research: Explanation and elaboration for the ARRIVE guidelines 2.0. *PLoS Biol.* 2020;18(7):e3000411.
18. Timmermans C, Rodriguez LM, Van Suylen RJ, et al. Catheter-based cryoablation produces permanent bidirectional cavotricuspid isthmus conduction block in dogs. *J Interv Card Electrophysiol.* 2002;7(2):149-155.
19. Van de Water A, Verheyen J, Xhonneux R, Reneman RS. An improved method to correct the QT interval of the electrocardiogram for changes in heart rate. *J Pharmacol Methods.* 1989;22(3):207-217.
20. Patel S, Bhatt L, Patel R, et al. Identification of appropriate QTc formula in beagle dogs for nonclinical safety assessment. *Regul Toxicol Pharmacol.* 2017;89:118-124.
21. Payseur JD, Rigney JJ, Turner SL, Wu X, Murphy DJ, Rossman EI. Evaluation of a method utilizing PhysioFlow(R), a novel signal morphology-based form of impedance cardiography, to measure cardiac output in the conscious beagle. *J Pharmacol Toxicol Methods.* 2016;81:115-119.
22. Chang RR, Gurvitz M, Rodriguez S, Hong E, Klitzner TS. Current practice of exercise stress testing among pediatric cardiology and pulmonology centers in the United States. *Pediatr Cardiol.* 2006;27(1):110-116.
23. Karila C, de Blic J, Waernessyckle S, Benoist MR, Scheinmann P. Cardiopulmonary exercise testing in children: an individualized protocol for workload increase. *Chest.* 2001;120(1):81-87.

24. Wagner JA, Horvath SM, Dahms TE. Cardiovascular, respiratory, and metabolic adjustments to exercise in dogs. *J Appl Physiol Respir Environ Exerc Physiol.* 1977;42(3):403-407.
25. Khouri EM, Gregg DE, Rayford CR. Effect of exercise on cardiac output, left coronary flow and myocardial metabolism in the unanesthetized dog. *Circ Res.* 1965;17(5):427-437.
26. Starzl TE, Gaertner RA. Chronic heart block in dogs; a method for producing experimental heart failure. *Circulation.* 1955;12(2):259-270.
27. Wessale JL, Geddes LA, Fearnot NE, Janas W, Grote LA. Cardiac output versus pacing rate at rest and with exercise in dogs with AV block. *Pacing Clin Electrophysiol.* 1988;11(5):575-582.
28. Beliveau L, Peronnet F, Bichet DG, Nadeau R. Atrial natriuretic peptide release from the ventricles in response to exercise in dogs with atrioventricular block. *Can J Physiol Pharmacol.* 1994;72(2):146-151.
29. Thomsen MB, Oros A, Schoenmakers M, et al. Proarrhythmic electrical remodelling is associated with increased beat-to-beat variability of repolarisation. *Cardiovasc Res.* 2007;73(3):521-530.
30. Blank AC, Hakim S, Strengers JL, et al. Exercise capacity in children with isolated congenital complete atrioventricular block: does pacing make a difference? *Pediatr Cardiol.* 2012;33(4):576-585.
31. Wang Y, Marshall RJ, Shepherd JT. Stroke volume in the dog during graded exercise. *Circ Res.* 1960;8:558-563.
32. Schweikert RA, Pashkow FJ, Snader CE, Marwick TH, Lauer MS. Association of exercise-induced ventricular ectopic activity with thallium myocardial perfusion and angiographic coronary artery disease in stable, low-risk populations. *Am J Cardiol.* 1999;83(4):530-534.
33. De Groot SH, Schoenmakers M, Molenschot MM, Leunissen JD, Wellens HJ, Vos MA. Contractile adaptations preserving cardiac output predispose the hypertrophied canine heart to delayed afterdepolarization-dependent ventricular arrhythmias. *Circulation.* 2000;102(17):2145-2151.
34. Xu F, Rhodes EC. Oxygen uptake kinetics during exercise. *Sports Med.* 1999;27(5):313-327.
35. Shanks J, Abukar Y, Lever NA, et al. Reverse re-modelling chronic heart failure by reinstating heart rate variability. *Basic Res Cardiol.* 2022;117(1):4.

Supplementary material

Suppl. table 1. Electrophysiological parameters, stroke volume, cardiac output, chamber humidity and temperature from dogs (n=12) at sinus rhythm (SR) and two days (AVB2d), three weeks (CAVB3) and six weeks (CAVB6) after AV block induction at rest, during exercise (2, 5, and 10 minutes) and 5 minutes of recovery (recov.).

Parameter		Rest	2 min	5 min	10 min	Recov.
Atrial rate	SR	100 ± 29	162 ± 28*	167 ± 18*	176 ± 16*	114 ± 23
	AVB2d	141 ± 19^	231 ± 13*^	220 ± 27*^	223 ± 17*^	166 ± 12*^
	CAVB3	126 ± 22^	230 ± 11*^	233 ± 11*^	239 ± 12*^	148 ± 24*^
	CAVB6	126 ± 20^	221 ± 10*^#	224 ± 12*^#	229 ± 13*^#	137 ± 20^&
Ventricular rate	SR	100 ± 29	162 ± 28*	167 ± 18*	176 ± 16*	114 ± 23
	AVB2d	47 ± 10^	63 ± 9*^	66 ± 15*^	66 ± 10*^	45 ± 11^
	CAVB3	45 ± 8^	61 ± 9*^	63 ± 8*^	64 ± 7*^	43 ± 7^
	CAVB6	43 ± 7^	60 ± 8*^	62 ± 7*^	63 ± 9*^	40 ± 6^
QRS	SR	73 ± 6	67 ± 5	67 ± 6	67 ± 6	72 ± 8
	AVB2d	96 ± 9^	87 ± 6^	87 ± 5^	87 ± 8^	94 ± 9^
	CAVB3	103 ± 13^	93 ± 13^	96 ± 12^	95 ± 11^	100 ± 12^
	CAVB6	98 ± 11^	99 ± 12^	101 ± 12^&	104 ± 12^&	101 ± 12^
QT	SR	234 ± 24	196 ± 21*	192 ± 11*	189 ± 11*	222 ± 16*
	AVB2d	296 ± 24^	261 ± 20*^	256 ± 16*^	253 ± 25*^	288 ± 28^
	CAVB3	338 ± 35^&	285 ± 20*^&	281 ± 26*^&	281 ± 22*^&	325 ± 35^&
	CAVB6	332 ± 30^&	300 ± 25*^&	298 ± 29*^&	294 ± 28*^&	332 ± 25^&
QTc	SR	265 ± 15	250 ± 15*	247 ± 9*	246 ± 9*	261 ± 10
	AVB2d	269 ± 19	264 ± 19^	261 ± 18	259 ± 24	254 ± 21
	CAVB3	306 ± 28^&	285 ± 15^&	284 ± 18^&	286 ± 18*^	287 ± 25*^&
	CAVB6	296 ± 24^	300 ± 17^&	299 ± 25^&	297 ± 21^&	286 ± 18^&
JT	SR	161 ± 19	128 ± 18*	125 ± 12*	122 ± 11*	150 ± 13
	AVB2d	201 ± 23^	173 ± 19*^	169 ± 16*^	166 ± 27*^	193 ± 24^
	CAVB3	235 ± 25^&	192 ± 17*^&	185 ± 19*^	186 ± 15*^	225 ± 25^&
	CAVB6	234 ± 24^&	201 ± 17*^&	196 ± 22*^&	190 ± 20*^	230 ± 19^&
JTc	SR	193 ± 12	182 ± 13	181 ± 11*	179 ± 9*	189 ± 9
	AVB2d	173 ± 17^	176 ± 16	173 ± 14	172 ± 23	160 ± 20^
	CAVB3	203 ± 19&	192 ± 11&	188 ± 12&	190 ± 10	187 ± 19&
	CAVB6	198 ± 18	201 ± 12^&	198 ± 18^&	192 ± 14^	184 ± 15&
Stroke volume	SR	46 ± 9	66 ± 15*	65 ± 16*	66 ± 21*	49 ± 10
	AVB2d	68 ± 20^	96 ± 21*^	95 ± 21*^	94 ± 12	70 ± 25
	CAVB3	63 ± 18^	91 ± 13*^	89 ± 16*^	89 ± 21*^	56 ± 20
	CAVB6	69 ± 24^	85 ± 24	88 ± 22*^	86 ± 21*	69 ± 23^
Cardiac output	SR	4.7 ± 0.8	11.1 ± 2.2*	11.2 ± 3.2*	11.6 ± 3.8*	5.5 ± 1.1
	AVB2d	3.5 ± 1.3	6.5 ± 1.7*^	6.4 ± 1.6*^	6.9 ± 1.0	3.7 ± 1.6
	CAVB3	2.9 ± 1.1^	5.7 ± 1.1*^	5.7 ± 1.4*^	5.8 ± 1.7*^	2.6 ± 1.2^

	CAVB6	3.2 ± 1.1^	5.4 ± 1.9*^	5.7 ± 1.7*^	5.7 ± 1.8*^	3.1 ± 1.1^
Chamber humidity	SR	44.5 ± 3.9	52.0 ± 7.1*	55.7 ± 10.3*	58.6 ± 9.7*	52.1 ± 8.2*
	AVB2d	42.6 ± 4.3	50.4 ± 5.9*	54.1 ± 7.4*	54.7 ± 7.4*	47.4 ± 6.2
	CAVB3	43.7 ± 4.4	51.7 ± 5.1*	57.1 ± 7.6*	61.3 ± 7.7*	50.0 ± 6.6
	CAVB6	41.1 ± 4.5	52.5 ± 7.2*	57.2 ± 9.5*	63.0 ± 6.8*	47.6 ± 7.2
Chamber temperature	SR	19.5 ± 2.2	20.1 ± 2.2*	20.7 ± 2.0*	21.6 ± 1.9*	21.3 ± 1.9*
	AVB2d	19.9 ± 2.8	20.4 ± 2.8*	20.7 ± 2.5*	21.6 ± 2.4*	21.3 ± 2.4*
	CAVB3	19.8 ± 1.1	20.2 ± 1.0*	20.9 ± 1.1*	21.8 ± 0.9*	21.5 ± 1.0*
	CAVB6	19.9 ± 1.8	20.6 ± 1.9*	21.4 ± 1.9*	22.2 ± 1.6*	21.9 ± 1.7*

QTc and JTc were obtained by QT and JT correcting for heart rate using the Van de Water formula. Ventricular and atrial rate in beats per minute, ECG intervals in milliseconds, stroke volume in ml, cardiac output in l/min, chamber humidity in %, and chamber temperature in °C. Data are presented as mean ± SD. For AVB2d exercise: n=8-12, for CAVB6 exercise: n=11, and for stroke volume and cardiac output at AVB2d: n=10 at rest and n=4-9 at exercise, and at CAVB6: n=11. Repeated measures two-way ANOVA with Tukey's multiple comparisons test. *p<0.05 compared to rest, ^p<0.05 compared to SR, $^{\&}$p<0.05 compared to AVB2d, and $^{\#}$p<0.05 compared to CAVB3.

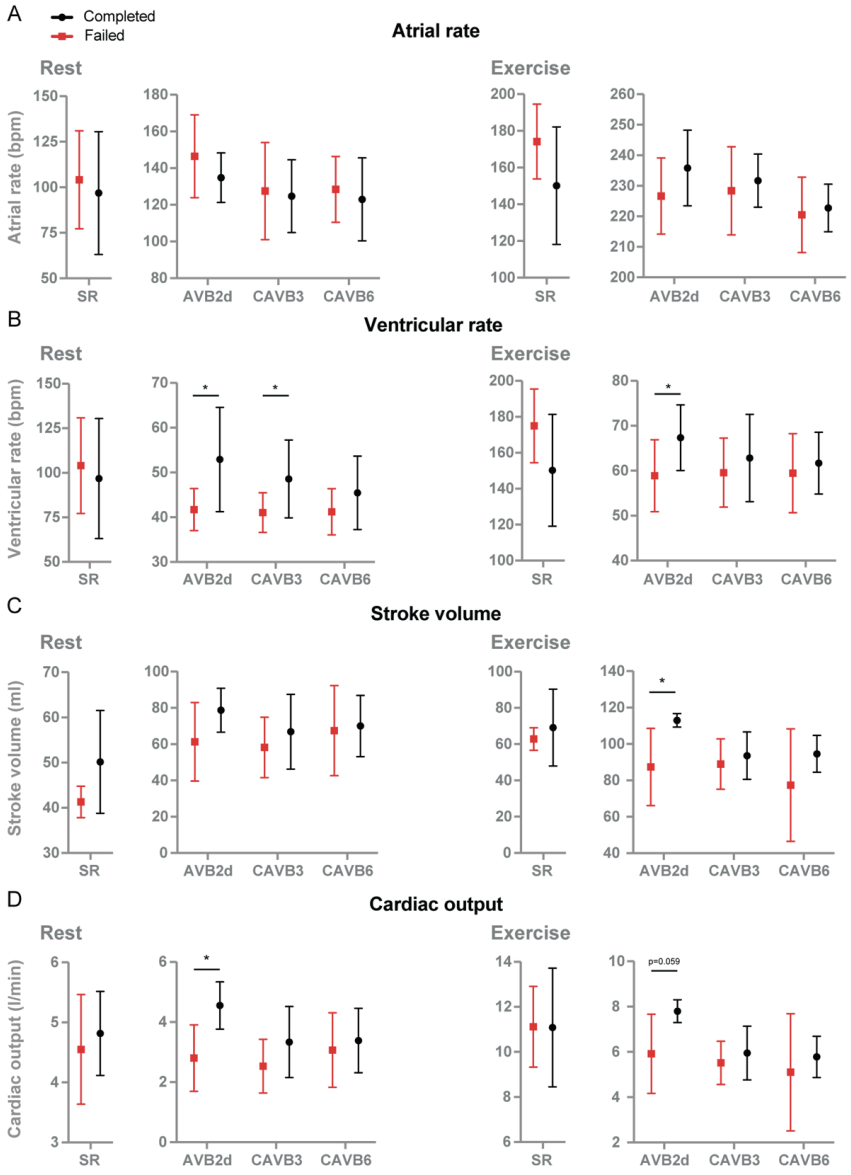

Suppl. figure 1. A) Atrial rate, **B**) ventricular rate, **C**) stroke volume, and **D**) cardiac output of dogs at timepoints rest (left panel) and exercise (right panel) separated in the failed (red, n=6) and completed (black, n=6) group determined at AVB2d. Data are presented as mean ± SD. For the completed group at AVB2d, parameters stroke volume and cardiac output at exercise: n=3. Unpaired t-test for comparison of failed vs completed group, *p<0.05.

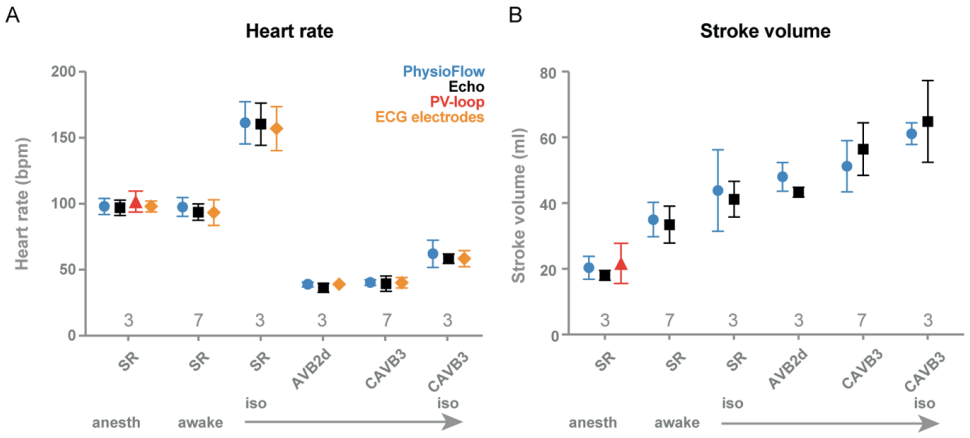

Suppl. figure 2. PhysioFlow evaluation in dogs by **A**) heart rate and **B**) stroke volume at sinus rhythm (SR) under anesthesia (anesth.), and in awake state at SR, two days (AVB2d) and three weeks (CAVB3) after AV block induction in baseline or after isoprenaline (iso). PhysioFlow data (in blue) was compared to echocardiography (echo, in black), pressure-volume loop measurements (PV-loop, in red), and electrocardiogram (ECG, in yellow). Data (numbers below data symbols refer to group size) are presented as mean ± SD.

8

Heart rate variability is severely impaired in the AV block dog model independent of cardiac remodeling duration

Joanne J.A. van Bavel[1], Cornelia W. van Dijk[1], Henriëtte D.M. Beekman[1], Arend Schot[2], Tim Takken[3], Marcel A.G. van der Heyden[1], Marc A. Vos[1]

[1] Department of Medical Physiology, Division of Heart and Lungs, University Medical Center Utrecht, Utrecht, the Netherlands
[2] Department of Clinical Sciences, Division of Anatomy and Physiology, Faculty of Veterinary Medicine, Utrecht University, the Netherlands
[3] Child Development and Exercise Center, Wilhelmina Children's Hospital, University Medical Center Utrecht, Utrecht, the Netherlands

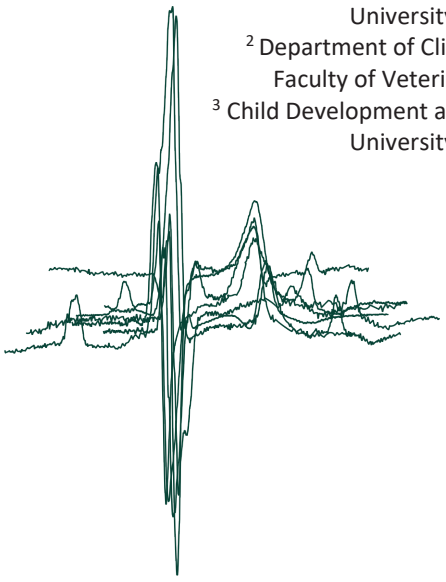

Abstract

Heart rate variability (HRV) refers to the fluctuations in cardiac beat-to-beat durations and is regulated by the autonomic input to the heart. An impaired HRV is observed in patients with heart failure and cardiopulmonary diseases, and is regarded as a predictive factor for sudden cardiac death. Restoring HRV with its potential positive effect on cardiac function is of high interest. In this study, we investigated HRV in the chronic AV block (CAVB) dog model.

Awake mongrel dogs (n=7) were tested in sinus rhythm (SR), and after AV block induction: two days (AVB2d), three weeks (CAVB3) and six weeks (CAVB6). Surface ECG and respiratory signals were recorded for 5 minutes in resting conditions.

The traditional time domain parameters (SDPP, SDRR, ΔPP mean, ΔRR mean, RMSSD, and pNN50) were reduced at all timepoints after AV block, predominantly for the RR intervals. The E:I ratio reduced for the PP intervals from 2.80 ± 0.36 at SR to 1.97 ± 0.61 at AVB2d ($p<0.05$), and for the RR intervals from 2.82 ± 0.37 at SR to 1.21 ± 0.16 at AVB2d, 1.23 ± 0.13 at CAVB3 and 1.31 ± 0.18 at CAVB6 ($p<0.05$).

Variability in atrial and ventricular rate are decreased in the awake chronic AV block dog. These results indicate that the CAVB dog can function as a model for examining the beneficial effect of restoring heart rate variability on the cardiopulmonary function.

Keywords

Heart rate variability, respiratory sinus arrhythmia, AV block, CAVB dog model

Introduction

Beat-to-beat variation in heart rate, or the variation in RR interval on the ECG, is known as heart rate variability (HRV) and in general depends on a complex balance between the sympathetic and parasympathetic tone.[1] Via this system, the heart rate is adapted to stimuli from various aspects on a physiological, pathological and environmental level.[2] Regarding the physiological aspect, fluctuations in heart rate can strongly synchronize with respiration, with an increased heart rate during inspiration and a decreased heart rate during expiration.[3] This phenomenon was first described by the German physiologist Carl Ludwig in 1847 and is referred to as respiratory sinus arrhythmia (RSA).[4]

HRV in synchrony with respiration is most prevalent at a younger age and in athletes,[5] in healthy subjects,[6] and in resting conditions upon high vagal activation.[7] It is therefore recognized as indicator of youth, health, and physical fitness. Though, the (beneficial) mechanisms underlying RSA are controversial[8] and range from origin in changes in intrathoracic pressure and stroke volume,[9] optimization of pulmonary gas exchange and oxygen delivery,[10] and reduction of cardiac workload.[11] One aspect that has been agreed on within this research field is that loss of RSA is strongly associated with heart failure and its comorbidities, such as chronic obstructive pulmonary disease and sleep apnea.[12-14]

Analysis of HRV and RSA is standardized over the last three decades and includes different approaches in terms of parameter calculation,[15] posture, breathing test, and length of the measurement. The HRV parameters are used in clinical studies as index of cardiac vagal tone and as prognostic value in various pathological conditions with mortality prediction,[16,17] and has therapeutic value focusing on improving cardiopulmonary function. Where exercise reduces RSA due to enhanced sympathetic tone, physical activity can restore RSA in rest [18] as can cardiac pacing: respiratory-modulated cardiac pacing enhanced RSA and thereby reversed heart failure-induced cardiac remodeling in rat and sheep.[19,20]

Dogs show a highly pronounced HRV and RSA with specific non-linear beating patterns.[21,22] The chronic atrioventricular block (CAVB) dog is a well-established preclinical model[23] applied in researching pro- and antiarrhythmic strategies such as new device entities.[24] Upon the weeks succeeding AV block induction, remodeling occurs at a contractile, electrical, and

structural level[25] and therefore experimental timepoints can be controlled. The CAVB dog's heart lacks any electrical conduction from the atria to the ventricles, which is substituted by the idioventricular rhythm at ±40-60 bpm. It indicates a promising role for this preclinical model in testing respiratory-modulated cardiac pacing. We studied the atrial and ventricular rate variability at different remodeling stages after AV block; at 2 days with limited remodeling, at three weeks, and six weeks with completed remodeling.

Methods

Animals

Seven purpose-bred Mongrel dogs (Marshall, New York, USA, three females and four males, bodyweight: 25 ± 2 kg, age: 14 ± 1 months) were included in this study. Dogs were housed in pairs in wooded-bedded kennels and had ad libitum access to water. They received food pellets twice a day and were allowed to play outside once a day with access to playing toys and then their welfare was checked daily. Animal care and experimentation were approved by the committee for Experiments on Animals of Utrecht University (application approval number: AVD5002016531). They were in accordance with the Directive 2010/63/EU of the European Parliament and the Dutch law on animal experimentation.

Surgical procedure: AV block induction

Prior to the surgical procedure, animals were fasted overnight. They received premedication (0.02 mg/kg i.m. atropine, 0.5 mg/kg i.m. methadone, 0.5 mg/kg i.m. acepromazine and 0.1 mg/kg s.c. meloxicam) 30 minutes before induction of general anesthesia. The latter included sodium pentobarbital (pentobarbital, 25 mg/kg i.v.) for induction, and 1.5 % isoflurane in O_2 and N_2O (1:2 ratio) via mechanical ventilation at 12 breaths per minute for maintenance. By radiofrequency ablation of the bundle of His, complete AV block was induced following our standard procedure.[26] Risk for inflammation and pain was prevented by administration of ampicillin (1000 mg) before (i.v.) and after (i.m) surgery, and buprenorphine (0.3 mg i.m.) after surgery.

Signal acquisition

The dogs were familiarized with the environment and researchers present. The commercially available Hexoskin shirt (Carré Technologies Inc, Montreal, Canada) was placed around the

thorax of the dog and the Hexoskin device located in the shirt pocket was connected to the Hexoskin application on a mobile phone using telemetry. The Hexoskin provides a 1-lead ECG signal (256 Hz) based on two electrodes in the thoracic regions and one electrode in the abdominal region. The respiratory signal (128 Hz) is measured by inductive plethysmography detecting thoracic and abdominal expansion. Surface ECG signals were obtained using EP tracer (Cardiotek, Maastricht, The Netherlands) with a frequency of 1,000 Hz. Prior to signal recording, all animals were secured to stand still on a table and the ECG and respiratory signals were checked. Resting ECG and respiratory signals were recorded for a period of 5 minutes. The recordings were performed in series at four different timepoints: sinus rhythm, and two days (AVB2d), three weeks (CAVB3), and six weeks (CAVB6) after AV block induction. Raw signals were converted to a .csv format using the HxConvertSourceFile program. Hexoskin ECG and respiratory signals – with a reduced respiratory signal output corresponding to inspiration and increased output corresponding to expiration – are visualized in **Figure 1A**.

Data analysis

R peaks from the Hexoskin ECG signal were selected using a Matlab (The MathWorks, Inc., Natick, Massachusetts, USA, version 2016a) script exporting RR intervals. A similar script was used to detect the PP intervals (for atrial rate analysis) from sinus rhythm dogs. For PP interval detection after AV block, one hundred PP intervals were manually measured from the surface ECG using the selection tools in EP tracer. Intervals including P waves in QRS complexes and ectopic beats were excluded. Based on the PP and RR intervals, standard and common parameters grouped under the time-domain quantifying heart rate variability were calculated, including: the standard deviation of the PP and RR intervals (SDPP and SDRR in ms, respectively), the average difference between all selected successive intervals (ΔPP mean and ΔRR mean in ms), the root mean square successive difference (RMSSD in ms), and the proportion of successive intervals that differ more than 50 ms (pNN50 in %). The E:I ratio was obtained by dividing the longest PP or RR interval during expiration by the shortest PP or RR interval during inspiration based on the respiratory signals.

Statistical analysis

Data are presented as mean ± standard deviation (SD). Serial data were analyzed using a repeated measures one-way analysis of variance (ANOVA) with Bonferroni's or Tukey's

multiple comparisons test. A value of $p<0.05$ was considered statistically significant. Analyses were performed using GraphPad Prism (version 9.3.1, GraphPad Software, San Diego, USA).

Results

Atrial rate variability is reduced after AV block

At sinus rhythm, variability in atrial rate ranges between 53 and 147 bpm (**Figure 1B, Table 1**). After AV block, the atrial rate increases compared to SR (**Figure 2A**), which is mainly caused by an increase in the minimal rate (**Table 1**). Variability in atrial rate is still present, though certainly reduced after AV block (**Figure 1B**) as shown by a reduction of HRV parameters SDPP, ΔPP mean, RMSSD and pNN50 after AV block (**Figure 2B-E, Table 1**). Although only significant for AVB2d, similar results were seen for the E:I ratio (**Figure 2F, Table 1**). The reduction in HRV parameters is less dominant at CAVB6 compared to AVB2d and CAVB3.

Variability in idioventricular rhythm is severely impaired after AV block

The AV block-induced bradycardia can be clearly observed from the tachograms in **Figure 1C**, which is stable at all AV block timepoints (45 ± 8 bpm at AVB2d, 45 ± 10 at CAVB3, and 45 ± 7 at CAVB6, **Table 1**). Despite the variation in ventricular rate at SR, it is severely impaired after AV block and can be appreciated from the Poincaré plots in **Figure 1C** (where the triangular pattern at SR is converted towards a clustered pattern after AV block) and the HRV parameters. AV block significantly reduced SDRR, ΔRR mean, RMSSD, pNN50 and E:I ratio at all timepoints (**Figure 2B-F, Table 1**).

When comparing the atrial and ventricular rhythm behavior upon AV block, we determine a significant increase in atrial rate and an extreme reduction in ventricular rhythm (**Figure 2A**). Regarding rate variability, impairment is more dominant in the ventricles compared to the atria as mainly demonstrated by the E:I ratio (**Figure 2F**).

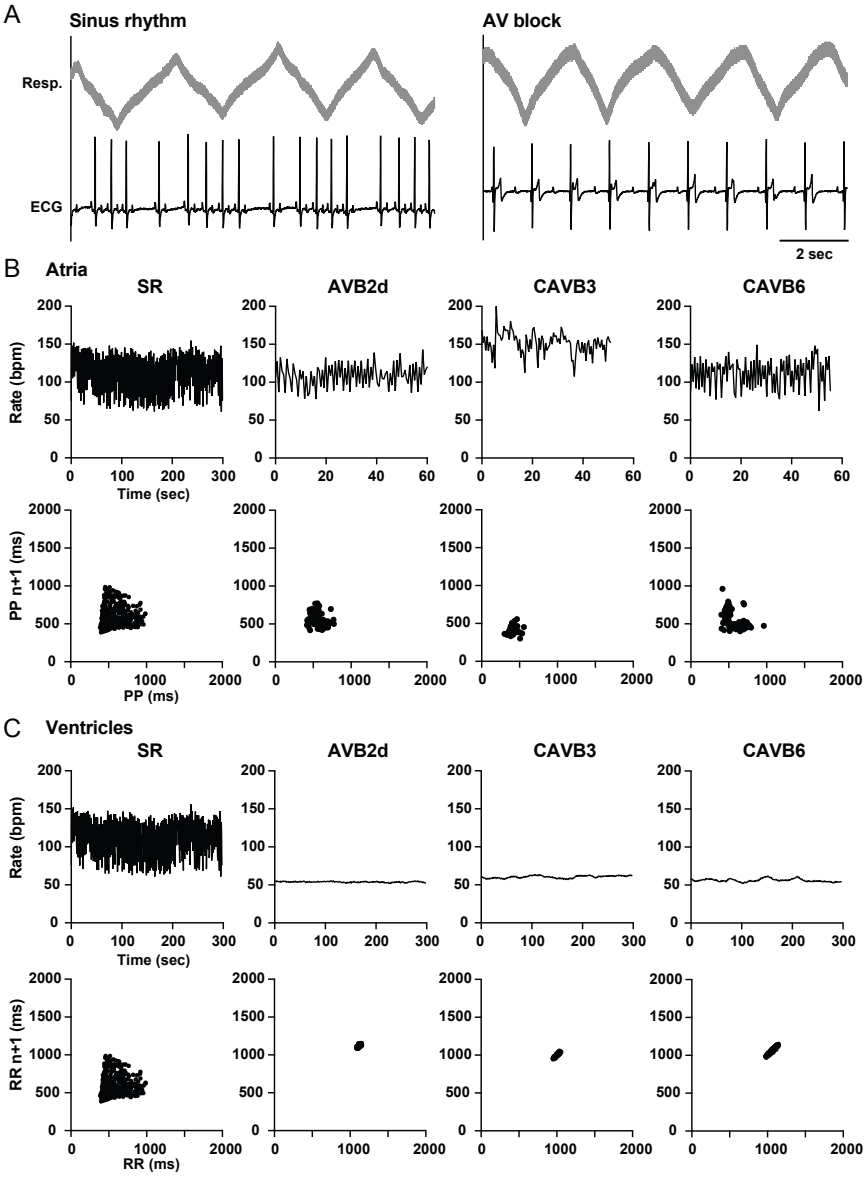

Figure 1. Overview of atrial and ventricular rate variability at sinus rhythm (SR) and after AV block at two days (AVB2d), three weeks (CAVB3) and six weeks (CAVB6). **A)** Respiratory (Resp.) and ECG signals of Hexoskin at sinus rhythm and AV block. A decreasing respiratory value refers to inspiration and an increasing value refers to expiration. **B)** Atrial rate variability in tachogram with corresponding Poincaré plot below. **C)** Ventricular rate variability in tachogram with corresponding Poincaré plots below. Results in series from dog h167607.

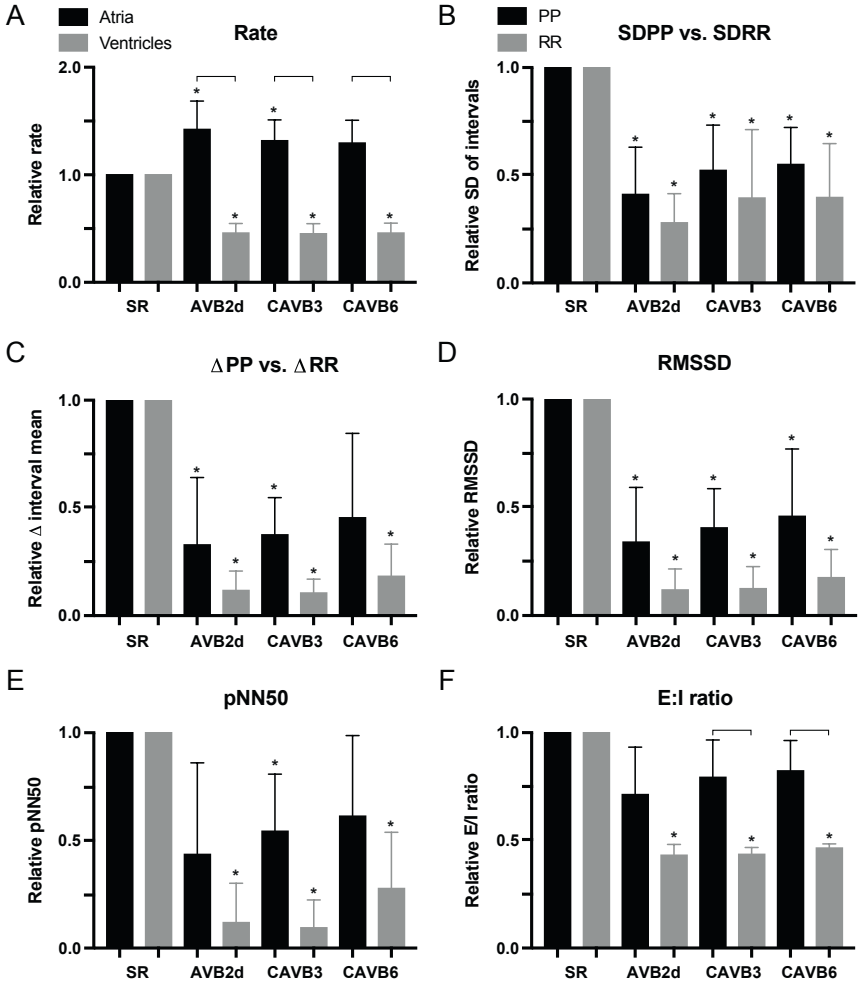

Figure 2. Overview of heart rate variability parameters of awake AV block dogs (n=7). Timepoints: sinus rhythm (SR) and three timepoints after AV block induction: two days (AVB2d), three weeks (CAVB3) and six weeks (CAVB6). **A**) Relative atrial and ventricular rate, **B**) standard deviation of selected intervals (SDPP vs. SDRR), **C**) delta mean of succeeding intervals (ΔPP vs. ΔRR), **D**) root mean square successive difference (RMSSD) **E**) proportion of successive intervals exceeding 50 ms (pNN50), **F**) longest interval during expiration divided by the shortest interval during inspiration (E:I ratio). Ratios are relative to RR of atria/PP intervals (black bars) and ventricles/RR intervals (grey bars). Data presented as mean ± SD. Repeated measures one-way ANOVA with Bonferroni's multiple comparisons test, *p<0.05 compared to SR, and bars refer to *p<0.05.

Table 1. Atrial and ventricular rate variability parameters of awake AV block dogs (n=7).

	SR	AVB2d	CAVB3	CAVB6
Atria				
Rate mean (bpm)	100 ± 18	140 ± 23 *	130 ± 20 *	127 ± 16 *
Rate min (bpm)	53 ± 8	98 ± 37 *	83 ± 27 *	74 ± 14 *
Rate max (bpm)	147 ± 25	175 ± 19	172 ± 28	165 ± 16
PP interval (ms)	658 ± 115	452 ± 79 *	487 ± 85 *	494 ± 63 *
SDPP (ms)	177 ± 54	75 ± 53 *	93 ± 50 *	94 ± 30 *
ΔPP mean (ms)	200 ± 88	61 ± 47 *	74 ± 50 *	77 ± 48
RMSSD (ms)	254 ± 98	86 ± 64 *	104 ± 69 *	103 ± 52 *
pNN50 (%)	74 ± 12	33 ± 30 *	40 ± 22 *	45 ± 27
E:I ratio	2.80 ± 0.36	1.97 ± 0.61 *	2.21 ± 0.53	2.28 ± 0.31
Ventricles				
Rate mean (bpm)	100 ± 18	45 ± 8 *	45 ± 10 *	45 ± 7 *
Rate min (bpm)	53 ± 8	41 ± 9	41 ± 9	39 ± 8
Rate max (bpm)	148 ± 25	49 ± 7 *	49 ± 10 *	51 ± 8 *
RR interval (ms)	658 ± 115	1365 ± 231 *	1398 ± 286 *	1378 ± 231 *
SDRR (ms)	176 ± 52	51 ± 32 *	64 ± 39 *	67 ± 37 *
ΔRR mean (ms)	197 ± 85	22 ± 17 *	20 ± 13 *	31 ± 16 *
RMSSD (ms)	250 ± 96	29 ± 25 *	31 ± 27 *	40 ± 21 *
pNN50 (%)	74 ± 11	9 ± 13 *	7 ± 10 *	19 ± 17 *
E:I ratio	2.82 ± 0.37	1.21 ± 0.16 *	1.23 ± 0.13 *	1.31 ± 0.18 *

Timepoints: sinus rhythm (SR) and three timepoints after AV block induction: two days (AVB2d), three weeks (CAVB3) and six weeks (CAVB6). SDPP vs. SDRR: standard deviation of selected intervals; ΔPP mean vs. ΔRR mean: delta mean of succeeding intervals; RMSSD: root mean square successive difference; pNN50: proportion of successive intervals exceeding 50 ms; E:I ratio: longest interval during expiration divided by the shortest interval during inspiration. Data presented as mean ± SD. Repeated measures one-way ANOVA with Tukey's multiple comparisons test, *p<0.05 compared to SR.

Discussion

This study presents the effect of complete AV block on atrial and ventricular rate variability in a preclinical animal model. The HRV time domain parameters were significantly reduced at the different remodeling timepoints after AV block compared to SR. The ventricular rate variability was more impaired than the atrial rate.

Atrial rate response upon AV block

The autonomic nervous system innervates the sinus node by targeting G-protein coupled receptors.[27] The intrinsic rate of the canine pacing cells in the sinus node varies from 90 to 140 bpm and is more affected by the vagal tone compared to human.[22,28] Though, the canine and human sinus node resemble to a great extent in structure and function.[29] Evaluation of HRV in conditions of complete AV block exposes very limited studies in literature. The general focus is on ventricular rate variability related to sleep, bradycardia, pacing, and first- or second-degree AV block. Nonetheless, Hsiao and coworkers revealed a significant reduction in atrial rate variability quantified by the traditional time domain parameters in thirteen human AV block patients.[30] In the CAVB dog, the atrial rate is increased upon AV block as presented in the current study and formerly reported.[31] This can be clarified by the enhanced sympathetic activity[32] in the form of e.g., increased norepinephrine plasma levels[33] as response to the AV block induced bradycardia and accompanying drop in cardiac output. Moreover, the AV block induced beat-to-beat variation in ventricular preload (due to the independent behavior of the atria compared to the ventricles) enhances the spontaneous pacemaker rate via stretch activated channels as mechano-electric feedback.[34,35] While HRV is appreciated as an indirect indicator of autonomic modulation,[36] enhanced sympathetic activity and an associated higher heart rate correspond with a reduced rate variability explaining the reduced atrial rate variability in the CAVB dog. The trend towards a less dominant reduction of atrial HRV parameters and atrial rate at CAVB6 compared to AVB2d coincide with a study in awake dogs by Boucher and coworkers reporting a lower atrial rate after six weeks.[37]

Ventricular rate response upon AV block

In conditions of complete atrioventricular dissociation as in the AV block dog model, the pulmonary and systemic circulation depend on an alternative pacemaker than the sinus node which generates the idioventricular rhythm. Directly after AV block induction, the heart starts to adapt to the bradycardia-induced drop in cardiac output in a compensatory approach by e.g., enhancing the contractility and - in a more time-consuming response - biventricular hypertrophy.[25] While the heart undergoes remodeling at different levels, the ventricular rate remains stable and below 60 bpm after AV block induction, as shown in the this study and reported previously.[37] Yet, this rhythm can somewhat increase by exercise and enhanced pacemaker activity (accelerated idioventricular rhythm).[31,38] Until now, effects of respiratory oscillations in the AV block dog model focused on modulation of action potential duration rather than heart rate in the anesthetized and mechanically ventilated AV block dog.[32] In dogs at rest, the current study shows that HRV is severely impaired after complete AV block, which is consistent over time.

The variability in atrial rate is less decreased after AV block compared to the ventricular rate. While the atrial rate finds variation upon the return of parasympathetic influences over time following AV block, ventricular pacemaker cells maintain the slow and stable generation of the idioventricular rhythm.[37] The latter seems, despite response upon sympathetic activation during exercise and stellate ganglion stimulation,[39] not affected by the autonomic nervous system in terms of variability in resting conditions.

Clinical implications

The loss of HRV and RSA in the AV block dog model, already from the onset of AV block induction, implies a valuable role of this preclinical model in the field of respiratory-modulated pacing. Chronic pacing (>2 weeks) on each respiratory cycle, with an increase in ventricular rate upon inspiration and a decrease in rate upon expiration, can establish improvement of cardiac function compared to healthy and monotonically paced conditions. A combination of the highly present RSA in healthy state and loss upon AV block, the arrhythmic sensitivity, and controlled timepoints in this standardized model appreciates its role in improving cardiac rhythm management devices,[39] as applied by Krause and

coworkers.[40] From a clinical perspective, the RMSSD value from a 5-minute recording is advised for risk prediction as it is most stable and robust.[6]

Study limitations

While RSA has a dominant presence in resting dogs at sinus rhythm, this study includes ultrashort (<5min, for PP intervals after AV block) and short term (±5 min) recordings instead of 24-hour recordings, of which the latter represent a rate behavior in a circadian rhythm including a wider range of environmental influences. Moreover, despite the detailed analysis under the time domain, this study does not display frequency domain analysis which gives more specific insight in parasympathetic effects compared to time domain analysis.

Conclusion

Variability in ventricular and atrial rate in the awake chronic AV block dog is impaired, predominantly in the ventricles. These results indicate that the CAVB dog can function as a potential model for examining the beneficial effect of restoring heart rate variability on the cardiopulmonary function.

Funding

This study, as part of the CResPace project, has received funding from the European Union's Horizon 2020 research and innovation programme under grant number 732170.

References

1. Levy MN. Sympathetic-parasympathetic interactions in the heart. *Circ Res.* 1971;29(5):437-445.
2. Fatisson J, Oswald V, Lalonde F. Influence diagram of physiological and environmental factors affecting heart rate variability: an extended literature overview. *Heart Int.* 2016;11(1):e32-e40.
3. Angelone A, Coulter NA, Jr. Respiratory sinus arrhythemia: A frequency dependent phenomenon. *J Appl Physiol.* 1964;19:479-482.
4. Ludwig C. Beitrage zur kenntniss des einflusses der respirationsbewegungen auf den blutlauf im aortensysteme. *Arch Anat Physiol Leipzig.* 1847;13:242-302.
5. Simoyi M. Respiratory sinus arrhythmia in athletes, the young, and the old. *Biomed J Sci & Tech Res.* 2020;30(3):23359-23363.
6. Jarczok MN, Weimer K, Braun C, et al. Heart rate variability in the prediction of mortality: A systematic review and meta-analysis of healthy and patient populations. *Neurosci Biobehav Rev.* 2022;143:104907.
7. Hayano J, Yasuma F. Hypothesis: respiratory sinus arrhythmia is an intrinsic resting function of cardiopulmonary system. *Cardiovasc Res.* 2003;58(1):1-9.
8. Beckers F, Verheyden B, Aubert AE. Aging and nonlinear heart rate control in a healthy population. *Am J Physiol Heart Circ Physiol.* 2006;290(6):H2560-2570.

9. Toska K, Eriksen M. Respiration-synchronous fluctuations in stroke volume, heart rate and arterial pressure in humans. *J Physiol.* 1993;472:501-512.
10. Hayano J, Yasuma F, Okada A, Mukai S, Fujinami T. Respiratory sinus arrhythmia. A phenomenon improving pulmonary gas exchange and circulatory efficiency. *Circulation.* 1996;94(4):842-847.
11. Ben-Tal A, Shamailov SS, Paton JF. Central regulation of heart rate and the appearance of respiratory sinus arrhythmia: new insights from mathematical modeling. *Math Biosci.* 2014;255:71-82.
12. De Jong MJ, Randall DC. Heart rate variability analysis in the assessment of autonomic function in heart failure. *J Cardiovasc Nurs.* 2005;20(3):186-195; quiz 196-187.
13. Reis MS, Deus AP, Simoes RP, Aniceto IA, Catai AM, Borghi-Silva A. Autonomic control of heart rate in patients with chronic cardiorespiratory disease and in healthy participants at rest and during a respiratory sinus arrhythmia maneuver. *Rev Bras Fisioter.* 2010;14(2):106-113.
14. Qin H, Keenan BT, Mazzotti DR, et al. Heart rate variability during wakefulness as a marker of obstructive sleep apnea severity. *Sleep.* 2021;44(5):zsab018.
15. Draghici AE, Taylor JA. The physiological basis and measurement of heart rate variability in humans. *J Physiol Anthropol.* 2016;35(1):22.
16. Nolan J, Batin PD, Andrews R, et al. Prospective study of heart rate variability and mortality in chronic heart failure: results of the United Kingdom heart failure evaluation and assessment of risk trial (UK-heart). *Circulation.* 1998;98(15):1510-1516.
17. Brouwer J, Van Veldhuisen DJ, Man in 't Veld AJ, et al. Prognostic value of heart rate variability during long-term follow-up in patients with mild to moderate heart failure. The Dutch Ibopamine Multicenter Trial Study Group. *J Am Coll Cardiol.* 1996;28(5):1183-1189.
18. Oliveira NL, Ribeiro F, Alves AJ, Teixeira M, Miranda F, Oliveira J. Heart rate variability in myocardial infarction patients: effects of exercise training. *Rev Port Cardiol.* 2013;32(9):687-700.
19. Shanks J, Abukar Y, Lever NA, et al. Reverse re-modelling chronic heart failure by reinstating heart rate variability. *Basic Res Cardiol.* 2022;117(1):4.
20. O'Callaghan EL, Lataro RM, Roloff EL, et al. Enhancing respiratory sinus arrhythmia increases cardiac output in rats with left ventricular dysfunction. *J Physiol.* 2020;598(3):455-471.
21. Hamlin RL, Smith CR, Smetzer DL. Sinus arrhythmia in the dog. *Am J Physiol.* 1966;210(2):321-328.
22. Moise NS, Flanders WH, Pariaut R. Beat-to-Beat patterning of sinus rhythm reveals non-linear rhythm in the dog compared to the human. *Front Physiol.* 2019;10:1548.
23. Loen V, Vos MA, Van der Heyden MAG. The canine chronic atrioventricular block model in cardiovascular preclinical drug research. *Br J Pharmacol.* 2022;179(5):859-881.
24. Smoczyńska A, Loen V, Aranda A, Beekman HDM, Meine M, Vos MA. High-rate pacing guided by short-term variability of repolarization prevents imminent ventricular arrhythmias automatically by an implantable cardioverter-defibrillator in the chronic atrioventricular block dog model. *Heart Rhythm.* 2020;17(12):2078-2085.
25. Oros A, Beekman JD, Vos MA. The canine model with chronic, complete atrio-ventricular block. *Pharmacol Ther.* 2008;119(2):168-178.
26. Timmermans C, Rodriguez LM, Van Suylen RJ, et al. Catheter-based cryoablation produces permanent bidirectional cavotricuspid isthmus conduction block in dogs. *J Interv Card Electrophysiol.* 2002;7(2):149-155.
27. Cifelli C, Rose RA, Zhang H, et al. RGS4 regulates parasympathetic signaling and heart rate control in the sinoatrial node. *Circ Res.* 2008;103(5):527-535.
28. Evans JM, Randall DC, Funk JN, Knapp CF. Influence of cardiac innervation on intrinsic heart rate in dogs. *Am J Physiol.* 1990;258(4 Pt 2):H1132-1137.
29. Kalyanasundaram A, Li N, Hansen BJ, Zhao J, Fedorov VV. Canine and human sinoatrial node: differences and similarities in the structure, function, molecular profiles, and arrhythmia. *J Vet Cardiol.* 2019;22:2-19.

30. Hsiao HC, Chiu HW, Lee SC, Kao T, Chang HY, Kong CW. Heart rate variability in patients with atrioventricular block. *Zhonghua Yi Xue Za Zhi (Taipei).* 1997;60(2):81-85.
31. Van Bavel JJA, Beekman HDM, Schot A, et al. Remodeling in the AV block dog is essential for tolerating moderate treadmill activity. *Int J Cardiol Heart Vasc.* 2023;44:101169.
32. Sprenkeler DJ, Beekman JDM, Bossu A, Dunnink A, Vos MA. Pro-arrhythmic ventricular remodeling is associated with increased respiratory and low-frequency oscillations of monophasic action potential duration in the chronic atrioventricular block dog model. *Front Physiol.* 2019;10:1095.
33. Vos MA, de Groot SH, Verduyn SC, et al. Enhanced susceptibility for acquired torsade de pointes arrhythmias in the dog with chronic, complete AV block is related to cardiac hypertrophy and electrical remodeling. *Circulation.* 1998;98(11):1125-1135.
34. Stams TR, Oosterhoff P, Heijdel A, et al. Beat-to-Beat variability in preload unmasks latent risk of torsade de pointes in anesthetized chronic atrioventricular block dogs. *Circ J.* 2016;80(6):1336-1345.
35. Reed A, Kohl P, Peyronnet R. Molecular candidates for cardiac stretch-activated ion channels. *Glob Cardiol Sci Pract.* 2014;2014(2):9-25.
36. Michael S, Graham KS, Davis GMO. Cardiac autonomic responses during exercise and post-exercise recovery using heart rate variability and systolic time intervals – A review. *Front Physiol.* 2017;8:301.
37. Boucher M, Dubray C, Duchene-Marullaz P. Long-term observation of atrial and ventricular rates in the unanesthetized dog with complete atrioventricular block. *Pflugers Arch.* 1982;395(4):341-343.
38. Gildea TH, Levis JT. ECG diagnosis: accelerated idioventricular rhythm. *Perm J.* 2018;22:17-173.
39. Nogaret A, O'Callaghan EL, Lataro RM, et al. Silicon central pattern generators for cardiac diseases. *J Physiol.* 2015;593(4):763-774.
40. Krause R, Van Bavel JJA, Wu C, Vos MA, Nogaret A, Indiveri G. Robust neuromorphic coupled oscillators for adaptive pacemakers. *Sci Rep.* 2021;11(1):18073.

Results from this chapter contributed to:

Abu-Hassan KJ, Taylor JD, **Van Bavel JJA**, Vos MA, Nogaret A.
Silicon Central Pattern Generator Model of Cardiac Contraction Behavior.
2020 11th Conference of the European Study Group on Cardiovascular Oscillations (ESGCO). 2020;1-2

Krause R, **Van Bavel JJA**, Wu C, Vos MA, Nogaret A, Indiveri G.
Robust neuromorphic coupled oscillators for adaptive pacemakers. *Scientific Reports.* 2021;11:18073

Taylor JD, Abu Hassan KJ, **Van Bavel JJA**, Vos MA, Nogaret A.
Robust design of inhibitory neuronal networks displaying rhythmic activity.
In: Awrejcewicz, J. (eds) Perspectives in Dynamical Systems III: Control and Stability. DSTA 2019.
Springer Proceedings in Mathematics and Statistics. 2021;364:187-198

9

The role of the AV block dog model in developing the cardiorespiratory pacing (CResPace) device

Joanne J.A. van Bavel[1], Henriëtte D.M. Beekman[1], Arend Schot[2], Søren Aasmul[3], Martin Leonhardt[4], Kamal J. Abu-Hassan[4], Chandrabhan Kushwah[4], Alain Nogaret[4], Marcel A.G. van der Heyden[1], Marc A. Vos[1]

[1] Department of Medical Physiology, Division of Heart & Lungs, University Medical Center Utrecht, Utrecht, The Netherlands
[2] Department of Clinical Sciences, Division of Anatomy and Physiology, Faculty of Veterinary Medicine, Utrecht University, The Netherlands
[3] Medtronic Bakken Research Center, Maastricht, The Netherlands
[4] Department of Physics, University of Bath, United Kingdom

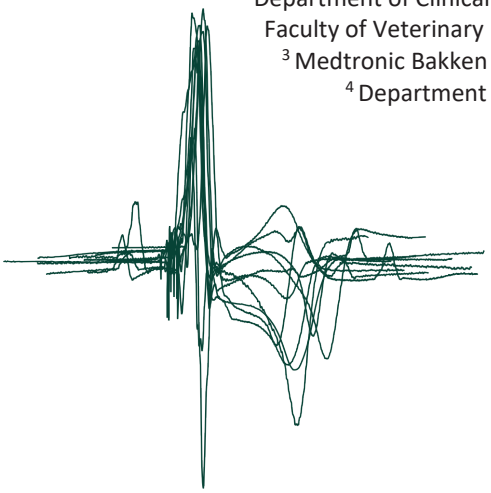

Abstract

The cardiorespiratory pacing (CResPace) device is based on small neuronal networks which can respond and adapt to physiological feedback from sensors in real time. These sensors include measurement of blood pressure, lung inflation, pO_2 and SpO_2. The developed bioelectronics (central pattern generators, CPG) and sensors are evaluated in the atrioventricular (AV) block dog model. Over the last four decades, this standardized experimental model of compensated hypertrophy was involved in pro- and antiarrhythmic drug screening and device testing. In this study, we set up a database with cardiorespiratory signals for data assimilation and development of the CPG device. Moreover, dummy sensors were implanted to evaluate long-term tissue and animal acceptance, and working sensors were tested under different conditions to show CPG adaptation to sensor input.

Keywords

Cardiac device, AV block dog model, respiratory sinus arrhythmia, sensors, pacing

Introduction

Incidence rates of the global epidemic heart failure (HF) have stabilized due to improvements of preventive strategies in terms of risk factors.[1] However, long-term data on HF reports mortality over 50% within five years after onset.[2] Several comorbidities such as hypertension, chronic obstructive pulmonary disease (COPD) and sleep apnea are commonly associated with HF and are linked to worse clinical outcomes.[3,4] Here, the apparent interaction between the cardiac and pulmonary system comes into view. Variation in heart rate upon each respiratory cycle, with an increased rate during inspiration and decreased rate during exhalation, is known as respiratory sinus arrhythmia (RSA).[5] This physiological phenomenon has substantial beneficial effects such as optimal gas exchange and efficient cardiac energy expenditure.[6,7] Where RSA is highly present in athletes and the young,[8,9] its absence is a hallmark of HF characterized by adverse changes in autonomic function.[10] Analysis of heart rate variability shows a loss of RSA in patients with chronic HF.[11]

Increasing heart rate variability by restoring RSA may be beneficial for patients with a reduced cardiac function as a result from cardiopulmonary disease. Heart rate regulation, based on diaphragmatic electromyogram signals, was successfully performed in rats using a hardware central pattern generator (CPG) based on outputs and dynamics of neurons.[12,13] Moreover, restoring RSA by this similar method in sheep with chronic heart failure improved cardiac function and reduced apnea incidence.[14] Current pacing strategies lack the complex biofeedback to restore RSA in real time. Moreover, incorporation of multiple cardiorespiratory parameters besides RSA including blood pressure, oxygen saturation (SpO_2), and oxygen and carbon dioxide partial pressure (pO_2, pCO_2) would more accurately approach the physiological setting of the respiratory and cardiac neuronal networks.[15]

The cardiorespiratory pacing (CResPace) consortium (EU Horizon 2020, grant no 73170) aims to develop an adaptive pacing device based on small neuronal networks which can respond and adapt to physiological feedback from sensors in real time. This will improve pacing treatment and thereby enhance cardiac function for patients suffering from heart failure and cardiorespiratory comorbidities. The regulation of the cardiorespiratory system by biological CPGs in the human brainstem (**Figure 1**) is modelled using computational neuron models.[15] The tri-phasic respiratory CPG integrates fluctuating signals of SpO_2, pO_2, pCO_2, lung inflation

and blood pressure as physiological input from implanted sensors to provide respiratory modulation to the tetra-phasic cardiac CPG. These, in turn, produce rhythmic patterned outputs to regulate heart chamber contractions influenced by the respiratory cycles.

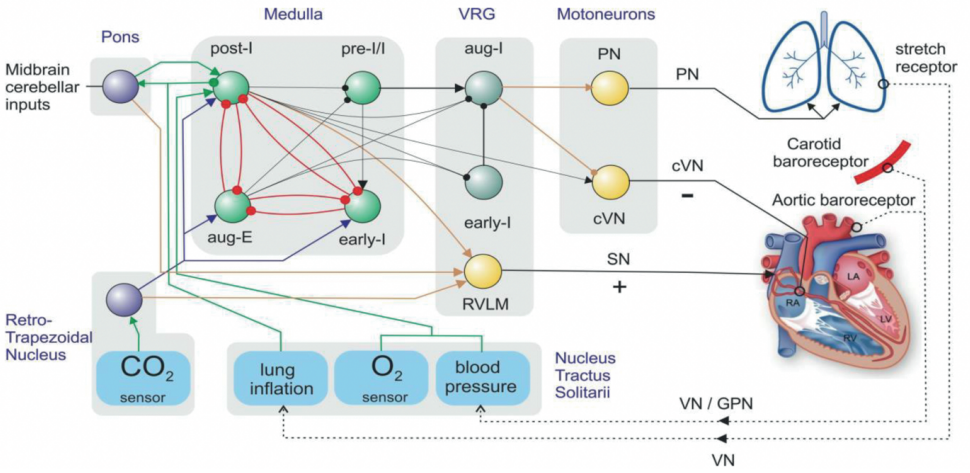

Figure 1. Regulation of the cardiorespiratory system by biological central pattern generators (bCPGs). The three-phasic respiratory bCPG integrates physiological feedback from arterial gas levels, lung inflation, and blood pressure to regulate heart rate.[15-17]

The developed bioelectronics and sensors are evaluated in the atrioventricular (AV) block dog model. The canine and human heart share a moderate resemblance in cardiac electrophysiology[18] and RSA is highly present in the dog.[19] Induction of AV block in combination with bradycardia-induced remodeling, anesthesia, and a pharmacological hit makes this heart vulnerable for induction of ventricular arrhythmias with high reproducibility.[20] Over the last four decades, this standardized experimental model of compensated hypertrophy was therefore involved in pro- and antiarrhythmic drug screening and device testing.[18,21] The aims for the current study included 1) setup of a database with cardiorespiratory signals, 2) evaluation of long-term implantation and animal acceptance of dummy sensors, 3) testing of working sensors under anesthesia, in awake state at rest and during exercise, and 4) demonstration of CPG adaptation to sensor input.

Methods

Animals

Animal handling and care were in accordance with the Directive 2010/63/EU of the European Parliament and the Council of 22 September 2010 on the protection of animals used for scientific purposes and the Dutch law on animal experimentation. Experiments were approved by the Central Authority for Scientific Procedures on Animals. Application approval numbers: AVD115002016531 and AVD11500202114910. Animal studies are reported in compliance with the ARRIVE guidelines.[22] The current study has no implications for replacement, refinement, or reduction. Data from adult purpose-bred mongrel dogs (n=22, Marshall, New York, USA) and healthy surplus beagle dogs (n=2, Charles River Laboratories, 's Hertogenbosch, The Netherlands) were included in the study. Dogs were housed in pairs in kennels containing wooden bedding material, had ad libitum access to drinking water and received food pellets twice a day. Furthermore, animals played outside every day and their welfare was checked daily. Animals were not randomized in the present study, and operators were not blinded.

Anesthesia procedure and AV block

Before each experiment containing anesthesia, dogs were fasted overnight and received premedication (0.02 mg/kg atropine, 0.5 mg/kg methadone, and 0.5 mg/kg acepromazine i.m.) 30 minutes before to the surgical procedure. General anesthesia was induced by sodium pentobarbital (Nembutal, 25 mg/kg i.v.) and maintained by 1.5% isoflurane in O_2 and N_2O (ratio 1:2) via mechanical ventilation with 12 breaths per minute. Pain and the risk for inflammation were minimized by analgesics (0.1 mg/kg Metacam s.c. before surgery and 0.3 mg/kg Temgesic i.m. after surgery) and antibiotics (1,000 mg/kg ampicillin i.v. before and i.m. after surgery). After measurements in sinus rhythm, complete and irreversible AV block was induced by radiofrequency ablation of the His bundle.[23]

Database of ECG and monophasic action potentials

Surface electrocardiogram (ECG) lead II tracings (recorded in EP tracer software, Cardiotek, Maastricht, The Netherlands), monophasic action potential (MAP) signals (catheter from Hugo Sachs Elektronik, Germany), and left ventricular pressure signals (LV-P, 7F pressure catheter from CD Leycom Inc., Zoetermeer, The Netherlands) with a sampling rate of 1 kHz

during baseline (1 minute) were collected from anesthesia experiments performed in the past (yr 2013, 2018 and 2019). Signals from healthy sinus rhythm (SR) dogs included ECG lead II (n=8), MAP from the left ventricular apex (n=10), right ventricular free wall (n=6) and right atrium (n=4), and LV-P signals (n=2). Signals from dogs with AV block for three weeks (n=2) and four weeks (n=2) included ECG lead II and MAP from the left and right ventricle.

Database of respiratory signals

Healthy SR dogs (n=5) got acquainted to stand still wearing the Hexoskin shirt (Carré Technologies Inc, Montreal, Canada) around the thorax. The shirt provides a 1-lead ECG signal with a sampling rate of 256 Hz based on two sensors in the thoracic region and one reference electrode in the abdominal region. The respiratory signal with a sampling rate of 128 Hz is measured by respiratory inductive plethysmography which detects thoracic and abdominal expansion with positive values for exhalation and negative values for inhalation. Signals were visualized and recorded for 5 minutes using the Hexoskin application on a mobile phone, and raw signals were later converted using HxConvertSourceFile software.

Database of physiological variables in awake state

Blood pressure signals originated from dorsal pedal artery of the left front paw (n=2). For cardiorespiratory measurements during exercise, an experimental protocol of moderate exercise was developed for which dogs were placed on a treadmill with a custom-build closed chamber of Plexiglass. A detailed description of the experimental setup and measurements are previously reported.[24] The database was completed with continuous surface ECG tracings from dogs in SR (n=3) at rest and during exercise, and venous (n=8) and arterial (n=2) blood parameters of dogs at sinus rhythm and AV block three weeks at rest, during exercise (2, 5, and 10 minutes) and recovery.

Evaluation of dummy sensors

Four dummy sensors (ethylene oxide sterilized) representing the weight and size of the new developed gas sensors (pO_2, SpO_2) and bioelectronics devices were implanted subcutaneously on the right side of the thorax under general anesthesia in one dog. Inflammation risk was minimized by oral administration of 250 mg synulox (twice-daily) and 0.1 mg/kg Metacam for five days after implantation as standardized after subcutaneous implantation of devices.

During 8.5 weeks of implantation, the location of the sensors was checked daily, and pictures were taken at the time of implantation, during implanted stages and when excised.

The dummy blood pressure sensor consisted of a silicon band and a surrounding clamp placed around the concerning artery. Under anesthesia, the dummy blood pressure sensor was implanted on the carotid artery or femoral artery in two dogs. For evaluation of implanting the lung inflation sensor, a Cooner wire (AS633-3SSF, Cooner Wire, Chatsworth, CA, USA, 1 mm) was placed through the lateral side of the diaphragm using a large needle after opening of abdominal region under the lowest rib. The wire was knotted after establishing a proper contact between the wire and the muscle tissue. This type of implantation was tested in two dogs. Implantation of the sensors was evaluated, pictures were taken and results were discussed within the CResPace consortium for sensor adjustments.

Testing of working sensors

Lung inflation signals were based on electromyography as measured by two Cooner wires implanted in the muscular part of the animal's right diaphragm in a 5 cm distance. Under anesthesia, spontaneous breathing was induced by reduction of isoflurane administration in a dog with chronic AV block. Muscle contractions upon each respiratory cycle were recorded in EP tracer software with a sampling rate of 1 kHz.

The gas sensors were implanted subcutaneously on the thorax and tested during six anesthesia experiments (n=2 beagle dogs and n=2 chronic AV block dogs). The SpO_2 sensor is based on spectroscopic measuring of hemoglobin absorption at 660 and 940 nm and the pO_2 sensor contains an optically interrogated oxygen sensitive assay for measuring alterations in tissue pO_2. Data was collected via a custom-build application on a tablet using telemetry. After a 1-hour baseline measurement, gas changes were induced by a respiratory maneuver including a reduction of the respiratory volume and flow which was confirmed by standard measurements of SpO_2 levels from the tongue. Respiratory volume and flow were normalized after reaching tongue SpO_2 levels of ±65%. Rate adaptation by the CPG electronics (n=1) was programmed based on data of former respiratory maneuvers. SpO_2 sensor output levels corresponding to SpO_2 levels of 99% were coupled to 64 bpm pacing output, whereas the reducing SpO_2 levels upon a respiratory maneuver increased the pacing output maximal to 74

bpm. Gas sensor testing was performed upon exercise during three experiments in one chronic AV block dog at day 1, day 7 and day 12 after sensor implantation.

Results

Database as use for the development of CPG models

A database with cardiorespiratory signals of dogs, with healthy and AV block-remodeled hearts, was used for the development of bioelectronic implants that adapt to physiological feedback. Representative cardiorespiratory tracings - including ECG, MAP signals from individual heart chambers, blood pressure, and respiratory signals - forming the database for modeling of the cardiac and respiratory neurons are presented in **Figure 2**. ECG and MAP signals from the RA and LV (**Figure 2A**) of an anesthetized healthy dog were used to extract heart chamber activation timings which were incorporated in the hardware CPG model consisting of four neurons.[25,26] Besides the cardiac CPG, respiratory sinus arrhythmia as physiological phenomenon was implemented in a hardware model. Respiratory signals simultaneously recorded with ECG of healthy and awake dogs via the Hexoskin shirt (**Figure 2C**) formed the basis for demonstrating the robustness of the developed neuromorphic electronic circuits and reproduction of heart rate modulation upon respiration was presented.[27] Moreover, exercise as physiological condition completed the database with e.g., ECG signals (**Figure 2E**), venous blood parameters, oxygen uptake and carbon dioxide exhalation.[24]

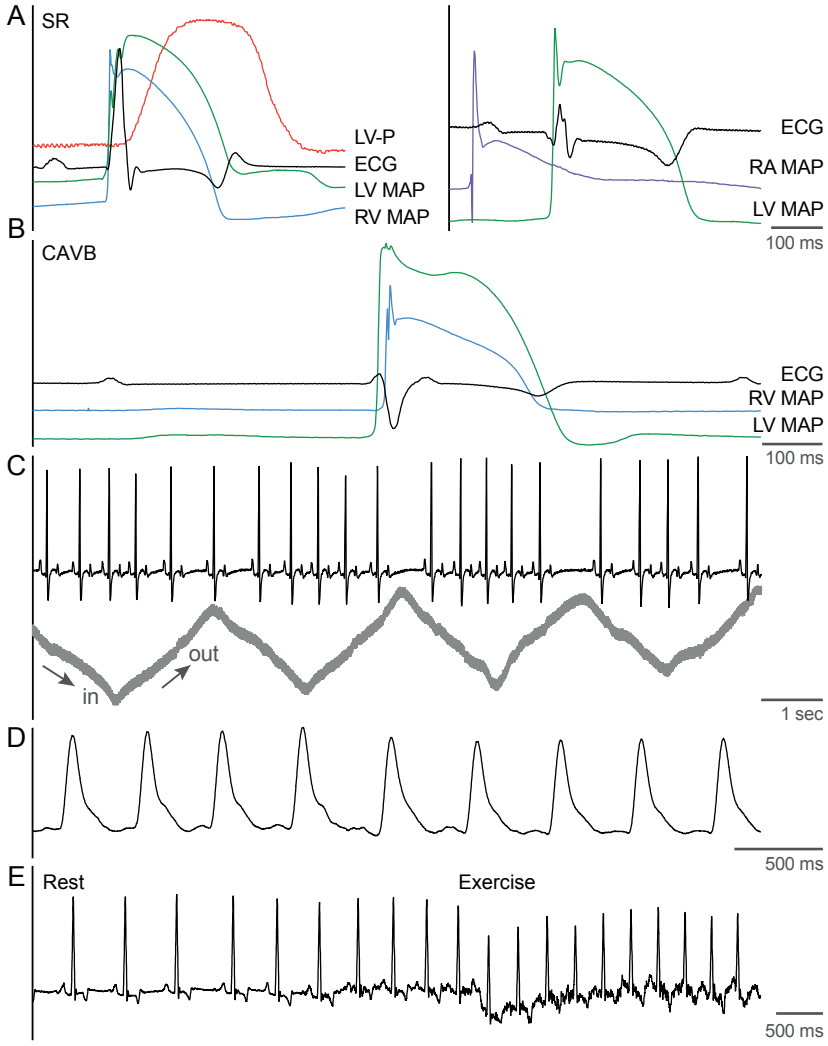

Figure 2. Overview of the cardiorespiratory signals representing the database for modeling of cardiac and respiratory networks. **A**) Left ventricular pressure (LV-P), ECG, LV, and RV monophasic action potential (LV MAP, RV MAP) and right atrial (RA) MAP signals from healthy and **B**) chronic AV block dog. **C**) ECG and respiratory signals and **D**) blood pressure signals from healthy dog in awake state. **E**) ECG from healthy dog at rests and during exercise.

Evaluation of dummy sensors

Different versions of the blood pressure sensor were tested in the form of a silicon ribbon wrapped around the artery and tightened with a clamp (**Figure 3A**). Suggestions on the implantation procedure, use of a screw and extent of tightening were shared with the engineering colleagues for further optimization. Implantation of the lung inflation sensor to

the diaphragm was optimal when the Cooner wire was sutured to the diaphragm (**Figure 3BII**) instead of through (**Figure 3BI**) the muscular tissue. Subcutaneous implantation of the dummy sensors representing the size and weight of the gas sensors and pacing device (**Figure 3C, D**) was successful for 8.5 weeks without any signs of inflammation. Moreover, the implantation pockets were clean after removal of the dummy devices (**Figure 3E**).

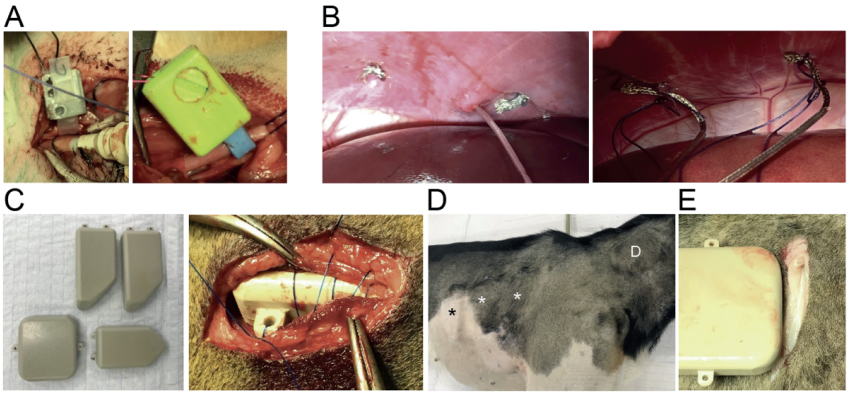

Figure 3. Overview of implanted dummy sensors in chronic AV block dogs. **A**) Blood pressure clamp around femoral artery and carotid artery. **B**) Cooner wires on diaphragm. **C**) Dummy sensors representing gas sensors and pacing device. **D**) Subcutaneous implantation of sensors (*) and device (D). **E**) Explanted sensor after 8.5 weeks with clean pocket.

Sensor response under anesthesia

Electromyography signals from the muscular part of the diaphragm using a Cooner wire upon each respiratory cycle of a chronic AV block dog under anesthesia were successfully obtained simultaneously with ECG (**Figure 4A**). Next, gas sensor response was evaluated during a respiratory maneuver (**Figure 4B**). The respiratory maneuver was confirmed by the reduced SpO_2 levels measured from the tongue ($tSpO_2$). The sensor SpO_2 ($sSpO_2$) responded immediately after initiation of the reduction in oxygen administration, whereas the pO_2 sensor had a response time of several minutes.

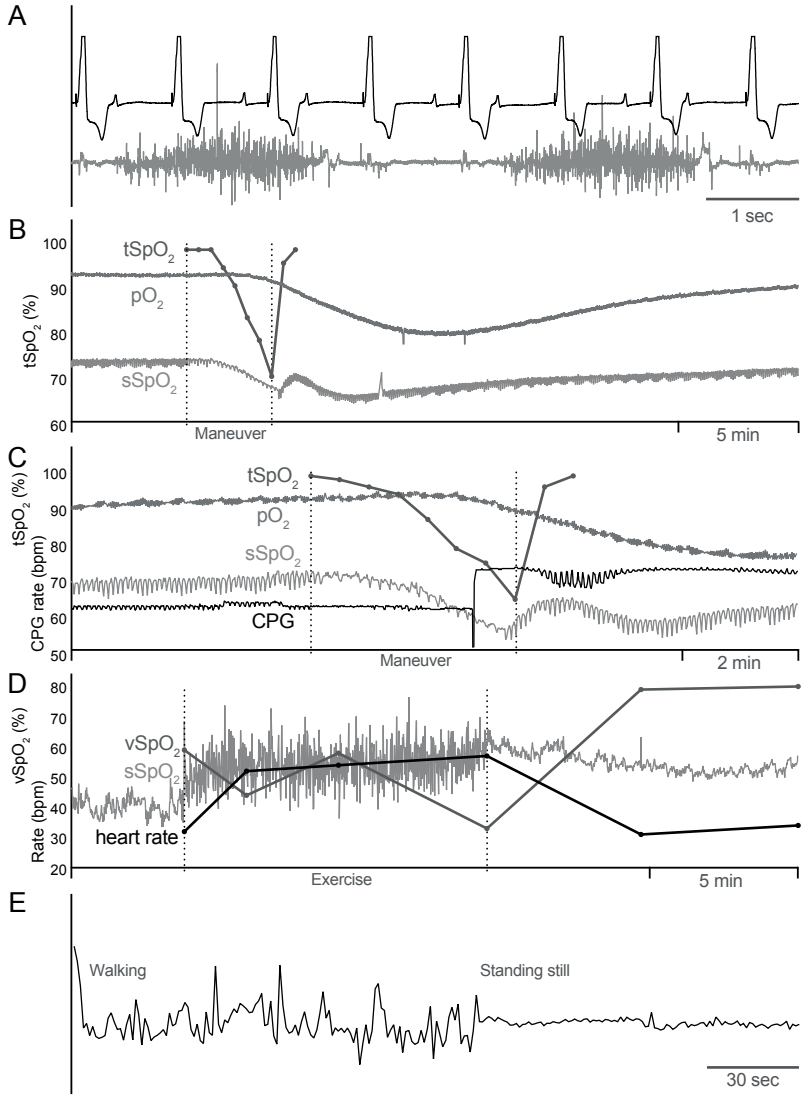

Figure 4. Representative overview of signals obtained from sensor testing. **A**) ECG and electromyography signals from diaphragm upon each respiratory cycle. **B**) pO_2 and SpO_2 ($sSpO_2$) sensor output and tongue SpO_2 ($tSpO_2$) during the respiratory maneuver. **C**) $sSpO_2$, pO_2 sensor output and $tSpO_2$ during a respiratory maneuver with heart rate adaptation via the CPG. **D**) $sSpO_2$ output, venous SpO_2 ($vSpO_2$) levels and heart rate during exercise. **E**) Movement artefacts from SpO_2 sensor in awake state. Output of gas sensors in arbitrary unit. Testing in chronic AV block dog.

Heart rate adaptation based on SpO_2 sensor input

Input of the fast-responding SpO_2 sensor was coupled to the CPG device based on data from a former performed respiratory maneuver within the same animal. **Figure 4C** again shows the

reduced $tSpO_2$ levels upon the maneuver and the response of the SpO2 and pO_2 sensors. The CPG output is presented by the black line and shows a certain increase in pacing output (from 64 to 72 bpm). This, upon the reducing $sSpO_2$ sensor input during the respiratory maneuver, which shows the adaptation possibilities of the CPG based on physiological input.

Sensor response in awake state

For evaluation of the sensors under more physiological circumstances than anesthesia, sensors were tested in awake state during rest and exercise (**Figure 4D**). Exercise was induced by a running protocol on a treadmill for 10 minutes and sensor output was obtained based on telemetry. Upon exercise, heart rate increased from 38 ± 6 bpm to 59 ± 3 bpm and venous blood SpO_2 ($vSpO_2$) levels reduced from 65 ± 14% to 44 ± 13% (n=3 experiments). The output of the SpO_2 sensor contained significantly more noise than during anesthesia which was further confirmed by the simple movement versus standing still recording (**Figure 4E**). While the wireless connection of the sensors was successfully over 15 days after implantation, sensor testing (with a focus on reducing artifacts and noise levels) upon exercise needs further optimization.

Discussion

The chronic AV block dog was involved in the CResPace project as a preclinical model to test the different components of the new developed cardiorespiratory device. As input for developing the cardiac and respiratory CPG, multiple cardiorespiratory tracings were shared, and an exercise model was created. Next, dummy sensors were successfully implanted for several weeks without signs of infection. Moreover, evaluation of dummy and final versions of the new developed sensors under several conditions resulted in demonstration of SpO_2 and pO_2 sensor response upon respiratory maneuvers. Finally, coupling of the SpO_2 sensor output to the CPG resulted in heart rate adaptation under anesthesia.

The AV block dog as preclinical model in CResPace – a future role

Testing circumstances of new cardiac devices often include anesthetic conditions as a first approach, even though awake and exercising conditions better represent the physiological situation as incorporated in the current study. For the first time in history of the standardized AV block dog model, an exercise protocol at different stages of cardiac remodeling (limited to

completed) was validated. It was suggested that dogs with limited cardiac remodeling after AV block and their reduced exercise tolerance would benefit most from new cardiac device properties - such as the CResPace device - by improving cardiac function and thereby exercise tolerance.[24] With regards to reinstating respiratory sinus arrhythmia in order to improve cardiac function, chronic pacing on each respiratory cycle – increased rate upon inspiration and decreased rate upon exhalation – for several weeks in the chronic AV block dog can show the benefits of the CResPace device when compared to monotonic pacing. It is expected that these results will partly confirm the former reported study outcome by Shanks and colleagues,[14] but will also gain further insight as the dog as preclinical model has significant presence of RSA and a moderate resemblance of its electrophysiology to that of a human. At an innovative level, yet outside of the current study scope, demonstration of the cardiorespiratory benefits by incorporation of multiple physiological sensors in combination with the self-adapting CPG device needs to be pursued further.

CResPace: a translational perspective

Where loss of RSA is a hallmark for cardiorespiratory disease,[10] reinstating RSA in the form of pacing on respiration should be the focus of implementation improvements in current pacing treatments. RSA is a physiological phenomenon with beneficial effects after all. The development of hardware CPGs based on realistic neuronal networks is preferred over digital electronics for rhythm regulation.[15] The study and implementation of biological CPGs in the field of bioelectric medicine perfectly fits into the currently popular field of artificial intelligence which will certainly further evolve in the upcoming decade. Current patients with HF and cardiorespiratory comorbidities can benefit from cardiac resynchronization therapy, yet a significant portion belongs to non-responders and further improvements are suggested.[28] The disadvantages of chronic pacing in a contemporary rhythm including adverse cardiac remodeling[29] can be minimalized when pacing the heart chambers individually based on self-adaptation in an RSA rhythm. Improvement of the cardiac function with 20% after reintroducing RSA in a large animal model[14] is clinically relevant and promising in order to improve patients experiences of their daily life routine. Still, awareness for sex differences is also important in this research field due to differences in autonomic function.[30]

Conclusion

A database with cardiorespiratory signals from healthy and AV block dogs resulted in modeling and validation of the cardiac and respiratory CPG, and corresponding joined publications. The AV block dog model was prepared under anesthetic and exercising conditions in order to fulfill a role in the development of the CResPace device by sensor evaluation and demonstration of device adaptation. The final version of this device will be beneficial for patients with heart failure and its cardiorespiratory comorbidities.

Acknowledgement

The authors thank dr. Tim Takken (Child Development and Exercise Center, Wilhelmina Children's Hospital, UMC Utrecht, The Netherlands) for provision of the Hexoskin shirt. This study, as part of the CResPace consortium, has received funding from the European Union's Horizon 2020 research and innovation programme under grant number 732170.

References

1. Tsao CW, Lyass A, Enserro D, et al. Temporal trends in the incidence of and mortality associated with heart failure with preserved and reduced ejection fraction. *JACC Heart Fail.* 2018;6(8):678-685.
2. Roger VL. Epidemiology of heart failure: a contemporary perspective. *Circ Res.* 2021;128(10):1421-1434.
3. Bavishi A, Patel RB. Addressing Comorbidities in heart failure: hypertension, atrial fibrillation, and diabetes. *Heart Fail Clin.* 2020;16(4):441-456.
4. Cittadini A, Bossone E, Ventura HO. Emerging comorbidities in heart Failure. *Cardiol Clin.* 2022;40(2):xi-xiv.
5. Starr I, Friedland CK. On the cause of the respiratory variation of the ballistocardiogram, with a note on sinus arrhythmia. *J Clin Invest.* 1946;25(1):53-64.
6. Hayano J, Yasuma F, Okada A, Mukai S, Fujinami T. Respiratory sinus arrhythmia. A phenomenon improving pulmonary gas exchange and circulatory efficiency. *Circulation.* 1996;94(4):842-847.
7. Ben-Tal A, Shamailov SS, Paton JF. Evaluating the physiological significance of respiratory sinus arrhythmia: looking beyond ventilation-perfusion efficiency. *J Physiol.* 2012;590(8):1989-2008.
8. Hrushesky WJ, Fader D, Schmitt O, Gilbertsen V. The respiratory sinus arrhythmia: a measure of cardiac age. *Science.* 1984;224(4652):1001-1004.
9. Abreu RM, Porta A, Rehder-Santos P, et al. Cardiorespiratory coupling strength in athletes and non-athletes. *Respir Physiol Neurobiol.* 2022;305:103943.
10. De Jong MJ, Randall DC. Heart rate variability analysis in the assessment of autonomic function in heart failure. *J Cardiovasc Nurs.* 2005;20(3):186-195; quiz 196-187.
11. Reis MS, Deus AP, Simoes RP, Aniceto IA, Catai AM, Borghi-Silva A. Autonomic control of heart rate in patients with chronic cardiorespiratory disease and in healthy participants at rest and during a respiratory sinus arrhythmia maneuver. *Rev Bras Fisioter.* 2010;14(2):106-113.
12. Nogaret A, Zhao L, Moraes DJ, Paton JF. Modulation of respiratory sinus arrhythmia in rats with central pattern generator hardware. *J Neurosci Methods.* 2013;212(1):124-132.
13. O'Callaghan EL, Chauhan AS, Zhao L, et al. Utility of a novel biofeedback device for within-breath

modulation of heart rate in rats: A quantitative comparison of vagus nerve vs. right atrial pacing. *Front Physiol.* 2016;7:27.

14. Shanks J, Abukar Y, Lever NA, et al. Reverse re-modelling chronic heart failure by reinstating heart rate variability. *Basic Res Cardiol.* 2022;117(1):4.
15. Nogaret A, O'Callaghan EL, Lataro RM, et al. Silicon central pattern generators for cardiac diseases. *J Physiol.* 2015;593(4):763-774.
16. CResPace Grant Agreement, number 732170. *European Commission H2020-FETPROACT*2016.
17. Smith JC, Abdala AP, Koizumi H, Rybak IA, Paton JF. Spatial and functional architecture of the mammalian brain stem respiratory network: a hierarchy of three oscillatory mechanisms. *J Neurophysiol.* 2007;98(6):3370-3387.
18. Loen V, Vos MA, Van der Heyden MAG. The canine chronic atrioventricular block model in cardiovascular preclinical drug research. *Br J Pharmacol.* 2022;179(5):859-881.
19. Hamlin RL, Smith CR, Smetzer DL. Sinus arrhythmia in the dog. *Am J Physiol.* 1966;210(2):321-328.
20. Oros A, Beekman JD, Vos MA. The canine model with chronic, complete atrio-ventricular block. *Pharmacol Ther.* 2008;119(2):168-178.
21. Smoczyńska A, Loen V, Aranda A, Beekman HDM, Meine M, Vos MA. High-rate pacing guided by short-term variability of repolarization prevents imminent ventricular arrhythmias automatically by an implantable cardioverter-defibrillator in the chronic atrioventricular block dog model. *Heart Rhythm.* 2020;17(12):2078-2085.
22. Percie du Sert N, Ahluwalia A, Alam S, et al. Reporting animal research: Explanation and elaboration for the ARRIVE guidelines 2.0. *PLoS Biol.* 2020;18(7):e3000411.
23. Timmermans C, Rodriguez LM, Van Suylen RJ, et al. Catheter-based cryoablation produces permanent bidirectional cavotricuspid isthmus conduction block in dogs. *J Interv Card Electrophysiol.* 2002;7(2):149-155.
24. Van Bavel JJA, Beekman HDM, Schot A, et al. Remodeling in the AV block dog is essential for tolerating moderate treadmill activity. *Int J Cardiol Heart Vasc.* 2023;44:101169.
25. Abu-Hassan KJ, Taylor, J.D., Van Bavel, J.J.A., Vos, M.A., and Nogaret, A. Silicon central pattern generator model of cardiac contraction behavior. 2020 11th Conference of the European Study Group on Cardiovascular Oscillations; 2020.
26. Taylor JD, Abu Hassan, K.J., Van Bavel, J.J.A., Vos, M.A., & Nogaret, A. Robust design of inhibitory neuronal networks displaying rhythmic activity. Perspectives in Dynamical Systems III: Control and Stability. DSTA 2019, Springer Proceedings in Mathematics & Statistics; 2021; Cham, Switzerland.
27. Krause R, Van Bavel JJA, Wu C, Vos MA, Nogaret A, Indiveri G. Robust neuromorphic coupled oscillators for adaptive pacemakers. *Sci Rep.* 2021;11(1):18073.
28. Katbeh A, Van Camp G, Barbato E, et al. Cardiac resynchronization therapy optimization: A comprehensive approach. *Cardiology.* 2019;142(2):116-128.
29. Tops LF, Schalij MJ, Bax JJ. The effects of right ventricular apical pacing on ventricular function and dyssynchrony implications for therapy. *J Am Coll Cardiol.* 2009;54(9):764-776.
30. Arshi B, Geurts S, Tilly MJ, et al. Heart rate variability is associated with left ventricular systolic, diastolic function and incident heart failure in the general population. *BMC Med.* 2022;20(1):91.

10

General discussion

Joanne J.A. van Bavel

Cardiovascular disease is the leading cause of mortality worldwide and sudden cardiac death is in most cases related to the occurrence of severe ventricular arrhythmias.[1,2] Arrhythmogenesis with its substrates, triggers, and underlying electrophysiological mechanisms is a complex process and optimization of (patient-specific) prevention of ventricular arrhythmia occurrence requires continuous research. Arrhythmia management in the field of cardiovascular research focusses on the discovery of new pharmacological targets, the evaluation of pro- and antiarrhythmic drug effects, and the development and improvement of cardiac device features. The canine heart shares a moderate resemblance in cardiac electrophysiology with that of the human. The remodeled heart of the anesthetized chronic atrioventricular block (CAVB) dog is sensitive to Torsade de Pointes (TdP) arrhythmias[3] and is therefore standardized for testing 1) proarrhythmic and antiarrhythmic effects of drugs, and 2) testing new device properties as antiarrhythmic strategy. Both elements are incorporated in this thesis to explore targeting of PI3K and I_{Ks} in the CAVB dog model, and to prepare and use the model for testing the CResPace device.

Drug testing and its insight into proarrhythmic mechanisms

Autophagy proteins as therapeutic target and their link to antiarrhythmic drugs have gained limited attention thus far. A cardiac view on autophagy is therefore described in **Chapter 2.** Targeting autophagy acts protective for e.g., cell growth and survival and seems therefore crucial for cardiomyocytes in ischemic and hypertrophic conditions.[4,5] Moreover, autophagy-related proteins are an interesting target in cancer treatment[6] with the original purpose to affect solely these. Though, targeting of the proteins in, for example, the PI3K pathway seems to affect the cardiac action potential with a potential risk for cardiac arrhythmias.[7]

Omipalisib is one of the compounds that targets the PI3K pathway by inhibition of both PI3K and mTOR[8] and is currently in phase I clinical trials with the potential to treat a variety of cancer types.[9] We evaluated the potential proarrhythmic risk of drug-induced PI3K inhibition by chronic treatment of omipalisib in the AV block dog model, presented in **Chapter 3.** One component of the AV block-induced remodeling includes a downregulation of repolarizing currents I_{Ks} and I_{Kr} resulting in repolarization prolongation.[10] In our study, after AV block induction, the ventricular rate in sinus rhythm was maintained in the form of pacing at VDD mode, to replace AV block-induced electrical remodeling by omipalisib-induced electrical

remodeling. Twice-daily dosing of omipalisib prolonged repolarization duration, already at baseline and further with dofetilide, and mildly enhanced the proarrhythmic outcome (**Table 1**). In essence, the effectiveness of anticancer treatment should outweigh the proarrhythmic risk induced by the PI3K inhibiting compounds. Over the last decade, the cardio-oncology field has emerged and communication crossing both cardiology and oncology disciplines is crucial for optimizing clinical practice.[11]

On a cellular level, isolated cardiomyocytes treated with PI3K inhibitors showed reduced I_{Ks} and I_{Kr} currents.[12] We found diminished repolarizing current density for I_{Ks} in cardiomyocytes isolated from the omipalisib-treated animals which thus in part reflects AV block-induced electrical remodeling. Though, the induction of TdP arrhythmias is certainly successful by inhibiting the main repolarizing current I_{Kr},[3] and I_{Ks} as second main potassium current is less dominant in prolonging the action potential and often demands an additional trigger such as exercise for arrhythmia induction when impaired.[13,14] Targeting of the repolarizing potassium currents and thereby challenging the repolarization reserve is of high interest when reflecting a clinical setting of the most common type of long QT syndrome: type 1 (*KCNQ1* mutations, impaired I_{Ks}).[15] Therefore, in **Chapter 4**, the repolarization and proarrhythmic outcome after repolarization reserve disturbance by I_{Ks} inhibitor JNJ303 was evaluated in the CAVB dog model. Inhibition of the remaining I_{Ks}, after its impairment upon AV block and the anesthetic regime, affects cardiac repolarization by prolongation of the QT interval and initiation of ectopic beats (**Table 1**). Though, perpetuation of ectopic beats into more severe arrhythmic events demands an additional trigger, here facilitated by enhanced contractility (by ouabain) or ending of the anesthetic regime. This further supports clinical findings, where LQT1 patients under enhanced sympathetic conditions, mostly upon exercise, are of high arrhythmic risk.[14] The opposite concept; activation of I_{Ks} by ML277 is described in **Chapter 5**. A mild antiarrhythmic effect was found in terms of delaying dofetilide-induced repolarization prolongation and a reduction in arrhythmic events. Though, activation of I_{Ks} by ML277 had a temporary effect and was unable to completely prevent dofetilide-induced TdP arrhythmias (**Table 1**). Both I_{Ks} and I_{Kr} are crucial in maintaining a stable repolarization. In the CAVB dog, targeting of I_{Kr} by dofetilide in anesthetic conditions has a drastic proarrhythmic outcome, while I_{Ks} inhibition demands an additional trigger.

A further analysis on proarrhythmic characteristics of the CAVB dog model is presented in **Chapter 6**. Our database with previously performed induction experiments using dofetilide was explored to unravel unpublished characteristics of the CAVB dog to get more insight into why 75% of the animals are inducible for TdP arrhythmias and the other quarter is not. Inducible dogs showed a TdP incidence of 100%, while non-inducible dogs with ≤2 TdP episodes presented a TdP incidence of 18% (**Table 1**). It was found that sex, time of the experiment, and heart weight were not related to TdP inducibility. Though, TdP inducibility was indicated by enhanced repolarization duration and LVdP/dt_{max} in inducible dogs at baseline (**Table 1**). Short term variability (STV), quantifying temporal dispersion of repolarization and associated with TdP arrhythmia occurrence, did not distinguish inducible from non-inducible dogs in our study (**Table 1**). A role for 1) sensitivity in STV analysis and 2) spatial dispersion of repolarization dependent perpetuation of TdP arrhythmias was raised.[16,17]

Table 1. Overview of the discussed drug testing studies in the AV block dog model.

	Omipalisib (*3*)	**JNJ303** (*4*)	**ML277** (*5*)	**Inducible** (*6*)	**Non-inducible** (*6*)
Details	PI3K inhibitor	I_{Ks} inhibitor	I_{Ks} activator	CAVB	CAVB
QTc	↑	↑	=	↑	=,↑
STV	=	↑	=	=	=
LVdP/dt_{max}	=	↑	ND	↑	=,↑
Arrhythmias	EB 20%	EB 100%	None	None	None
Trigger	Dofetilide	Ouabain	Dofetilide	Dofetilide	Dofetilide
QTc	↑↑	↓	↑↑	↑↑	↑↑
STV	↑↑	ND	↑	↑↑	↑↑
LVdP/dt_{max}	↑	↑↑↑	ND	↑↑	↑↑
Arrhythmias	TdP 20%	TdP 67%	TdP 100%	TdP 100%	TdP 18%

Numbers in brackets behind drugs, inducible and non-inducible refer to thesis chapters. QTc interval and STV in ms, LVdP/dtmax in mmHg/s. EB: ectopic beats, TdP: Torsade de Pointes arrhythmias. Symbols refer to increase (↑), decreased (↓), unchanged (=), or not determined (ND).

Apparent variations in the drug testing approaches result in the evaluation of different parameters predicting and presenting arrhythmic outcome (**Table 1**). Here, new insights show a more dominant role for certain parameters already at baseline and thus before addition of proarrhythmic trigger dofetilide. Altogether, a complex interplay between underlying substrates, triggers and electrophysiological mechanisms certainly creates the ultimate

condition for initiation and perpetuation of severe arrhythmias. In that matter, a chance for 'grey' pro- and antiarrhythmic outcomes is undeniably there.

Preparing a preclinical arrhythmia model for complex device testing

The development of device properties has expanded over the last decades in parallel with the ageing population, increasing life expectancy, and certainly the rise in possibilities among computational technology and the use of digital devices.[18] This is accompanied with a rise in challenges and dilemmas such as selection of device type, lead replacement, and time-dependent cardiac remodeling upon chronic pacing. The focus currently lies on the optimization and individualization of the pacing strategies. One example here is a complex cardiac device with adaptive electronics based on sensors providing physiological input in order to adapt beat-to-beat regulation.[19] To date, testing of device properties was performed in the anesthetized CAVB dog model. We prepared the AV block dog model in conditions of physical exercise of which the results are presented in **Chapter 7**. Exercise tolerance and corresponding physiological parameters were determined in dogs at sinus rhythm, and at two days (AVB2d, limited cardiac remodeling), three weeks (CAVB3) and six weeks (CAVB6, completed remodeling) after AV block. Furthermore, we validated the PhysioFlow® technique with echocardiography and ventricular pressure measurements to non-invasively determine cardiac output at rest and exercise. Exercising dogs after AV block were unable to maintain the cardiac output despite the increase in atrial and ventricular rate and stroke volume. More interestingly, 50% of the dogs with limited remodeling at AVB2d were unable to complete the exercise protocol, and showed signs of hypoxemia and acidification, and more arrhythmic events. The dogs with a higher stroke volume and ventricular rate – resulting in a higher cardiac output – were able to complete the exercise protocol. As discussed earlier, a common additional trigger for arrhythmias with I_{Ks} impairment in the background includes sympathetic activation such as exercise. Indeed, exercising dogs with limited remodeling at AVB2d, yet significant electrical remodeling in the first week after AV block, showed increased proarrhythmic effects. In the succeeding weeks, stabilization of the ectopic origin and cardiac remodeling at other levels apparently reduced the arrhythmic outcome. We suggest AVB2d as experimental timepoint to examine the beneficial effects in device testing. Moreover, AV block- and drug-induced impairment of I_{Ks} as model of LQT1 with exercise as additional trigger

can be of interesting therapeutic value for a LQT1 patient in a daily-life situation with increased arrhythmic risk.

Besides conditions of physical exercise, a principal component of biofeedback in cardiac rhythm regulation is the respiratory cycle at rest. Fluctuations in heart rate are reduced in patients with heart failure and other respiratory diseases.[20] This physiological phenomenon of fluctuations in heart rate upon respiration is called respiratory sinus arrhythmia (RSA) and cardiac beneficial effects are suggested when clinically reinstating RSA.[21,22] The aim of the study in **Chapter 8** was to examine RSA in the AV block dog model. Variability in atrial and ventricular rate was severely impaired after AV block, and the reduction was predominantly present in ventricular rate. It implies a valuable role of the AV block dog model in reestablishing RSA via cardiac pacing using an electrical biofeedback device. Reversed remodeling by reinstating RSA was found in a preclinical heart failure model, [22] and further evaluation of this in a preclinical model sensitive to cardiac arrhythmias with impaired RSA is of interest.

The two preceding studies were part of the CResPace consortium in order to prepare the AV block dog model for device testing. The aim was to develop a biofeedback device with the ability to adapt to changes in physiological variables using input from sensors. An overview of the consortium plan and experimental results are presented in **Chapter 9**. A database of cardiorespiratory signals from dogs was setup and used for development of the bioelectronics. Next, dummy and working SpO_2, pO_2 and blood pressure sensors were evaluated in dogs under anesthesia and awake conditions. We were able to detect pacing adaptation during changes in SpO_2 levels upon a respiratory maneuver used as input for the CResPace device in a dog under anesthesia. The AV block dog with impaired RSA was adjusted for device testing by including exercising conditions. Though, the sensors and bioelectronics demand further optimization to show the beneficial effects upon chronic implantation and physical challenges such as exercise.

Concluding remarks and future perspective

The AV block dog is a valuable model in drug and device testing because it contains the ability to target AV block-induced remodeling timepoints, anesthetic vs. awake (resting and

exercising) conditions, and evaluation at baseline and upon proarrhythmic triggers in serial conditions. Valid limitations of the CAVB dog model are in the scope of the required expertise, challenges in societal acceptance, high costs, and conflicts of interest when cooperating with industry.[23] It is of high interest and value to further optimize alternative methods for animal testing, yet, for now the AV block dog model closely approaches clinical proarrhythmic conditions and led us to a diverse insight into arrhythmia initiation and perpetuation, and clinical prevention. The AV block dog model in conditions of physical activity combined with a pharmacological block of I_{Ks} would be a next and relevant step in approaching the electrophysiological translation to the clinic. In general, the scope of research will further focus on precision medicine by targeting a specific subgroup of patients instead of a 'one drug fits all' approach in which we can no longer ignore the role of artificial intelligence (AI).[24] Current examples are 4D-printing of biomedical devices,[25] use of AI in ECG analyses,[26] and incorporation of artificial neurons in a pacemaker[19] as the CResPace device. Patient-specific treatment based on AI algorithms using real-time data from a single implanted device has become a realistic approach for the future.

References

1. World Health Organization. The top 10 causes of death. 2020; https://www.who.int/news-room/fact-sheets/detail/the-top-10-causes-of-death.
2. Goldberger JJ, Buxton AE, Cain M, et al. Risk stratification for arrhythmic sudden cardiac death: identifying the roadblocks. *Circulation.* 2011;123(21):2423-2430.
3. Oros A, Beekman JD, Vos MA. The canine model with chronic, complete atrio-ventricular block. *Pharmacol Ther.* 2008;119(2):168-178.
4. Sciarretta S, Yee D, Shenoy V, Nagarajan N, Sadoshima J. The importance of autophagy in cardioprotection. *High Blood Press Cardiovasc Prev.* 2014;21(1):21-28.
5. Li Y, Chen C, Yao F, et al. AMPK inhibits cardiac hypertrophy by promoting autophagy via mTORC1. *Arch Biochem Biophys.* 2014;558:79-86.
6. Onorati AV, Dyczynski M, Ojha R, Amaravadi RK. Targeting autophagy in cancer. *Cancer.* 2018;124(16):3307-3318.
7. Ballou LM, Lin RZ, Cohen IS. Control of cardiac repolarization by phosphoinositide 3-kinase signaling to ion channels. *Circ Res.* 2015;116(1):127-137.
8. Knight SD, Adams ND, Burgess JL, et al. Discovery of GSK2126458, a highly potent inhibitor of PI3K and the mammalian target of rapamycin. *ACS Med Chem Lett.* 2010;1(1):39-43.
9. Munster P, Aggarwal R, Hong D, et al. First-in-human phase I study of GSK2126458, an oral pan-class I phosphatidylinositol-3-kinase inhibitor, in patients with advanced solid tumor malignancies. *Clin Cancer Res.* 2016;22(8):1932-1939.
10. Volders PG, Sipido KR, Vos MA, et al. Downregulation of delayed rectifier K(+) currents in dogs with chronic complete atrioventricular block and acquired torsades de pointes. *Circulation.* 1999;100(24):2455-2461.
11. Alvarez-Cardona JA, Ray J, Carver J, et al. Cardio-Oncology Education and Training: JACC Council

Perspectives. *J Am Coll Cardiol.* 2020;76(19):2267-2281.
12. Lu Z, Wu CY, Jiang YP, et al. Suppression of phosphoinositide 3-kinase signaling and alteration of multiple ion currents in drug-induced long QT syndrome. *Sci Transl Med.* 2012;4(131):131ra150.
13. Volders PG, Stengl M, van Opstal JM, et al. Probing the contribution of IKs to canine ventricular repolarization: key role for beta-adrenergic receptor stimulation. *Circulation.* 2003;107(21):2753-2760.
14. Schwartz PJ, Priori SG, Spazzolini C, et al. Genotype-phenotype correlation in the long-QT syndrome: gene-specific triggers for life-threatening arrhythmias. *Circulation.* 2001;103(1):89-95.
15. Krahn AD, Laksman Z, Sy RW, et al. Congenital Long QT Syndrome. *JACC Clin Electrophysiol.* 2022;8(5):687-706.
16. Dunnink A, Stams TRG, Bossu A, et al. Torsade de pointes arrhythmias arise at the site of maximal heterogeneity of repolarization in the chronic complete atrioventricular block dog. *Europace.* 2017;19(5):858-865.
17. Smoczynska A, Aarnink EW, Dunnink A, et al. Interplay between temporal and spatial dispersion of repolarization in the initiation and perpetuation of torsades de pointes in the chronic atrioventricular block dog. *Am J Physiol Heart Circ Physiol.* 2021;321(3):H569-H576.
18. Bradshaw PJ, Stobie P, Knuiman MW, Briffa TG, Hobbs MS. Trends in the incidence and prevalence of cardiac pacemaker insertions in an ageing population. *Open Heart.* 2014;1(1):e000177.
19. Nogaret A, O'Callaghan EL, Lataro RM, et al. Silicon central pattern generators for cardiac diseases. *J Physiol.* 2015;593(4):763-774.
20. Reis MS, Deus AP, Simoes RP, Aniceto IA, Catai AM, Borghi-Silva A. Autonomic control of heart rate in patients with chronic cardiorespiratory disease and in healthy participants at rest and during a respiratory sinus arrhythmia maneuver. *Rev Bras Fisioter.* 2010;14(2):106-113.
21. O'Callaghan EL, Lataro RM, Roloff EL, et al. Enhancing respiratory sinus arrhythmia increases cardiac output in rats with left ventricular dysfunction. *J Physiol.* 2020;598(3):455-471.
22. Shanks J, Abukar Y, Lever NA, et al. Reverse re-modelling chronic heart failure by reinstating heart rate variability. *Basic Res Cardiol.* 2022;117(1):4.
23. Loen V, Vos MA, van der Heyden MAG. The canine chronic atrioventricular block model in cardiovascular preclinical drug research. *Br J Pharmacol.* 2022;179(5):859-881.
24. Johnson KW, Torres Soto J, Glicksberg BS, et al. Artificial intelligence in cardiology. *J Am Coll Cardiol.* 2018;71(23):2668-2679.
25. Faruque O, Lee Y, Wyckoff GJ, Lee CH. Application of 4D printing and AI to cardiovascular devices. *Journal of Drug Delivery Science and Technology.* 2023;80:104162.
26. Attia ZI, Harmon DM, Behr ER, Friedman PA. Application of artificial intelligence to the electrocardiogram. *Eur Heart J.* 2021;42(46):4717-4730.

Appendix

Samenvatting in het Nederlands

Hartritme en stoornissen

De samentrekking en ontspanning van de hartkamers verlopen in een gelijkmatig ritme. Veranderingen in de elektriciteit in hartcellen leiden tot de vorming van een actiepotentiaal, die door het verloop over de hartkamers resulteert in het hartritme en de samentrekking van het spierweefsel. De actiepotentiaal ontstaat door veranderingen in stromen welke veroorzaakt worden door beweging van verschillende ionen, zoals natrium, calcium en kalium door specifieke kanalen. Dit zorgt voor de verschillende fases van de actiepotentiaal: een samentrekking (depolarisatie) en ontspanning (repolarisatie) van de hartcellen. De snelle instroom van natrium leidt tot de depolarisatie. Daarna volgt een kleine repolarisatie door de verminderde natrium stroom en opening van kalium kanalen, en een plateau fase door de instroom van calcium ionen en een balans met de kalium stroom. Tenslotte zijn de kalium stromen (I_{Kr} en I_{Ks}) verantwoordelijk voor de repolarisatie fase. De complete som van alle elektrische activiteit over het hart wordt weergegeven op het elektrocardiogram (ECG).

Verstoringen in de elektrische geleiding in het hart kunnen leiden tot verschillende ritmestoornissen, waarvan fibrilleren van de onderste kamers (ventrikels) de meest ernstige vorm is door het stilvallen van de bloedstroom. Plotse hartdood leidt nog steeds tot een hoog aantal sterfgevallen wereldwijd en 50-70% hiervan is gerelateerd aan ernstige ventrikelritmestoornissen. Het onderliggende proces van het ontstaan en de voortgang van ritmestoornissen is complex. Een combinatie van verschillende zogenoemde substraten, triggers en onderliggende elektrofysiologische mechanismen liggen hieraan ten grondslag. Een hogere leeftijd, familiegeschiedenis, leefstijl (dieet, roken, alcohol inname, te weinig lichaamsbeweging), medicijngebruik en andere ziekten zoals nierfalen, longproblemen en slaapapneu, kunnen het risico op hartritmestoornissen vergroten. Vervolgens kunnen onderliggende verstoringen in het elektrisch systeem een extra hartslag veroorzaken. Bij een combinatie van eerder genoemde condities kan dit leiden tot een initiatie en verder verloop van de ritmestoornis. Ingrijpen op het ontstaan of beëindigen van een ritmestoornis kan door middel van medicatie en de implantatie van een hartapparaat, zoals een pacemaker of implanteerbaar cardioverter defibrillator (ICD).

De focus van onderzoek naar hartritmestoornissen ligt op het ontdekken van farmacologische aangrijpingspunten, de ontwikkeling van nieuwe medicatie en de verbetering van hartapparaten. Hiervoor wordt gebruik gemaakt van computermodellen, celmodellen, kleine en grote proefdieren en mensen in zieke en gezonde condities. Er worden steeds betere alternatieven voor proefdieren ontwikkeld om dierproeven te verminderen en te voorkomen. Toch bezitten de huidige alternatieven cruciale gebreken en is het onrealistisch om op dit moment compleet afstand te doen van dierproeven. Een grondige beredenering over het gebruik van het type diermodel met de hoogste betekenis voor de patiënt is van groot belang.

Preklinisch model gevoelig voor hartritmestoornissen

Op elektrofysiologisch vlak toont het hart van de hond veel gelijkenissen met die van de mens. Daarom wordt het gebruik van dit dier in elektrofysiologisch onderzoek naar medicatie benoemd in de ICH S7B richtlijnen. Onder normale omstandigheden in sinusritme (**Figuur 1A**) verloopt de elektrische geleiding door beide bovenste kamers (atria) en vervolgens via het tussenschot door de beide ventrikels. Middels het maken van een blokkade in de elektrische geleidingen tussen de atria en de ventrikels ontstaat er een atrioventriculaire (AV) blok in het hondenhart. Dit resulteert in de vorming van een nieuw en laag ritme (**Figuur 1B**) in de ventrikels dat leidt tot een sterke vermindering van de hoeveelheid bloed dat per minuut wordt rondgepompt. Hierdoor gaat het hart zich op verschillende vlakken aanpassen (remodeleren) aan de nieuwe situatie: de samentrekking wordt krachtiger, de hartspier wordt dikker en de duur van de repolarisatie verlengt. Dit model wordt het chronisch AV blok (CAVB) hondenmodel genoemd. Door het remodeleren is het hondenhart onder anesthesie vatbaar voor ernstige ritmestoornissen: Torsade de Pointes ritmestoornissen. Zoals de naam zegt, worden deze gekenmerkt door het draaien van de toppen rondom de middenlijn op het ECG (**Figuur 1C**). Deze ritmestoornissen kunnen onder gestandaardiseerde omstandigheden met een medicament worden opgewekt.

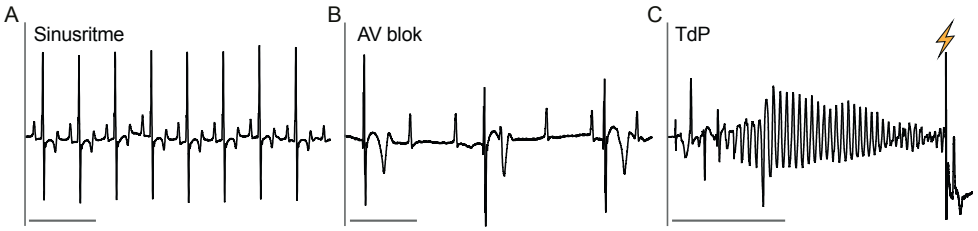

Figuur 1. ECG lead II signalen representatief voor honden in **A**) sinusritme, **B**) atrioventriculair (AV) blok, en **C**) Torsade de Pointes (TdP) ritmestoornis beëindigd door defibrillatie, weergegeven door het schok symbool. Schaal horizontale lijnen: 1 seconde voor panelen A en B, en 5 seconde voor paneel C.

Doel van het onderzoek

Het testen van zowel medicijnen als een nieuw hartapparaat ligt centraal in deze thesis (**Figuur 2**) met als overkoepelend doel om de huidige behandelstrategieën van hartritmestoornissen te optimaliseren.

Deel I: medicijn testen start met het bespreken van de rol van een biologische route in hartritmestoornissen en de effecten van medicatie daarop (**hoofdstuk 2)**. Het gaat hier om het biologische proces autofagie wat zorgt voor de afbraak van afvalmateriaal in cellen. Inzichten in het effect van zowel antiaritmische medicatie (medicatie tegen hartritmestoornissen) als andere medicatie op de remming en activatie van autofagie wordt steeds meer beschreven. Dit suggereert dat autofagie meer erkenning moet krijgen in toekomstig onderzoek naar de (neven)effecten van medicatie. Een voorbeeld hiervan is de PI3K route die naast autofagie ook een belangrijke rol speelt in celgroei en celdeling. Hiermee is deze route ook een aantrekkelijk aangrijpingspunt in therapieën tegen kanker. Toch is er bewijs gevonden dat remming van deze route effect kan hebben op ion kanalen in hartcellen. Daarom is het pro-aritmische effect van PI3K remmer omipalisib getest in de CAVB hond (**hoofdstuk 3**). Chronische behandeling leidde tot een verlenging van de repolarisatie duur en een milde aanwezigheid van hartritmestoornissen. Daarnaast lieten de hartcellen een verminderde activatie van repolarisatiestroom I_{Ks} zien. Voor de studie van **hoofdstuk 4** is het pro-aritmische effect van I_{Ks} remmer JNJ303 getest. Korte behandeling in de CAVB hond leidde ook tot een verlenging van de repolarisatie duur en een milde aanwezigheid van hartritmestoornissen. Ernstigere ritmestoornissen konden worden opgewekt na het verhogen van de samentrekking van het hart. Een tegenovergestelde benadering is beschreven in

hoofdstuk 5, namelijk het activeren van I_{Ks} door ML277. Dit medicament kon tijdelijk het optreden van ritmestoornissen voorkomen als deze werden opgewekt in het CAVB hondenmodel. Een verdere analyse van pro-aritmische kenmerken van het CAVB hond model is beschreven in **hoofdstuk 6**. Honden die vatbaarder zijn voor ritmestoornissen laten een verlengde repolarisatie duur en verhoogde samentrekking van het linker ventrikel zien. Deze studies geven meer inzicht in de rol van autofagie/PI3K en I_{Ks} onder pro-aritmische opstandigheden. Dit betreft veel voorkomende klinische situaties gezien de hoge frequentie van kankerbehandeling, medicatiegebruik en genetische afwijkingen.

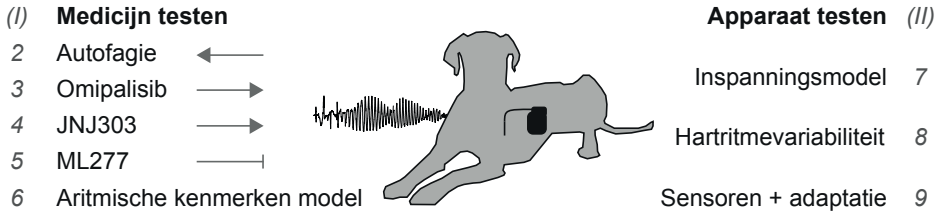

Figuur 2. Overzicht van de hoofdstukken in dit proefschrift, opgedeeld in deel *I*: Medicijn testen en deel *II*: Apparaat testen.

Deel II: apparaat testen gaat over het voorbereiden van het CAVB hondenmodel op het testen van een verder ontwikkeld hartapparaat (sensor-gestuurde pacemaker). Om deze te testen onder dagelijkse omstandigheden met verhoogde fysieke activiteit is er een inspanningsmodel opgezet (**hoofdstuk 7**). Daarnaast zijn de inspanningstolerantie en bijbehorende parameters vastgesteld op verschillende tijdspunten na het maken van AV blok. Hieruit werd geconcludeerd dat voor toekomstige experimenten het voordelige effect van de nieuwe pacemaker het best kan worden aangetoond als er nog weinig remodelering van het hart heeft plaatsgevonden na AV blok. Een andere functie van de nieuwe pacemaker is het terugbrengen van hartritmevariabiliteit door het hartritme aan te passen op de ademhaling. In de gezonde situatie is het hartritme hoger tijdens inademing en lager tijdens uitademing. Deze variatie in hartritme is sterk verminderd bij mensen met hartfalen. Analyses van de hartritmevariabiliteit laten zien dat zowel het ritme van de atria als het ritme van de ventrikels een sterk verminderde variatie laten zien na AV blok (**hoofdstuk 8**). Het CAVB hondenmodel is dus een interessant model voor het aantonen van het voordelige effect van het terugbrengen van hartritmevariabiliteit door de nieuwe pacemaker. De werking en functie van de nieuwe

pacemaker worden besproken in **hoofdstuk 9**. Informatie over zuurstof, bloeddruk en ademhaling gemeten door sensoren wordt in de pacemaker verwerkt en dit leidt tot een adaptatie van het hartritme. De werking en lange-termijn implantatie van de sensoren werd getest in de CAVB hond. Vervolgens is er aangetoond dat de pacemaker het hartritme kon aanpassen als de zuurstofwaarden in de hond onder narcose actief werden verlaagd. Deze nieuwe pacemaker zal na verdere optimalisatie een waardevolle therapie kunnen zijn voor patiënten met hartfalen, longziekten en slaapapneu.

Conclusie

Het testen van medicatie en hartapparaten is van groot belang voor de behandeling van hartritmestoornissen. Het CAVB hondenmodel is hiervoor gestandaardiseerd en is daarom een belangrijk preklinisch model in elektrofysiologisch onderzoek. De studies in dit proefschrift geven meer inzicht in de complexe combinatie van factoren in het opwekken en voorkomen van ritmestoornissen door met medicatie in te grijpen op een belangrijk cellulair proces en de repolarisatie stroom I_{Ks}. Facetten van de nieuw ontwikkelde pacemaker zijn getest in de CAVB hond en het apparaat zal na optimalisatie een waardevolle betekenis kunnen hebben voor mensen met hart- en longziekten.

Dankwoord

Wat heb ik hier lang naar uitgekeken: het schrijven van mijn dankwoord. Ik ben de afgelopen jaren op veel vlakken uitgedaagd en heb veel geleerd. Laat het overduidelijk zijn dat je ‘in je eentje’ een PhD niet kunt voltooien.

Prof. dr. Vos, **Marc**, jouw enthousiasme was zeer aanstekelijk toen je me vertelde over het onderwerp van dit PhD traject. Je gaf me het vertrouwen de experimentplanningen uit te voeren nadat ik die trots in de vorm van flowcharts aan je presenteerde. Zeer gedetailleerd spraken we over musicals en speciaal-bier-rijtjes en samen met Rian stelden jullie je huis beschikbaar voor de Marc-bbq’s die bijdroegen aan de fijne sfeer in de groep. Vanaf halverwege het traject heb ik veel zelfstandig kunnen invullen, waarvan ik veel heb geleerd. Je hebt een mooie onderzoekslijn op- en voortgezet waaraan ik trots heb mogen bijdragen.

Dr. Van der Heyden, **Marcel**, acht jaar geleden was jij de eerste die ik van de Medische Fysiologie mocht ontmoeten. Sindsdien was jij een stabiele factor, altijd aanwezig en bereikbaar, in voor een goed gesprek en een borrel, en bovenal enthousiast over onderzoek en onderwijs. Jij was er als ik zoekende was, je luisterde dan geduldig, zocht naar een oplossing en stelde twee vragen die niet vanzelfsprekend zijn: hoe gaat het met je en wat kan ik voor je doen? Heel terecht heb jij de titel PhD Supervisor of the year 2022 gewonnen. Wat was ik trots. Bedankt voor al jouw hulp.

Prof. dr. **Jeroen Bakkers**, dr. **Martin Pešl**, prof. dr. **Harold van Rijen**, prof. dr. **Daniela Salvatori** and prof. dr. **Dick Thijssen**, thank you for accepting being part of my assessment committee and for critically reading my thesis.

Mijn dank is groot aan de (oud) collega’s van de Medische Fysiologie: ‘een gesloten afdeling waar de deuren altijd open staan’. Het is een eer dat ik, zo bleek tijdens de introductie voor mijn Dutch Physiology Day praatje, onderdeel mocht worden van het MedFys meubilair.

Jet, aan woorden niet genoeg hoe groot mijn dank is voor alles wat je voor mij hebt gedaan. Vanaf dag één heb jij aan mijn zijde gestaan en een persoon zoals jij gun ik iedereen in het PhD traject. Door jouw ervaring, expertise en enthousiasme werden zorgen rondom experimenten van me afgenomen. Jij bezit de mooie eigenschap om op natuurlijke wijze te schakelen tussen het jezelf in dienststellen van een ander en de verantwoordelijkheid nemen. Ik heb onze samenwerking als natuurlijk en enorm prettig ervaren, want alles ging altijd op dezelfde manier, het was duidelijk en overal konden we wel een praktische oplossing voor vinden. 'Als het goed is, is het goed, hè?'. Naast het mogen delen van een enkele traan, hebben we heel veel gelachen. Nadat je met pensioen ging, heb ik je het afgelopen jaar uiteraard erg gemist op de afdeling. Heel fijn dat we elkaar, ook met Esther erbij, zijn blijven zien.

Toon, al even geleden begon ik bij jou in de groep voor mijn masterstage. Een fijne omgeving waarin ik me kon ontwikkelen tot het moment dat jij me het vertrouwen gaf om een stage in New York te gaan doen. Ook daarna bleef jij een vast aanspreekpunt voor mij. Met je prachtige opmerkingen draag je tijdens de leuke MedFys momenten (o.a. taart eten om 11.00 uur, labstapdagen en etentjes) bij aan de goede sfeer. Bedankt voor de momenten dat je met empathie en zorg voor me klaar stond. **Teun**, dank voor jouw kritische vragen tijdens besprekingen en dat ik altijd bij je terecht kon voor hulp rondom patch clamp en het werkend blijven houden van mijn laptop. Ik heb je bijdrage erg gewaardeerd. **Sanne**, jouw grote glimlach verblijdt altijd de hele ruimte. Bedankt voor je scherpe vragen en het delen van je enthousiasme. **Marti**, vol droge humor vergezelde je mij regelmatig in de kamer van Linda. Dank voor jouw hulp binnen het PhD programma Cardiovascular Research. **Linda**, jouw kamer was de afgelopen jaren mijn centrale punt van de MedFys. Ik werd altijd blij als ik jou zag zitten bij binnenkomst. In jouw kamer voelde ik me welkom en deelden we graag wat ons bezighield: eten, musicals, vakantietripjes, kerstversiering, McDooonald's, Wie is de mol?, noem maar op. Het was een fijne afleiding. Ik heb je betrokkenheid, hulp en gezelligheid heel erg gewaardeerd. **Marien**, heel wat patch clamp parties heb ik met je mogen meedoen. Ik bewonder jouw patch-expertise en dank je voor het delen van de mooiste verhalen in het elektrofysiologielab.

Vera, alle facetten van de afdeling hebben wij met elkaar gedeeld. Onderdeel zijn van de Marc-groep, experimenten uitvoeren, het organiseren van de labstapdag, Papendal cursus, lesgeven, MedPhys Productions en promotiefeestjes. Jij denkt wat meer out-of-the-box en gaf me daardoor vaak waardevolle inzichten tijdens onze fijne gesprekken. Heel veel succes met het afronden van je PhD. Ik heb er alle vertrouwen in. **Stephanie**, voor het overgrote deel zijn wij roomies geweest op de MedFys en was je dus een vast gezicht van mijn MedFys omgeving. Met een lach was je altijd in voor een gezellig praatje en deelde je je waardevolle kennis over de belangrijke zaken van een PhD buiten de MedFys om. Dank je wel daarvoor. **Meye**, onze extra inzet voor de afdeling heb ik altijd fijn met je kunnen delen. Bedankt voor jouw eindeloze interesse, dat siert je. **Encan**, I really appreciated your invitation for the nice dinner you organized for us at your house. Together we taught my final ECG practicals, thank you for your kindness and help.

Tonny, ik kijk fijn terug op de tijd dat jij als secretaresse, klankbord en al met al als warm mens een vast gezicht was van de MedFys. **Leonie**, het lab was dankzij jou altijd geordend en overzichtelijk en daardoor een genot om ’s ochtends vroeg aan mijn blotjes te beginnen. Het was heel fijn om een rol als paranimf met je te delen. **Elise**, vanaf dat ik startte op de MedFys was jij, als mijn stagebegeleider, mijn voorbeeld. Van jou heb ik geleerd om zo efficiënt mogelijk veel dingen tegelijk te doen en dat in combinatie met gezelligheid. Je bureauplekken op de afdeling heb ik mogen opvolgen en mede daardoor heb ik nog vaak aan je gedacht. **Lotte**, wat genoot ik van jouw structurele aanpak als wij samen een experiment begonnen tijdens mijn stage. Bij het pakken van een Post-it dacht ik daarna altijd aan jou! Bedankt voor jouw scherpe feedback wat heeft bijgedragen aan mijn basis van onderzoek doen. **Alex**, thank you for sharing the patch clamp parties and your expertise on pharmacology and cardiac electrophysiology. I know that the times I had to bother you with my questions are uncountable. You took the time to clearly explain every single detail, which I really appreciated. **David**, ik werd altijd vrolijk als jij je met grote stappen enthousiast over de afdeling bewoog. Jouw enthousiasme over de elektrofysiologie van het hart is enorm aanstekelijk. Dank je wel dat je dat met mij wilde delen. **Alan**, when I think of you, I think about food: tuna salad, this specific muffin type, tiramisu and pastaaa! To clarify: that is a good thing. It was nice to have you around at the MedPhys. **Helen**, uiteraard keek ik altijd extra op als jij in de mooiste creaties binnenkwam. Bedankt voor je gezelligheid tijdens

borrels, etentjes en promotiefeestjes. **Chantal**, jouw hulp voordat ik naar New York ging is me altijd veel waard geweest. Tijdens kwetsbare gesprekken kwam het naar voren dat je besloot weer terug te gaan en ik bleef op de hoogte van je mooie prestaties daar. **Muge**, you are one of the sweetest people I got the opportunity to meet during my PhD. Thank you for sharing your story with me. I am glad we are still in touch via emails and as we always end them: 'I wish you all the best'. **Aurore**, het laatste jaar met regelmaat mijn kamergenootje betekende in alle rust werken afgewisseld met gezellig kletsen. Ik wens je veel succes met je verdere carrière. **Valerie**, ik heb altijd veel bewondering gehad voor je enorme concentratievermogen, doorzettingsvermogen en hoeveelheid kennis. Bedankt voor het beantwoorden van mijn vragen en je input.

Vier studenten heb ik mogen begeleiden waardoor ik enorm veel over mezelf heb geleerd. **Caroline**, op de eerste dag van mijn PhD begon jij jouw masterstage. Onze samenwerking ging vanzelf en dat ging gepaard met veel humor. Ik voel me stiekem toch wel vereerd dat jij mensen laat denken dat ik de wasmachine-mevrouw op jouw mok ben. Heel veel succes met de afronding van je PhD. **José** en **Tobias**, dank voor jullie inzet en samenwerking. **Nelia**, je pannenkoekenplant op de vensterbank naast mijn bureau heeft me vaak herinnerd aan onze gezellige samenwerking. Veel succes met je verdere carrière. **Huidige studenten**, een succesvol verloop van jullie stage gewenst.

Mijn dank is ook groot voor de samenwerkingen buiten de afdeling Medische Fysiologie. **Arend Schot**, ik heb genoten van onze samenwerking. Jij bezit veel enthousiasme voor je vak, bent enorm flexibel en ging feilloos mee in de vaste manier van werken van Jet en mij. Ik wil je bedanken voor het in werking brengen en houden van de loopbandkamer, de ontelbaar aantal keren 'goedzooo' en het in alle rust laten verlopen van de inspanningsexperimenten. Zelfs de corona-periode kon ons niet tegenhouden om door te gaan. **Maarten van Emst**, bedankt voor jouw interesse en gedachtewisselingen rondom complexe fysiologie vraagstukken. **Rolf Sparidans**, dank voor het delen van jouw expertise en geduldige uitleg over LC-MS/MS. **Philippe Wouters**, dank je wel dat jij vele keren in alle flexibiliteit klaarstond voor het maken van de echo's. Ons geduld werd dan nog wel eens op de proef gesteld, maar het was het allemaal waard. **Henk van der Linde**, van een spontane ontmoeting op het Safety Pharmacology Congress in Barcelona en het naast elkaar presenteren van onze posters, naar

een mooie samenwerking rondom de JNJ303 studie. Dank voor jouw kritische blik en het delen van jouw kennis. **Tim Takken**, onze samenwerking startte al vroeg in mijn PhD traject. Je was altijd bereikbaar voor het delen van materiaal en kennis. Ik heb genoten van jouw Summerschool course en ik dank je voor je input. Ons gesprek over de welbekende schrijfuitdagingen heeft me veel inzicht gegeven.

I had the opportunity to be part of the CResPace consortium. **Alain Nogaret** thank you for leading the project. **Mariann Gyöngyösi**, thank you for sharing your thoughts and ideas and for hosting our meeting in Vienna. **Martin Riesenhuber**, it was a comforting idea that you were there so we, as PhD students, could share our thoughts and concerns throughout the project. Our professional discussions went in parallel with a lot of laughter. **Martin Leonhardt**, thank you for joining the last couple of experiments and for the interesting conversations and brainstorm sessions, which led to the successful measurements. **Kamal** and **Chandrabhan**, thank you for our collaboration and for sharing your expertise with me. **Renate** and **Elisa**, despite our short cooperation, I really appreciated the kindness you brought into our very efficient meetings and other moments of contact. I wish you all the best for your future careers. **Martin Pešl**, thank you for your interest and input, and for sharing your knowledge with me. **Soren**, I look back on the pleasant moments we shared during the consortium meetings, dinners, and the successful experiments we have performed together. I really enjoyed working with you. With only a few comforting words you gave me more confidence already early in my PhD, which I really appreciated. **Yankí**, you were the stable and reliable factor within the consortium. I thank you for your friendly and coordinated contribution. To all **CResPace colleagues**, thank you and I wish you all the best.

Dierverzorgers van H0, dank voor jullie inzet betreft het dierenwelzijn. Jullie werk is een fundamenteel onderdeel geweest van dit onderzoek. **Jeroen**, het was dankzij jou altijd gezellig in de stal en je extra hulp naast de gebruikelijke werkzaamheden heb ik erg gewaardeerd. **Helma**, dank dat jij als vast gezicht in het GDL ons adviseerde en altijd in was voor een vrolijk praatje in de vroege ochtend. **Marlijn**, wij hebben we heel wat keertjes samen op de OK mogen gestaan. Hoe vroeg ook, altijd stond jij fris en fruitig klaar om te starten en hebben we samen met Jet mooie momenten mogen delen. **Fred Poelma** en **Ivo Tiebosch**, dank voor jullie advies rondom het schrijven van de nieuwe projectaanvraag.

Mijn vrienden, vriendinnen en familie gaven afleiding tijdens mijn PhD en zijn heel erg belangrijk voor me.

Myrna, jouw aanwezigheid vult de ruimte met positiviteit. Jij geniet van het geluk van mensen om jou heen en dat delen wij. Ik ben graag in jouw buurt en lach dan heerlijk om onze zelfspot. Dit uit zich op een hoogtepunt wanneer wij 'Ashes' door de microfoon laten klinken. **Kevin**, met jou kan ik op een zeer professionele manier de verpakking, ervaring, geur en structuur van snoep evalueren. Bedankt voor jouw doortastende vragen, openheid, warmte en dikke knuffels. **Rianne** en **Doreth**, van Tony's Chocolonely behang tijdens onze stage bij de MedFys naar serieuze banen in de wetenschap. Dank je wel voor het samen delen van de frustraties die daarbij horen. **Pauline** en **Eliane**, als echte Gossip Girls startte onze vriendschap in New York. Nu houden we elkaar op de hoogte tijdens decadente etentjes in Amsterdam en Utrecht. XOXO **Milou**, cheers op nog veel wijnavondjes. Dank je wel voor onze fijne gesprekken en de Abbey-content die mijn laatste schrijffase heeft opgevrolijkt. **Coen**, wanneer beginnen wij nou een podcast? Al is het misschien toch verstandiger om onze ongezouten mening binnen vier muren te houden. Elk feestje is mooier als jij er bent en hopelijk hebben we er nog veel samen in het vooruitzicht. **Jacques** en **Marga**, bedankt voor de fijne avondjes in jullie achtertuin. Het bierglas staat altijd voor me klaar en ik geniet volop als we iedere keer weer het duet van Andrea Bocelli en Laura Pausini ten gehore brengen. **Marian**, bedankt voor de gezelligheid en jouw hulp in het vinden van de perfecte promotiejurk. **Anne**, wijntjes, dinertjes, een serieus gesprek, feesten, heel hard lachen, alles kan met jou! Bedankt voor jouw gezelligheid en adviezen. **Jelle**, de grootste met een groot hart. Bedankt dat je er was op belangrijke momenten. Ik kijk uit naar nog vele spelletjesavonden. **Fedde**, sinds vorige zomer ben je een vrolijke aanwinst in Giesbeek en Arnhem. Na de oprichting van de 'rijke en zielige club' gingen wij met Suusje langs de McDrive en vieren wij de feestdagen. Dank je wel voor je interesse.

Agnieszka, van collega naar vriendin. Wat hebben wij mooie dingen binnen en buiten de MedFys mogen delen. #opPapendal, onze werkplekken binnen 4 m^2, eerste publicaties en spannende presentaties, het samen organiseren van de labstapdag en PhD retreat, Marc bbq's, Marc meetings, MedPhys Productions, de lekkerste etentjes van jou en Jeroen, en natuurlijk jouw promotie. Mijn promotie zal jij gaan vastleggen en jouw positieve uitstraling

in mijn buurt die dag geeft me nu al rust. Jouw advies en geruststelling de afgelopen jaren, specifiek op die ene zeer vroege vrijdagochtend afgelopen januari, heb ik heel erg op prijs gesteld. 'Ik ben zó trots op jou'.

Birgit, als mijn frustraties even hoog opliepen, zocht ik jou zo snel mogelijk op. Ik vond je dan zeer geconcentreerd in een labjas met de mooiste muziek op de achtergrond. Je liet dan alles uit je handen vallen, luisterde, stelde me gerust en bood áltijd je hulp aan. Ik zie je graag lachen en dat hebben we dan ook veel gedaan samen! Tijdens de lunch werden tv-programma's pittig geanalyseerd en planden we onze uitjes zoals de Piano Guys en Meimaand snoepjesmaand bij de Tilburgse kapel. Eén van de hoogte- (of diepte) punten is toch wel dat we 'op BHV-niveau' zijn natgeregend in de voorraadkamer. Bedankt voor jouw steun op ontelbaar veel momenten.

Mijn 'lieverds' van het Arentheem, ik geniet als we samen zijn en ben heel trots op ieder van jullie. **Julia**, onze vriendschap begon toen we, als twee brugpiepers die 'van ver' kwamen, met zware Kipling tassen de Raapopseweg trotseerden. Nu zijn jouw gedetailleerde beschrijvingen van al onze herinneringen een fijne afleiding naar 'toen'. Een dagje Rotterdam met jouw rondleiding en ontbijtplankje voelt als een ontspannende vakantiedag. **Noor**, heerlijk hoe we altijd onze mening klaar hebben, als echte rechercheurs iedereen wel weten te vinden, gek zijn op kinderen en Momo, en elkaar de liefde gunnen. **Roos**, wat ben jij altijd lief voor mij. Tijdens de laatste schrijffase heb je tijdens jouw kostbare tijd geïnteresseerd geluisterd en meegedacht. Mijn geluk kon niet op toen je me tijdens die ene wandeling op die ene plek vertelde dat Sophia eraan zou komen. Je doet het goed Rosie. **Emmy**, heel erg sterk en mooi ben jij. Ik ben blij dat jij in mijn leven bent en we iedere zondagavond bellend alles met elkaar kunnen delen. Welke zorgen of tranen er ook voorbij komen, altijd sluiten we lachend af! Ik ben er zeker van: er ligt veel moois in het verschiet.

Tessa, of het nou tijdens de voorbereidingen van de KIKA Run is, of het verhuizen van Arnhem naar Utrecht en weer terug: wij gaan elkaar achterna. Jij bent mijn voorbeeld in hoe jij jouw leven inricht. Ik hoop dat we samen nog heel veel restaurants in Arnhem gaan ontdekken en van veel 'plankjes van Tes' met kaassoufflés uit de pan gaan genieten. **Shanice**, Janien Denies, sinds onze ontmoeting in de collegezaal op de VU heb ik veel van mijn belangrijke momenten

met jou mogen delen, want jij bent er altijd voor mij. Met niemand anders kan ik van echte nerd-momenten in een splitsecond volledig opgaan in muziek van het Mega Piraten Festijn en Celine Dion. Bedankt dat jij altijd in onze vriendschap blijft investeren. **Jennifer**, jouw aanstekelijke lach bezorgt mij altijd een overweldigend gevoel aan vrolijkheid. Van dichtbij heb ik jouw kracht mogen meemaken sinds mijn grote vriend Olivier is geboren. Wij gunnen elkaar de wereld. Van ons plan om onze week in New York nog eens te herbeleven, kan ik blijven fantaseren. Ik weet dat we dat gaan bewerkstelligen.

Familie aan de kant van Aanstoot, vroeger kwamen we elke zondag bij elkaar in de Naaldwijkstraat en daar kijk ik fijn op terug. Nu zetten we onze band voort tijdens verjaardagen, belletjes en zijn we er wanneer dat nodig is. **Familie aan de kant van Van Bavel**, de band tussen ons is mij veel waard. Als het nodig is, zullen we er altijd voor elkaar zijn. Op naar een nieuwe familiebijeenkomst.

Mijn paranifm, **Willem**, wat heb jij mij geholpen. Er zijn menig zakken Tikkels en broodjes Ben in onze mondjes gegaan alsoffff het Malteeeesers zijnnnn. Jij zorgde voor een enorme lading humor en, ook al lachte jij net iets harder om de memes die je deelde, die vrolijkheid sleepte mij door de uitdagende momenten heen. Vaak was mijn blik in 'jouw kantoor' voldoende om voor een gezellige afleiding samen te komen. Je was er ook voor het beantwoorden van mijn vele inhoudelijke vragen, het sparren over figuren en statistiek, en het nalezen van teksten die ik je stuurde. Jij kijkt verder en ziet waar je van waarde kunt zijn. Ik heb dat gewaardeerd. Bedankt voor je enorme steun.

Mijn paranimf, **Daniek**, 25 jaar aan vriendschap achter ons en hopelijk nog vele jaren voor ons. Als buurmeisjes en samen spreekbeurten geven vanaf groep 2 tot bruidsmeisje en paranimf. We hebben in die tijd al heel wat hoogte- en dieptepunten met elkaar gedeeld. Bij jou kan ik mezelf zijn, want jij geeft me het vertrouwen dat dat genoeg is. Wij kunnen heel goed en lang praten, jij luistert aandachtig en geeft dan op een fijne manier advies. Daarnaast kunnen we heel hard lachen, elkaar de waarheid zeggen en met elkaar feesten. Al met al zijn wij een goed team. Bedankt voor alle steun en gezelligheid! Ik kijk er naar uit nog veel mooie herinneringen te maken in de toekomst, 'want toeval bestaat niet, hè?'.

En dan mijn vangnet waar ik spreekwoordelijk ieder moment in kan vallen als het nodig is. Dat is nogal wat keren gebeurd de afgelopen jaren. Dalen en heel veel mooie pieken beleven wij samen. Van onbeschrijflijke waarde, onvoorwaardelijk en het allerbelangrijkste in mijn leven, want 'wij zijn de kern'.

Mijn lieve zusjes. 'Wij zijn zussen.' **Eline**, lieve Lien, verschillend maar niemand op de wereld is meer hetzelfde als wij. Jij bent mijn vriendin, 'spiegoloog', personal shopper, degene met wie ik alles deel en als eerste op bel. Ik hou van jouw 'spijker-op-de-kop' analyses en adviezen. Met jou kan ik zo hard lachen dat de tranen over onze wangen rollen. Lufjoe Lien. **Marieke**, lieve Marie, jouw komst in het gezin is het mooiste dat ons is overkomen. Jij bent de knapste, een levensredder, mijn chauffeur en degene waarmee ik het enthousiasme voor spelletjes (vooral 'turdie sekunts'), het Nederlandse lied, het menselijk lichaam, garnalenpasta en karaoke/silent disco feestjes kan delen. I like all dit. Lym.

Mijn lieve ouders. **Felix**, lieve papa, 'ik lijk steeds meer op jou'. Het lijkt wel alsof dat met de dag meer wordt. Afgelopen jaar hebben we de waarde van onderzoek naar hartritmestoornissen ondervonden wat ons nóg dichter bij elkaar bracht. Wij delen de interesse in bèta-onderwerpen en ik ambieer je enthousiasme en gedachtegang over de oneindigheid van het universum. Je hebt me altijd het gevoel gegeven dat ik alles kan en mag doen, en dat je me overal zal komen ophalen als dat nodig is. Een dikke knuffel volgt dan. Bedankt voor je onvoorwaardelijke steun. Lufjoe daddy. **Irma**, lieve mama, 'als ik mijn hartslag voel, dan voel ik die van jou'. Elke dag begint met een berichtje van jou en dit zou ik niet meer weg kunnen denken. De afgelopen jaren hebben we een ontelbaar aantal keren gebeld, gespard en de Giesbeekse dijken afgewandeld. Je laat me altijd welkom voelen en geniet dan, net als ik, het meest als we als gezin samenzijn. Jij bent de allersterkste persoon die ik ken en ik bewonder je. Mijn dank voor jouw zorg en steun is niet in woorden uit te drukken. Bedankt voor alles mommy. I love you.

Lieve oma, altijd in ons hart. Ik zal mijn zegeningen blijven tellen.

’t Komt wel goed.

PhD portfolio

Education	**Year**	**Workload (EC*)**
General courses		
Summerschool Paediatric Sport and Exercise Medicine	2018	1.5
Introductory Biostatistics for Researchers	2019	4.5
PhD day: Transparent Science	2019	0.3
PhD day: Creativity in Science	2021	0.2
Scientific Artwork – Adobe Illustrator	2021	0.7
Responsible Conduct of Research	2021	0.15
Theoretical courses		
PhD Retreat Cardiovascular Research (organization + attendance)	2018	1.0
Dutch Heart Foundation – Vascular Biology	2018	1.5
Dutch Heart Foundation – Cardiac Function & Adaptation	2019	1.5
Sophisticated Laboratory Techniques in Cardiovascular Research	2020	3.0
Jongbloed Seminars	2017-2022	1.5
Research Colloquia Cardiology	2017-2022	3.0
External courses and meetings		
Safety Pharmacology Society Congress, Barcelona	2019	1.2
Hartfunctiebijscholing – Ergometrie	2020	0.3
Heart Rhythm Society Congress, Online	2021	1.2
		21.55

Teaching		
Supervision of students	**Year**	**Weeks**
Caroline Pham	2017-2018	53
José Inia	2018	11
Tobias Vast	2019	13
Nelia van Dijk	2020	42
Teaching activities	**Year**	**Hours**
Practicals	2018-2022	32
Working groups	2018-2021	42

* 1 EC, European Credit, is equal to a time-investment of 28 hours.

List of publications

Van Bavel JJA, Beekman HDM, Smoczyńska A, Van der Heyden MAG, Vos MA. I_{Ks} activator ML277 mildly affects repolarization and arrhythmic outcome in the CAVB dog model. *Biomedicines.* 2023;11(4):1147

Van Bavel JJA, Beekman HDM, Schot A, Wouters PC, Van Emst MG, Takken T, Van der Heyden MAG, Vos MA. Remodeling in the AV block dog is essential for tolerating moderate treadmill activity. *Int J Cardiol Heart Vasc*. 2023;44:101169

Van Bavel JJA, Beekman HDM, Van Weperen VYH, Van der Linde HJ, Van der Heyden MAG, Vos MA. I_{Ks} inhibitor JNJ303 prolongs the QT interval and perpetuates arrhythmia when combined with enhanced inotropy in the CAVB dog. *Eur J Pharmacol.* 2022;932:175218

Van Bavel JJA, Pham C, Beekman HDM, Houtman MJC, Bossu A, Sparidans RW, Van der Heyden MAG, Vos MA. PI3K/mTOR inhibitor omipalisib prolongs cardiac repolarization along with a mild proarrhythmic outcome in the AV block dog model. *Front Cardiovasc Med.* 2022;9:956538

Taylor JD, Abu Hassan KJ, **Van Bavel JJA**, Vos MA, Nogaret A (2021). Robust design of inhibitory neuronal networks displaying rhythmic activity. In: Awrejcewicz, J. (eds) Perspectives in Dynamical Systems III: Control and Stability. DSTA 2019. *Springer Proceedings in Mathematics and Statistics.* 2021;364:187-198

Krause R, **Van Bavel JJA**, Wu C, Vos MA, Nogaret A, Indiveri G. Robust neuromorphic coupled oscillators for adaptive pacemakers. *Sci Rep.* 2021;11:18073

Abu-Hassan KJ, Taylor JD, **Van Bavel JJA**, Vos MA, Nogaret A. Silicon central pattern generator model of cardiac contraction behavior. *2020 11th Conference of the European Study Group on Cardiovascular Oscillations (ESGCO)*. 2020;1-2

Kessler EL, Van Stuijvenberg L, **Van Bavel JJA**, Van Bennekom J, Zwartsen A, Rivaud MR, Vink A, Efimov IR, Postma AV, Van Tintelen JP, Remme CA, Vos MA, Banning A, de Boer TP, Tikkanen R, Van Veen TAB. Flotillins in the intercalated disc are potential modulators of cardiac excitability. *J Mol Cell Cardiol*. 2019;126:86-95

Van Bavel JJA, Vos MA, Van der Heyden MAG. Cardiac arrhythmias and antiarrhythmic drugs: an autophagic perspective. *Front Physiol.* 2018;9:127

Cerrone M, Montnach J, Lin X, Zhao YT, Zhang M, Agullo-Pascual E, Leo-Macias A, Alvarado FJ, Dolgalev I, Karathanos TV, Malkani K, Van Opbergen CJM, **Van Bavel JJA**, Yang HQ, Vasquez C, Tester D, Fowler S, Liang F, Rothenberg E, Heguy A, Morley GE, Coetzee WA, Trayanova NA, Ackerman MJ, Van Veen TAB, Valdivia HH, Delmar M. Plakophilin-2 is required for transcription of genes that control calcium cycling and cardiac rhythm. *Nat Commun.* 2017;1:106

About the author

Joanne van Bavel was born on the 18th of September 1993 in Giesbeek, The Netherlands. She attended pre-university education at the Thomas á Kempis College, Arnhem. Her educational profile focused on nature, health, and techniques to work towards her childhood dream to become a reconstructive surgeon. However, growing up hearing about the diseased heart being present within her family, raised her interest towards the cardiovascular field, which grew even further during biology classes educated by F. ter Beke.

In 2012, Joanne started the bachelor programme of Biomedical Sciences at the Vrije Universiteit Amsterdam. As extracurricular activities she became a member of the Student Representatives, and the Faculty Student Council Earth and Life Sciences as Head Public Relations. The bachelor was finished with an internship of four months at the Department of Medical Physiology, UMC Utrecht, on localization of the flotillin protein in cardiac tissue of various species supervised by dr. Teun de Boer.

In 2014, Joanne continued her studies with the master programme Biology of Disease, including the cardiovascular track, and got the opportunity to further expand her bachelor internship research. This internship was performed under supervision of dr. Toon van Veen and dr. Elise Kessler, and partly under supervision of prof. dr. Jeroen Bakkers and dr. Lotte Koopman at the Hubrecht Institute. During the last six months of her master programme, Joanne had the opportunity to go abroad by attending the group of prof. dr. Mario Delmar as an intern at the NYU Langone Medical Center, New York. Here, she looked into intercalated disc proteins and the use of single-molecule localization microscopy. By returning to the Department of Medical Physiology, the master programme was completed with a thesis on autophagy, calcium, and the cardiac contraction mechanism under supervision of dr. Marcel van der Heyden.

In September 2017, Joanne started her PhD position under supervision of prof. dr. Marc Vos and dr. Marcel van der Heyden, again at the Department of Medical Physiology. Her thesis, entitled ‘Drug and device testing in a preclinical model sensitive to cardiac arrhythmias’, will be defended on the 28th of September 2023. From June 2023, Joanne continued her career as project employee/researcher at the Dutch Heart Foundation.

Sudden cardiac death is still the leading cause of mortality worldwide and in 50-70% of the cases related to ventricular arrhythmia. The process of initiation and perpetuation of ventricular arrhythmias is complex and coincides with (a combination of) diverse substrates, triggers, and underlying electrophysiological mechanisms. Arrhythmia management is still improving and focusses on evaluating proarrhythmic responses of new developed compounds, the discovery of new pharmacological targets, and the improvement of antiarrhythmic strategies.The remodeled heart of the anesthetized chronic atrioventricular (AV) block dog is sensitive to ventricular arrhythmias and is therefore a valuable model in testing pro- and antiarrhythmic strategies.

The studies incorporated in this thesis concentrate on two parts for targeting ventricular arrhythmias. 1) Drug testing: with a focus on targeting the second main repolarizing current I_{Ks} and the establishment of underlying proarrhythmic triggers for ventricular arrhythmias, and 2) Device testing: by establishing exercise and respiratory behavior of the AV block dog model for testing a new pacing strategy.